



THE PREPARATION AND APPLICATION OF THORIUM- BASED NUCLEAR FUELS

A thesis submitted to the Department of Materials Science and Engineering,
The University of Sheffield

by

Ross Peel, MEng

In support of the application for the degree of

Doctor of Philosophy (PhD)

Originally submitted December 2016

Final version submitted with minor amendments September 2017

SUMMARY

Thorium is currently produced primarily as an impure by-product of the mining and processing of the rare earth phosphate mineral monazite. Thorium concentrates are currently purified industrially by solvent extraction with PC-88a, but this extractant cannot separate uranium and iron from thorium. In this work mixtures of PC-88a and HDEHP were investigated for the mutual separation of uranium, thorium and iron. The extracted complexes were identified. U and Fe were extracted by cation exchange, while Th was extracted by a mixed cation exchange/solvation mechanism. It was found that three contact stages could extract > 99% of the thorium. A flowsheet was proposed.

The first modern use of thorium as a nuclear fuel is most likely to be as an oxide fuel within Generation III+ nuclear reactors. In this work a uranium-plutonium mixed oxide was investigated as a fissile driver for thorium in the Enhanced CANDU 6 reactor, as an alternative to the proposed UK CANMOX fuel for irradiation of the UK plutonium inventory. A large number of fuel concepts were considered, and several were analysed by Monte Carlo simulation. It was found that U-Pu-Th fuels could offer transmutation of the plutonium, irradiate UK reprocessed uranium and give improved coolant void reactivities, while irradiating thorium and converting it to fissile ^{233}U .

Thorium and uranium may be recovered from spent nuclear fuel by the Acid THOREX process, which uses TBP solvent extraction. However, TBP has a number of disadvantages. In this work several alternative solvent extraction systems were investigated for the separation of Th, U, Fe and Zr. PC-88a was mixed with ten other extractants as potential synergists, extracting from hydrochloric, nitric and sulfuric acids. Several promising systems were identified based on distribution ratios and separation factors.

ACKNOWLEDGEMENTS

The work presented in this thesis would not have been possible without the contribution of a great number of people, who have helped to shape my ideas and provide me with those opportunities and experiences which have been vital to me in reaching the point of submitting a doctoral thesis and successfully completing a *viva voce* examination.

At the University of Sheffield I must begin by acknowledging the contribution of my academic supervisory team, which has undergone some significant changes over the three years (and twenty seven months) of my Ph.D. programme. Professor Karl Whittle provided the impetus for this work and encouragement and support through the process, continuing to do so even since taking up a new post at the University of Liverpool. Professor John Provis has provided much needed continuity through the process. Dr. Mark Ogden has been instrumental in providing day-to-day advice and guidance in the technical aspects of the work, particularly regarding the thorium separations work presented in Chapters 3 and 6, in addition to the necessary counselling when the scope of the work seemed overwhelming. I would also like to thank Dr. Iain Hannah for his assistance in the role of a thesis writing mentor for providing the necessary kick up the bottom required for me to get into the process of writing.

The elemental concentration analyses by ICP-MS and ICP-OES presented in this work were performed by external services. ICP-MS was carried about by Dr. Gabriella Kakonyi and Dr. Andrew Fairburn in the Groundwater Protection and Restoration Group of the Kroto Research Institute, University of Sheffield. ICP-OES was carried out by Mr. Martin Jennings of the University of Manchester and Dr. Sarah Pepper, with much advice on the technique to the author from both parties.

Due to this work being completed through the Nuclear FiRST Doctoral Training Centre, many people at the University of Manchester have also been very helpful at various stages of the work. In particular, Dr. Clint

Sharrad and Dr. Richard Foster provided technical insights and help in accessing analytical facilities at the institution. The mineral samples analysed in Appendix A, and a good number of other samples besides, were provided by Dr. David Gelsthorpe at the Manchester Museum on a highly extended loan. For assistance with the work presented on neutronic simulation in Chapter 5 I would like to thank Professor Tim Abram at the University of Manchester for providing access to the Redqueen and CFS2 high power computing infrastructures, and also Seddon Atkinson at the University of Sheffield for his help in working with Redhat Scientific Linux.

Also related to the simulation work presented in Chapter 5, I would like to thank Dr. Jim Kuijper of NUCLIC for his expert input and feedback on the work done in this chapter, leading towards to publication of this work.

The work described in Chapter 4 was originally carried out during a 12 week industrial placement with AREVA S.A. in Paris, France, under the direction of Dr. Luc Van Den Durpel. This contact was provided by Dr. Stephanie Cornet, now at the OECD Nuclear Energy Agency, for which the author is extremely grateful. All those in the AREVA Research, Development and Innovation management team are thanked for their patience and understanding as I rediscovered my French-speaking abilities after over four years of letting them go to rust. In particular I wish to thank Patrick Chaucheprat for his many inspirational tales of managing research projects on the Superphénix experimental fast reactor, and Isabelle Perraud for her assistance with matters of administration and organisation.

There are also a great number of people who have supported me personally during the Ph.D. process. I must begin by thanking my parents, without whose unending love and support over the last 28 years I would never have been able to reach this point. In particular, their provision of free full-board accommodation during the final 12 months of the Ph.D. process are appreciated beyond measure. On that note I must also say thank you to Dr.

Richard Walker, friend and landlord, for allowing me to continue living in his property even when paying the rent became problematic.

I also thank my partner Laura Bird for keeping me sane and happy during the last 2.5 years, making sure I did not forget that there is a life beyond research, and in particular being willing to bear with me during the intensive work period of the last few months. She has provided me with a new outlook on life, and a vision of a happier future than I had heretofore imagined possible.

Finally, the work reported in this thesis would also not have been possible without:

- ~£75,000 in stipends, consumables and travel/conference expenses, plus however much more in on-costs. Thank you EPSRC!
- Three laptops (two which gradually became too slow to tolerate)
- 21 GB of online cloud data storage
- ~250 hours underwater on SCUBA diving holidays
- ~3000 Tesco finest cookies (various flavours)
- ~250 litres of cappuccino
- ~3 litres of espresso at AREVA (because when in Rome....)
- A truly inestimable quantity of real ale, primarily supplied by the Red Deer (18 Pitt Street, Sheffield), the Cobden View (40 Cobden View Road, Sheffield), and the Hallamshire House (49-51 Commonsides, Sheffield).

“As for me, I had the time of my life.”

– Stephan King, *“On Being Nineteen
(And a Few Other Things)”*

TABLE OF CONTENTS

Summary	i
Acknowledgements	ii
Table of Contents.....	v
List of Tables	xiii
List of Figures	xvi
List of Nomenclature.....	xxvi
1 Introduction	1
1.1 Aims.....	1
1.2 The Structure of This Thesis.....	2
1.3 Global Context – The Need for Nuclear Energy.....	3
1.4 The Modern Nuclear Power Industry	4
1.4.1 Uranium-based Nuclear Fuel – Supply and Demand.....	4
1.4.2 Reducing Fuel Resource Utilisation	5
1.4.3 Options for Sustainable Nuclear Fuel Management.....	6
1.5 Thorium as an Alternative Fuel to Uranium	6
1.5.1 The Limitations of Thorium	7
1.5.2 The Use of Thorium as a Nuclear Fuel.....	7
1.6 Nuclear Power in the United Kingdom.....	9
1.6.1 Historical and Current Nuclear Operations	9
1.6.2 The UK Plutonium Inventory.....	9
1.7 Aqueous Separations Processes	12
1.8 Chapter Summary.....	14
2 Introductory Theory, Thorium Resources and Literature	
Review 15	
2.1 Overview of Nuclear Power Reactor Operating Principles and	
Basic Physics.....	15
2.1.1 Neutron Interactions with Matter.....	16

2.1.2	The Critical Nuclear Fission Chain Reaction	21
2.1.3	Neutron Moderation.....	23
2.1.4	Neutron Loss	24
2.1.5	Core Heat Management and Removal.....	25
2.1.6	Core Control Systems	25
2.1.7	Fuel Fertile Conversion and Breeding.....	27
2.1.8	Reactor Stability and Coefficients of Reactivity.....	27
2.1.9	Used Nuclear Fuel.....	29
2.1.10	Plutonium and Proliferation.....	29
2.2	Thorium as a Nuclear Fuel	30
2.2.1	Nuclear Interaction Properties of Thorium.....	30
2.2.2	Thorium Spent Fuel	32
2.2.3	The Thorium Oxide Fuel Form	33
2.2.4	Thorium-fuelled Molten Salt Reactors	34
2.3	Thorium Resources	35
2.3.1	Primary Sources of Thorium	36
2.3.2	Secondary Thorium Resources	40
2.3.3	Thorium Resource Utilisation Scenarios.....	40
2.4	Thorium Fuel Cycle Front End.....	41
2.4.1	Overview of Thorium Production from Monazite Ore	41
2.4.2	Monazite Concentrate Leaching.....	42
2.4.3	Thorium Concentrate Purification	44
2.4.4	Fuel Form Conversion.....	45
2.4.5	Thorium Oxide Pellet Fabrication	45
2.5	Thorium Fuel Cycle Back End	45
2.6	Principles of Solvent Extraction.....	46
2.6.1	Solvent Extraction Example: The PUREX Process.....	48
2.7	Historical Thorium Purification Processes.....	50
2.7.1	The Acid THOREX Process	51
2.7.2	The Interim-23 Process.....	55
2.8	Solvent Extraction of Thorium	55
2.8.1	Solvent Extraction Mechanisms	57
2.8.2	Tributyl Phosphate Extraction	58

2.8.3	Phosphine Oxides.....	59
2.8.4	Phosphorous Acids	60
2.8.5	Carboxylic Acid Extractants	64
2.8.6	Sulfur-based Extractants	64
2.8.7	Thiophosphorous Acid Extractants.....	65
2.8.8	Amine Extractants.....	66
2.8.9	Aminophosphorous Extractants.....	71
2.8.10	Calixarene Extractants	71
2.8.11	Crown Ethers	72
2.8.12	LIX Extractants	72
2.8.13	Room Temperature Ionic Liquids	73
2.8.14	Summary of Prior Research into Thorium Separations	75
2.9	Thorium-based Nuclear Fuels.....	76
2.9.1	Thorium Fuelled Reactor Core Design Considerations	77
2.9.2	Thorium Dioxide Fuels in Reactor Operation.....	79
2.9.3	Thorium in Pressurised Heavy Water Reactors	86
2.9.4	Summary of Prior Research into Solid Thorium Fuels	92
2.10	Novel Research Areas Identified and Developed in this Thesis	
	93	
2.10.1	Thorium Solvent Extraction from Monazite	93
2.10.2	Thorium-Uranium-Plutonium Fuels in Pressurised Heavy Water Reactors	94
2.10.3	Recovery of Thorium and Uranium from Spent Fuels	95
2.11	Chapter Summary.....	96
3	Development of the PC-88a/ HDEHP/HCl Solvent Extraction System	97
3.1	Introduction	97
3.1.1	Properties of PC-88a and HDEHP	98
3.1.2	Selection of Organic Diluent.....	101
3.1.3	Literature Review on the Extraction of Th, U and Fe by PC- 88a and HDEHP	101

3.1.4	Extraction Studies Performed.....	107
3.2	Methods	108
3.2.1	Reagents and Stock Solutions	108
3.2.2	Analytical Instruments and Techniques	109
3.2.3	Experimental Technique.....	111
3.2.4	Variations in Methodology.....	113
3.2.5	Error Calculation.....	114
3.2.6	Data Analysis	115
3.2.7	Prediction of Extraction Isotherms.....	119
3.3	Results.....	122
3.3.1	Determination of Extraction Mechanism	122
3.3.2	Calculation of Number of Required Extraction Contacts	131
3.4	Discussion	135
3.4.1	Determination of Extracted Complexes	135
3.4.2	Extractant Aggregation.....	136
3.4.3	Extraction Isotherm and Contact Stages.....	137
3.4.4	Proposed Thorium Separations Flowsheet	138
3.5	Conclusions on the Developed Process	140
3.5.1	Future Work in this Area	141
3.6	Chapter Summary	144
4	Plutonium-Thorium Fuel Options for Irradiation in Heavy	
	Water Reactors.....	146
4.1	Introduction	146
4.1.1	The UK CANMOX Proposal	148
4.1.2	The Enhanced CANDU 6 Reactor	148
4.1.3	UK CANMOX Fuel	151
4.1.4	The UK Uranic Materials Inventory	155
4.1.5	Use of Uranic Materials in the EC6.....	156
4.1.6	Alternative EC6 Fuels.....	156
4.1.7	Fuel Material Resources.....	158
4.2	Neutronic Analysis Method.....	161
4.2.1	Neutronic Comparison Factors	163
4.2.2	Homogeneous Core Isotopic atomic Density Estimation	164

4.2.3	Neutron Interaction Data Library	165
4.2.4	One Group Reactor Theory	165
4.3	Neutronic Analysis Results.....	166
4.4	Neutronic Analysis Discussion.....	168
4.4.1	Concepts for Development.....	169
4.5	Multiplication Factor Calculation	169
4.5.1	Natural Uranium Reference Fuel.....	171
4.5.2	UK CANMOX Mimic Reference Fuel.....	172
4.5.3	Buckling Constant Method.....	174
4.5.4	Concept Fuels 17 and 19 Results.....	181
4.6	Nuclear Materials Availability For Fuel Concepts	183
4.6.1	Plutonium Inventory Utilisation.....	184
4.6.2	Uranium Inventory Utilisation	186
4.6.3	EPR Reprocessing Product Availability and Support Ratio	188
4.7	Conclusions	190
4.7.1	Recommendation	192
4.8	Future Work	193
4.8.1	Neutronic Interactions in a Heterogeneous Core	193
4.8.2	Impact of Irradiation History on Reactivity and Power	193
4.8.3	Fuel Cycle Integration.....	194
4.9	Summary and Development.....	194
5	Three-component Nuclear Fuel Simulation in the Enhanced CANDU 6 Reactor	196
5.1	Introduction	196
5.1.1	Nuclear Reactor Core Behaviour Simulation.....	197
5.1.2	The Monte Carlo Method.....	198
5.1.3	Fuel and Core Parameters Calculated	199
5.2	Methodology.....	201
5.2.1	The Serpent Neutronics Code	201
5.2.2	Geometry Simplification	202
5.2.3	Neutron Population and Iteration Number Independence.....	204

5.2.4	Fuel Concepts Analysed.....	206
5.2.5	Analysis Case Set-up.....	208
5.2.6	Void Coefficient of Reactivity.....	209
5.3	Neutronic Simulation Results	209
5.3.1	Natural Uranium Fuels	209
5.3.2	UK CANMOX Fuel	211
5.3.3	Plutonium Loading in Three-component Fuel	215
5.3.4	Fuel Concept Comparison – Use of EPR Reprocessed MOX	223
5.3.5	Effect of MDU-TPU Blending	227
5.4	Discussion and Materials Requirements	227
5.4.1	Validation against Natural Uranium CANDU Fuels.....	227
5.4.2	UK CANMOX Fuels	228
5.4.3	Three component fuels.....	229
5.5	Future Work.....	233
5.6	Conclusions and Chapter Summary.....	236
6	Comparison of Thorium Separation by Ten Solvent Extraction	
Mixtures		238
6.1	Introduction	238
6.1.1	Aqueous Phase Selection	239
6.1.2	Metals of Interest in the Aqueous Feed.....	239
6.1.3	Selection of Organic Extractants for Synergism Testing	240
6.2	Materials and Methods.....	241
6.2.1	Reagents and Stock Solutions	241
6.2.2	Experimental Technique.....	244
6.3	Results.....	245
6.3.1	Error Calculation.....	245
6.3.2	Third Phase Formation by Diocylamine.....	249
6.4	Discussion	249
6.4.1	Identification of Potential Separation Systems.....	249
6.4.2	Extraction from Hydrochloric Acid.....	257
6.4.3	Extraction from Nitric Acid.....	260
6.4.4	Extraction from Sulfuric Acid.....	262
6.4.5	Summary of Extraction Behaviours.....	265

6.4.6	Suggested Separations Systems for Further Development.....	267
6.5	Conclusions	271
6.6	Future Work	271
6.7	Chapter Summary	272
7	Overall Conclusions and Future Work	273
7.1	Motivation for Work and Aims.....	273
7.2	Thorium Purification from Monazite and Monazite Residues 275	
7.3	Three-component U-Pu-Th Fuels in the EC6 Pressurised Heavy Water Reactor	276
7.4	Recovery of Thorium and Uranium from Spent Thorium Nuclear Fuel.....	277
7.5	Monazite Requirements for UK Plutonium Irradiation and Spent Fuel Production.....	278
7.6	Future Work	279
7.7	Conclusion	279
	References	281
	APPENDIX A. Monazite Sample Electron Microscopy Studies	316
A.1	Analysis of some Monazite Samples.....	316
A.1.1	Scanning Electron Microscopy	316
A.1.2	Sample Preparation and Analytical Procedure.....	317
A.1.3	Results and Discussion.....	317
	APPENDIX B. Mathematical Derivations of Solvent Extraction	
	Equations 324	
B.1	Equilibrium Extraction Constants for Cation Exchange Liquid- Liquid Distribution.....	324
B.1.1	Basic cation exchange reaction and equilibrium extraction constant for an acidic extractant	324
B.1.2	Cation exchange reaction and equilibrium extraction constant for a dimeric acidic extractant.....	325

B.1.3	Mixed cation exchange and solvation with one dimeric extractant	325
B.1.4	Mixed cation exchange and adduct formation with two extractants	326
B.1.5	Slope Analysis to find Parameters n , q and r	326
B.2	McCabe-Thiele Extraction Isotherm	328
B.1.6	Cation Exchange with a Single Extractant	328
B.1.7	Mixed Solvation and Cation Exchange by Multiple Extractants	330
APPENDIX C. Serpent Input File for 3% plutonium in Fuel Concept 19		
	332	
C.1	Serpent Code Interpretation	332
C.2	Input File Text	333
APPENDIX D. Screening Study Distribution ratio Results Tables		336

LIST OF TABLES

Table 2.1– Average mass composition data across 9 monazite samples [142, 144, 151-161].....	37
Table 2.2 – Estimated reserves of thorium in some major source countries, in tonnes of thorium metal, and estimated thorium oxide fraction where available [34].....	39
Table 2.3 – Accompanying notes for Figure 2.19. Between each step are included notes on how to proceed to the following step.	53
Table 2.4 – Biphasic extraction equilibria of three key complexation mechanisms [76].....	57
Table 3.1 – pK_a and pK_{dimer} data for PC-88a and HDEHP [391, 392].	99
Table 3.2 – Concentration of each metal across three replicates for determination of experimental errors, determined by ICP-MS. Samples prepared by adding 0.04 ml of metal spike solution to 4.95 ml of 3 M hydrochloric acid. Also given are the calculated percentage errors in the metal distribution ratios.....	116
Table 3.3 – Integer slope of fitted lines on log-log plots of DM against pH with coefficient of determination R^2 for fitted lines.	123
Table 3.4 – Synergic factors for thorium, uranium and iron for extraction by 0.1 M PC-88a and 0.05 M HDEHP in <i>n</i> -dodecane from hydrochloric acid...	124
Table 3.5 – Integer slope of fitted lines on log-log plots of DM against [PC-88a] and [HDEHP] plotted in Figure 3.13, with coefficient of determination R^2 for fitted lines.	127
Table 3.6 – slope of fitted lines on log-log plots of DM against $[Cl^-]$ and $[SO_4^-]$, with coefficient of determination R^2 for fitted lines. Non-integer values are used where no reasonable integer slope could be fitted.....	130
Table 3.7 – Stability constants for thorium chloride, nitrate and sulfate complexes in aqueous solution [83].....	130
Table 3.8 – Thorium distribution ratio, thorium concentration in the organic phase and calculated modified logarithmic extraction constant from each	

experiment at the reference extraction conditions (3 M HCL, 0.1 M PC-88a, 0.05 M HDEHP).....	132
Table 3.9 – Inputs required for prediction of an isotherm using Equation (3.25) for thorium, uranium and iron, as used or determined in this work.	133
Table 3.10 – Number of extraction stages required for 99% uranium recovery for different extraction constants. Number of stages for an extraction constant of 2.5 included to indicate sensitivity in this region....	135
Table 3.11 – Loading capacities for each metal with 0.1 M PC-88a, 0.05 M HDEHP from 3.0 M HCl.	138
Table 4.1 – Main Geometric and operating parameters of the CANDU 6 reactor [383] and the Enhanced CANDU 6 reactor [63, 382, 437, 438, 442].	152
Table 4.2 – Geometric parameters and mass data for a CANFLEX fuel bundle. A calculated mass is given for UK CANMOX fuel, based on 2.5% dysprosium loading and 96.6% theoretical density [382, 443].....	154
Table 4.3 – Selected data on UK uranic materials inventories as of 1 April 2013 [61, 382, 445].....	156
Table 4.4 – Isotopic composition of uranium sources considered [62, 450].	159
Table 4.5 – Isotopic composition of plutonium sources considered [451, 452].	160
Table 4.6 – Details of fuel concepts considered by components of MOX and whether a thorium blanket was included. Concepts 10-18 are the three-component fuel versions of two-component fuel concepts 1-9 respectively.	162
Table 4.7 – Calculated neutron reproduction factors η and fission:capture ratios $\alpha - 1$ for a selection of fuels either previously reported in the literature or in operation. Results are also shown normalised against natural uranium for comparison with this reference fuel.	166
Table 4.8 – Calculated relative reproduction factors and fission:capture ratios for two and three-component mox concepts with 1%, 2% and 3% by	

mass plutonium loading in mox fuel elements. Normalised to natural uranium values.....	167
Table 4.9 – Mass of materials in homogeneous core.	170
Table 4.10 – Calculated initial effective multiplication factor and contributing variables for natural uranium fuel in a 37-element CANDU bundle [331]. Fast fission factor ϵ assumed to equal unity. Also shown are typical values for natural uranium-fuelled CANDU reactors [431].	172
Table 4.11 – Fuel materials requirements with proposed three-component fuels. Required masses given per reactor.year and for a fleet of units capable of irradiating the whole plutonium inventory over 30 years.....	187
Table 4.12 – Potential fuelling options for an EC6 reactor fleet based on reprocessing products from four EPR units.....	189
Table 5.1 – Burnup at which $k_{inf} = 0.986$, the average value at which natural uranium fuels are discharged from CANDU 6 reactors.....	214
Table 5.2 – Comparison of normalised power distributions in intermediate and outer rings of UK CANMOX fuel and three-component fuel concept 19.	219
Table 5.3 – Discharge burnups achievable with fuel concept 19 plutonium loadings suggested in Chapter 4.....	230
Table 5.4 – Discharge burnups achievable with fuel concept 17 plutonium loadings suggested in Chapter 4.....	233
Table 6.1 – Selected extractants examined in this thesis.....	242
Table 6.2 – Calculated percentage errors in metal separation factors.	245

LIST OF FIGURES

Figure 2.1 – Selected neutron interaction cross sections for Th-232 and -233 for a range of incident neutron energies. Data taken from ENDF/B-VII.1 library [96].	17
Figure 2.2 – Selected neutron interaction cross sections for uranium-233 for a range of incident neutron energies. Data taken from ENDF/B-VII.1 library [96].	17
Figure 2.3 – Selected neutron interaction cross sections for uranium-235 for a range of incident neutron energies. Data taken from ENDF/B-VII.1 library [96].	18
Figure 2.4 – Selected neutron interaction cross sections for uranium-238 for a range of incident neutron energies. Data taken from ENDF/B-VII.1 library [96].	18
Figure 2.5 – Selected neutron interaction cross sections for plutonium-239 for a range of incident neutron energies. Data taken from ENDF/B-VII.1 library [96].	19
Figure 2.6 – Selected neutron interaction cross sections for plutonium-240 for a range of incident neutron energies. Data taken from ENDF/B-VII.1 library [96].	19
Figure 2.7 – Selected neutron interaction cross sections for plutonium-241 for a range of incident neutron energies. Data taken from ENDF/B-VII.1 library [96].	20
Figure 2.8 – The nuclear fission chain reaction. A neutron causes fission in a fissile atom, producing two fission fragments, a number of fast neutrons and energy in the form of heat. Figure based on source [97].	21
Figure 2.9 – Elastic scattering (N,EL) and radiative capture (N,G) cross sections for hydrogen (H-1), deuterium (H-2), oxygen (O-16) and graphite (C-0) for a range of incident neutron energies. Data taken from ENDF/B-VII.1 library [96].	24
Figure 2.10 – Selected key components of a boiling water reactor [100].	26

Figure 2.11 – Key components in the nuclear containment structure for two other common plant types, the Pressurised Water Reactor (PWR, left) and the Pressurised Heavy Water Reactor (PHWR, right) [100].	26
Figure 2.12 – Selected neutron capture interactions and radioactive decay reactions for thorium-based nuclear fuels. Shown in green is the pathway from ^{232}Th to ^{233}U , with possible routes to even-numbered uranium isotopes in blue. Reactions shown are neutron capture-production (n,2n), radiative neutron capture (n, γ), and beta decay (β^-). Radiative capture cross sections are shown for 0.025 eV incident neutrons and n,2n cross sections are average values for fission spectrum neutrons, as this reaction has a threshold energy of 6-7 MeV [45].	31
Figure 2.13 – Selected neutron capture cross sections for protactinium isotopes for a range of incident neutron energies. Data taken from the ENDF/B-VII.1 library [96].	32
Figure 2.14 – Ingestion radiotoxicity of four PWR fuels against time post-irradiation. Image reproduced from data published in [116].	33
Figure 2.15 – Schematic diagram of the main elements of a molten salt reactor (MSR) system. The “Freeze Plug” is composed of a material which will melt if the reactor temperature becomes too high, allowing the fuel salt to drain into sub-critical “dump tanks” to cool and solidify [137].	35
Figure 2.16 – Monazite group mineral crystals from Landaas, Norway (left). Sand containing Monazite from Brazil (right). Scale in Centimetres.	37
Figure 2.17 – Block flow diagram overview of thorium concentrate preparation by hydrometallurgical route. Prepared based on information available in [142]	42
Figure 2.18 – Distribution ratios for tetravalent and hexavalent uranium, neptunium and plutonium as a function of nitric acid concentration with 30% TBP in odourless kerosene diluent. Image reproduced from data published in [70].	49
Figure 2.19 – Key stages of the PUREX process, represented in separatory funnels. The TBP in kerosene organic phase (yellow) is lighter than the	

nitric acid aqueous phase (blue), and sits above it when not undergoing agitation to contact the phases. FP = Fission Products; MA = Minor Actinides. See accompanying notes in Table 2.3 below	52
Figure 2.20 – Effect of TBP concentration in organic phase on thorium extraction from 5 M HNO ₃ with 8 g/l phosphate and 9.5 g/l sulphate ions. Y-axis corrected to a diluent-free basis. Image reproduced based on data published in [142].	54
Figure 2.21 – The THRUST process, used in India to recover thorium, uranium and rare earth elements from monazite [34].	62
Figure 2.22 – Example of an LWR core with three fuelling regimes, using plutonium as an example fissile driver for thorium. View onto the core is from the top-down. Typically, LWR fuel is inserted into the reactor core as fuel assemblies, each of which consists of a number of fuel rods. Assemblies are typically of the order of 10-20 cm along a side in end profile and are several metres tall, with a mass of several hundred kilograms. Rod diameters are of the order of 1 cm, being composed of stacks of fuel oxide pellets in a zirconium alloy cladding [15, 17].	78
Figure 2.23 – Diagram showing key components of CANDU nuclear reactors with PHWR notation (left). Calandria with extended fuel channel (right)....	87
Figure 3.1 – Form of the PC-88a and HDEHP dimers, where R1 represents the alkyl or alkoxide ester group.	98
Figure 3.2 – Distribution ratio for thorium as a function of pH under extraction by several concentrations of PC-88a in kerosene from sulfuric acid media. Image reproduced from data published in [255].	100
Figure 3.3 – Distribution ratio for thorium as a function of acidity and PC-88a concentration in dodecane when being extracted from hydrochloric acid (left) and mixed HCl/NaCl solutions (right). Images reproduced from data presented in [251].	100
Figure 3.4 – Distribution ratio for thorium as a function of nitric acid concentration when extracted by 0.75M PC-88a in <i>n</i> -dodecane. Image reproduced from data published in [253].	101

Figure 3.5 – Distribution ratios for thorium, uranium and cerium from acidic chloride media by 0.7 M HDEHP in xylene diluent. Image reproduced from data published in [87].....	104
Figure 3.6 – Extraction of uranium from nitric acid media as a function of acidity at constant nitrate concentration. 0.005 M PC-88a, 3 M nitrate, 25°C. Image reproduced from data published in [400].....	105
Figure 3.7 – Extraction efficiency of iron(III) from hydrochloric acid media by 30% PC-88a (aqueous:organic ratio 2, 25°C, contact time 15 mins. Image reproduced from data published in [406].	105
Figure 3.8 – Extraction of iron(III) by four concentrations of HDEHP from hydrochloric acid media. [HDEHP] levels are 0.05 M, 0.1 M, 0.2 M and 0.4 M, bottom to top (30°C, one hour contact time). Image reproduced from data published in [403].	106
Figure 3.9 – The experimental variables studied in this associated with each phase.....	107
Figure 3.10 – Diagram of main functional components of a mass spectrometry system with inductively coupled plasma ion source and quadrupole mass analyser.	110
Figure 3.11 – Example of a McCabe-Thiele isotherm as applied to solvent extraction.....	120
Figure 3.12 – Th, U and Fe distribution ratios as a function of pH, fitted with lines of integer slope (left). Metal extraction fraction as a function of acidity for thorium, uranium and iron (right). Extraction performed from HCl of various concentrations with 5 min contact time at room temperature with 100 ppm each metal. Extractant concentrations were 0.1 M PC-88a and 0.05 M HDEHP.	125
Figure 3.13 – Distribution ratio of Th, U and Fe as a function of variable extractant concentration. Top: Variable [PC-88a] with [HDEHP] = 0.05 M. Bottom: Variable [HDEHP] with [PC-88a] = 0.1 M. Extraction performed from 3.0 M HCl with 5 min contact time at room temperature with 100 ppm each metal.....	126

Figure 3.14 – Job's Plot showing distribution ratios of four metals as a function of the HDEHP fraction in the extractant mixture. Extraction performed from 3.0 M HCl with 5 min contact time at room temperature with 100 ppm each metal, using 0.15 M total extractant concentration. Lines only intended as a guide to the eye.....127

Figure 3.15 – Distribution ratio for Th, U and Fe as a function of added chloride (left) or sulfate (right) in the aqueous phase. Extraction performed from 3.0 M HCl with 5 min contact time at room temperature with 100 ppm each metal, using 0.1 M PC-88a and 0.05 M HDEHP in n-dodecane as extractants. Note that axis labels are in the left-most column/bottom row of the table.....129

Figure 3.16 – Distribution ratio for thorium as a function of total extractant concentration, with PC-88a:HDEHP ratio 2. Extraction performed from 3.0 M HCl with 5 min contact time at room temperature with 100 ppm thorium.133

Figure 3.17 – Predicted McCabe-Thiele extraction isotherm, for extraction of thorium from hydrochloric acid ($[H^+]_{eq} = 1.5 \text{ M}$) using 0.1 M PC-88a and 0.05 M HDEHP in n-dodecane.....134

Figure 3.18 – Uranium extraction isotherm with lines of varying slope through origin, representing possible operating lines for sensitivity analysis.134

Figure 3.19 – Suggested process flowsheet for separation of thorium, uranium and iron from saline hydrochloric acid media. HCl concentrations are marked as 3+x and 3-x M. The difference in concentration should be set such that the acidity in the extraction section is 3 M.....139

Figure 4.1 – CANDU reactor Fuel channel cutaway diagram. Fuel bundle outer diameter is approximately 10 cm. The bundle shown is the new CANFLEX design.....149

Figure 4.2 – CANDU 6 calandria with pressure tubes installed. Scale of core may be inferred from workers visible standing at the base of the calandria vessel on the left and on top of the vessel on the right [439]......149

Figure 4.3 – Full CANDU core diagram, showing calandria vessel, three fuel channels and coolant feeders, and end shielding assemblies. Inset: Close-up

of fuel bundles within fuel channel, with pressure and calandria tubes and annulus gas space. Core diameter OF EC6 reactor is 7.6 metres. Core control devices omitted for clarity [440]. 150

Figure 4.4 – Left: Photograph of 43 fuel element CANFLEX fuel bundle. Right: Diagram showing CANFLEX fuel elements in pressure tube (red) with annulus gas space (green) contained within calandria tube (orange). 153

Figure 4.5 – Evaluated values of neutronic factors as affected by dysprosium burnable absorber loading in UK CANMOX fuel. Fast fission factor and leakage factors were very close to unity for all Dy loading fractions, and so are not shown. 173

Figure 4.6 – Cylindrical core shape labelled with geometric annotations as used in buckling constant derivation..... 177

Figure 4.7 – Ratio of materials buckling constant to geometric buckling constant in UK CANMOX fuel as a function of burnable absorber loading.. 179

Figure 4.8 – Evaluated values of neutronic factors affected by plutonium loading in proposed fuel concept 19. Variability between concept 19 and concept 17 is minimal. Fast fission factor, thermal utilisation factor and leakage factors were all close to unity..... 181

Figure 4.9 – Variation in ratio of materials buckling constant to geometric buckling constant as a function of average plutonium loading in outer and intermediate fuel elements..... 182

Figure 5.1 – Fuel channel geometry used in computational experiments. Core is considered to be an infinite lattice of infinitely long fuel channels, containing equivalent fuel throughout. For scale, calandria tube outer diameter is 66 mm. 205

Figure 5.2 – Effect of neutron population size (left) and number of cycles (right) on effective multiplication factor and calculation running time. 206

Figure 5.3 – Evolution of infinite multiplication factor k_{inf} and conversion ratio C with natural uranium oxide fuel in the Enhanced CANDU 6 reactor. 210

Figure 5.4 – Evolution of normalised power profile in natural uranium fuel in 37-element bundle elements (top) and CANFLEX bundle elements (bottom) with burnup. Values averaged over all elements in each ring, normalised relative to average power of a bundle in the core.....212

Figure 5.5 – Effect of reduced coolant density on k_{inf} for natural uranium fuel in the CANFLEX fuel bundle.213

Figure 5.6 – Isotopic density of selected U and Pu isotopes in fuel bundle as a function of burnup for natural uranium fuel in the CANFLEX bundle.213

Figure 5.7 – Evolution of k_{inf} with burnup for UK CANMOX fuels with different dysprosium fractions. Also shown is the conversion ratio, which was found to be almost identical for all dysprosium fractions.214

Figure 5.8 – Power profiles across the UK CANMOX fuel elements at 0%Dy (top), 2.5%Dy (middle) and 10%Dy (bottom). Power density set to 25.8 kW/kgHM.....216

Figure 5.9 – Evolution of plutonium isotopic vector, consumption of ^{235}U , and depletion of key dysprosium isotopes in UK CANMOX bundle with 2.5% dysprosium loading. Left: Outer and intermediate rings with MOX. Right: Inner ring and centre elements with dysprosium and depleted uranium. .217

Figure 5.10 – Normalised change in k_{inf} at 1 MWd/kgHM UK CANMOX fuel with 2.5% Dy as a function of fuel burnup for several coolant densities.....217

Figure 5.11 – Evolution of k_{inf} (top) and C (bottom) with burnup for fuel concept 19 with different average plutonium fractions in the MOX seed region. Marked on graphs are the assumed multiplication factor and calculated conversion ratio at discharge.220

Figure 5.12 – Power profiles across the bundle in fuel concept 19. Plutonium fractions in the MOX driver are 1% (top), 3% (middle) and 6% (bottom).221

Figure 5.13 – Isotope mass variation with burnup in fuel concept 19 with average Pu fraction of 3%. Intermediate ring with 4.29% initial plutonium loading (left) and outer ring with 2.14% initial plutonium loading (right).222

Figure 5.14 – Evolution of selected isotope masses in fuel concept 19 with 3% initial plutonium loading. Total across intermediate and outer rings with U-Pu MOX (left), and inner ring and centre pin with ThO_2 (right).222

Figure 5.15 – Effect of void fraction on k_{inf} for fuel concept 19 with 3% average plutonium loading at 1 MWd/kg, presented as change in k_{inf} from unvoided condition.....	223
Figure 5.16 – Evolution of k_{inf} and C with burnup in two three-component fuel concepts 17 (reprocessed EPR MOX) and 19 (inventory MOX) with two plutonium loading fractions.....	225
Figure 5.17 – power profiles across the bundle in fuel concept 17 with 3% average plutonium loading.....	226
Figure 5.18 – Evolution of selected isotope masses in fuel concept 17 with 3% initial plutonium loading. Total across intermediate and outer rings with U-Pu MOX (left), and inner ring and centre pin with ThO ₂ (right).....	226
Figure 5.19 – Reduction in k_{inf} with fuel burnup for fuel concept 21 with 3% plutonium loading with 3 levels of MDU blending fraction (left). Variation in burnup at which $k_{inf} = 0.986$ (right).....	227
Figure 5.20 – Evolution of selected isotope masses in fuel concept 17 with 1.4% initial plutonium loading. Total across intermediate and outer rings with U-Pu MOX (left), and inner ring and centre pin with ThO ₂ (right).....	232
Figure 5.21 – Suggested simulation geometry for initial studies into the effect of control rods in PHWR cores [483].....	234
Figure 6.1 – Chemical structures of organic extractants used in the study.	243
Figure 6.2 – Logarithmic Distribution ratios with 0.5 M hydrochloric acid (top) and 3.0 M hydrochloric acid (bottom) as the aqueous phase. Results for 5 ml acid with 100 ppm each metal against 5 ml of 0.1 M PC-88a and 0.05 M other extractant in <i>n</i> -dodecane, with 5 min contact time at room temperature.....	246
Figure 6.3 – Logarithmic Distribution ratios with 0.5 M Nitric acid (top) and 3.0 M Nitric acid (bottom) as the aqueous phase. Results for 5 ml acid with 100 ppm each metal against 5 ml of 0.1 M PC-88a and 0.05 M other extractant in <i>n</i> -dodecane, with 5 min contact time at room temperature..	247
Figure 6.4 – Logarithmic Distribution ratios with 0.5 M Sulfuric acid (top) and 3.0 M Sulfuric acid (bottom) as the aqueous phase. Results for 5 ml acid	

with 100 ppm each metal against 5 ml of 0.1 M PC-88a and 0.05 M other extractant in *n*-dodecane, with 5 min contact time at room temperature. .248

Figure 6.5 – Logarithmic distribution ratio for thorium (line) and Logarithmic separation factors for co-contaminants against thorium (bars) with 0.5 M Hydrochloric acid (top) or 3.0 M hydrochloric acid (bottom) as the aqueous phase. Results for 5 ml acid with 100 ppm each metal against 5 ml of 0.1 M PC-88a and 0.05 M other extractant in *n*-dodecane, with 5 min contact time at room temperature.....251

Figure 6.6 – Logarithmic distribution ratio for thorium (line) and Logarithmic separation factors for co-contaminants against thorium (bars) with 0.5 M nitric acid (top) or 3.0 M nitric acid (bottom) as the aqueous phase. Results for 5 ml acid with 100 ppm each metal against 5 ml of 0.1 M PC-88a and 0.05 M other extractant in *n*-dodecane, with 5 min contact time at room temperature.252

Figure 6.7 – Logarithmic distribution ratio for thorium (line) and Logarithmic separation factors for co-contaminants against thorium (bars) with 0.5 M sulfuric acid (top) or 3.0 M sulfuric acid (bottom) as the aqueous phase. Results for 5 ml acid with 100 ppm each metal against 5 ml of 0.1 M PC-88a and 0.05 M other extractant in *n*-dodecane, with 5 min contact time at room temperature.253

Figure 6.8 – Logarithmic distribution ratio for uranium (line) and Logarithmic separation factors for co-contaminants against uranium (bars) with 0.5 M hydrochloric acid (top) or 3.0 M hydrochloric acid (bottom) as the aqueous phase. Results for 5 ml acid with 100 ppm each metal against 5 ml of 0.1 M PC-88a and 0.05 M other extractant in *n*-dodecane, with 5 min contact time at room temperature.....254

Figure 6.9 – Logarithmic distribution ratio for uranium (line) and Logarithmic separation factors for co-contaminants against uranium (bars) with 0.5 M nitric acid (top) or 3.0 M nitric acid (bottom) as the aqueous phase. Results for 5 ml acid with 100 ppm each metal against 5 ml of 0.1 M PC-88a and 0.05 M other extractant in *n*-dodecane, with 5 min contact time at room temperature.255

Figure 6.10 – Logarithmic distribution ratio for uranium (line) and Logarithmic separation factors for co-contaminants against uranium (bars) with 0.5 M sulfuric acid (top) or 3.0 M sulfuric acid (bottom) as the aqueous phase. Results for 5 ml acid with 100 ppm each metal against 5 ml of 0.1 M PC-88a and 0.05 M other extractant in <i>n</i> -dodecane, with 5 min contact time at room temperature.....	256
Figure 6.11 – Interpolation of distribution ratios for thorium and uranium extracted from sulfuric acid at acidities 0.5 M and 3.0 M by a mixture of 0.1 M PC-88a and 0.05 M HDEHP in <i>n</i> -dodecane.	269
Figure A.1 – Secondary Electron (left) and Backscatter Electron (right) Images of Norwegian bulk monazite, taken at 90x magnification (top) and 350x magnification (bottom).....	318
Figure A.2 – EDS spectrum for Position A in bulk monazite sample. Phase suggested to be thorite, huttonite, or uranothorite (Th,U)SiO ₄	318
Figure A.3 – EDS spectrum for Position B in bulk monazite sample. Phase suggested to be allanite (Ce,Ca,Y,La) ₂ (Al,Fe ³⁺) ₃ (SiO ₄) ₃ (OH), or similar.	319
Figure A.4 – EDS spectrum for Position C in bulk monazite sample. Phase suggested to be microcline or other potassium feldspar KAlSi ₃ O ₈	319
Figure A.5 – EDS spectrum for Position D in bulk monazite sample. Phase suggested to be monazite (Ce,La,Ca,Th)PO ₄	320
Figure A.6 – EDS spectrum for Position E in bulk monazite sample. Phase suggested to be xenotime YPO ₄	320
Figure A.7 – Secondary Electron Image of Brazilian monazite sand sample, taken at 100x magnification.....	321
Figure A.8 – EDS spectrum for Position A in monazite sand sample . Phase suggested to be xenotime YPO ₄	322
Figure A.9 – EDS spectrum for Position A in monazite sand sampleFigure A.7. Phase suggested to be thorite, huttonite, or uranothorite (Th,U)SiO ₄ .	322
Figure A.10 – EDS spectrum for Position A in monazite sand sample. Phase suggested to be monazite (Ce,La,Ca,Th)PO ₄	323

LIST OF NOMENCLATURE

As they are only mentioned very briefly, the list of abbreviations here does not include most solvent extraction materials listed in Chapter 2. Definitions are given within the text.

ABBREVIATION	FULL TERM
AAS	Atomic Absorption Spectroscopy
ABWR	Advanced Boiling Water Reactor
ACR-700	Advanced CANDU 700
ADS	Accelerator Driven System
AECL	Atomic Energy of Canada Ltd.
AGR	Advanced Gas-cooled Reactor
Aliquat-336	Tricaprylmethylammonium chloride
AMEX	Amine Extraction process
AP1000	Advanced Passive 1000 (reactor)
BMIM	1-butyl-3-methylimidazolium (chloride)
BOL	Beginning of Life
BWR	Boiling Water Reactor
CANDU	Canadian Deuterium Uranium (reactor)
CANMOX	A proposal to irradiate UK plutonium in EC6 reactors
CCS	Carbon Capture and Sequestration
CGN	China General Nuclear Power Corporation
CMPO	Carbamoyl methyl phosphine oxide
Cyphos 101	Trihexyl(tetradecyl)phosphonium chloride
DECC	UK Department of Energy & Climate Change
DEHPA	See "HDEHP"
DU	Depleted uranium
DUPIC	Direct Use of Used PWR fuel in CANDU
EC6	Enhanced CANDU 6 (reactor)
EDS	Energy Dispersive X-ray Spectroscopy
ENDF	Evaluated Nuclear Data File
EOL	End of Life
EPR	European Pressurised Reactor –or– Evolutionary Power Reactor. Now known officially as simply EPR.
EXAFS	X-ray Absorption Fine Structure Spectroscopy
eV	Electron volt, a unit of energy equal to 1.6×10^{-19} joules
FP	Fission Products
FTIR	Fourier Transform Infrared spectroscopy

GE	General Electric
HDEHP	Di(2-ethylhexyl) phosphoric acid
HEHEHP	See "PC-88a"
HPR1000	Name of reactor type formally designated "Hualong One"
HTR	High Temperature Reactor
IAEA	International Atomic Energy Agency
IBOS	Inner blanket, outer seed
ICP	Inductively Coupled Plasma spectroscopy
ICP-MS	Inductively Coupled Plasma Mass Spectroscopy
ICP-OES	Inductively Coupled Plasma Optical Emission Spectroscopy
IOBMS	Inner and outer blanket, middle seed
ISOB	Inner seed, outer blanket
JEFF	Joint Evaluated Fission and Fusion File
JENDL	Japanese Evaluated Nuclear Data Library
kgHM	Kilograms of heavy metal
LEU	Low enriched uranium (< 5% ²³⁵ U)
LFTR	Liquid fluoride thorium reactor
LWR	Light water reactor
MA	Minor actinides (actinides in spent nuclear fuel besides those which make up the main fuel component, i.e. U, Pu, Th).
MAGNOX	Magnesium non-oxidising, the designation of a magnesium-aluminium alloy used as a fuel cladding material in the UK's first generation of nuclear power plants, which were also known as MAGNOX reactors or MAGNOX plants.
MDU	MAGNOX Depleted Uranium
MFR	Moderator to Fuel Ratio
MOX	Mixed Oxide (fuel)
MSR	Molten Salt Reactor
NatU	Natural uranium
NDA	Nuclear Decommissioning Authority
NMR	Nuclear Magnetic Resonance spectroscopy
NNL	National Nuclear Laboratory
NUE	Natural uranium equivalent
PC-88a	Di-(2-ethylhexyl) xxviihosphonic acid mono 2-ethylhexyl ester
PHWR	Pressurised Heavy Water Reactor
PLEx	Plant Lifetime Extension

PLS	Pregnant Liquor Solution
PRISM	Power Reactor Innovative Safe Module
PUREX	Plutonium Uranium Redox Extraction
PWR	Pressurised Water Reactor
QUADRISO	Quadruple isotropic fuel
RepU	Reprocessed uranium
ROX	Rock-like Oxide fuel
RTIL	Room Temperature Ionic Liquid
SBU	Seed-blanket unit fuel
SEM	Scanning Electron Microscopy
SLM	Supported Liquid Membrane
SMR	Small Modular Reactor
SSET	Self-sufficient Equilibrium Thorium fuel cycle
TBP	Tributyl phosphate
tHM	Tonnes of heavy metal
THOREX	Thorium Extraction process
ThORP	Thermal Oxide Reprocessing Plant
THPO	Trihexyl phosphine oxide
TOA	Trioctylamine
TOPO	Trioctylphosphine oxide
TPU	ThORP Product Uranium
TRISO	Triple isotropic fuel
UK	United Kingdom
UK CANMOX	See "CANMOX"
USA	United States of America

MATHEMATICAL TERM	DESCRIPTION
[]	Concentration of material named in square brackets
$\overline{\text{overbar}}$	Species in the organic phase in solvent extraction
A	Atomic mass number
B	Materials buckling constant
B_g	Geometric buckling constant
B_U	Fuel discharge burnup (MWd/tHM)
c	Charge on metal ion
C_f	Reactor design capacity factor
C_r	Conversion ratio
CVR	Coolant Void Reactivity
D	Diffusion constant
D_M	Distribution ratio of element M

f	Thermal utilisation factor
F	Annual fuel requirement (tHM)
i	Index representing fuel isotope
j	Total number of fuel isotopes
\mathbf{J}	Neutron density vector, or neutron current
K_{dimer}	Dimerisation constant
k_{eff}	Effective multiplicity factor
K_{ex}	Equilibrium extraction constant
K'_{ex}	Modified equilibrium extraction constant
k_{inf}	Infinite multiplicity factor
l	Neutron leakage rate
L	Thermal neutron diffusion length in the moderator
L_R	Thermal neutron diffusion length in the reactor
L_S	Neutron slowing down length in the moderator
m	A perturbation in reactor conditions
$[M_0]$	Total concentration of element M in system
MR	Moderating ratio
n	Number of protons exchanged in metal complexation
N	Isotopic atomic density
p	Resonance escape probability
P_{FNL}	Fast neutron non-leakage probability
P_{th}	Reactor thermal power (MW)
P_{TNL}	Thermal neutron non-leakage probability
Q	The result of a quotient operation (in error analysis)
R^2	Coefficient of determination
S	Total extractant concentration in system
s	Thermal neutron production rate
$t_{0.5}$	Isotope half-life
V	Volume
x	Equilibrium concentration in the aqueous phase
X_F	Fraction of ^{235}U in the uranium feed
X_P	Fraction of ^{235}U in the enriched product
X_T	Fraction of ^{235}U in the depleted tails
y	Equilibrium concentration in the organic phase
α^{-1}	Fission:capture ratio
$\alpha_{M,Th}$	Separation factor of element M against thorium
ε	Fast fission factor
η	Neutron reproduction factor

$\bar{\mu}$	Average cosine of neutron scattering angle
ν	Average number of neutrons released per fission
ξ	Logarithmic energy decrement/neutron lethargy gain
ρ	Enrichment feed-to-product mass ratio
σ_a	Microscopic neutron absorption cross section
σ_c	Microscopic radiative neutron capture cross section
σ_f	Microscopic neutron-induced fission cross section
σ_s	Microscopic elastic neutron scattering cross section
σ_t	Microscopic total neutron interaction cross section
Σ_i	Macroscopic neutron cross section, where $i = c, f, s$ etc.
ϕ	Neutron flux
ψ_M	Synergic factor of element M
ω	Reactor coefficient of reactivity

1 INTRODUCTION

This academic thesis presents work carried out into the preparation of nuclear-grade thorium for nuclear fuel production, specifically the use of HDEHP as a synergist for PC-88a for the separation of thorium from uranium and iron in nuclear fuel preparation. In addition, a novel use of thorium in heavy water-moderated nuclear power reactors is presented for plutonium irradiation, using fertile thorium oxide driven by a fissile mixture of reprocessed uranium and plutonium. A study is also reported into the separation of Th, U, Zr and Fe in thorium spent fuel, comparing ten potential synergists for PC-88a from three mineral acids as the aqueous phase.

1.1 AIMS

This work described in this thesis covers three principal aims:

- 1) Determine the extracted complexes and number of contact stages required to extract 99% of the dissolved thorium within an acidic monazite leachate using mixtures of PC-88a and HDEHP.
- 2) Determine the evolution of k_{inf} with burnup for mixed U-Pu-Th oxide nuclear fuels as an alternative to the proposed UK CANMOX fuel of U-Pu MOX with dysprosium absorber in the Enhanced CANDU 6 reactor. Also to determine the isotopic composition of the fuel actinides upon discharge from the core and the effect of coolant voiding on reactivity with this fuel.
- 3) Identify potential synergists for PC-88a for the separation of uranium, thorium, zirconium and iron for spent thorium nuclear fuel reprocessing by determining the distribution ratios and separation factors against thorium and uranium for these metals.

1.2 THE STRUCTURE OF THIS THESIS

This thesis is presented in seven chapters.

In this first chapter, a general introduction is given, presenting a justification for thorium-based nuclear energy and introducing the areas for potential improvement in the thorium nuclear fuel cycle which are herein addressed.

In Chapter 2 is presented relevant background theory required for a fuller understanding of the literature review and the novel work reported. A review of the state-of-the-art in the areas of work is also presented.

Scientific literature relevant to the aims given above is considered, and gaps are identified for further study, leading to the aims of the thesis above.

In Chapter 3, a liquid-liquid distribution system using PC-88a and HDEHP for the separation of thorium, uranium and iron is developed in detail for thorium minerals processing, with the extracted complexes identified and the number of contact stages for 99% thorium extraction determined.

In Chapter 4, an application for thorium is investigated as a component of pressurised heavy water reactor fuel. The neutronic feasibility of the fuel is assessed in a homogeneous, infinite reactor core at the beginning of its life.

In Chapter 5, a computational simulation is presented to validate and develop the work presented in Chapter 4, extending the homogeneous core to an infinite two-dimensional lattice of fuel channels and including burnup behaviour, isotopic composition evolution and coolant void reactivity.

In Chapter 6, a screening study is presented into ten potential liquid-liquid distribution extractants in combination with PC-88a and three minerals acids as aqueous media in order to separate uranium, thorium, iron and zirconium in spent thorium nuclear fuel.

Finally, Chapter 7 concludes the thesis and reviews and summarises the work carried out and the suggested next steps for further development.

1.3 GLOBAL CONTEXT – THE NEED FOR NUCLEAR ENERGY

Predictions of increasing world population and economic growth are a warning signal for increased global energy consumption, particularly in the rapidly developing nations of India and China [1, 2]. Secure and independent access to energy and supplies of other natural resources is becoming increasingly important globally [3-7].

Energy supplies in the modern world have to meet several criteria to be effective and acceptable. Energy systems must offer reliable supply, be environmentally sustainable, be acceptable to the public and policy makers, and be within the scope of appropriate legal and regulatory frameworks. Systems should also offer independence from outside influences, for example impacts from primary fuel price rises or supply shortages, or attack by hostile actors. The system must also be economically competitive [8, 9].

Today the world is shifting towards a very different mixture of electrical supply technologies than has been used historically, with fossil fuelled power plants being increasingly pushed aside in favour of low carbon technologies as a response to global climate change, as evidenced most recently by the Paris Agreement [10, 11]. In the UK, for example, it is anticipated that within 15 years all coal-fired power stations will be closed, with a transition to low carbon nuclear and renewable energy sources [12].

If globally increasing energy demand is to be met in a way that respects the requirements outlined above, nuclear power must form a part of the global energy mix [8, 13]. Nuclear power is the only reliable, technologically mature and low carbon energy source which is neither dependant on external factors beyond human control such as the weather, nor extremely limited by geographical requirements such as the need for fast flowing water supplies. Nuclear power is predicted to become an increasingly important for all world-regions, over a range of timescales depending on the region in question [14].

1.4 THE MODERN NUCLEAR POWER INDUSTRY

In order to discuss nuclear reactor technology in this thesis, it is necessary to begin with a general overview of nuclear power reactors and their operating principles. This topic is discussed at length in the scientific and popular science literature, and the reader may consult numerous sources for further information [15-20]. A summary overview of the relevant topics required for an understanding of this thesis is given in Section 2.1.

Of the various reactor types in the world, the most common is the Light Water Reactor (LWR), accounting for 85% of operating reactors in 2014 [21], which combines the Pressurised Water Reactor (PWR) and Boiling Water Reactor (BWR) categories. The other common type is the Pressurised Heavy Water Reactor (PHWR), making up 11% of operating reactors.

Following the Fukushima Daiichi nuclear accident in 2011 public confidence in nuclear power was severely reduced across the world, causing a number of countries to re-evaluate their own nuclear programmes [22]. However, many other countries are now planning an expansion or renewal of their nuclear power programmes [23]. A recent indicator of returning public confidence was the November 2016 referendum in Switzerland regarding early closure of nuclear plants. The early closure proposal was rejected and plants will continue to operate to their planned end of life (EOL) dates [24].

1.4.1 URANIUM-BASED NUCLEAR FUEL – SUPPLY AND DEMAND

Approximately 95% of operable civil power reactors are fuelled with mined “primary” uranium, and the remainder are fuelled from “secondary” uranium resources, principally reclaimed or repurposed materials from existing inventories and/or weapons programmes, or reprocessed materials from uranium-fuelled reactors [25]. Plutonium separated from used nuclear fuel is often mixed with recycled uranium or depleted uranium tails from enrichment processing in these secondary uranium fuelled reactors [26].

Primary uranium resources are assured for the next 20 years, even under high demand scenarios driven by aggressive expansion of nuclear power [25]. Given that the planned operating lifetimes of modern plants is 40-60 years, and that now it is common to carry out Plant Lifetime Extension (PLEx) operations on existing stations [27], it may be difficult to supply sufficient fuel for plants built today in the latter part of their lives based on current uranium estimates.

1.4.2 REDUCING FUEL RESOURCE UTILISATION

In the current generation of LWRs and PHWRs, improvements in uranium resource utilisation have been limited by three main factors. The first is that the conversion ratio (the fraction of the fuel fissioned which was produced within the reactor through neutron capture on fertile materials) has not been considered as an important design criterion, and is of the order of 0.5-0.6 for LWRs and 0.8 for PHWRs [15, 20].

The second reason is that the production of enriched uranium oxide UO_2 reactor fuel requires a very large amount of mined uranium per fuel element in the core. Approximately 8-9 t of natural uranium are required per tonne of 4.5% enriched uranium product in a modern LWR [15], and 100-1000 times this mass of uranium ore may need to be extracted to produce this [28].

Thirdly, when the fuel is removed from the reactor, a significant quantity of the fissile material remains as unburnt plutonium and uranium-235, of the order of 2% total, and this is rarely recovered and reused. Only France and Japan regularly reprocesses waste and reuse the products as fuel [29]. The fraction of spent fuel not reprocessed and reused is difficult to estimate, but reuse may reduce uranium requirements by approximately 25-30% [30].

Taken together these factors indicate that LWRs, which represent 82% of the world's reactors, use barely 1% of the uranium that is mined to supply them.

1.4.3 OPTIONS FOR SUSTAINABLE NUCLEAR FUEL MANAGEMENT

There is significant room for improvement in many areas of nuclear energy systems for fuel resource utilisation, and these options and possibilities will need to be exploited as the price of uranium increases over the coming decades.

In the short term, possible areas for improvement include reducing the depleted uranium tails assay in fuel enrichment from the current typical value of 0.25% [30]. Additionally, increasing spent fuel reprocessing and reuse of the separated fissile products in Mixed Oxide (MOX) fuels will give reductions in natural uranium requirements. In the coming decades, increased conversion ratios in reduced moderation reactors and fast breeder reactors could further improve this [31-33].

1.5 THORIUM AS AN ALTERNATIVE FUEL TO URANIUM

In addition to uranium there also exists thorium, another naturally occurring potential fuel. Full details of the thorium fuel cycle, its opportunities and challenges are presented in [34]. A physics-based comparison of uranium and thorium fuels is presented in Section 2.2. However, a qualitative description of the key differences is presented here.

The comparison of uranium and thorium fuel cycles in order to determine whether adoption of thorium is advantageous is partly subjective from the viewpoint of the fuel cycle operator or country. Countries which have access to plentiful thorium resources, limited uranium resources, and the need to develop a largely indigenous fuel cycle, such as India, are very much motivated to adopt thorium fuel cycles [35].

Developed countries with established nuclear fuel cycles are much more reserved when considering thorium fuel cycles. For the USA and UK, thorium fuel cycles are not currently seen as sufficiently attractive to displace U-Pu fuels [36-38]. Of course, this assessment may change depending on the development of the thorium fuel cycle globally.

1.5.1 THE LIMITATIONS OF THORIUM

Thorium nuclear energy makes regular appearances in popular science reporting [39, 40]. Thorium provides a complementary material to supplement uranium resources, particularly with the decline in limited secondary uranium resources [41]. However, thorium is often presented by a sector of the scientific and technical community as a “silver bullet” – a wonder fuel which can save the planet from climate change and energy shortages in general, and the problems of uranium-fuelled nuclear energy in particular. However, any nuclear fuel must be evaluated within the context of a whole nuclear energy system in order to evaluate its potential benefits.

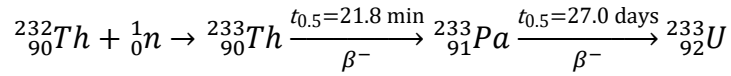
1.5.2 THE USE OF THORIUM AS A NUCLEAR FUEL

1.5.2.1 RESOURCE AVAILABILITY

Thorium is approximately four times more abundant than uranium in the environment, and much of it is in the readily accessible ore monazite, which concentrates as a sand in river beds and beaches, and in the ore bastnasite, which is heavily mined for rare earths and iron in China [42]. A detailed discussion of monazite resources is presented in Section 2.3 of this thesis.

1.5.2.2 THERMAL BREEDING WITH THE THORIUM-²³³U FUEL CYCLE

Unlike uranium, thorium is naturally monoisotopic in the environment, found only as ²³²Th. This isotope is fertile, and can be converted to the fissile ²³³U by capturing a neutron and undergoing two β^- decays, as shown in the reaction below, where $t_{0.5}$ is the radioactive decay half-life [43]



Where $t_{0.5}$ is the half-life of the parent isotope, and β^- indicates beta decay (electron emission).

Nuclear reactors require an amount of fissile material in the core in order to be operable, the fission of which is driven by neutrons. The nuclear fission process releases additional neutrons, which go on to cause further fissions, sustaining a critical nuclear chain reaction [17]. Criticality may be expressed through the neutron multiplication factor k_{inf} , the ratio of neutron population in a generation to that of the previous generation. As thorium is not fissile, a reactor cannot be fuelled with thorium alone, and requires a source of neutrons, at least until the fraction of ${}^{233}\text{U}$ reaches a level which is sufficient to sustain a chain reaction without additional neutron sources. The neutron producing fissile driver can be another fissile isotope, for example ${}^{239}\text{Pu}$, or an external neutron source, as is used in an Accelerator Driven System [44].

For a wide range of incident thermal neutron energies, the fission of ${}^{233}\text{U}$ releases more than two neutrons per neutron absorbed, with enough margin to allow for two neutrons to remain after accounting for parasitic neutron absorption or leakage in many cases. Thus, fuel breeding is possible in thorium fuelled reactors with a thermal neutron spectrum [34, 45]. For a breeding core, once the amount of ${}^{233}\text{U}$ in a suitable geometry reaches equilibrium no further fissile driver is required, and only additional thorium needs to be introduced.

As 100% of primary thorium may be irradiated in a nuclear reactor, with no enrichment losses and the possibility of complete thorium fissile conversion in a thermal neutron spectrum, the resource utilisation of thorium compares favourably to uranium, giving much reduced requirements for mining [46].

1.6 NUCLEAR POWER IN THE UNITED KINGDOM

1.6.1 HISTORICAL AND CURRENT NUCLEAR OPERATIONS

The United Kingdom was one of the first countries to use nuclear power, operating the Windscale Piles at low burnups for weapons-grade plutonium production from 1950 to 1957. Since then, a generation of 26 MAGNOX-type reactors have operated from 1956 to 2015 [47]. These were followed by seven Advanced Gas-cooled Reactor (AGR) stations, which were connected to the grid between 1976 and 1988 [48, 49]. These plants continue to operate today and are scheduled to close between 2024 and 2030. In 1995 a single PWR was built at Sizewell [50]. Sizewell B is currently planned to operate until 2035. Fuller histories of the UK nuclear programme are available in the literature [51, 52].

The UK is now at the beginning of a so-called nuclear renaissance, and aims to allow the construction of approximately 16-18 GWe of new nuclear generating capacity over the coming twenty years [53]. Eight sites have been designated as potential sites for new nuclear stations, and it is currently suggested that at least six of these will be used for new reactors. These reactors will be built, owned and operated by private bodies, with financial guarantees from the UK government on energy prices and loan underwriting [54-60].

1.6.2 THE UK PLUTONIUM INVENTORY

Since reactor operations began in the UK, plutonium and uranium have been separated from MAGNOX and AGR spent fuel and held in national inventories [61]. MAGNOX reactors have a low burnup compared to modern reactors, with the earliest reactors purposefully operating for highly fissile plutonium production. AGR burnups were higher, but still relatively low compared to modern LWRs [62].

The resulting plutonium inventory is divided into “lots”, each of which has a variable isotopic composition, due to the material having been produced from a number of reactor types with different power and burnup histories, and then aged in storage for up to 60 years, during which time decay products have built up, notably the neutron absorber americium-241 [63].

The inventory is expected to reach 140 tHM when current reprocessing contracts end in 2018, including ~25 tHM of foreign-owned plutonium [64]. It has been suggested that the annual cost of safely storing and safeguarding this material may be approximately £80 million [65]. The Government views this material as a “zero value asset”, rather than a waste, and is seeking options through which the overall risk of the material may be reduced or eliminated. The current preferred option is reuse of the plutonium in a fuel form, as opposed to direct disposal as a waste [64]. The plutonium management decision in government is owned by the Nuclear Decommissioning Authority (NDA).

The UK National Nuclear Laboratory (NNL) has the task of assessing options for plutonium disposition. They are considering four main options [64]:

1. Immobilisation and disposal in a suitable engineered waste form.
2. Production of MOX fuel for use in a suitable LWR. Previous efforts to operate a MOX plant in the UK have been unsuccessful [66].
3. Production of a MOX fuel suitable for use in the SNC-Lavalin Enhanced CANDU 6 (EC6), a PHWR.
4. Production of a metallic alloy fuel of plutonium, zirconium and uranium suitable for use in the GE-Hitachi Nuclear Energy PRISM reactor, a liquid sodium-cooled fast reactor.

The criteria used by NDA in selecting plutonium management options have not been published. However, from the details of the various proposals put forward to the NDA it would appear that the UK wishes to reduce the risks of its separated plutonium inventory over a relatively short period of time,

and that it is desirable for the final product of the dispositioning process to be beyond use as a weapons material. In the case of reuse proposals, this would mean that the plutonium would need to undergo significant irradiation in a reactor in order to reduce the proportion of fissile isotopes and to provide a degree of radiogenic self-protection from fission products and minor actinides, followed by immobilisation in a final spent fuel form. Furthermore it is assumed that the NDA would wish to maximise the electrical energy value that may be recovered from the plutonium, and to minimise the waste volumes arising from these activities.

The AREVA and GE-Hitachi proposals have a number of merits, but these proposals will not be discussed further in this thesis. Instead this work will focus on the proposal from SNC-Lavalin, called UK CANMOX. The proposal is detailed further in Chapter 4 of this thesis. There are a number of problems with the proposed fuel, the main of which being that it generates additional plutonium and will lead to the irradiation of large quantities of depleted uranium and the valuable rare earth element dysprosium. To counter these problems, in Chapters 4 and 5 alternative fuel concepts for Pu irradiation in PHWRs are proposed based on the use of thorium and reprocessed uranium in place of dysprosium and depleted uranium. The aim was to determine whether such a fuel concept would be neutronically feasible, by determining how the neutron multiplication factor k_{inf} compares to that of natural uranium and UK CANMOX fuels, and to determine the achievable discharge burnup (energy release per unit mass of fuel), isotopic compositions on discharge, thorium conversion to ^{233}U , and whether the fuel could give an improvement in core coolant void reactivity [67], a common problem and potential regulatory hurdle for the Enhanced CANDU 6 reactor in the UK [20, 68].

1.7 AQUEOUS SEPARATIONS PROCESSES

Nuclear fuels have very strict requirements on chemical purity. All nuclei absorb neutrons to some degree, and the presence of contaminants reduces the availability of neutrons to sustain the fission chain reaction [69]. As such, processes are required which separate contaminants from fuel components. After irradiation, spent fuel reprocessing techniques may be used to separate useful elements from waste materials, and may in future be used to separate individual elements from spent fuel for advanced waste treatments [70-73]. Currently the majority of used nuclear fuel separations activities are carried out in aqueous media, from which the desired elements are selectively extracted, leaving waste material behind. Front end processing activities are more variable, depending on the process feed material, but aqueous methods remain very common [74].

The methods most used in the nuclear industry are solvent extraction and ion exchange [74-76]. These methods involve bringing the aqueous solution of multiple metals into contact with an extraction medium. In solvent extraction, the extraction medium is a liquid, while in ion exchange processes the extraction medium is a solid. The metals distribute to some extent between the aqueous medium and the extraction medium, which is immiscible with the aqueous medium. The different affinity of each metal towards the extraction media is used to separate them.

In this thesis several liquid-liquid distribution studies are discussed, and a brief overview of the technique is presented in the following chapter. Many detailed descriptions of solvent extraction theory are available in the scientific literature, and the reader may consult the following sources for further information [76-79].

Separations processes for thorium have been studied in great detail in the literature, considering a very wide range of extractants in a variety of situations and from a large set of aqueous media. These are detailed in

Section 2.8. These studies have almost all examined individual extractants, including the very well-established tributyl phosphate (TBP) [80-82], the more industrially relevant phosphorous extractants such as PC-88a [83-85] and HDEHP [86-88], and the more recent synthesis of experimental extractants such as crown ethers [89-91] and calix-4-arenes [92-94]. PC-88a in particular is the currently used extractant of choice for thorium recovery [34]. However, in industrial use iron and uranium must be separated in a separate step from the mineral solution feed before PC-88a may be used to recover the thorium. In Chapter 3 is presented a possible system which aimed to allow thorium to be separated selectively from a mixture of iron and uranium, based on synergic mixtures of PC-88a and HDEHP, a combination which has not previously been reported in the literature. The aim was to determine the extracted complexes and number of contact stages required to extract 99% of the dissolved thorium from an acidic solution of uranium, thorium and iron.

The separation of thorium and uranium will also be required if it is desired to recover ^{233}U which has been produced in the reactor from thorium in order to reintroduce this uranium into new thorium fuel, for instance if a thorium- ^{233}U "equilibrium" fuel is needed to start a full thorium fuel cycle. In CANDU reactors the fuel is surrounded by a zirconium alloy sheath, which deforms under the pressure and temperature in the core and is compressed onto the fuel pellets, making it difficult to mechanically separate the zirconium from the fuel [20]. The separation of thorium, uranium, zirconium and iron has not been well studied in the literature. In Chapter 6 a screening study is presented of a set of ten potential synergists for PC-88a, including HDEHP, for the separation of these metals. The aim was to determine the distribution ratios of each metal and the separation factors of iron, uranium and zirconium against thorium with the various synergic mixtures from nitric, hydrochloric and sulfuric acids, in order to identify promising systems for further detailed development.

1.8 CHAPTER SUMMARY

In this chapter the case has been made for nuclear power, particularly thorium-based nuclear power. While thorium has fallen out of favour with the mainstream nuclear industry, in the right applications it can complement the existing uranium nuclear fuel cycle, enhancing the sustainability credentials of nuclear energy and allowing improvements in a number of areas such as resource utilisation, non-proliferation, and as a fertile host material for plutonium stockpile irradiation. Despite this, the thorium fuel cycle is relatively under-developed compared to the uranium fuel cycle.

In addition background information has been given on the current status of nuclear power in the UK, with a focus on plutonium management options, as well as an introduction to solvent extraction as a means of separating metal ions in aqueous solutions.

In the next chapter, the current state-of-the-art in thorium fuel preparation and reactor irradiation are discussed, as well as the historical context of thorium nuclear power research and development efforts. From this review gaps in the scientific literature were identified for further study.

2 INTRODUCTORY THEORY, THORIUM RESOURCES AND LITERATURE REVIEW

Having established the need for additional work in thorium separations chemistry and thorium nuclear fuels in Chapter 1, this chapter begins with a more detailed overview of reactor physics phenomena and the front end of the thorium nuclear fuel cycle. Following this is a discussion of the current scientific literature on the separation of thorium from other elements by solvent extraction and the use of thorium dioxide as a nuclear fuel in Generation III+ nuclear power reactors, particularly PHWRs.

2.1 OVERVIEW OF NUCLEAR POWER REACTOR OPERATING PRINCIPLES AND BASIC PHYSICS

This section provides an introduction to nuclear reactor physics and operations theory, as required for an understanding of the topics in this thesis. Fuller details of these topics are available in the literature [15-20], and these sources were used to compile the information reported in this section.

Similar to a fossil fuelled power plant, electricity is produced in a nuclear plant by turning a generator, using the mechanical work from a connected steam or gas turbine. The heat required to turn this turbine is produced by a nuclear fission reaction. Nuclear fission is the splitting of suitable heavy atomic nuclei to release energy, occurring when these nuclei absorb neutrons, become unstable, and split into two smaller fragments and a small

number of neutrons. This is as opposed to nuclear fusion, where light atomic nuclei are brought together to release energy [95].

2.1.1 NEUTRON INTERACTIONS WITH MATTER

Besides fission, several other important neutron-nucleus interactions are possible. A neutron may be captured by a nucleus without inducing fission, resulting in the formation of a heavier nucleus, which may then undergo radioactive decay to form other isotopes. Neutrons may also be scattered by nuclei, transferring a portion of their energy to the target nucleus and thus changing their velocity.

The probability of a given neutron interacting with a nucleus is a function of the target nucleus' composition and the energies of the nucleus and the incident neutron. These probabilities are often expressed as microscopic neutron cross sections σ , usually expressed in barns (b), where $1 \text{ b} = 10^{-24} \text{ cm}^2$. The cross sections for neutron-induced fission σ_f , radiative neutron capture σ_c , and elastic neutron scattering σ_s for some selected actinide isotopes of importance in this work over a range of neutron energies are shown in Figure 2.2 to Figure 2.7. Two further combined interaction cross-sections are defined as the absorption cross section σ_a and the total interaction cross section σ_t , as shown in Equation (2.1).

$$\sigma_t = \sigma_s + \sigma_a = \sigma_s + \sigma_c + \sigma_f \quad (2.1)$$

It can be seen that in general, the lower the energy of the incident neutron, the greater the chance of it being absorbed. In the central part of the neutron energy range, approximately $10^1 - 10^5 \text{ eV}$, the cross section is characterised by a series of close peaks. These are known as neutron resonances, and occur due to the fact that the possible energy states of a nucleus are discrete, and neutrons are much more likely to be absorbed if they have the correct energy to form a compound nucleus [17].

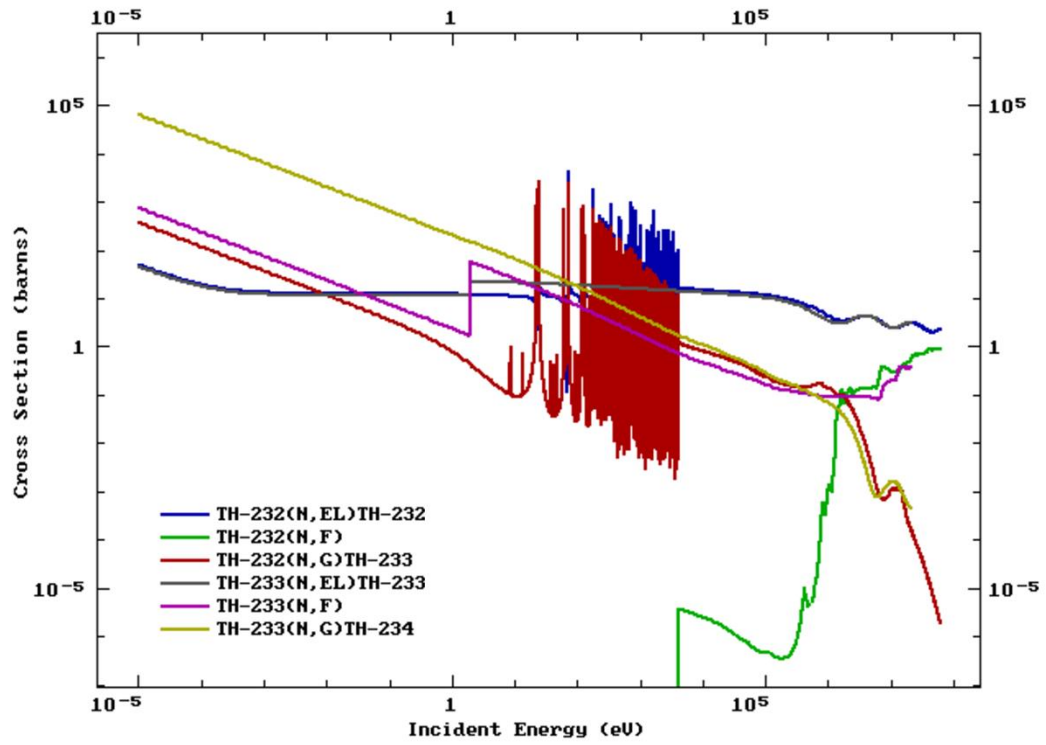


FIGURE 2.1 – SELECTED NEUTRON INTERACTION CROSS SECTIONS FOR Th-232 AND -233 FOR A RANGE OF INCIDENT NEUTRON ENERGIES. DATA TAKEN FROM ENDF/B-VII.1 LIBRARY [96].

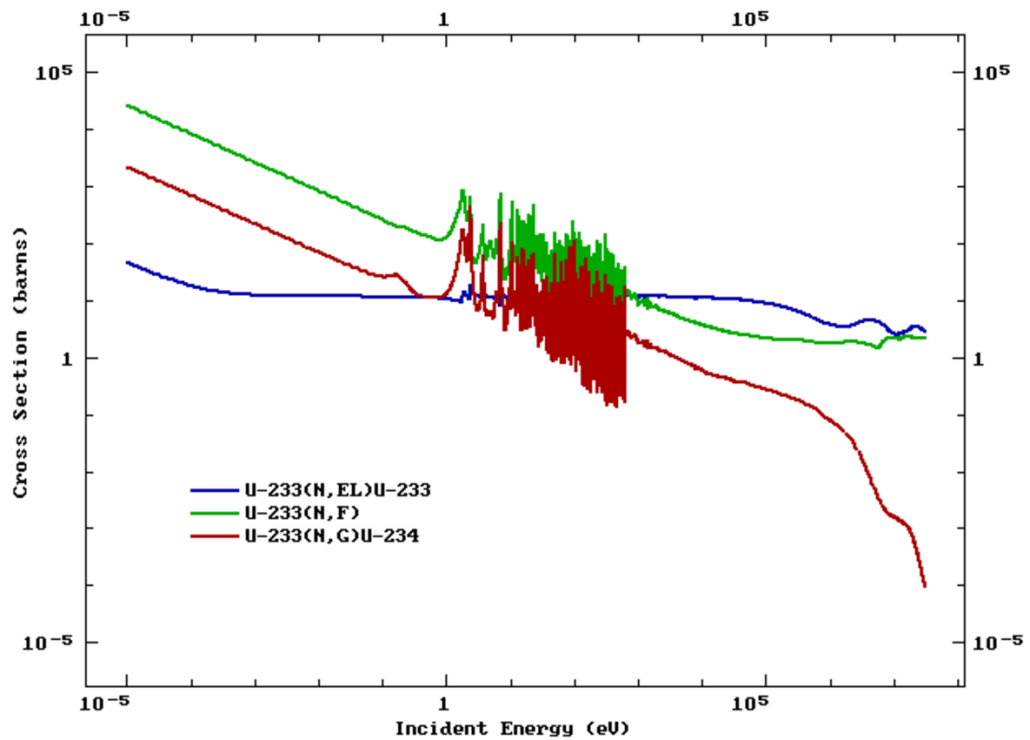


FIGURE 2.2 – SELECTED NEUTRON INTERACTION CROSS SECTIONS FOR URANIUM-233 FOR A RANGE OF INCIDENT NEUTRON ENERGIES. DATA TAKEN FROM ENDF/B-VII.1 LIBRARY [96].

THE PREPARATION AND APPLICATION OF THORIUM-BASED NUCLEAR FUELS

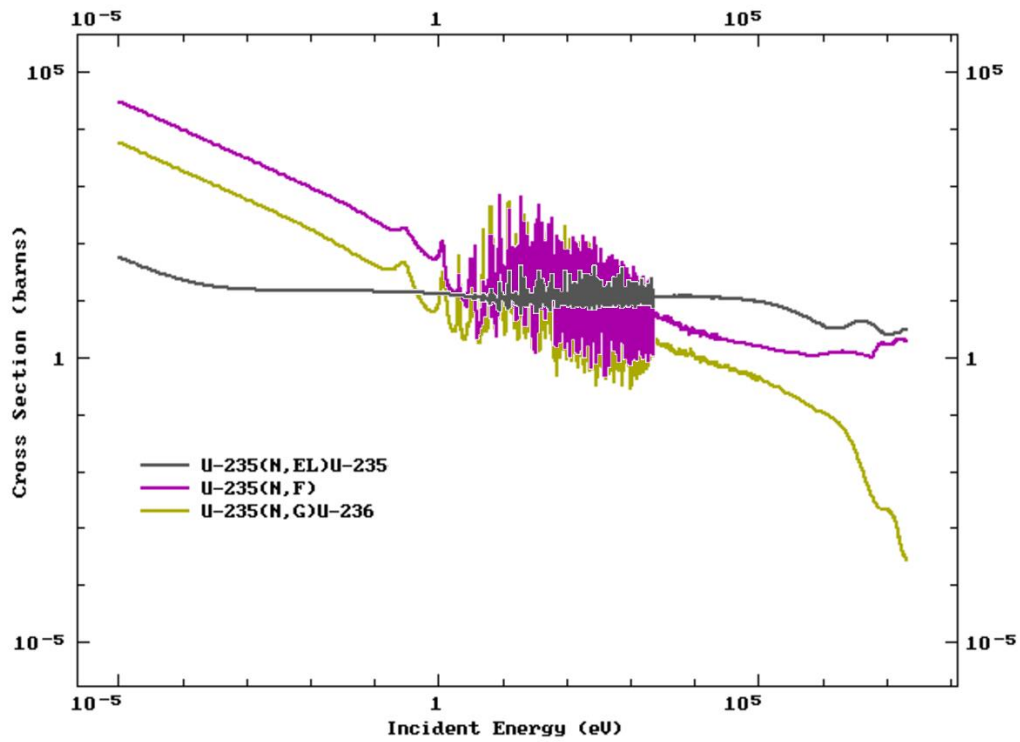


FIGURE 2.3 – SELECTED NEUTRON INTERACTION CROSS SECTIONS FOR URANIUM-235 FOR A RANGE OF INCIDENT NEUTRON ENERGIES. DATA TAKEN FROM ENDF/B-VII.1 LIBRARY [96].

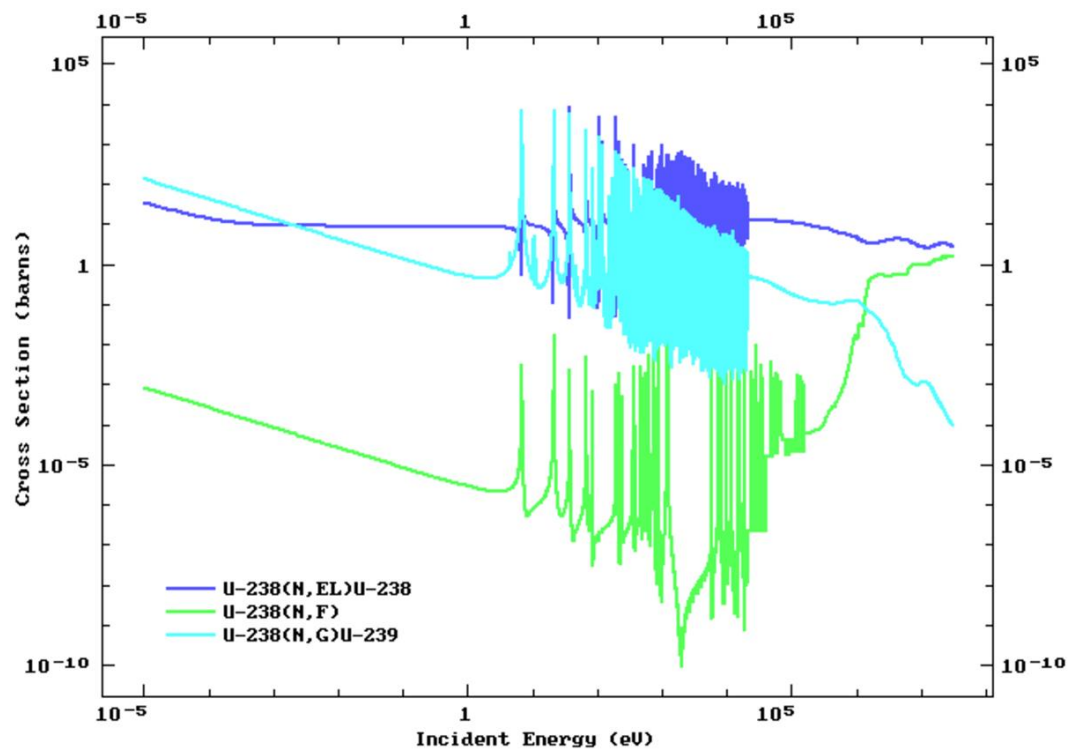


FIGURE 2.4 – SELECTED NEUTRON INTERACTION CROSS SECTIONS FOR URANIUM-238 FOR A RANGE OF INCIDENT NEUTRON ENERGIES. DATA TAKEN FROM ENDF/B-VII.1 LIBRARY [96].

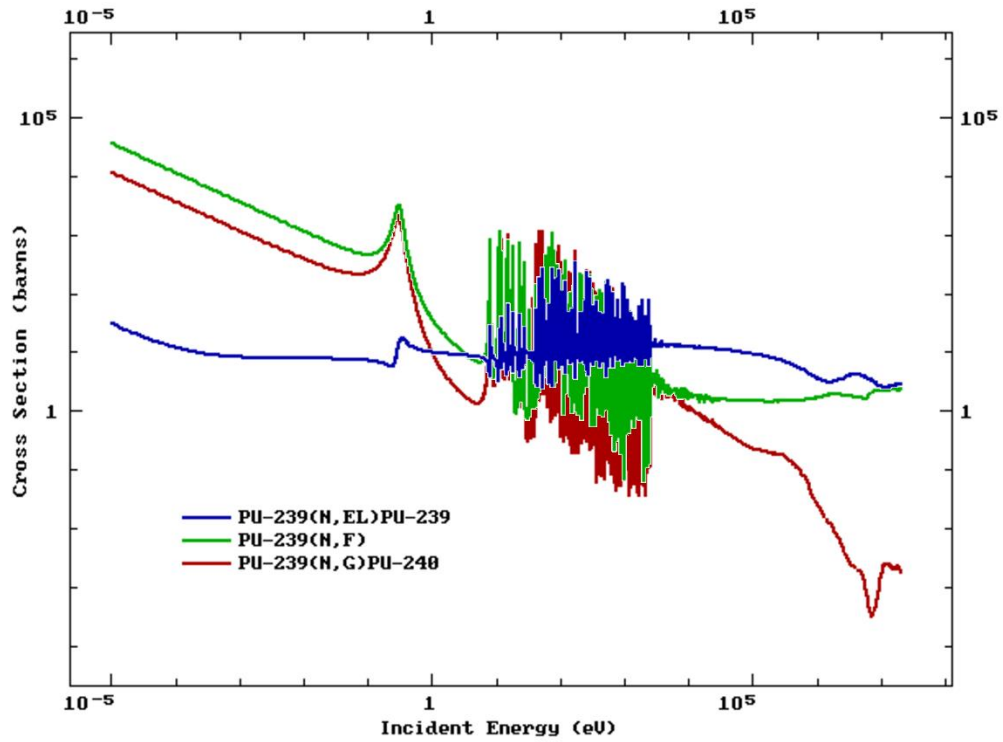


FIGURE 2.5 – SELECTED NEUTRON INTERACTION CROSS SECTIONS FOR PLUTONIUM-239 FOR A RANGE OF INCIDENT NEUTRON ENERGIES. DATA TAKEN FROM ENDF/B-VII.1 LIBRARY [96].

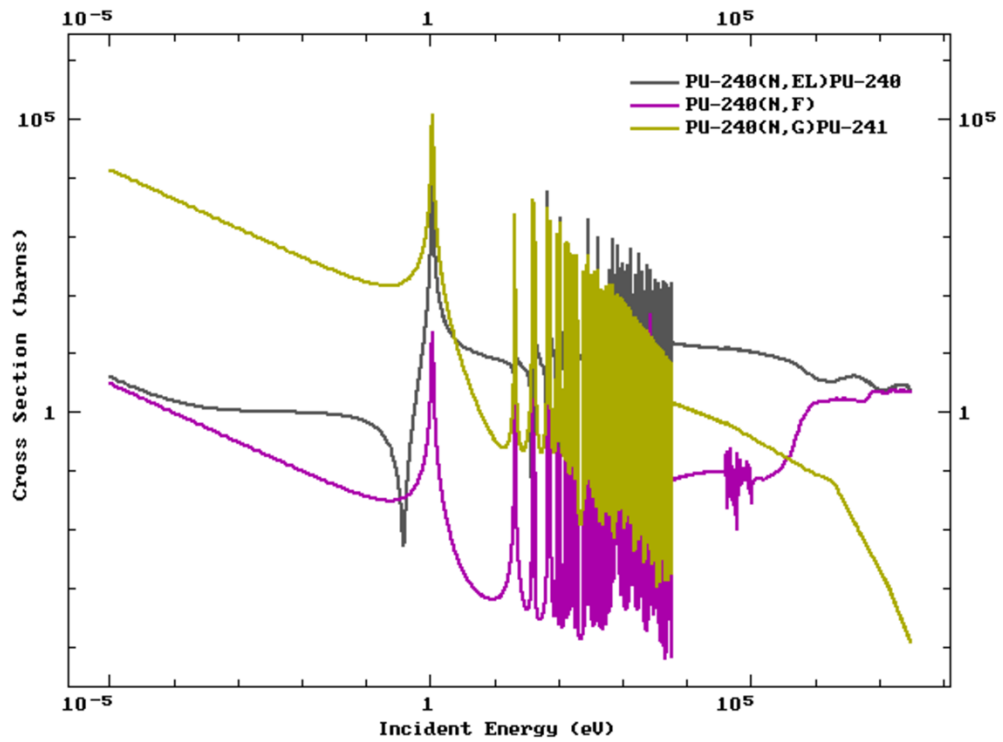


FIGURE 2.6 – SELECTED NEUTRON INTERACTION CROSS SECTIONS FOR PLUTONIUM-240 FOR A RANGE OF INCIDENT NEUTRON ENERGIES. DATA TAKEN FROM ENDF/B-VII.1 LIBRARY [96].

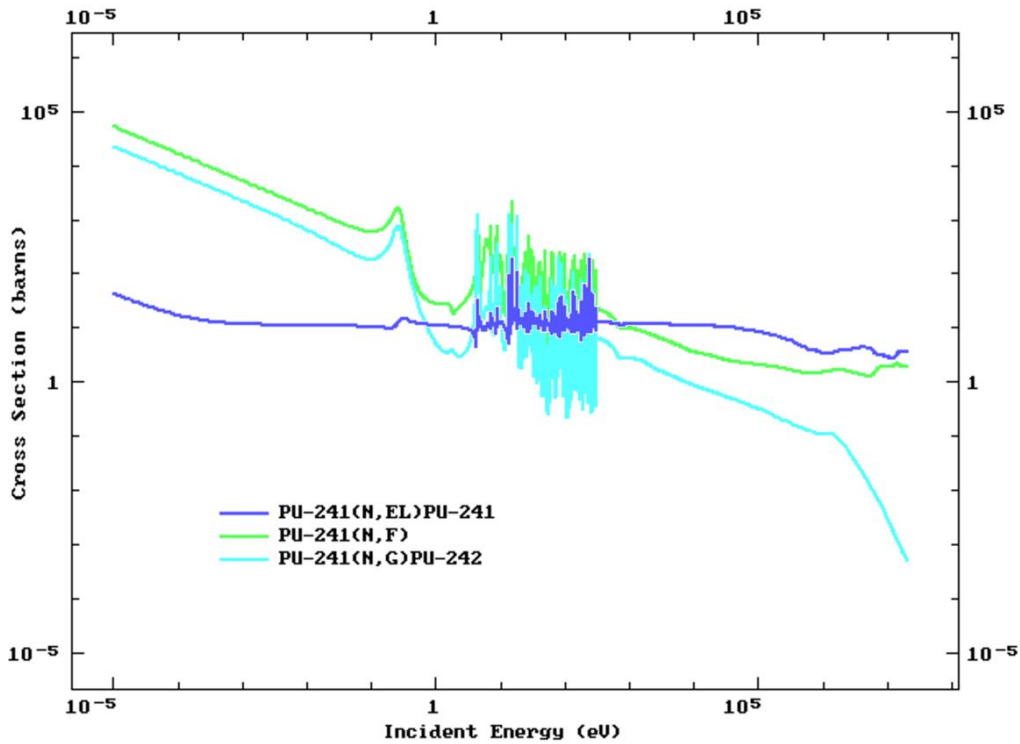


FIGURE 2.7 – SELECTED NEUTRON INTERACTION CROSS SECTIONS FOR PLUTONIUM-241 FOR A RANGE OF INCIDENT NEUTRON ENERGIES. DATA TAKEN FROM ENDF/B-VII.1 LIBRARY [96].

Microscopic cross sections vary as a function of target nucleus temperature due to the Doppler broadening of peaks in the interaction spectra. As the target nucleus temperature increases it vibrates more rapidly, leading to an increase in the range of relative velocities between the incident neutron and the target nucleus. Thus, with increasing temperature the interaction peaks become more diffuse, with a lower maximum magnitude [16].

In addition to the microscopic neutron interaction cross section σ , there exists the macroscopic neutron interaction cross section Σ , which is the microscopic cross section multiplied by the atomic density of the isotope, as shown in Equation (2.2).

$$\Sigma_i = N\sigma_i \quad (2.2)$$

Where Σ_i is the macroscopic neutron cross section for interaction i , and N is the atomic density of the isotope of interest.

2.1.2 THE CRITICAL NUCLEAR FISSION CHAIN REACTION

Nuclear fuels are prepared from “fissile” materials (those which have a high fission capture cross section) [18]. Most commonly used is the isotope uranium-235, which releases 2-3 fast neutrons upon fission. These fast neutrons have energies of ~ 2 MeV. The released neutrons may then go on to cause fission in other ^{235}U atoms. If exactly one released neutron goes on to cause an additional fission, and this process is repeated, a self-sustaining “critical” chain reaction can be created, as illustrated in diagrammatic form in Figure 2.8. This may be achieved by bringing together a “critical mass” of fissile material in a suitable geometry, number of neutrons being produced by fission is balanced by the number of neutrons either being captured or leaking from the critical mass. A nuclear reactor is critical when the number of neutrons within the core is constant over time. This may be expressed by the parameter k_{inf} , as given in Equation (2.3), which accounts for neutron production and absorption within an infinite reactor core, without neutron leakage [19].

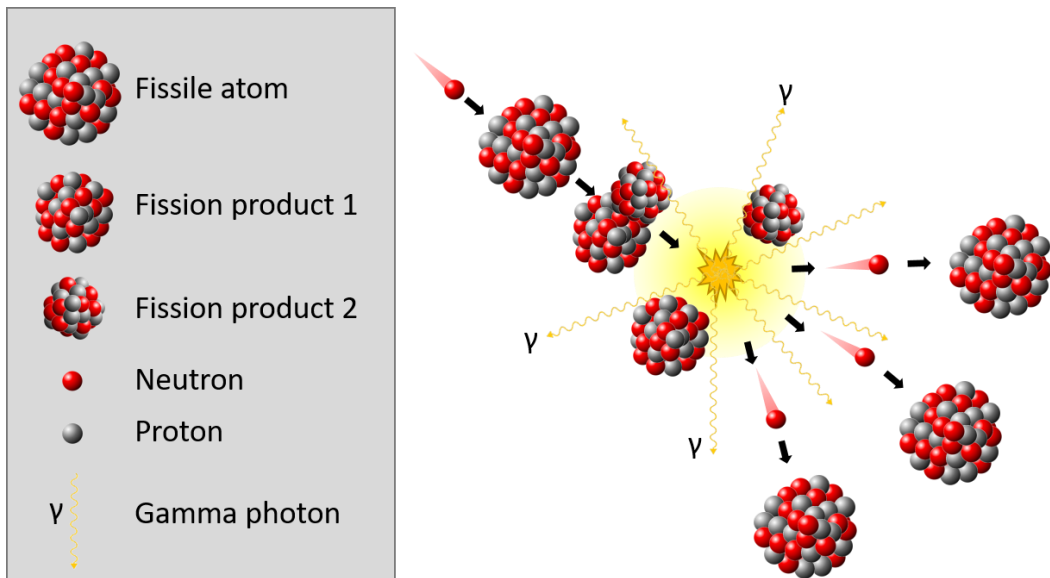


FIGURE 2.8 – THE NUCLEAR FISSION CHAIN REACTION. A NEUTRON CAUSES FISSION IN A FISSILE ATOM, PRODUCING TWO FISSION FRAGMENTS, A NUMBER OF FAST NEUTRONS AND ENERGY IN THE FORM OF HEAT. FIGURE BASED ON SOURCE [97].

$$k_{inf} = \frac{n_i}{n_{i-1}} \quad (2.3)$$

Where k_{inf} is the infinite neutron multiplication factor,
 n_i is the number of neutrons in the current generation, and
 n_{i-1} is the number of neutrons in the previous generation.

Real reactors are naturally not infinitely large, and have some degree of neutron leakage from the core. To account for this the effective neutron multiplication factor k_{eff} is also defined, as given in Equation (2.4) [16].

$$k_{eff} = k_{inf} P_{NL} \quad (2.4)$$

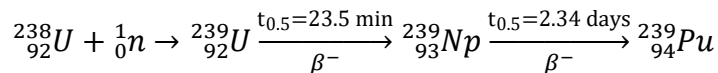
Where k_{eff} is the effective neutron multiplication factor, and
 P_{NL} is the probability of neutron non-leakage.

When $k_{eff} = 1$, the reaction is critical. When $k_{eff} > 1$ the core is supercritical, and when $k_{eff} < 1$ the core is subcritical. Further to this, another parameter, the core reactivity ρ , is defined in Equation (2.5) [16].

$$\rho = \frac{k_{eff} - 1}{k_{eff}} \quad (2.5)$$

Thus for a critical core, $\rho = 0$. A supercritical core will have positive reactivity, and a subcritical core will have negative reactivity.

Uranium-235 forms 0.71% of natural uranium, with the remainder being made up almost completely by uranium-238, which is not fissile, although it can be converted to fissile plutonium-239 through radiative neutron capture and beta decay as shown in the following reaction [17].



Similarly, thorium-232 is converted to the fissile isotope uranium-233 by neutron capture, as was described in Section 1.5.2.2.

2.1.3 NEUTRON MODERATION

As can be seen in Figure 2.2 and Figure 2.3, neutrons are most likely to cause fissions in ^{235}U and ^{233}U when their energies are lowered to the “thermal” range, which is defined as ~ 0.025 eV. A 2 MeV fast neutron is approximately 500 times less likely to induce a fission in ^{233}U than a thermal neutron, based on the difference in their effective neutron cross sections [45]. Most reactors slow down fast fission neutrons to thermal energies, thus increasing the probability of fission reactions occurring, using a so-called moderator [17].

The moderator will be a material of low atomic mass, which reduces the neutron energy through elastic collisions between the neutrons and moderator nuclei. The lighter the scattering nucleus, the more energy is lost by the neutron per scattering event, known as the lethargy gain, or logarithmic energy decrement, notated ξ [16]. Moderators should not be absorbent of neutrons and should have a high scattering cross section. Common moderators include light (ordinary) water, heavy (deuterated) water and graphite. The elastic scattering and radiative capture cross sections for the key isotopes of these moderators are given in Figure 2.9.

Moderators may be compared through the moderator ratio parameter MR , as defined in Equation (2.6), where the greatest ratio indicates the most effective neutron moderator [16].

$$MR = \frac{\xi \Sigma_s}{\Sigma_a} \quad (2.6)$$

Typical values for MR are 71 for light water, 5670 for heavy water, 143 for beryllium and 192 for graphite [98]. Moderators which give rapid neutron thermalisation are preferred, as they allow neutrons to more rapidly pass through the resonance energy range with a lower chance of being captured.

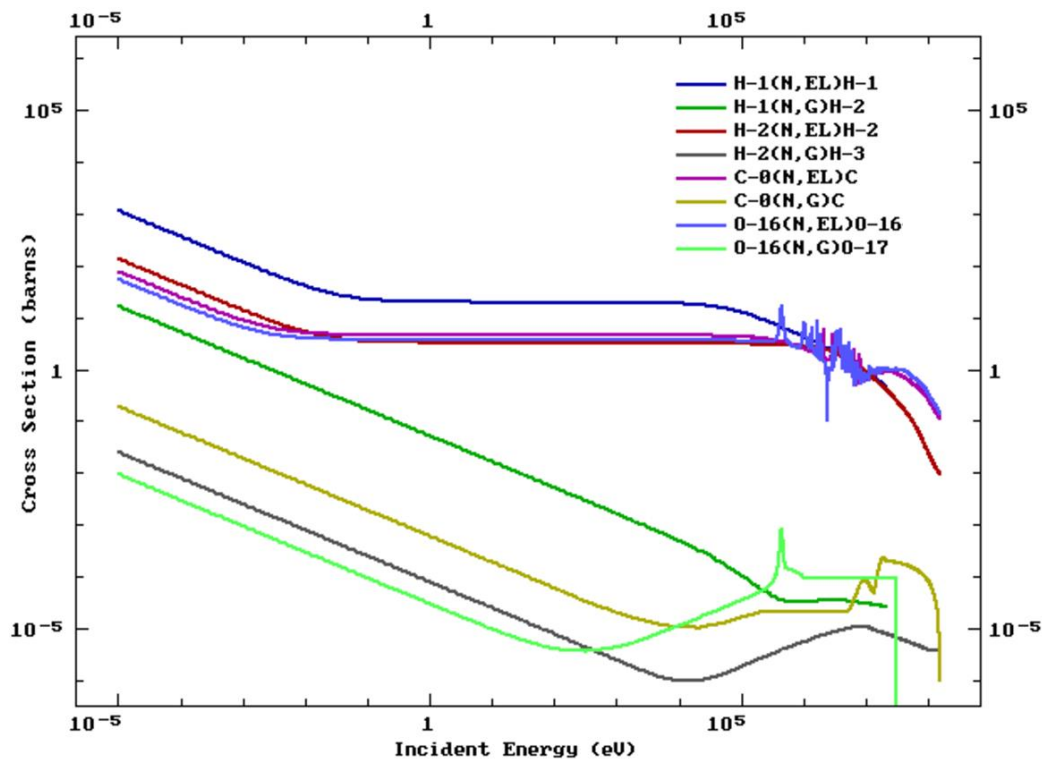


FIGURE 2.9 – ELASTIC SCATTERING (N,EL) AND RADIATIVE CAPTURE (N,G) CROSS SECTIONS FOR HYDROGEN (H-1), DEUTERIUM (H-2), OXYGEN (O-16) AND GRAPHITE (C-0) FOR A RANGE OF INCIDENT NEUTRON ENERGIES. DATA TAKEN FROM ENDF/B-VII.1 LIBRARY [96].

Reactors are often categorised into types based on their moderator materials, i.e. Light Water Reactors (LWRs) and Pressurised Heavy Water Reactors (PHWRs).

2.1.4 NEUTRON LOSS

In a reactor, neutrons may be lost through several mechanisms. They may be absorbed by fuel without causing a fission, be absorbed in other materials present in the reactor or leak from the core [19].

Neutron loss due to absorption in the moderator is a key parameter in reactor materials selection. Light water is a good moderator, as ^1H has a large scattering cross section and energy decrement. However, the neutron absorption of light water is much greater than that of heavy water, leading to significant absorption in the moderator for LWRs. For this reason, these reactors are generally fuelled with enriched uranium, where the fraction of

^{235}U has been increased to give greater fuel reactivity. PHWRs do not require enrichment, as the moderator has minimal neutron absorption [20].

2.1.5 CORE HEAT MANAGEMENT AND REMOVAL

Heat removal in the reactor is achieved by passing a coolant through the core. In addition to extracting useful energy, this controls heat build-up in the reactor, primarily in order to prevent materials from failing at high temperature, both in normal operation as well as under accident scenarios. LWRs usually use light water as both coolant and moderator [17]. Current PHWRs use heavy water as both coolant and moderator, although the coolant water and moderator water are segregated [20].

A simplified diagram of the key elements of a boiling water reactor (BWR) system is shown in Figure 2.10. Structures outside of the containment building are broadly similar for almost all reactor types, although many plants use large bodies of open water for condensate cooling, rather than cooling towers. However, systems inside the containment building vary significantly according to reactor type. The reactor systems for two other common reactor types, the PWR and PHWR, are shown in Figure 2.11.

Other thermal reactor types operating today include the Advanced Gas-cooled Reactor, a graphite-moderated, carbon dioxide gas-cooled reactor which only exists in the United Kingdom [49], and Russian RBMK and EGP-6 reactors, which are light water-cooled and graphite-moderated [99].

2.1.6 CORE CONTROL SYSTEMS

A nuclear reactor core must begin its life with some level of positive reactivity, as otherwise it would instantaneously become sub-critical as soon as the first nucleus underwent fission. Over the period of operation the excess reactivity must be suppressed in order to achieve critical operation ($k_{eff} = 1$). This is commonly achieved by using neutron absorbing materials

to reduce the population of neutrons in the core, allowing critical operation over a fuel irradiation cycle [18, 19].

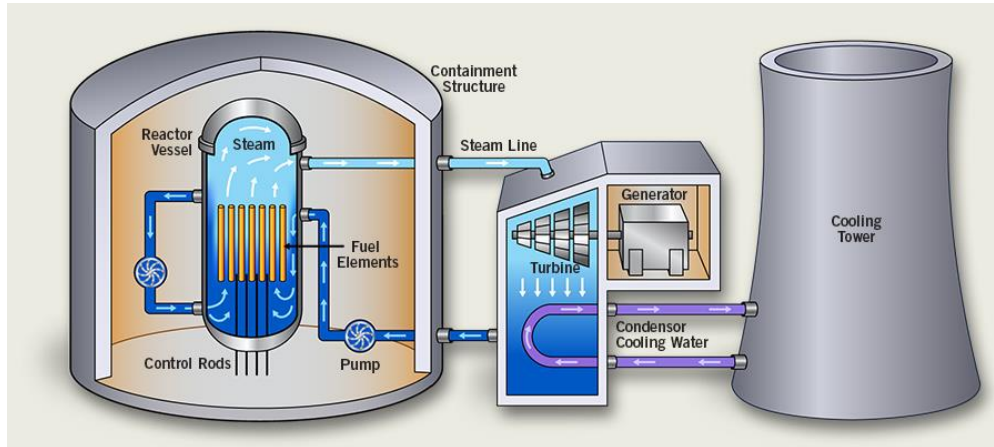


FIGURE 2.10 – SELECTED KEY COMPONENTS OF A BOILING WATER REACTOR. ILLUSTRATION COURTESY OF CAMECO CORPORATION-URANIUM 101 [100].

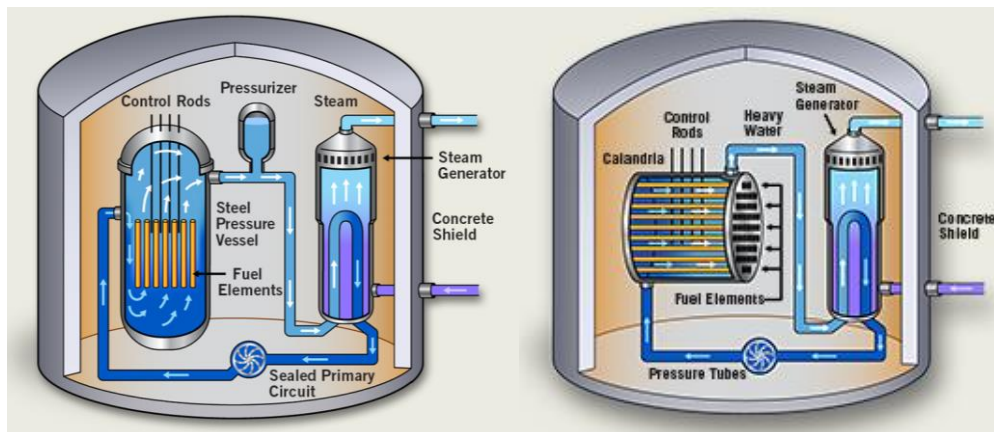


FIGURE 2.11 – KEY COMPONENTS IN THE NUCLEAR CONTAINMENT STRUCTURE FOR TWO OTHER COMMON PLANT TYPES, THE PRESSURISED WATER REACTOR (PWR, LEFT) AND THE PRESSURISED HEAVY WATER REACTOR (PHWR, RIGHT). ILLUSTRATIONS COURTESY OF CAMECO CORPORATION-URANIUM 101 [100].

A number of systems are used in reactors to control the neutron population. The most common are control rods. Control rods are solid bars which may be driven into or out of the core, and contain neutron absorbing materials such as boron, cadmium or gadolinium [17].

Neutron absorbing materials may also be built into the fuel assemblies, and are thus fixed in position within the core. These are used as burnable

neutron absorbers, which are intended to gradually be converted from highly absorbent to low absorbent materials over the course of irradiation, generally to smooth out large excesses of positive reactivity associated with fresh nuclear fuel or temporarily reduce local neutron flux [16].

The third common method of reactivity control is “chemical shim” control, where a soluble neutron absorber is added to the reactor coolant and/or moderator. Generally this is boron, although gadolinium is also used [20].

PHWRs often feature Liquid Zone Control in addition, where vertical tubes within the core may be filled with or emptied of light water in order to alter the moderation and neutron capture profile [20, 68].

2.1.7 FUEL FERTILE CONVERSION AND BREEDING

Some nuclear fuel materials are not fissile, but are fertile, meaning that they are converted by neutron capture to form fissile materials. ^{238}U and ^{232}Th are examples of fertile materials. The quotient of the rates of production and consumption of fissile material is termed the conversion ratio, C_r , with $C_r \geq 1$ indicating fuel breeding. Thermal reactors generally have $0 < C_r < 1$, producing an amount of fissile plutonium as they consume ^{235}U , which will in turn be partially consumed [17].

2.1.8 REACTOR STABILITY AND COEFFICIENTS OF REACTIVITY

An operating reactor is not a machine in a steady state, and perturbations in operating conditions can cause changes in the neutron population, thus changing the core reactivity, leading to changes in core power and temperature, leading in turn to variations in the density of core materials.

The effects of perturbations in reactor operating conditions on the neutron population and core reactivity are expressed through reactivity coefficients ω , as defined in Equation (2.7) [16, 17, 19].

$$\omega = \frac{d\rho}{dm} \quad (2.7)$$

Where ω is the reactivity coefficient,
 ρ is the core reactivity, and
 m is the perturbation causing a change in reactivity.

It is always an aim of reactor design to have negative coefficients of reactivity, as this means that any perturbation leads to a change in reactivity which self-corrects the perturbation, giving a stable reactor [16, 17, 19].

Some key reactivity coefficients include the fuel temperature coefficient, also known as the Doppler coefficient, where m in Equation (2.7) is the fuel temperature [17]. As the fuel temperature increases so does the Doppler broadening effect, leading to increased neutron absorption in the resonance region. Additionally, there is the moderator temperature coefficient, where m in Equation (2.7) is the moderator temperature. Increased moderator temperature leads to decreased moderator density and thus less moderation, hardening the neutron energy spectrum and giving lower neutron absorption in the moderator [17].

The void coefficient is where m in Equation (2.7) is the fraction of voiding in liquid coolants/moderators due to vaporisation. If the heat flux from the fuel surpasses a critical value then the coolant may undergo a departure from nucleate boiling, leading to fuel rods becoming surrounded by an insulating vapour layer and thus being less able to discharge heat to the coolant, potentially also giving reduced moderation [20].

When designing reactors, it is vital that the effect of these and many other factors on the core be considered in order to ensure that the reactor will be stable in operation over its life and during fault conditions [68].

2.1.9 USED NUCLEAR FUEL

When nuclear fuel can no longer sustain the critical chain reaction, it is removed from the reactor. The level of fuel irradiation achieved is often described in terms of fuel “burnup”, measured as the amount of thermal energy released from a unit mass of fuel, commonly in megawatt.days/kilogram of heavy metal [16].

For most uranium-fuelled reactors the used fuel still contains approximately 95% uranium, with the remainder converted to fission products and other actinides including plutonium, which are generally extremely radioactive [101, 102]. This used fuel may be reprocessed to separate out the uranium and plutonium from the other actinides and fission products, which are considered as waste, or the whole used fuel may be classified as waste for suitable disposal. The uranium and plutonium may be reused as nuclear fuel [26]. In thorium-fuelled reactors the fuel might be reprocessed to recover the ^{233}U for reuse in a ^{233}U -Th “equilibrium” fuel [103, 104].

2.1.10 PLUTONIUM AND PROLIFERATION

Besides being reused in reactors, plutonium may also be used in the manufacture of nuclear weapon “pits”, the fissile core of a nuclear bomb. The fissile isotope ^{239}Pu has a critical mass of approximately 10 kg [105], and it is this isotope that forms the majority of plutonium in spent nuclear fuel.

Separated plutonium is hence highly attractive to individuals and groups who wish to create a nuclear weapon. The illicit acquisition of nuclear materials is known as plutonium proliferation [106].

2.2 THORIUM AS A NUCLEAR FUEL

2.2.1 NUCLEAR INTERACTION PROPERTIES OF THORIUM

In addition to those presented previously in Section 1.5, thorium has a number of other differences as a fuel when compared to uranium. Many of these are linked to the nuclear properties of ^{233}U and ^{232}Th , as distinct from ^{235}U and ^{238}U respectively [43, 107].

As can be seen in Figure 2.1 and Figure 2.4, ^{232}Th is approximately three times more likely to capture a thermal neutron than ^{238}U , meaning it converts more readily to a fissile isotope. This property means that thorium is an advantageous “host” material for the irradiation of separated fissile materials such as plutonium, allowing longer irradiation cycles and higher levels of fuel burnup to be achieved than with ^{238}U , without producing additional ^{239}Pu [108]. Thorium fuels are also much less likely to form transuranic elements, as the neutron capture cross section of ^{233}U is less than that of either ^{235}U or ^{239}Pu , but the fission cross sections are similar, as can be seen in Figure 2.2, Figure 2.3 and Figure 2.5. In addition, plutonium production is almost eliminated, as more neutron captures are required on ^{232}Th than ^{238}U to produce the element [107, 109].

Neutron capture on ^{232}Th does not always lead to the production of ^{233}U . Some neutron interactions can lead to the formation of heavier ^{234}U nuclei following neutron capture on ^{233}Pa or ^{233}U , as shown in Figure 2.12 [110-112]. Alternatively, neutron captures on ^{232}Th , ^{233}Pa or ^{233}U may result in the formation of ^{232}U , again as shown in Figure 2.12 [112-115]. The relatively long half-life of ^{233}Pa ($t_{0.5} = 27.0$ d), compared to the equivalent decay of ^{239}Np in the U-Pu fuel cycle ($t_{0.5} = 2.36$ d), exacerbates this, providing a large window of time in which ^{232}U may be formed. The microscopic cross sections for some selected neutron capture reactions on protactinium isotopes are shown in Figure 2.13. Such even-numbered

uranium isotopes have very low fission cross sections. Additionally, ^{232}U has a number of high-energy gamma ray emitting decay daughters and a half-life of 68.9 years, meaning that if uranium were to be separated from thorium spent fuel the separations process and uranic products would require significant radiation shielding to be made safe, likely necessitating remote handling. Sufficient time must also be allowed for any remaining ^{233}Pa in the spent fuel to decay to ^{233}U prior to reprocessing [116].

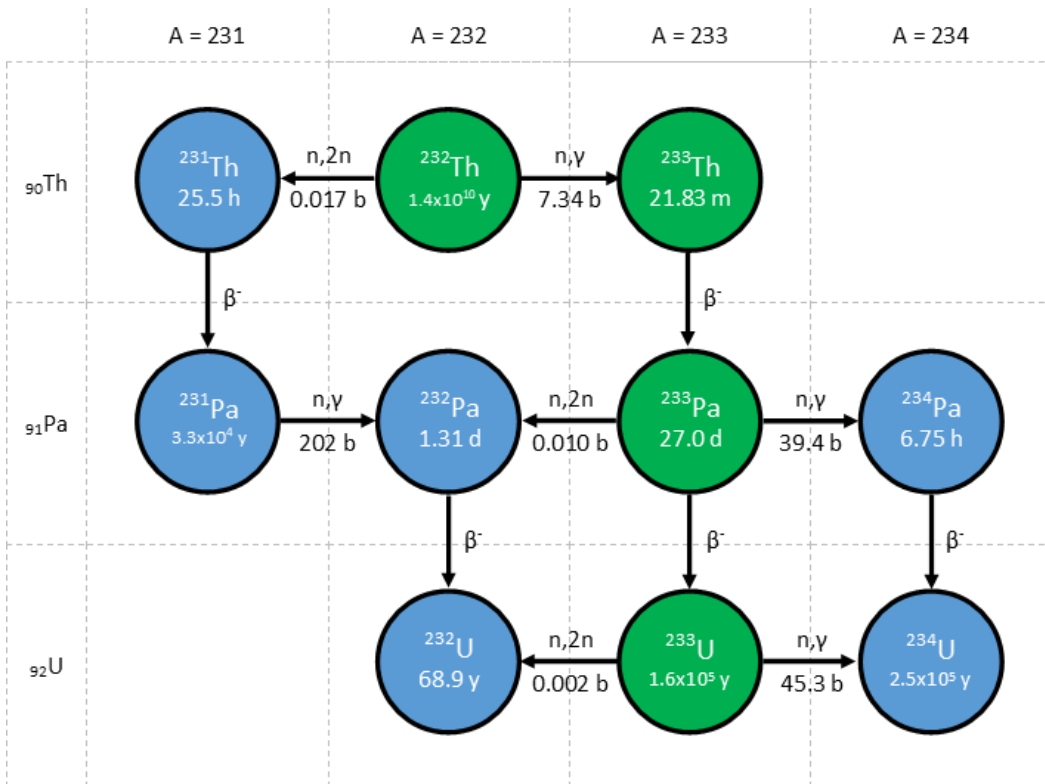


FIGURE 2.12 – SELECTED NEUTRON CAPTURE INTERACTIONS AND RADIOACTIVE DECAY REACTIONS FOR THORIUM-BASED NUCLEAR FUELS. SHOWN IN GREEN IS THE PATHWAY FROM ^{232}Th TO ^{233}U , WITH POSSIBLE ROUTES TO EVEN-NUMBERED URANIUM ISOTOPES IN BLUE. REACTIONS SHOWN ARE NEUTRON CAPTURE-PRODUCTION (n,2n), RADIATIVE NEUTRON CAPTURE (n, γ), AND BETA DECAY (β^-). RADIATIVE CAPTURE CROSS SECTIONS ARE SHOWN FOR 0.025 eV INCIDENT NEUTRONS AND n,2n CROSS SECTIONS ARE AVERAGE VALUES FOR FISSION SPECTRUM NEUTRONS, AS THIS REACTION HAS A THRESHOLD ENERGY OF 6-7 MeV [45].

The positive side of ^{232}U is that it can be useful in providing radiogenic self-shielding, giving inherent proliferation resistance to the spent thorium fuel. Highly attractive proliferation materials may also be shielded by blending

with ^{232}U [38, 116, 117]. However, such self-shielding weakens over time as the short-lived radiotoxic materials decay. Unfortunately ^{233}U is an attractive material for proliferation itself, being similarly effective in a weapon as ^{239}Pu [118, 119], and it must be protected and safeguarded with the same level of care and diligence [109, 120, 121].

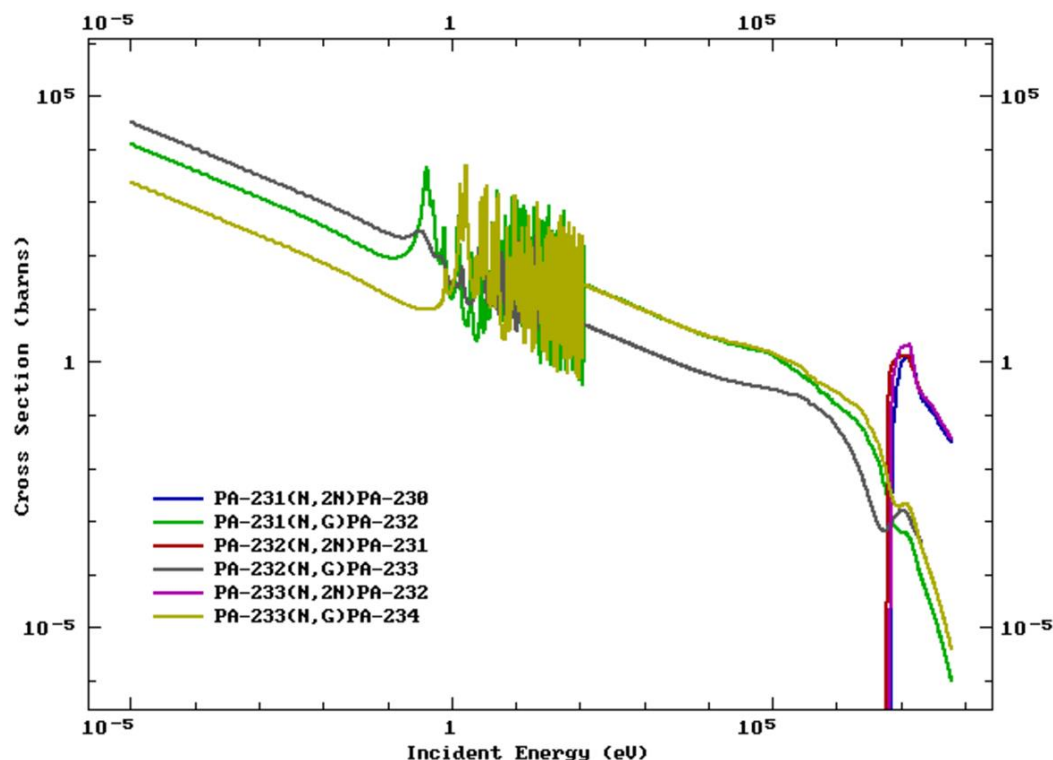


FIGURE 2.13 – SELECTED NEUTRON CAPTURE CROSS SECTIONS FOR PROTACTINIUM ISOTOPES FOR A RANGE OF INCIDENT NEUTRON ENERGIES. DATA TAKEN FROM THE ENDF/B-VII.1 LIBRARY [96].

2.2.2 THORIUM SPENT FUEL

The radiotoxicity and heat generation rate of thorium spent nuclear fuel is generally comparable to or lower than that of uranic spent fuel [102]. As in shown in Figure 2.14, for the first 200 years following discharge from the core the spent fuel radiotoxicity is comparable, with ^{90}Sr dominating. Over the period 200-2000 years Th spent fuels are less radiotoxic than U spent fuels, due to ^{241}Am dominating in high plutonium fraction fuels. However,

from 2000-2,000,000 post-irradiation ^{233}U -thorium spent fuels are more radiotoxic due to the ^{233}U and ^{234}U decay chains.

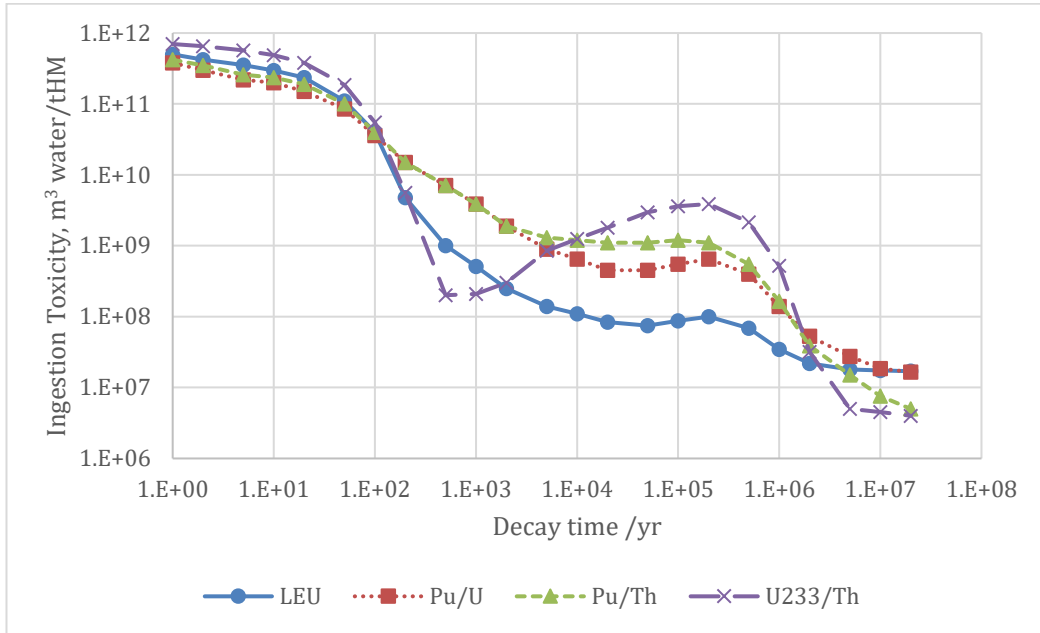


FIGURE 2.14 – INGESTION RADIOTOXICITY OF FOUR PWR FUELS AGAINST TIME POST-IRRADIATION. IMAGE REPRODUCED FROM DATA PUBLISHED IN [116].

The spent fuel heat generation rate will be a crucial parameter in sizing a nuclear waste geological repository, which is driven by the heat generation at 1000 years post-irradiation [68]. The heat generated by a thorium-uranium spent fuel is less than that of uranium-plutonium spent fuel over a timescale of 1000 years [68, 102].

2.2.3 THE THORIUM OXIDE FUEL FORM

Thorium dioxide ThO_2 as a fuel has a number of advantages and challenges compared to uranium oxide fuel. Of the two, thorium dioxide is more resistant to high temperatures, radiation damage and oxidation [122-125].

The chemical stability of ThO_2 means that its behaviour in long term storage and disposal is more predictable than UO_2 fuels, which can convert to UO_3 and U_3O_8 [126]. The downside of this chemical stability is that spent fuel dissolution for reprocessing is also more complex, requiring mixtures of

hydrofluoric acid and concentrated nitric acid in order to dissolve the spent fuel [104, 127].

ThO₂ is also more refractory than UO₂, meaning that higher fuel temperatures in the core can be reached without fuel failure. However, this also necessitates the use of higher temperatures in fuel pellet sintering, which are more difficult to achieve [128-130].

2.2.4 THORIUM-FUELLED MOLTEN SALT REACTORS

When thorium nuclear fuel is discussed, it is almost inevitable that a discussion of Molten Salt Reactors (MSRs) will follow. A description of the current status of thorium-fuelled MSRs is given in [131]. MSRs have some key differences from LWRs, which are briefly outlined here. MSRs have been built and successfully operated historically [132], but today are still considered to be an experimental concept which require detailed development across materials science, reactor chemistry, and fuel production and processing in order to be realised. A diagram of an example MSR system is presented in Figure 2.15.

When fuelled by thorium, once at Th-²³³U equilibrium these reactors would ideally be fuelled only by the addition of thorium, with ²³³U being produced and burnt within the reactor system and not being separated. However, there are many variations of the design, and many possible fuel cycles and applications, making the above outline an example only.

Proponents of the technology insist that liquid fluoride thorium reactors (LFTRs) may be available within as little as ten years [133]. In reality with the requirements for research and development, power plant design, fuel qualification, regulatory approval, fuel processing capacity deployment, and the myriad other challenges facing such a revolutionary nuclear technology, the timescale for commercial operation is more likely to be at least the mid-21st century [134]. The first irradiations of thorium in commercial reactors

will likely be as thorium oxide in LWRs [135] or PHWRs [136]. In this thesis, fuels are considered for use in PHWRs.

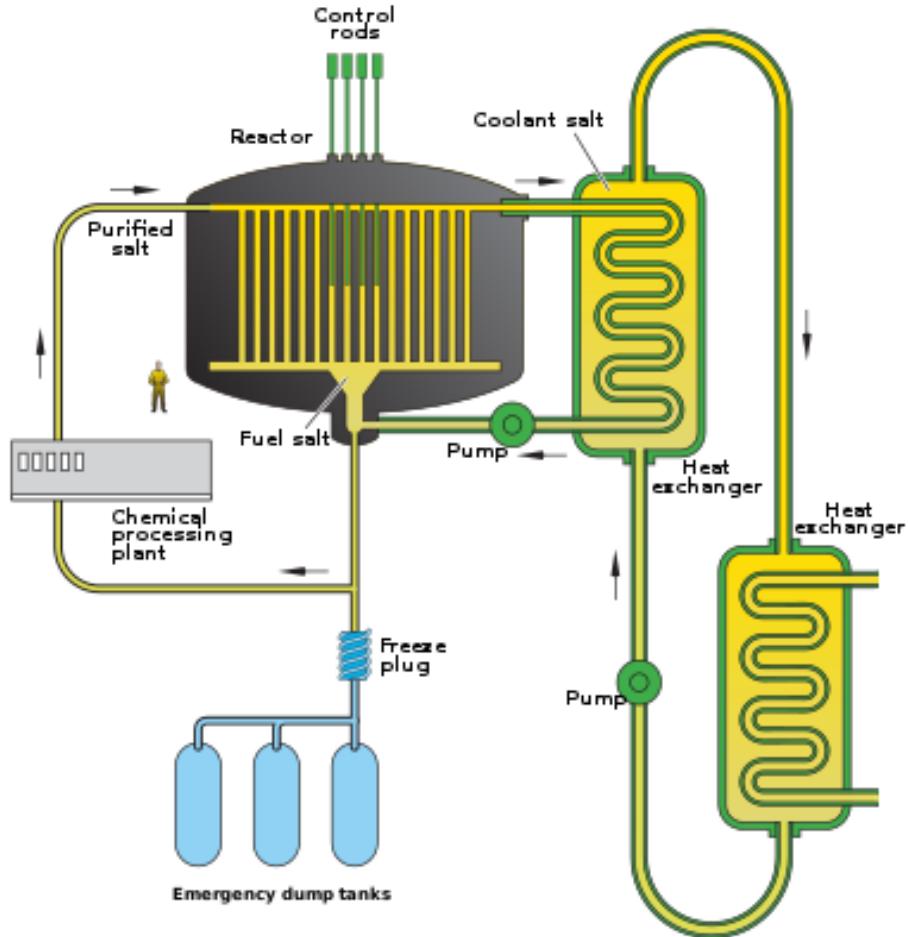


FIGURE 2.15 – SCHEMATIC DIAGRAM OF THE MAIN ELEMENTS OF A MOLTEN SALT REACTOR (MSR) SYSTEM. THE “FREEZE PLUG” IS COMPOSED OF A MATERIAL WHICH WILL MELT IF THE REACTOR TEMPERATURE BECOMES TOO HIGH, ALLOWING THE FUEL SALT TO DRAIN INTO SUB-CRITICAL “DUMP TANKS” TO COOL AND SOLIDIFY [137].

2.3 THORIUM RESOURCES

Thorium resources can be classified as primary or secondary. Minerals containing thorium are considered as primary thorium resources. Secondary thorium resources include existing separated thorium inventories and mineral processing residue stocks. The actual thorium

resources used in fuel fabrication will be selected on the basis of resource cost, ease of treatment, product value, and demand amongst other factors.

2.3.1 PRIMARY SOURCES OF THORIUM

Thorium currently has no large scale application and mineral resources which contain it are currently not worked for their thorium content [138]. Thorium occurs in the natural environment as a component of a number of minerals [139, 140]. Thorium is the major component of the minerals thorianite ThO_2 and thorite ThSiO_4 [141, 142]. These minerals often include some fraction of uranium alongside the thorium [142]. Such uranium-bearing minerals may be worked for their uranium content, but the thorium is regularly discarded as a waste product, having little to no commercial value today with the exception of research uses [143].

2.3.1.1 THE THORIUM-BEARING MINERAL MONAZITE

Monazite is the collective name for a group of monoclinic rare earth phosphate minerals which may contain thorium in addition to elements including cerium, lanthanum, neodymium, gadolinium and samarium [144, 145]. The general structure of monazite is given as $(\text{Ce,La,Nd,Th})(\text{PO}_4,\text{SiO}_4)$ [141, 145]. The group includes several minerals designated by their dominant cation, including Monazite-(Ce), Monazite-(La), Monazite-(Nd) and Monazite-(Sm), as well as other minerals such as Gasparite-(Ce) $(\text{Ce,RE})(\text{AsO}_4)$ and Cheralite $(\text{Ce,Ca})(\text{Ce,Th})\text{PO}_4$ [146].

While monazite does exist in bulk crystals as shown in Figure 2.16, it also concentrates as a sand on beaches and in rivers due its high density and greater resistance to erosive weathering processes than its' common host rocks [144]. The monazite forms a component of heavy mineral sands, alongside other heavy, weathering-resistant minerals such as zircon ZrSiO_4 and ilmenite FeTiO_3 . Such "placer" deposits are extensively worked for the rare earth content of the monazite [147] and thus large quantities of

thorium are produced as a by-product [148, 149]. An example of such a sand is shown in Figure 2.16. The shown monazite samples were examined by scanning electron microscopy, and the results of these examinations are presented in Appendix A of this thesis.



FIGURE 2.16 – MONAZITE GROUP MINERAL CRYSTALS FROM LANDAAS, NORWAY (LEFT). SAND CONTAINING MONAZITE FROM BRAZIL (RIGHT). SCALE IN CENTIMETRES.

A wide range of monazite composition data is available in the scientific literature [142, 150-160]. The mass fractions of 9 different monazites from different locations across four continents have been averaged to give the composition of a “typical” monazite, which is given in Table 2.1. However, the composition of any given mineral which might be processed for its rare earth, thorium or uranium content may vary significantly from these average values.

TABLE 2.1– AVERAGE MASS COMPOSITION DATA ACROSS 9 MONAZITE SAMPLES [142, 144, 151-161].

COMPONENT	MASS FRACTION	COMPONENT	MASS FRACTION
ThO ₂	8.82%	Al ₂ O ₃	0.33%
P ₂ O ₅	26.38%	Fe ₂ O ₃	1.19%
SiO ₂	1.66%	CaO	1.33%
U ₃ O ₈	1.17%	MgO	0.11%
Ce ₂ O ₃	24.22%	PbO	0.27%
La ₂ O ₃	29.58%	H ₂ O	0.49%
Y ₂ O ₃	4.45%		

2.3.1.2 OTHER THORIUM-BEARING MINERALS

Thorium forms a minor component of over one hundred other minerals, including niobates, tantalates, titanates, phosphates and silicates [142, 161]. These minerals are usually very low in thorium, or are not considered amongst the primary sources of thorium for some other reason such as rarity or lack of economic motivation.

2.3.1.3 GEOGRAPHICAL DISTRIBUTION OF THORIUM-BEARING MONAZITE RESOURCES

Thorium mineral resources occur in a number of countries. Numerous reports of monazite, thorianite and thorite resources give all three minerals in carbonatites, pegmatites, vein deposits and placer deposits [142, 150-152, 154, 161-166]. This thesis focusses on monazite. It is estimated that total world thorium resources in major deposits are at least 6 million tonnes [166], with total global resources estimated to be 12 million tonnes [34]. The largest thorium-rich mineral resources are Indian beach sands along the country's eastern coast. It is estimated that these sands alone contain one million tonnes of thorium [166]. The Indian nuclear strategy relies on the exploitation of these thorium resources in a closed fuel cycle, as the country has little indigenous uranium and has for a long time been prevented from importing the uranium and nuclear technology due to its status as a non-signatory to the Nuclear Non-Proliferation Treaty [35, 167].

Significant monazite reserves containing ~6% thorium oxide also exist in Brazil, and monazite was worked for its rare earth content in the country from 1949-1992, producing thousands of tonnes of thorium hydroxide concentrate by-product [168]. This thorium hydroxide by-product residue is discussed further in Section 2.3.2.

Rare earth exploration and processing of monazites containing thorium was underway in 2015 in Australia, Brazil, Sweden, North America (Canada, Greenland and the United States), Asia (India, Kazakhstan, Russia, Thailand,

Turkey, Vietnam) and Africa (Kenya, Madagascar, Malawi, Mozambique, Namibia, South Africa, Tanzania) [166]. In addition, valuable thorium resources are available, but not currently worked, in Sri Lanka [169, 170], Malaysia [171] and Norway [151]. India and China are the main producers of monazite, producing of the order of 5000 t/yr in 2005. The economically recoverable thorium resources for countries with large resources are listed in Table 2.2.

TABLE 2.2 – ESTIMATED RESERVES OF THORIUM IN SOME MAJOR SOURCE COUNTRIES, IN TONNES OF THORIUM METAL, AND ESTIMATED THORIUM OXIDE FRACTION WHERE AVAILABLE [34].

COUNTRY	REASONABLY ASSURED RESOURCES /tHM	ESTIMATED ADDITIONAL RESERVES /tHM	THORIUM OXIDE FRACTION IN MONAZITE
India	650,000	–	8.88%
Brazil	606,000	700,000	6.5%
Turkey	380,000	500,000	–
United States	137,000	295,000	3.1% (Florida beach sand)
Norway	132,000	132,000	–
Greenland	54,000	32,000	–
Canada	45,000	128,000	–
Australia	19,000	–	–
South Africa	18,000	–	5.9% (Bulk monazite rock)
Korea	–	–	5.47%
Italy	–	–	11.34%
Malaysia	–	–	8.75%
Sri Lanka	–	–	14.32%

2.3.2 SECONDARY THORIUM RESOURCES

In addition to the primary monazite resources listed in Section 2.3.1, there are also approximately 25,000 t of thorium oxide in monazite processing residues, including those in Brazil discussed in Section 2.3.1.3 [34]. These monazite residues represent a pre-concentrated source of thorium compared to monazite, and are generally much more amenable to dissolution/digestion. Their chemical form is dependent upon the treatment they have received, but they are generally very low in rare earths while still containing the bulk of the actinides, potentially alongside transition metals and other materials whose recovery is not currently economically advantageous [168, 171-173]. A description of the main processes by which these residues are produced is given in Section 2.7. The separation of thorium from monazite residues has been studied in the literature [174, 175].

Separated thorium stocks are held in several nuclear-powered countries, with varying inventory size and material quality. The United States is known to hold a stockpile of 3200 tHM of separated thorium nitrate [176], and France holds a stockpile of 8500 tHM as nitrate and hydroxide [177]. It is highly likely that other countries, such as India and China, also have separated thorium inventories. The UK now holds only a small thorium inventory, being ~200 kgHM thorium oxide held at the Springfields site, with all other thorium materials having now been classified as wastes [61].

2.3.3 THORIUM RESOURCE UTILISATION SCENARIOS

Monazite residues would be an excellent first source for thorium in the event of increasing demand for the metal as a nuclear fuel [178]. While demand for thorium is limited, it is likely that these existing residues will form the primary sources of thorium, followed by new monazite processing by-products as the availability of these stocks becomes limited. However, if demand for thorium were to increase significantly due to the requirements

of a developing fuel cycle, other mineral resources such as thorite would be more likely to be worked for the element [138].

2.4 THORIUM FUEL CYCLE FRONT END

In this thesis a new process for thorium concentrate purification is presented, concerning the decontamination of thorium from some common co-contaminant metals found in monazite and its residues. An impure thorium concentrate feed is assumed, with the goal of producing a high purity thorium product. A brief overview is presented here of current monazite processing, focussing on thorium recovery by solvent extraction.

2.4.1 OVERVIEW OF THORIUM PRODUCTION FROM MONAZITE ORE

Five broad stages can be considered in the processing of monazite-bearing crude heavy mineral sands to produce a nuclear-grade thorium product [107].

1. Extraction of suitable crude heavy mineral sands.
2. Concentration of the monazite from the crude mineral sand (known as beneficiation).
3. Conversion of the monazite concentrate to thorium concentrate.
4. Purification of the thorium concentrate to nuclear grade.
5. Fuel form conversion and fuel fabrication.

A summary of the stages by which a thorium concentrate is produced is presented diagrammatically in Figure 2.17.

As was outlined in Section 2.3.1.1, the two broad types of monazite resources are bulk rock deposits and placer sand deposits. Sand is very much preferred, as collection of sands with little to no overburden is much less expensive than rock mining [34].

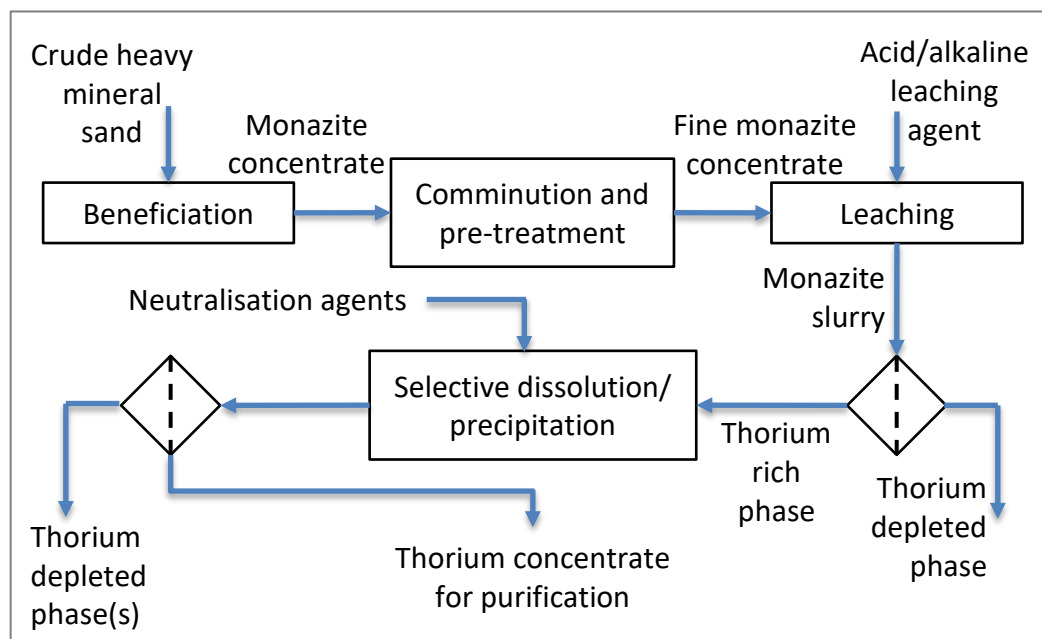


FIGURE 2.17 – BLOCK FLOW DIAGRAM OVERVIEW OF THORIUM CONCENTRATE PREPARATION BY HYDROMETALLURGICAL ROUTE. PREPARED BASED ON INFORMATION AVAILABLE IN [142]

The collected sand must next undergo beneficiation to separate the monazite from the crude mixed sand. Generally wet gravimetric separation is used as the first stage separation, followed by electrostatic and magnetic methods where necessary [179]. Alternatively, floatation separation can be performed using a variety of collectors, although work in this area is ongoing [142, 180, 181]. This produces a concentrated monazite sand, free from other sand components.

2.4.2 MONAZITE CONCENTRATE LEACHING

The next step in the production of nuclear grade thorium is the treatment of the monazite concentrate in order to make the thorium available for purification. Historically two processes were developed for this in the American National Laboratory system; the Sulfuric Acid Process [182, 183] was developed at Ames Laboratory, and the Caustic Soda Process [184, 185] was developed at Battelle Memorial Institute. Excellent information on the development of these processes during the 1940s and 1950s was published following the Atoms for Peace conference in 1958 [142].

Variations of these processes have been used since their development in the 1950s, although sulfuric acid as a monazite leachant had been in use for many years prior to this for the extraction of thorium, primarily for use in gas mantles [186-188]. Both processes call for comminution of the monazite concentrate to increase its surface area, followed by aqueous leaching in order to produce a thorium concentrate. The leaching product is known as a Pregnant Liquor Solution (PLS), and contains the elements leached from the mineral feed. This PLS is then taken through a series of selective precipitation and dissolution steps to produce a thorium concentrate that may be purified by solvent extraction.

These processes have been refined over time [18, 34, 180, 189-191]. Direct leaching with sulfuric acid is considered to be an outdated process, as no version of the process has been found which can separate thorium from the heavy lanthanide elements. Alkaline treatment with sodium hydroxide as a leachant is in use, remaining largely unchanged from the original Caustic Soda process [180, 192]. This process involves treating the finely ground monazite concentrate with 60-70% sodium hydroxide solution at $\sim 150^{\circ}\text{C}$, which dissolves much of the gangue material and converts the monazite to a hydrous metal oxide cake containing the bulk of the thorium, uranium and rare earths. The mineral feed may be heat treated prior to chemical treatment in order to improve digestion and dissolution behaviour [193, 194]. Following alkaline digestion the monazite hydroxide cake may be leached with water or acid to selectively extract the thorium, uranium and mixed rare earths as separate concentrates with varying degrees of purity.

Also in use is a process which reacts monazite with calcium chloride and calcium carbonate at high temperature. The reaction product may be leached with 3% hydrochloric acid to extract the rare earth content. While this reaction offers good thorium separation from rare earths compared to the established acid and alkaline leach processes, thorium is left behind in the solid residue as an impure, insoluble oxide, which is highly resistant to

dissolution [195]. As such the calcium chloride and calcium oxide conversion process will not be further considered in this thesis.

Today many industrial plants use an aqueous alkaline conversion followed by water/acid leaching to dissolve the monazite hydroxide cake [180]. In rare earth processing the rare earths tend to be selectively leached at low acidities, leaving the actinides in the cake, which is then dealt with as a radioactive waste material.

The literature related to monazite decomposition and digestion has been well covered in recent reviews [139, 180], and is a subject of ongoing research [196]. Processes currently in use for rare earth separation include both sulfuric acid and sodium hydroxide leaching. However, for thorium separations, alkaline processing is preferred [34, 42].

2.4.3 THORIUM CONCENTRATE PURIFICATION

The next stage for a thorium fuel cycle is to take the thorium concentrate produced by the monazite leaching and purify it to the point where it may be converted to an appropriate chemical form for nuclear fuel fabrication.

Commonly such a purification step is performed by a hydrometallurgical method, typically solvent extraction, with the final product being purified thorium nitrate or thorium oxalate [34, 189]. The aim of this process is to decontaminate the thorium concentrate by removing any co-contaminants which would cause deleterious effects in the reactor, by either absorbing neutrons required for the fission chain reaction, or by affecting the thermal, physical or chemical properties of the fuel itself.

It is this stage of the front end processing which is treated in detail in this thesis, and so further detail on the current state-of-the-art in this area is given below in Section 2.8.

2.4.4 FUEL FORM CONVERSION

Following purification, the thorium product may be converted to the required chemical form for fuel production. Currently thorium oxide, chloride and fluoride are being considered for development, although metallic thorium or other novel fuel types are not outside the scope of consideration [197].

Thorium nitrate is often produced during thorium purification processes as a pre-cursor to it being converted to a final oxide, halide or metal form. The thorium hydroxide cake is dissolved in nitric acid and solvent extraction with TBP is used to produce a purified thorium product, similar to the PUREX process described in Chapter 1. Further details on this process are given in Section 2.7.1 below.

Thorium oxide may be calcined directly from the nitrate, or first by conversion to thorium oxalate, which gives improved properties in filtration, drying and calcination to produce a thorium oxide powder product [142, 198].

2.4.5 THORIUM OXIDE PELLET FABRICATION

Thorium oxide fuels must finally be fabricated into solid fuel pellets prior to assembly, which may be achieved by sintering a compressed powder pellet. Fuel pellet density is a key parameter which must be optimised in order to give the best reactor performance [20]. The sinterability of the thorium oxide powder is dependent on the process by which it was produced [129, 198].

2.5 THORIUM FUEL CYCLE BACK END

The back end of the thorium fuel cycle is largely akin to the back end of the uranium fuel cycle, with the key distinction being in the motivation for why the fuel may or may not be reprocessed. If the fuel cycle is closed, it is

usually to recover the uranium in order to reuse the ^{233}U , generally to produce a ^{233}U -Th “equilibrium” fuel. The thorium may also be recovered in order to minimise the requirement for fresh thorium [104, 199, 200]. The main proposed method for thorium fuel reprocessing is the Acid THOREX process, which is described in Section 2.7.1 [104, 201, 202]. Other solvent extraction processes may be able to give better separation of thorium and/or uranium from other components. However, recent separations studies for thorium reprocessing applications are limited in the scientific literature. Instead, the great majority of publications are related to the fuel cycle front end. However, once the spent fuel has been rendered into aqueous solution, there is little chemical difference between this solution and the pregnant leachate solution from minerals processing. As such, the literature related to front end processing is also useful when considering the back end, and *vice versa*. Therefore, the literature review of thorium solvent extraction studies presented in Section 2.8 below may be considered to be applicable both for the front end and the back end. The major difference between the two applications is the presence of a strong radiation field in the back end, which would need to be considered during the development of any reprocessing system.

If an open fuel cycle is preferred, this is usually for reasons for economics or non-proliferation [121]. Directly disposing of thorium fuel means that the ^{233}U is disposed alongside its ^{232}U , ^{232}Th and highly active fission products/minor actinides. This eliminates the high costs associated with reprocessing, while making it more difficult for a would-be proliferator to acquire and separate the fissile material [109, 116].

2.6 PRINCIPLES OF SOLVENT EXTRACTION

Full details on solvent extraction systems are provided in the literature [74-77, 79, 123, 203]. In solvent extraction systems, two immiscible solutions are dispersed into one another to give a large contact surface area between

them. The solutions are known in solvent extraction as phases. One phase, usually aqueous, will contain one or more target solutes and potentially some unwanted material such as contaminants. The second phase will be, or contain, an extractant which forms complexes with some of the solutes. This second phase is often termed the solvent, or organic phase, as many common extractants are organic materials, and tend to be dissolved in a non-polar organic solvent known as a diluent. Species from each phase react and bind to form new complexes which are extracted.

Individual complexes have different preferences for each phase, distributing to some level across the two phases. The degree of distribution across the phases of a given species is often expressed as a distribution ratio, as expressed in Equation (2.8) [77].

$$D_M = \frac{[\bar{M}]}{[M]} \times \frac{V_{aq}}{V_{org}} \quad (2.8)$$

Where D_M is the distribution ratio of species M,

$[\bar{M}]$ is the concentration of M in the organic phase,

$[M]$ is the concentration of M in the aqueous phase,

V_{aq} is the volume of the aqueous phase, and

V_{org} is the volume of the organic phase.

As such, for equal volumes of the aqueous and organic phase, an extracted species will have $D_M > 1$, while a rejected species will have $D_M < 1$. In addition, the separation factor for two metals $\alpha_{M,M'}$ is defined in Equation (2.9) [77].

$$\alpha_{M,M'} = \frac{D_M}{D_{M'}} \quad (2.9)$$

D_M may be controlled by careful selection of the contact conditions and phase chemistry. Generally systems are designed such that complexes comprising the target solutes and the extractant will be partitioned into the

organic phase, while any unwanted materials will be left behind in the aqueous phase [74, 76].

After a suitable time in contact, the phases are separated, and the organic phase containing the target ion(s) may then be contacted with another phase, known as the back-extraction or stripping phase. The contact time is determined by the kinetics of complex formation and phase separation, and the thermodynamic endpoint of the complexation reaction where the complex is in equilibrium with the free extractant and target solute [77]. This adjusts the conditions such that formation of the solute-extractant complex is no longer favoured, and the target solute is recovered into the stripping phase. In a well-designed system the contaminants and other solutes will have either remained in the aqueous phase, or not been stripped from the organic phase, leaving the purified target solute(s) in the stripping phase.

If required the loaded organic phase may be contacted with a “scrub” solution prior to back-extraction. This solution retains the target solutes in the organic phase, but should collect any unwanted material which must be removed prior to back-extraction of the target solutes.

An example of a solvent extraction process used in the nuclear industry is given below.

2.6.1 SOLVENT EXTRACTION EXAMPLE: THE PUREX PROCESS

Solvent extraction is a process which is used regularly in the nuclear industry in uranic spent fuel reprocessing, in the PUREX (Plutonium-Uranium Redox Extraction) Process [15, 75]. The PUREX process takes a feed of spent uranic nuclear fuel and produces three aqueous product streams of separated uranium, separated plutonium, and a mixed stream of fission products and minor actinides. Spent nuclear fuel is dissolved in strong nitric acid and then mixed with a solution of 30% tributyl phosphate

(TBP), termed the extractant, in an odourless kerosene diluent. The organic phase is hydrophobic, and so mechanical force is applied to disperse the organic and aqueous phases into one another, maximising the interfacial surface area between the phases during the contact period. After mixing, the two phases settle and separate, with the organic phase collecting on top of the aqueous phase [204, 205].

The distribution ratios for tetravalent and hexavalent uranium, plutonium and thorium as a function of nitric acid concentration are presented in Figure 2.18. The system redox conditions are set such that uranium exists in as U(VI) and plutonium as Pu(IV). It can be seen in Figure 2.18 that these ions preferentially form hydrophobic nitrate complexes with TBP at high acid concentration, which are partitioned into the organic phase. The unwanted fission products and transuranic elements do not form strongly extracted complexes with the TBP, and remain in the aqueous phase.

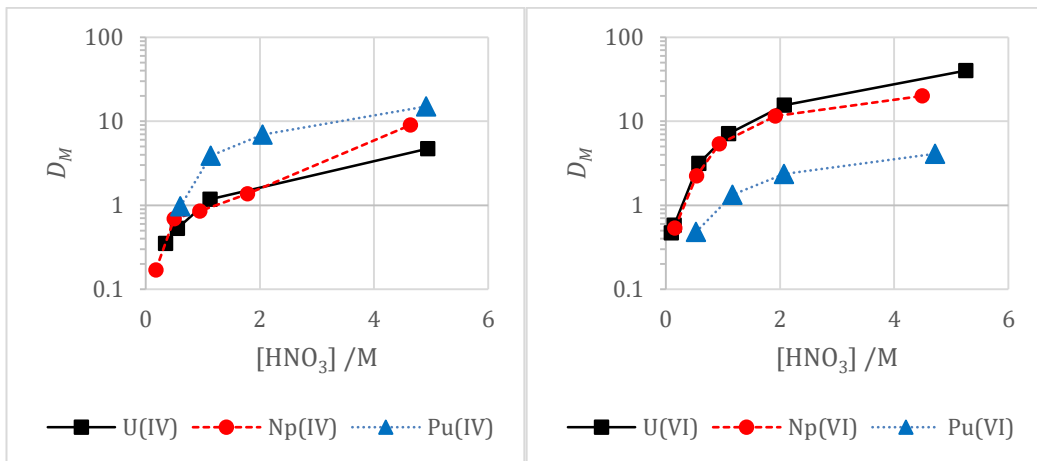


FIGURE 2.18 – DISTRIBUTION RATIOS FOR TETRAVALENT AND HEXAVALENT URANIUM, NEPTUNIUM AND PLUTONIUM AS A FUNCTION OF NITRIC ACID CONCENTRATION WITH 30% TBP IN ODOURLESS KEROSENE DILUENT. IMAGE REPRODUCED FROM DATA PUBLISHED IN [70].

The organic phase, loaded with U and Pu, is then contacted with a scrubbing solution, specifically fresh nitric acid without metals in solution, to which any fission products or minor actinides in the organic phase are returned. The scrubbed organic phase is then sequentially contacted with two back-

extraction, or “stripping”, media, each of which induce conditions such that one of the actinide complexes is no longer favoured, and the metal is selectively returned to the stripping medium. In the case of PUREX, the first stripping medium is ferrous sulfamate solution, which selectively reduces Pu(IV) to Pu(III). Trivalent Pu does not form an extractable TBP complex, and is rejected to the aqueous phase [70, 77]. U(VI) is then stripped with dilute nitric acid. The organic phase is finally stripped of all remaining metals and refreshed for reuse. Gradually the organic phase undergoes radiolytic damage and the TBP breaks down. TBP degradation products are removed during the solvent recycling circuit.

A diagram showing the key elements of the process is shown in Figure 2.19, with accompanying notes in Table 2.3. At-scale, the process is run continuously, in counter-current mixer-settlers or pulsed columns [75, 77]. However, for clarity it is presented here as a batch process in separatory funnels, as it might be performed in a laboratory.

Other solvent extraction processes have different target metals and contaminants, and use many different aqueous media, extractants, and diluents, as well as additional chemicals to perform functions such as the prevention of phase separation or plant equipment corrosion.

2.7 HISTORICAL THORIUM PURIFICATION PROCESSES

The purification of thorium concentrates was first carried out by solvent extraction in the 1950s, using extraction chemistry similar to that of the PUREX process. This process, known as Acid THOREX (THORium EXtraction), was originally designed for use in the back end of the fuel cycle for aqueous reprocessing of thorium fuels [104]. However, the Acid THOREX process is known to be currently in use for front end thorium purification from monazite residues [206]. Also developed at the time was the Interim-23 Process [202].

Solvent extraction is already well developed in the nuclear industry, and to switch to other processes, particularly non-aqueous processes, would be very difficult. The nuclear industry is very conservative, and does not adopt new processes easily. It is hoped that this work can supply an advantageous process chemistry for thorium separations, while retaining technologically mature approaches based on well-known and readily available extraction media.

Having said this, interesting developments in the application of solvent extraction chemistry are ongoing beyond traditional two-phase methods for thorium and uranium separation. Supported Liquid Membrane (SLM) methods offer advantages in meeting some of the difficulties of solvent extraction processes [207]. Supercritical fluid extraction and stripping is also under consideration [208, 209]. These advanced variations in solvent extraction methods are developing, and may form the basis of actinide separations processes in the future. However, in this thesis only traditional solvent extraction methods are considered in detail.

2.7.1 THE ACID THOREX PROCESS

In the back end application of the Acid THOREX Process, thorium and uranium are co-extracted from a dissolved spent fuel feed in strong nitric acid by 30-45% TBP in *n*-dodecane or *n*-paraffin, leaving fission products behind. The actinides are then separated by selective back-extraction using approximately 0.2 M nitric acid for thorium back-extraction, followed by 0.05 M nitric acid for uranium back-extraction, producing a thorium nitrate solution from which a thorium nitrate product may be precipitated. The distribution ratio for uranium extraction from 5 M nitric acid solutions by various concentrations of TBP in *n*-dodecane is presented in Figure 2.20. Versions of the process also exist where low TBP fractions (3-8%) are employed, selectively extracting uranium and leaving thorium in the aqueous raffinate [104, 210, 211].

THE PREPARATION AND APPLICATION OF THORIUM-BASED NUCLEAR FUELS

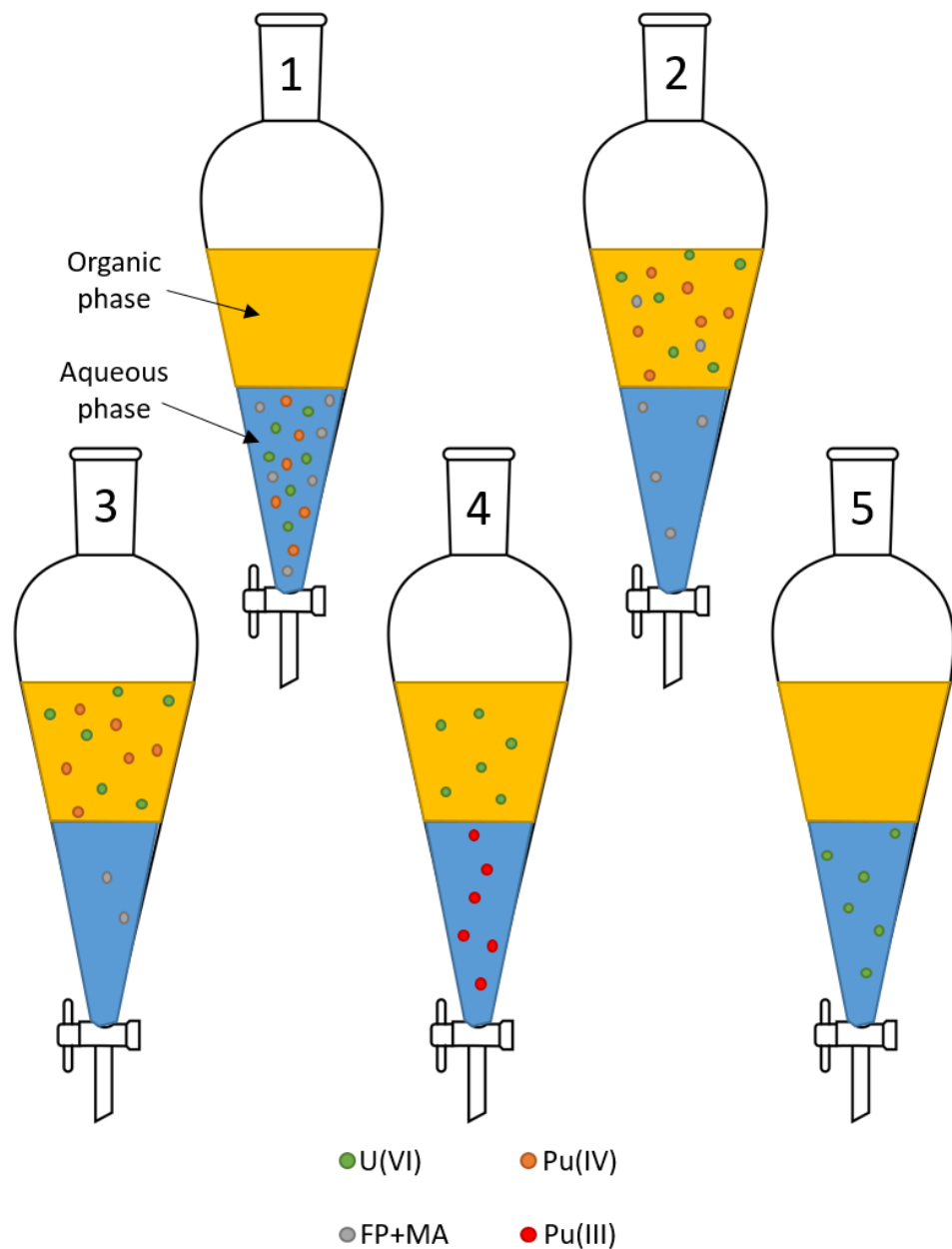


FIGURE 2.19 – KEY STAGES OF THE PUREX PROCESS, REPRESENTED IN SEPARATORY FUNNELS. THE TBP IN KEROSENE ORGANIC PHASE (YELLOW) IS LIGHTER THAN THE NITRIC ACID AQUEOUS PHASE (BLUE), AND SITS ABOVE IT WHEN NOT UNDERGOING AGITATION TO CONTACT THE PHASES. FP = FISSION PRODUCTS; MA = MINOR ACTINIDES. SEE ACCOMPANYING NOTES IN TABLE 2.3 BELOW

TABLE 2.3 – ACCOMPANYING NOTES FOR FIGURE 2.19. BETWEEN EACH STEP ARE INCLUDED NOTES ON HOW TO PROCEED TO THE FOLLOWING STEP.

#	AQUEOUS PHASE	ORGANIC PHASE	STATUS OF PROCESS
1	Spent fuel feed – nitric acid with U, Pu, FP+MA.	TBP in kerosene, no metals.	Before extraction contact.
Perform phase contact by agitating and allow to settle.			
2	Bulk of FP+MA in feed nitric acid.	Bulk of U and Pu complexed with TBP. Some FP/MA.	After extraction contact, but before scrubbing contact.
Remove aqueous phase. Contact with “fresh” nitric acid to scrub.			
3	Back extracted FP & MA in “fresh” nitric acid strip solution.	Actinide-TBP complexes in kerosene diluent.	After scrubbing contact, before Pu stripping contact.
Remove scrub acid. Add ferrous sulfamate in nitric acid as aqueous.			
4	Pu(III) stripped into ferrous sulfamate solution.	Uranium-TBP complexes in kerosene diluent.	After Pu stripping contact, before U stripping contact.
Remove aqueous phase containing Pu(III). Add dilute nitric acid.			
5	U(VI) stripped into dilute nitric acid.	Slight remainder of metals for clean-up prior to recycle.	After U stripping contact, prior to solvent recycling.
Clean up organic phase and reuse.			

Thorium is not particularly well extracted by TBP even at high acid concentrations, but under the correct conditions can be extracted sufficiently for the process [201, 202, 212]. Third phase formation is also an issue at high thorium loadings [80]. Third phases in solvent extraction are distinct phases which form during the solvent extraction contact, often due to a splitting of the organic phase into two parts, one of which is rich in diluent and the other of which is depleted in diluent, being a heavier organic

phase comprised of the extracted metal ligand complex. This is due to the organic diluent in the light organic phase reaching its solubility limit for the metal ligand complex, meaning that any additional complex forms a third phase [77].

In spite of these issues the process has been used historically for thorium separations in the USA and the UK, and is in use elsewhere today [104]. Perhaps the main reason for this is that the process can be run on lightly modified PUREX plants, and as such a good amount of relevant operational experience exists. A number of variations to the core process have been proposed and are in use at various scales around the world. Significant detail on the Acid THOREX process is given in various sources [104, 201, 202].

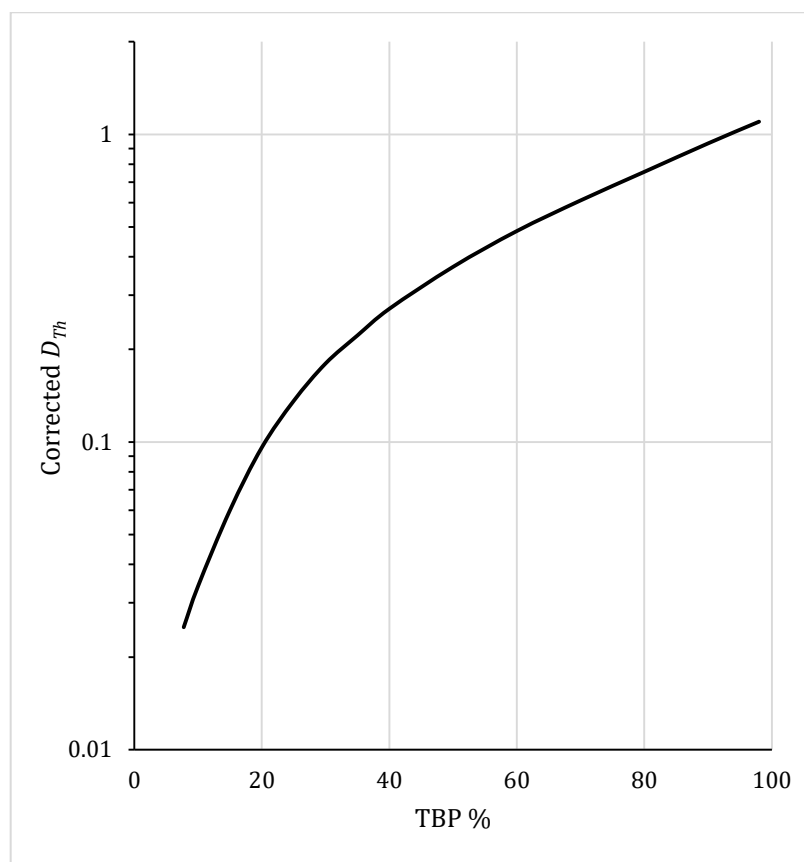


FIGURE 2.20 – EFFECT OF TBP CONCENTRATION IN ORGANIC PHASE ON THORIUM EXTRACTION FROM 5 M HNO_3 WITH 8 g/l PHOSPHATE AND 9.5 g/l SULPHATE IONS. Y-AXIS CORRECTED TO A DILUENT-FREE BASIS. IMAGE REPRODUCED BASED ON DATA PUBLISHED IN [142].

2.7.2 THE INTERIM-23 PROCESS

The Interim-23 Process was designed for spent fuel processing and recovers uranium only, leaving thorium in the aqueous raffinate, which was deemed desirable due to the highly active ^{228}Th decay daughter ^{208}Tl [213]. This is useful in a thorium fuel cycle to separate ^{233}U where thorium would not be recycled. The Interim-23 Process and related systems are therefore unsuitable for thorium recovery.

In the process either di-sec-butyl phenyl phosphonate in di-ethyl-benzene or low concentration TBP in *n*-dodecane are used as extractants against a nitrate feed, with an acid deficient scrub used to return thorium to the aqueous raffinate [202, 213].

2.8 SOLVENT EXTRACTION OF THORIUM

Much research has been carried out into alternative separations schemes for thorium. For the fuel cycle front end, solvent extraction schemes are the most often reported in the recently published scientific literature, followed by ion exchange approaches. Historically there is much data on selective precipitation/dissolution approaches, although advances in this area are now less often reported.

The first solvent extraction separations for thorium used tributyl phosphate in kerosene as the organic phase [142]. Since then many other extractants have been developed and investigated, with ongoing research being published into both existing extractants under new conditions as well as newly synthesised novel extractants. In this section the range of extractants tested for thorium separations in solvent extraction systems is reviewed.

In the development of extraction processes, much research effort is focussed on the development of new extractant chemicals capable of performing highly selective extraction of specific metals. However, there exist already

numerous extractants capable of performing metal separations with varying degrees of success which have not been fully investigated.

Mixtures of multiple extractants may be used to achieve synergic effects. The definition of synergism in solvent extraction is that greater extraction is given by a mixture of extractants than is achieved by the sum of the extractants working individually under similar conditions [214]. Synergism is most commonly observed with mixtures of chelating extractants and solvating extractants, and is thought to be due to the solvating extractant increasing the hydrophobicity of the metal ligand complex compared to the complex formed by the chelating ligand alone [214, 215]. This can occur through three mechanisms:

- The chelating extractant alone does not fill all metal coordination sites, some of which are occupied by hydration water. The solvating extractant fills these remaining sites.
- The solvating extractant opens up one or more of the chelate binding site rings and binds to these sites instead, increasing the number of bound extractant ligands.
- The metal coordination sphere does not change its hydration number, but expands to accept the solvating extractant.

Synergic effects are a subject of particular interest in this thesis, as combinations of well-established extractants may give improved extraction behaviour without the requirement for novel extractants. Synergic mixtures can give improved extraction compared to the individual extractants, with a relatively minor increase in cost and system complexity, while the development of a new extractant from scratch requires a long process of basic research and development into the nature and synthesis of the extractant and the possibility of novel and/or challenging extraction conditions.

The opposite of synergism is antagonism, where the extraction is less than the sum of the extraction given by the individual extractants. Antagonism is often due to extractants preferentially binding to one another rather than forming an extracted hydrophobic metal complex.

In the remainder of this section, a wide range of previously studied extractants for thorium are presented. It is necessary to understand how well the system separates thorium from other metals. In this case these other metals would include the rare earth elements and uranium from monazite, as well as any other elements in the monazite or thorium concentrate. The behaviour of other metals is not discussed here for the sake of brevity, however, the references cited here most often do consider separation of uranium and/or rare earth elements. The purification of uranium and individual rare earth elements are topics which receive much attention in the literature [42, 139, 180, 216-222].

2.8.1 SOLVENT EXTRACTION MECHANISMS

Extractants and extraction conditions are usually chosen in order to separate specific target ions with a high degree of selectivity. Hydrophobic metal-extractant complexes may form through a number of mechanisms, which are well-detailed in a variety of sources [74, 76, 77, 79]. Indicative interfacial reactions for the three key extraction mechanisms seen in this thesis are given in Table 2.4.

TABLE 2.4 – BIPHASIC EXTRACTION EQUILIBRIA OF THREE KEY COMPLEXATION MECHANISMS [76].

MECHANISM	INDICATIVE COMPLEXATION REACTION
Cation exchange	$M^{c+} + n\overline{HL} \rightleftharpoons \overline{ML}_n + cH^+$
Anion exchange	$M^{c+} + cX^- + \overline{A^+X^-} \rightleftharpoons \overline{MX}_{c+1}A$
Solvation	$M^{c+} + cX^- + n\overline{S} \rightleftharpoons \overline{MX}_cS_n$

In general, acidic extractants are cation exchangers, which exchange protons for metallic cations. The most common anion exchangers for thorium extraction are amine extractants, which form complexes with negatively charged metallic species. Solvating extractants form neutral adducts with charge neutral metallic species.

A special class of extraction reagents are chelating reagents, which are polydentate extractants which bind to multiple sites on the target ion, and as such generally form very strong complexes.

In the following sections, the previous literature related to thorium extraction is discussed.

2.8.2 TRIBUTYL PHOSPHATE EXTRACTION

TBP is a solvating extractant, which forms hydrophobic neutral adducts with uranium(VI), thorium(IV) and plutonium(IV). Tri-n-butyl phosphate remains a very commonly used extractant today, despite it being first developed in the 1940s and 50s [81, 82, 142, 223-225]. TBP is a phosphate ester, the general formula of which is $P(=O)(OR)_3$. As was discussed in Section 2.7.1, TBP does not complex thorium particularly well. It is also relatively soluble in water, and there is a possibility of third phase formation due to the limited solubility of the extracted $Th(NO_3)_4 \cdot TBP$ adduct in the organic diluent and the low stability constant of the thorium TBP complex [211]. Extractions from iodide and bromide media have also been studied [226].

Other phosphate esters have been investigated in an attempt to address the limitations of TBP. Tri-sec-butyl phosphate has been found to give better thorium separation from uranium and a reduced tendency to third phase formation compared to TBP [211]. Tri-isobutyl phosphate, tri-n-amyl phosphate, tri-isoamyl phosphate and tri-n-hexyl phosphate have also been investigated. Branched alkyl chains were found to have little effect on

thorium complex solubility, but increasing the length of the alkyl chain was found to greatly reduce tendency to third phase formation [227].

The addition of aliphatic alcohols or mixed halides to the aqueous media have been found to affect TBP extraction [228]. The effect of diluent has also been studied, with kerosene found to perform better than a range of other hydrocarbon diluents [229].

TBP is still undergoing research, although this is more into operational considerations rather than the extraction chemistry [230, 231]. Work is also ongoing into the use of TBP in synergic systems with other extractants. As a solvating extractant it is often paired with acidic cation exchange extractants to give synergic extraction. Further detail on such systems is given below.

2.8.3 PHOSPHINE OXIDES

In the mid-1950s, work was undertaken into phosphine oxides [232, 233], another solvation extractant family with general formula $P(=O)R_3$. The most commonly used of these is trioctyl phosphine oxide (TOPO), named commercially as Cyanex 921. There also exists Cyanex 923, a mixture of TOPO and trihexyl phosphine oxide (THPO). See Section 2.8.4.3 for further detail on the Cyanex family of extractants.

TOPO has been found to give better extraction of thorium from nitric and hydrochloric acid solutions than TBP [234-236]. TOPO has also been investigated in an SLM system, and was found to slightly extract thorium from nitrate media, back extracting into carbonate media [237]. Cyanex 923 has also been found to give good extraction of thorium in an SLM system from hydrochloric acid into ammonium carbonate solution [238]. Cyanex 923 gives good thorium extraction from concentrated sulfuric acid solutions [239].

Carbamoyl methyl phosphine oxides (CMPO) have also been investigated. Such extractants have been proposed for addition to the PUREX process in

order to extract transuranium elements from spent nuclear fuel [71]. Octyl(phenyl)-N,N-diisobutyl carbamoyl methyl phosphine oxide (O Φ CMPO) has been investigated for thorium extraction from nitric acid, particularly third phase formation in this system [240], and as part of an SLM system [205].

2.8.4 PHOSPHOROUS ACIDS

Phosphorous acid extractants have the general formula $X_2P(=O)(OH)$, where X represents alkyl, oxalkyl or other moieties. They can be subgrouped as phosphoric acids $(RO)_2P(=O)(OH)$, phosphonic acids $(RO)RP(=O)(OH)$ and phosphinic acids $R_2P(=O)(OH)$. The extraction mechanism for phosphorous acids is cation exchange, where the metal cation exchanges for the acid proton. The extractant basicity increases in the order phosphoric < phosphonic < phosphinic, due to the decreasing electronegativity brought by the reduced number of oxygen atoms in the phosphonic/phosphinic acid, thus strengthening the OH bond in the molecule.

2.8.4.1 PHOSPHORIC ACID EXTRACTANTS

In the late 1950s work began into the study of dialkyl phosphoric acid extractants for actinide separations [241, 242]. Of these the most reported in the literature today is di-(2-ethylhexyl) phosphoric acid (HDEHP, DEHPA or D2EHPA), also named as TOPS 99 and P204.

HDEHP extracts thorium well from sulfate media [86, 87, 193, 239], chloride media [87, 88] and nitrate media [243]. From sulfate media the best extraction is given by petroleum ether as diluent [86]. In another study HDEHP was found to extract thorium moderately under a range of conditions [244]. The effects of mixed acid media and water-soluble alcohols in the aqueous phase on thorium extraction by HDEHP have also been investigated, and these factors were found to strongly influence the extraction behaviour [87, 228]. Extractions from bromide and iodide media

have also been studied by HDEHP [226]. Mixtures of HDEHP and TOPO have been found to give slight synergism in chloride media [245]. Mixtures of HDEHP and Cyanex 923 have been found to extract thorium from sulfate media [239]. An SLM system using HDEHP has been studied, using an electric current to drive the extraction [246].

Other phosphoric acid extractants have also been studied. Bis para-octylphenyl phosphoric acid (HDO Φ P) extracts thorium well from chloride media [247]. The interfacial behaviour of di-n-octyl phosphoric acid (HDOP), bis(2,2-dimethylhexyl)phosphoric acid (HDNOP), bis(hexoxyethyl) phosphoric acid (HDHoEP) and bis(diisobutylmethyl) phosphoric acid (HD(DIBM)P) have been studied, and it is suggested that some of these may be used as extractants for thorium [248].

The extraction of thorium from nitrate media by bis(4-ethylcyclohexyl) hydrogen phosphate (D4ECHPA) and bis(4-cyclohexyl-cyclohexyl) hydrogen phosphate (D4DCHPA) were also investigated. These were found to give consistently higher extraction than HDEHP [243].

Di(1-methylheptyl) methyl phosphate, also known as P350, was found to give poor thorium extraction from hydrochloric acid media [249].

2.8.4.2 PHOSPHONIC ACID EXTRACTANTS

The study of phosphonic acids and phosphonate extractants also began in the late 1950s [250]. The most commonly reported of these in the literature is 2-ethylhexylphosphonic acid mono-2-ethylhexyl ester, known as PC-88a, and this extractant is used today for industrial thorium separations in India, in the THRUST process (Thorium Retrieval, Uranium Recovery and Restorage of Thorium Oxalate), which is shown in a block flow diagram in Figure 2.21. It can be seen in Figure 2.21 that a step is required prior to thorium extraction to separate uranium and iron.

Other acronyms for this extractant are HEHEHP and EHEHPA, and commercial names include P507 and Ionquest 801. In this work the extractant is referred to as PC-88a.

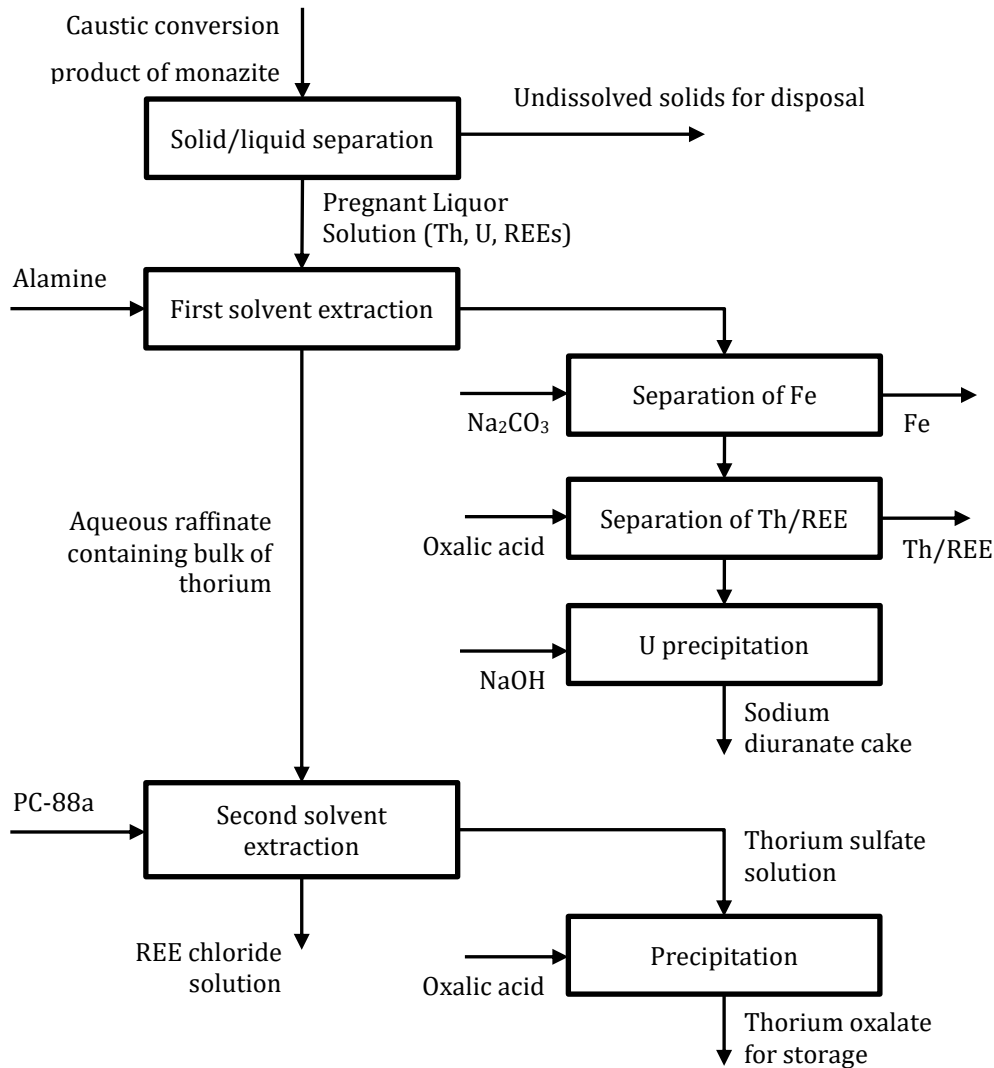


FIGURE 2.21 – THE THRUST PROCESS, USED IN INDIA TO RECOVER THORIUM, URANIUM AND RARE EARTH ELEMENTS FROM MONAZITE [34].

PC-88a has been investigated as an extractant for monazite separations from chloride media [221, 251, 252]. Extractions of thorium from nitrate media [84, 85, 236, 253] and sulfate media [254, 255] have also been studied. Stripping of thorium from PC-88a with sulfuric, nitric and hydrochloric acids found that sulfuric acid stripping was the most effective

[83]. Mixtures of PC-88a and Cyanex 923 give slight thorium extraction [239].

2-ethylhexyl phenylphosphonic acid HEHΦP has been found to extract thorium from nitric acid media [256, 257].

Two other phosphonates which have been studied are diamylbutyl phosphonate (DABP) and diamylamyl phosphonate (DAAP), which have been compared with TBP [258]. Di(1-methyl-heptyl) methyl phosphonate (DMHMP) was found to extract thorium well from nitrate media, giving good separation against uranium as compared to TBP [259].

Dibutylpropyl phosphonate (DBPrP) and Dibutylpentyl phosphonate (DBPeP) have also been studied for thorium separations from nitrate media, and found to perform better than TBP [260].

Thorium is extracted with slight synergism from HCl by mixtures of HDEHP and di-(2-ethylhexyl) 2-ethylhexyl phosphonate (DEHEHP) [245].

2.8.4.3 PHOSPHINIC ACID EXTRACTANTS

The most basic of the phosphorous extractants are the phosphinic acids. A number of commercial phosphinic acid extractants are produced by Cytec under the trade name Cyanex, and these are commonly studied in the literature [261].

Cyanex 272 (bis(2,4,4-trimethylpentyl) phosphinic acid) was found to be a poor thorium extractant from low concentrations of HCl, but the extraction could be improved by combination with PC-88a [252]. Extraction with Cyanex 272 is also poor from sulfate media, but is very strong from nitrate media [86, 244, 254, 262, 263]. TBP and TOPO were found to greatly increase thorium extraction with Cyanex 272 from nitrate media [264]. Mixtures of Cyanex 272 and Cyanex 923 give slight extraction of thorium [239]. Also investigated were mixtures of Cyanex 272 and TBP [265].

2.8.5 CARBOXYLIC ACID EXTRACTANTS

Carboxylic acids are another example of cation exchange extractant. They have received much less attention in thorium separations than phosphorous based extractants. One of the major problems with such extractants is their relatively high solubility in aqueous media, resulting in solvent loss and reduced extraction of the target metal [86].

The use of oleic, palmitic and lauric acids was investigated for thorium extraction from nitrate media, and these were found to load large amounts of thorium per gram of extractant, although thorium was not partitioned particularly strongly into the organic phase [266].

The addition of phosphoryl groups to carboxylic extractants for thorium extraction has also been studied [267]. Carboxyl groups often form a part of complex extractants, some of which will be detailed below.

2.8.6 SULFUR-BASED EXTRACTANTS

Sulfur based extractants have also been investigated for thorium separations, either as sulfoxides or sulfonic acids, to replace phosphine oxides and phosphonic acids respectively.

2.8.6.1 SULFOXIDE EXTRACTANTS

Sulphoxide extractants function by a solvation mechanism. Dipentyl sulfoxide (DPSO) has been found to give strong thorium extraction from concentrated hydrochloric acid media [268]. However, DPSO, diphenyl sulphoxide (DPhSO) and di-n-octyl sulphoxide (DOSO) were not found to give greater extraction than TBP, either alone or in combination [269]. Dihexyl sulfoxide (DHSO) was found to be a poor thorium extractant from hydrochloric acid, although the addition of lithium chloride improved extraction [235]. Petroleum sulfoxides likewise gave poor thorium extraction [270].

Five sulfoxides were compared to TBP and found to give broadly comparable thorium extraction to TBP from nitrate media. These were Di(2-ethylhexyl) sulfoxide (DEHSO), Di(1-methylheptyl) sulfoxide (DMHpSO), 2-ethyl hexyl-*p*-methylphenyl sulfoxide (EHMPSO), *n*-dodecyl *p*-methylphenyl sulfoxide (DpEPSO) and Di(*p*-methylphenyl) sulfoxide (DEPSO) [271].

2.8.6.2 SULFONIC ACID EXTRACTANTS

Aryl sulfonic acids are another type of sulfur-based extractant which has received some attention for use with thorium. These extractants function by cation exchange [256].

Dinonyl naphthalene sulfonic acid HDNNS very slightly extracts thorium, although the mixture with HEHΦP gives strong synergic extraction [256, 257]. HDNNS is more commonly used for magnesium extraction, under the trade name Synex 1051 [261].

The sulfonic acid extractant (2-[(2-arsenophenyl)-azo]-1,8-dihydroxy-7-[(2,4,6-tribromophenyl)azo]-naphthalene-3,6-disulfonic acid) has been studied for thorium extraction from monazite components by capillary electrophoresis [272]. Also studied for thorium separation was 2-carboxy-2'-hydroxy-3',5'-demethylazobenzene-4-sulphonic acid [273].

2.8.7 THIOPHOSPHOROUS ACID EXTRACTANTS

Sulfur and phosphorous combine in thiophosphorous extractants, which are cation exchangers. Cyanex 272 has two thiophosphorous analogues. Cyanex 301 is bis(2,4,4-trimethylpentyl)dithiophosphinic acid, and Cyanex 302 is bis(2,4,4-trimethylpentyl) monothiophosphonic acid.

On average, across a range of extraction conditions, Cyanex 302 was found to extract thorium less well than Cyanex 272 [262]. A Taguchi analysis was carried out on the two thiophosphorous Cyanex reagents and TBP, extracting from HCl, HNO₃ and H₂SO₄ media, and it was found that Cyanex 302 was a good extractant for thorium at a range of acidities in all studied

aqueous media [263]. Mixtures of Cyanex 272 and 302 were found to give greater extraction than Cyanex 272 alone from nitrate media, although extraction was less favourable than mixtures of Cyanex 272 and TOPO [264].

A variety of Cyanex 272, 301 and 302, and PC-88a combinations have been tested for thorium extraction from hydrochloric acid media [252]. The thiophosphonic acid extractants are less efficient than Cyanex 272 or PC-88a in nitric acid media, but more efficient in sulphuric acid media. Cyanex 301 and 302 give synergism when mixed with TBP or DOSO [254].

2.8.8 AMINE EXTRACTANTS

The above described acidic extractants function by a cation exchange mechanism. A large number of basic amine extractants exist also, which function by anion exchange. They may be classified by the number of substituents around the nitrogen centre.

Amine extraction for thorium dates again from the 1950s, when it was applied to the sulfuric acid digested monazite in the AMEX (Amine Extraction) process. Early research into a variety of amine extractants showed that primary amines are the strongest thorium extractants from sulfate media [274].

One of the main perceived advantages of amine extractants is that they can be completely decomposed at high temperatures, unlike phosphorous or sulfur extractants, leaving no solid/liquid nuclear wastes requiring management. This is due to their being composed of only of carbon, hydrogen, oxygen and nitrogen, and is known as the CHON principle [275, 276].

2.8.8.1 PRIMARY AMINES

Branched primary amine extractants generally give strong thorium extraction [274]. The tri-alkyl-methylamine extractant Primene JM-T $(\text{CH})_3\text{C}(\text{CH}_2\text{C}(\text{CH}_3)_2)_4\text{NH}_2$ is a relatively commonly used primary amine

extractant [277]. Extraction of thorium from citric acid media with Primene JM-T has been investigated [278].

The primary amine N1923 (NH_2CHR_2 where $\text{R} = \text{C}_8\text{-C}_{10}$ [279]), has been found to give good thorium extraction from nitrate media [280] and sulfate media [281].

Octylamine and the branched *tert*-octylamine were found to give comparable extraction kinetics in sulfate media to HDEHP and Cyanex 272. These amines extracted almost no thorium from sulphate media at pH 1, but extraction was >90% at pH 1.5 [86].

2.8.8.2 SECONDARY AMINES

Secondary amines may give slight or strong extraction of thorium according to the degree of alkyl branching. Generally speaking, as the branching approaches closer to the nitrogen centre, the strength of extraction reduces [274]. Comparatively little research has been carried out into secondary amines.

Amberlite LA-1 (dodecanyl-trialkylmethylamine) was found to give poor thorium extraction from hydrochloric acid media [282]. Di-*n*-octylamine (DNOA) and di-(tridecyl)amine (DTDA) were found to give strong thorium extraction from dilute sulfuric acid solutions [283].

2.8.8.3 TERTIARY AMINES

Tertiary amines are the most studied sub-group in the literature. A variety of commercial extractants are sold under the brand Alamine, particularly Alamine-308 (triisooctylamine), Alamine-310 (triisodecylamine) and Alamine-336 (a mixture of the above). A Chinese variant of Alamine-336 is known as N235 [231, 249].

Alamine-336 extraction is often reported in the literature. Thorium has been found to be well extracted from strong lithium chloride solutions at low

acidity by Alamine-336 in cyclohexane. Higher ionic strength is required if bromide were used instead of chloride in order to achieve the same extraction efficiency [284]. Other studies have also found thorium to be poorly extracted by Alamine-336 from strong HCl solutions [285, 286]. Strong nitric acid solutions however give good extraction [286]. Cyanex 301 and 302 have been found to give strong antagonism in combination with Alamine-310 from hydrochloric acid solutions [252].

Tri(iso-octyl)amine (TOA) in xylene was found to give poor extraction of thorium from hydrochloric acid media [287-289], with slightly stronger extraction given by nitric acid, and slightly weaker extraction by sulfuric acid [289]. Some small amount of extraction was observed from sulfuric acid, but scrubbing was able to remove this in a small number of contacts [290]. Strong extraction of thorium was observed from citric acid media, with weaker extraction from oxalic acid [291]. Across a range of acids and acid concentrations extraction of thorium by TOA was comparable to extraction by TBP [212]. A patent has protected the separation of thorium by mixtures of TOA and TBP from hydrochloric acid media, finding that thorium was not well extracted [231].

A number of other tertiary amines have been investigated for extraction of thorium from citric and oxalic acids. Tri-n-propyl amine was found not to extract thorium from either. Tri-n-dodecyl amine was found to give similar extraction behaviour to TOA. An Alamine reagent (number not specified) gave less extraction from citric acid than TOA, but extracted thorium completely from oxalic acid [291].

2.8.8.4 QUATERNARY AMMONIUM SALTS

A number of quaternary ammonium salts have been investigated, although of these the most commonly reported in the literature is Aliquat-336, tricaprilmethylammonium chloride. As anion exchangers, quaternary

ammonium salts commonly extract thorium as a metal nitrate, chloride, sulfate or other anion species.

In general, across a range of aqueous media, Aliquat-336 was found to extract thorium more strongly than TBP or TOA [212]. Aliquat-336 was found to give complete thorium extraction from oxalic acid, and variable extraction from citric acid, with greatest extraction at the lowest acid concentration [291]. Aliquat-336 also extracts thorium strongly from solutions of sodium succinate [292]. The extraction of thorium from alkaline digested monazite cake dissolved in nitric acid with Aliquat-336 has been studied, and it was found that thorium is extracted strongly, while the trivalent rare earths are extracted poorly and uranium distributes between the organic and aqueous phases [293].

Recently work has been carried out into solutions of phosphinated quaternary ammonium salts. Thorium was not well extracted from nitrate media by methyl-trioctyl-ammonium dialkyl-phosphinate in toluene [294].

2.8.8.5 ANILINE EXTRACTANTS

Anilines are a type of aromatic amine where one of the hydrogens is replaced by a phenyl group, thus giving an extractant with a mixture of phenyl and amino groups. Slow, incomplete extraction of thorium was observed by *n*-methylaniline (a secondary amine) and *n,n*-dimethylaniline (a tertiary amine) from sulfate media [86]. Better extraction was given by octylamine [295].

50:50 mixtures of TOA and *n,n*-octylaniline in xylene were found to give strong, synergic extraction from 1.5 M sulfuric acid [296].

2.8.8.6 AMIDE EXTRACTANTS

A number of amides have been tested for thorium extraction. The first of these were *N,N,N',N'*-tetraalkyldiamides, first investigated in the 1960s [297]. Latterly, *N,N,N',N'*-tetrabutyladipicamide (TBAA) was found to

extract thorium from 3 M and stronger solutions of HNO_3 [298]. This extractant was found to give the best performance of ten amides and TBP from nitrate media [299].

Other similar amides studied are the 4-oxaheptanediamide (OHA) extractants N,N,N',N'-tetraalkyl-4-oxaheptanediamide (TOOHA), N,N,N',N'-tetrabutyl-4-oxaheptanediamide (TBOHA), N,N,N',N'-tetrahexyl-4-oxaheptanediamide (THOHA) and N,N,N',N'-tetra isooctyl-4-oxaheptanediamide (Ti-OOHA). Under the correct conditions slight extraction of thorium could be achieved with these extractants [300].

The extraction of thorium from nitrate media by N,N-di-n-hexyl octanamide (DHOA) has been studied, and it was found that the bulk of thorium is not extracted, remaining in the aqueous phase [301]. However, slight extraction was found by another researcher under similar conditions [234].

The diglycolamides are a subject of research for actinide separations, particularly N,N,N',N'-tetraoctyl diglycolamide (TODGA) and N,N,N',N'-tetra-2-ethylhexyl diglycolamide (TEHDGA). Thorium is extracted by TODGA in n-dodecane from nitric acid solutions [72]. TEHDGA with isodecanol in n-dodecane was also found to extract thorium strongly from nitric acid [73].

2.8.8.7 PYRIDINE EXTRACTANTS

Some work has been carried out into pyridine based amine extractants.

A study into 5-(4-pyridyl)nonane in benzene found that it does not extract thorium from nitrate media [302]. However, work on the oxide form, 4-(5-nonyl)-pyridine oxide, found that the extractant in xylene extracted thorium from nitric acid for a range of acidities. Thorium was not extracted by the pyridine oxide from hydrochloric or sulfuric acids [289].

2.8.9 AMINOPHOSPHOROUS EXTRACTANTS

Some work has been carried out into the use of combined amine and phosphorous extractants. Both of the studies given below reported a solvation mechanism.

The alkylamide phosphorous extractant octaethyltetraamidopyrophosphate (OETAPP) was found to extract thorium as mono- and disolvate from strong hydrochloric acid media, and from a wide range of nitric acid concentrations [303].

2-ethylhexyl-N,N'-di (2-ethylhexyl) phosphorodiamidate was synthesised recently for the separation of thorium from rare earth elements, and was found to extract thorium quantitatively from nitric acid, quite strongly from some hydrochloric acid concentrations, and generally only slightly from sulfuric acid [304].

2.8.10 CALIXARENE EXTRACTANTS

Calixarenes are relatively large cyclic molecules, named for their vase-like shape. They have a cavity in the centre which is hydrophobic and can accommodate ions and molecules, including species extracted from the aqueous phase. Calixarenes are relatively new to actinide solvent extraction, compared to phosphorous and amine extractants, and synthesis and testing of new calixarenes is a developing area.

Thorium is slightly extracted from hydrochloric acid media by 25,26,27,28-tetracarboxymethyl-5,11,17,23-tetra-*tert*-butyl calix(4)arene by a cation exchange mechanism [94]. 5,11,17,23-tetra(diethoxyphosphoryl)-25,26,27,28-tetraacetoxycalix(4)arene extracts thorium well from nitric acid media [92], and stronger extraction was given by the tetrapropyl variant 5,11,17,23-tetra(diethoxyphosphoryl)-25,26,27,28-tetrapropoxy-calix(4)arene. A solvation mechanism is reported for these extractants [305]. Finally, the extractant 5,11,17,23-Tetra[(2-ethyl

acetoethoxyphenyl)(azo)phenyl]calix(4)arene was found to extract thorium strongly at pH 7 from nitrate media, but the extraction mechanism was not reported [93].

2.8.11 CROWN ETHERS

Crown ethers are cyclic molecules which can coordinate metals in their centres. They have received some attention in the literature for thorium separations.

The separation of thorium from rare earths may be carried out at pH 4.5 by α -(syndibenzo-16-crown-5-oxy)acetic acid or α -(syndibenzo-16-crown-5-oxy)phenylacetic acid, as thorium is quantitatively extracted by cation exchange and rare earths are almost completely rejected [90]. A number of other crown ethers have been shown to be capable of extracting thorium with the cation exchanger 3-phenyl-4-benzoyl-5-isoxazolone (HPBI) investigated alone and with other crown ethers as potential synergists from nitric acid solutions [89]. The separation of thorium from monazite with N-phenylbenzo-18-crown-6-hydroxamic acid (PBCHA) has also been investigated, and very strong extraction was given at pH 3-5 with dichloromethane diluent. The mechanism was identified as cation exchange [91].

2.8.12 LIX EXTRACTANTS

Studies related to a number of extractants produced under the brand LIX are given here, as they do not fit into the categorisation above.

LIX 26 is a chelating alkylated 8-hydroxyquinoline, and mixtures of this extractant and butanol in benzene have been found to extract thorium at pH 4-6. Extraction could be achieved at lower acidities with standard 8-hydroxyquinolene in methylisobutylketone (MIBK). Additionally, mixtures of salicylic acid and oxine were found to quantitatively extract thorium. In

mixtures of LIX 26 and DPSO, thorium extraction increases with LIX 26 fraction [306].

LIX 54 is 1-phenyldecanone-1,3-dione. Alone it does not strongly extract thorium from chloride media, but this may be increased slightly by the addition of TBP, and greatly by the addition of thenoyltrifluoroacetone (HTTA) as a mixed complex by cation exchange [307].

LIX 84 is 2-hydroxy-5-nonylaceto-phenone oxime. This extractant extracts thorium very poorly, even when mixed with TBP, neodecanoic acid, Alamine-336, HTTA or dibenzoylmethane [308].

2.8.13 ROOM TEMPERATURE IONIC LIQUIDS

Recently interest has grown in ionic liquids for solvent extraction, both as extractants and as diluents. Ionic liquids are simply ionic compounds which are liquid at ambient temperatures. They are often considered as advantageous over volatile organic solvents due to their being inflammable, stable at high temperatures and resistant to radiolysis [209, 309-313]. In particular, recent work into radiolytic degradation of extractants and diluents for thorium extraction has shown that ionic liquids protect the extractants themselves from radiation damage more than organic diluents [314].

In the literature the most commonly reported types of ionic liquid are Cyphos phosphonium compounds and imidazolium compounds. Several imidazolium compounds have been studied for thorium extraction.

Thorium is not well extracted from sulfuric acid by the amine extractant N1923 in 1-octyl-3-methylimidazolium hexafluorophosphate [C₈mim]PF₆ as diluent. The use of the ionic liquid diluent greatly reduced extraction compared to the use of a hydrocarbon diluent (*n*-heptane). However, the addition of sodium sulfate greatly increased thorium extraction by N1923 in the ionic liquid [315]. DEHEHP in *n*-heptane and in [C₈mim]PF₆ gave

differing extraction percentages as a function of pH. At pH 1 and below the hydrocarbon diluent gave better extraction, but above this pH the ionic liquid gave better extraction [316].

Other 1-alkyl-3-methylimidazolium hexafluorophosphate ionic liquid diluents (alkyl groups butyl, hexyl, octyl) have been investigated for thorium extraction with *N,N,N',N'*-tetrabutyl-3-oxapentane diamide (TBDA) and *N,N'*-dimethyl-*N,N'*-dibutyl-3-oxapentanediamide (MBDA), which are stronger complexants than TODGA. All extractant and diluent combinations were found to extract thorium well from dilute nitric acid solutions, with some combinations also giving good extraction for concentrated acid [317]. TODGA extraction from nitric acid media was improved by the use of ionic liquid diluents as compared to *n*-dodecane [72].

1-alkyl-3-methylimidazolium bis(trifluoromethylsulfonyl)imides ($C_n\text{mimNTf}_2$) with alkyl groups ethyl, butyl, hexyl and octyl have been studied as diluents, with HTTA as extractant. The shorter alkyl chains gave greater extraction from nitric acid media, and the extraction was greatest at low acidity [209].

$[C_4\text{mim}]PF_6$ was used as a diluent for TOPO for Th and Eu separations in nitrate media. The diluent alone and with TOPO were found to quantitatively extract thorium. Dichloromethane as diluent gave a much reduced extraction [318].

1-[3[[[(diphenylphosphinyl)acetyl]amino]propyl]-3-tetradecyl-1*H*-imidazol-3-ium hexafluorophosphate has been functionalised with CMPO, and this was found to strongly extract thorium from nitric acid solutions [319].

bis(chlorophosphoryl)decahydro-2,4-di(2-hydroxyphenyl)benzo[d][1,3,6]oxadiazepine (DPO) has been used as an extractant with $[C_6\text{mim}]PF_6$ as diluent, which efficiently extracted thorium from nitrate media [320].

A recent publication has studied piperidinium based ionic liquids as an alternative to imidazolium, with four sulfoxide extractants. The piperidinium diluent gave good thorium extraction from 1 M HNO₃, and more efficient extraction. Phenyl sulfoxides were found to give stronger extraction than alkyl sulfoxide [321].

Several patents for thorium separations using ionic liquids have been granted [322-324].

2.8.14 SUMMARY OF PRIOR RESEARCH INTO THORIUM SEPARATIONS

The range of possible solvent extraction systems for the separation of thorium from monazite leachates is very large, and many researchers over the past 70 years have produced significant data on a number of possible systems and their efficacy, with new conditions and extractants being studied all the time. The great majority of these studies are on the subject of thorium recovery from minerals, rather than reprocessing. However, the results should also be applicable to spent fuel separations.

Synergic systems using existing extractants have not been fully explored. The use of established extractants can bring advantages in terms of technological maturity and cost savings over the use of novel extractants which must undergo much development prior to being useable in a process. As was shown in Figure 2.21, PC-88a alone does not give suitable separation of thorium, uranium and iron from monazite liquor. In order to improve upon this, a synergic system is proposed. The selected synergist for investigation was the phosphoric acid extractant HDEHP, as described in Section 2.8.4.1. HDEHP can give good separation of thorium, uranium and trivalent cerium from hydrochloric acid [87], and has been found to give relatively poor extraction of iron [325] from hydrochloric acid solutions. Hydrochloric acid was used as the aqueous feed in the THRUST process, and so this acid was used as the aqueous medium in this work. It was therefore anticipated that mixtures of PC-88a and HDEHP might give good separation

of these metals. This combination of extractants has not previously been reported in the literature. An investigation of the mixture is reported in Chapter 3.

When considering the back end of the fuel cycle, the range of possible extractants for examination is very large. While the literature review above applies fairly equally across both the front end and back end, few specific studies have been carried out into thorium and uranium separations from spent fuel. Thus, it was considered valuable to perform a screening study to determine promising mixtures for development. PC-88a was retained as a primary extractant, and a subset of the extractants above were selected for testing as potential synergists. This work is reported in Chapter 6.

2.9 THORIUM-BASED NUCLEAR FUELS

Various thorium fuels are being studied for use in a number of reactor applications. Of these, the first application of thorium in a modern commercial reactor fuel will likely be as thorium dioxide in an LWR or PHWR, with some addition of thorium as a minor component of the fuel in the period to 2030, the use of thorium in fissile materials management over 2030-2050, and a full thorium fuel cycle from 2050 onwards [43].

The work in this thesis does not concern the fabrication of thorium nuclear fuels, although research work is ongoing into the preparation and production of high-quality thorium oxide powders and pellets [128, 129, 198, 326]. Synthesis of mixed thorium-uranium pellets is also an area of ongoing research [327-332].

Economic analyses of thorium-uranium oxide pellet fabrication processes have been carried out. It was determined that the cost of manufacturing fuels from ThO₂ and enriched UO₂ could increase by 25-64% compared to current costs of LEU fuel [333].

2.9.1 THORIUM FUELLED REACTOR CORE DESIGN CONSIDERATIONS

As was discussed in Section 1.5.2, thorium alone cannot be used to operate a reactor, and a source of neutrons is required to maintain a critical chain reaction. In the short and medium term this is most likely to be achieved by the addition of a fissile driver. Fissile drivers in the literature, as detailed below, include repurposed strategic materials such as highly enriched uranium (HEU) and weapons-grade plutonium, reprocessing products of other fuels including reactor-grade plutonium and recycled uranium, and low enriched uranium (LEU, up to 20% ^{235}U). Uranium previously bred from thorium, being primarily ^{233}U , may also be used.

The thorium and fissile driver may be arranged within the reactor in several ways:

- The thorium and fissile driver may be mixed homogeneously within the fuel pellets.
- Alternatively, a complete core of identical fuel assemblies may be used, with a heterogeneous fuel layout within the individual fuel rods or assemblies. This is known as microheterogeneity.
- Finally, a heterogeneous core may be used, with separate fissile and fertile zones, known as macroheterogeneity. This arrangement is typified by the seed and blanket concept, where fuel is organised into separate fissile and fertile regions at the level of the core.

These fuelling regimes are illustrated in Figure 2.22. Other heterogeneous fuel options include heterogeneous pellets and axial variation along the length of the fuel rod.

Completely homogeneous cores of uranium and thorium have been shown to be disadvantageous compared to standard uranium fuels in LWRs, as a significant loading fraction of relatively highly enriched uranium is required in order to match the irradiation cycle duration, and the achievable fuel burnup at discharge is reduced. However, spatial separation of the uranium

and thorium can increase the achievable burnup in the core per unit of ^{235}U , even if the fertile and fissile components are separated by only a few centimetres. This is at the cost of increased complexity in fuel management and core behaviour due to the presence of super-critical seed regions and sub-critical blanket regions, and the need to balance the heat and power distribution across the core [334].

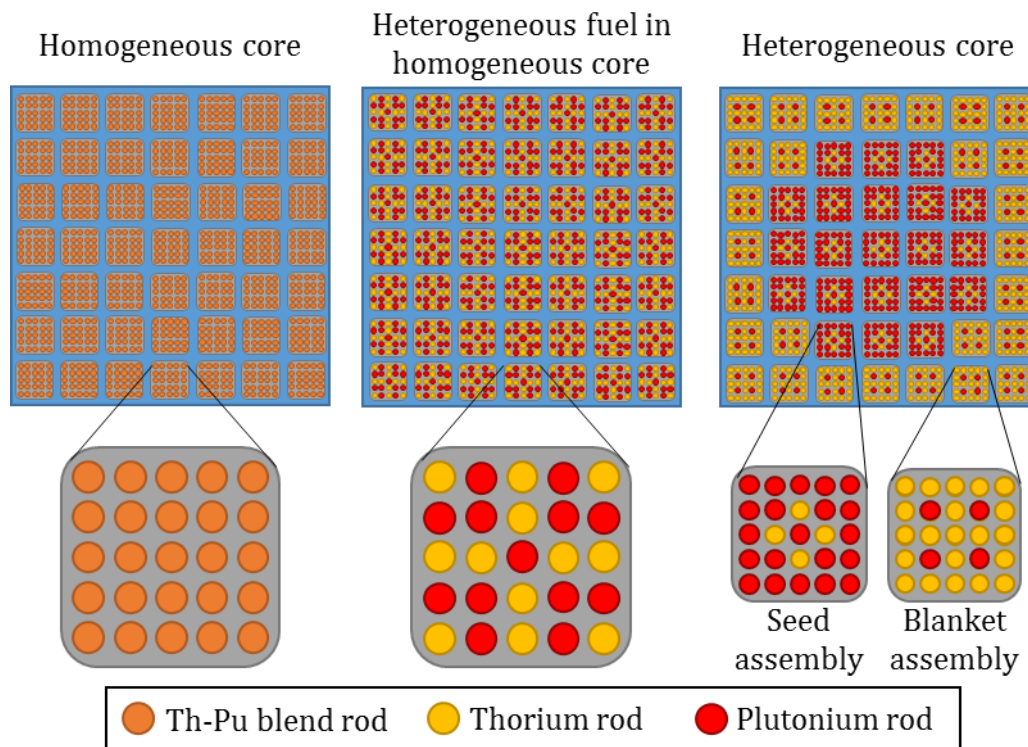


FIGURE 2.22 – EXAMPLE OF AN LWR CORE WITH THREE FUELLING REGIMES, USING PLUTONIUM AS AN EXAMPLE FISSILE DRIVER FOR THORIUM. VIEW ONTO THE CORE IS FROM THE TOP-DOWN. TYPICALLY, LWR FUEL IS INSERTED INTO THE REACTOR CORE AS FUEL ASSEMBLIES, EACH OF WHICH CONSISTS OF A NUMBER OF FUEL RODS. ASSEMBLIES ARE TYPICALLY OF THE ORDER OF 10-20 CM ALONG A SIDE IN END PROFILE AND ARE SEVERAL METRES TALL, WITH A MASS OF SEVERAL HUNDRED KILOGRAMS. ROD DIAMETERS ARE OF THE ORDER OF 1 CM, BEING COMPOSED OF STACKS OF FUEL OXIDE PELLETS IN A ZIRCONIUM ALLOY CLADDING [15, 17].

Heterogeneous fuels need not necessarily contain solely ThO_2 in the fertile “blanket” fuel rods. Some amount of uranium, particularly uranium-238, can be beneficial when mixed with the thorium as a proliferation resistance measure, as this means that the resulting uranium isotopic vector in the

spent fuel will not contain highly pure ^{233}U [115, 120, 335]. However, this significantly reduces the achievable fuel burnup [114, 336].

The fissile driver may also take the form of an external neutron source. A proton accelerator with neutron spallation target may be coupled to the sub-critical reactor core in order to supply the required neutrons for thorium conversion [199]. This is known as an Accelerator Driven System (ADS), and these reactors are often promoted as giving safety advantages compared to critical cores, as the core will immediately become sub-critical if the particle accelerator is made inactive [337, 338]. Research has also been undertaken into fission-fusion hybrid reactor systems for thorium transmutation, where a fusion neutron source is surrounded by a blanket of fissile/fertile material to achieve high breeding ratios in thorium and irradiation of transuranic waste [339-345].

2.9.2 THORIUM DIOXIDE FUELS IN REACTOR OPERATION

The work in this thesis studies reactor operation of ThO_2 PHWR fuels for separated plutonium and uranium management. However, before beginning to discuss PHWR fuels a review of the literature on thorium oxide fuels in other reactor types is given, in order to present a more complete view of the state-of-the-art in thorium fuel research and development.

2.9.2.1 ThO_2 FUELS IN PRESSURISED WATER REACTORS

Research into the mixing of thorium with highly enriched uranium and plutonium has shown that these materials may be successfully repurposed from military applications and irradiated in pressurised light water reactors. Compared to standard uranic fuels, Th-Pu fuels give a reduction in minor actinide waste generation, leading to more rapid reduction in spent fuel radioactivity as was discussed in Section 2.2.2 [125]. Thorium breeding in a homogeneous LEU-Th reactor core was calculated to greatly reduce ^{235}U requirements and produce much less plutonium. The spent fuel also had a

much weaker neutron radiation field, while the Pu-Th fuel reduced the need for natural fuel resources. Specifically, the total amount of thorium and uranium required to operate the core was 80% of the amount of LEU required over the same period [115].

Work by Weaver and Herring [130] into PWR cores using reactor-grade and weapons-grade plutonium as the fissile driver identified that the plutonium with the higher fissile fraction could be used to give higher end-of-life (EOL) burnups than reactor-grade plutonium. However, when a plutonium fraction of 4.4% was used with both depleted uranium and thorium as the fertile material, the U-Pu MOX achieved greater end of life burnups than the Th-Pu MOX. The breeding of ^{233}U as a function of burnup was little affected by the plutonium source or mass fraction.

Thorium-bearing fuel assemblies have been proposed for use in existing PWR cores. The Radkowsky Thorium Fuel core concept uses Seed-Blanket Units (SBUs), which are designed for one-to-one replacement of PWR fuel assemblies, featuring a microheterogeneous seed and blanket array within the SBU. The Westinghouse PWR fuel assembly has a 17x17 array of fuel rods. In the Radkowsky SBU the inner 133 fuel rods use a metallic alloy fuel of plutonium and zirconium, while the outer 156 fuel rod positions are replaced by thorium oxide blanket rods. The seed and blanket subassemblies are refuelled separately, with the blanket subassemblies irradiated over several cycles of seed fuel replacement. When used for plutonium irradiation, this concept can convert the plutonium more completely than standard MOX PWRs, with a 50%-70% mass reduction for the same energy output and a larger fraction of less fissile even-numbered plutonium isotopes. The use of plutonium as a fissile driver reduces the effectiveness, or “worth”, of neutronic control devices such as control rods, and so design changes are recommended to standard PWRs to adapt to this, specifically to enable the greater use of soluble boron as a neutron absorber [335, 346-351].

Whole cores of seed and blanket fuel assemblies in checkerboard patterns have also been considered by Todosow et. al. [334], and these were found to be broadly similar to the Radkowsky fuel in terms of fuel requirements and discharges, although fuel management is simplified considerably.

Detailed studies on the effect of burnable poisons around guide tubes and fuel rods have been carried out by Fridman and Kliem [352], and power distributions are reported for a full checkerboard core simulation over three irradiation cycles. The fuel used was 8.6% reactor-grade plutonium in thorium, with three fuel batches giving an 18 month fuel cycle. Guide tube poisons were found to reduce power peaking across the core over the duration of the irradiation cycle. It was further recommended to use stronger neutron absorbing materials in control rods for Pu-Th fuels.

Work by Lau, Demaziere et. al. [353] suggested the use of thorium as a partial replacement for burnable poisons, in order to flatten the neutron flux profile over the core, particularly at the beginning of core life. Mixed LEU-Th oxide fuel rods with some U-Gd rods as burnable poison were used. Most reactivity coefficients were only slightly changed, while the others (Doppler and moderator temperature coefficients) were within operating limits. The reduction in gadolinium fraction reduced beginning of life power peaking, thus giving improved thermal-hydraulic safety parameters. Another study by Subkhi, Su'ud and Waris [354] considered the addition of ^{231}Pa and ^{227}Np as burnable poisons for a long-life core fuelled with a fraction of ^{233}U at the start of life, as these materials are commonly present in the spent fuel of thorium reactors. A lifetime of 28 years is indicated, although this is based purely on calculations of core criticality and power profile.

Other hosts for plutonium irradiation have been considered besides thorium. Inert matrices of zirconium oxide, with and without thorium doping were investigated. It was found that the fissile fraction loading had to be kept relatively low in order to maintain a negative coolant void reactivity

in the core, which in turn led to a relatively short fuel irradiation cycle length. A multi-recycling scheme using such a fuel was proposed, with the need for small additions of thorium and depleted uranium after each irradiation cycle, as well as an addition of weapons-grade plutonium in order to allow continuous recycling (the use reactor-grade plutonium was found to allow a maximum of two cycles before the isotopic vector became too degraded for further use) [355]. These inert matrix fuels have been termed “rock-like” (ROX) fuels, and have a relatively low spent fuel radiotoxicity, as well as being able to achieve high plutonium transmutation [117, 356]. The addition of some thorium dioxide to the ROX fuel helps to maintain negative reactivity coefficients in the core [356].

An economic analysis of alternative fuel cycle options for PWRs has shown that 50% mixtures of thorium and uranium, both in the metallic and oxide forms, give economic advantages compared to uranium oxide fuel at a smear density of 0.95 and optimum burnup level from a cost perspective, using 6.5-7% enriched uranium [357].

An analysis of the safety parameters of PWRs with Pu-Th oxide fuels has considered a number of reactivity coefficients and accident scenarios, both at steady state and during transients, and has shown that such fuels should be able to be licensed for operation. Consequences of accident scenarios were found to be less severe than in UO₂ fuelled reactors, and within acceptable limits [358, 359].

Thorium-fuelled PWRs have also been investigated as minor actinide burners. It has been seen that decreasing the moderator-to-fuel ratio (MFR) hardens the neutron spectrum, thus improving minor actinide conversion [360].

Fuel breeding in large and small PWRs has been investigated and appears to be feasible under thermal reactor conditions with burnups in the range 20-

40 GWd/t. The greatest breeding ratio was given by high reactor power, but low power density [361].

Studies on complete thorium cores with ^{233}U as the fissile driver in PWRs have shown comparable behaviour to standard UO_2 fuels, with improvements in conversion ratio, reactivity depletion, natural resource utilisation, and a similar level of resistance to proliferation [362].

Pu-Th fuels in PWRs are suggested as a part of various transition and supplementary schemes for UO_2 fuels. One study by Takaki and Mardiansah [363] suggests Pu-Th fuels based on reactor-grade plutonium. This would breed ^{233}U , which could be separated and used as initial seed fuel in a ^{233}U -Th thermal breeding PHWR. Another study by Bi, Si and Liu [364] suggests a similar scheme with the further multi recycling of ^{233}U and potentially thorium in several PWR cycles.

A publication by Marshalkin and Povyshev [365] has reported on the breeding of ^{233}U from LEU-Th, Pu-Th and U-Pu-Th fuels in Russian VVER reactors, moderated by heavy and light water blends to modify the neutron spectrum over the irradiation cycle. It was determined that at most 85% heavy water must be used in order to maintain a negative void coefficient.

A comparison of Th-Pu MOX against low enriched UO_2 in a PWR has found that rather than an outer blanket of fertile material, an annulus of thorium oxide within the core can give much greater discharge burnups. The flux profile matches most closely to a 2.1-3.1% ^{235}U uranium oxide PWR core when the Pu loading fraction in the Th-Pu fuel is 5.5%, with greater axial and radial peaking at higher Pu fractions [366].

A recent study by Alhaj et. al. [367] into Pu-Th fuels found that 13.5% reactor-grade plutonium loading in Pu-Th oxide fuel assemblies could achieve the same irradiation cycle length as UO_2 fuel in a Westinghouse AP1000 reactor with fuel conversion factors increased by up to 10% compared to UO_2 fuel .

From these and other studies, it can be seen that thorium-based fuels for PWRs have been studied in some detail, from initial BOL neutronic feasibility studies to full core simulations with thermal-hydraulic analysis over transients and accident scenarios. The general consensus is that high conversion factors, and even fuel breeding, are possible in existing PWRs if correctly fuelled with thorium and a suitable fissile driver. LEU-Th fuels may be manufactured in existing fuel fabrication plants, and both LEU-Th and Th-Pu fuels may be irradiated within the safety limits of existing and planned reactors. If correctly applied, these fuels can bring benefits in terms of in-core fuel longevity, power profiles, non-proliferation, and economics.

2.9.2.2 ThO₂ FUELS IN BOILING WATER REACTORS

Much of what is applicable in PWRs regarding the addition of thorium remains true in boiling water reactors. However, several studies have focussed particularly on BWRs, and these are detailed here.

A cermet fuel of 50% porous LEU-Th oxide particles (75% ThO₂, 25% UO₂ with 19.5% ²³⁵U) dispersed in a metallic zirconium matrix was investigated as a potential fuel for the Simplified Boiling Water Reactor. The core design was optimised with burnable poison placement for minimal reactivity change with burnup, and studies into fuel fabrication were carried out. It was found that the fuel could be irradiated for eight years to a burnup of 54 GWd/t [368].

Four thorium oxide fuels for BWRs were compared to low enriched uranium fuel and U-Pu MOX fuel in the Forsmark-3 BWR. Open fuel cycles were considered using LEU-Th and reactor-grade Pu-Th, as well as closed fuel cycles using reprocessed U and Pu in a LEU-Pu-Th fuel, and a Th-²³³U fuel. The core infinite multiplication factor k_{inf} was found to increase by 0.2 in the first 10 GWd/t of irradiation for UO₂ and Th-²³³U fuels as the 4% Gd₂O₃ burnable neutron absorber is depleted, decreasing more rapidly thereafter than MOX fuel and fuels with Th and UO₂ or plutonium, which do not have a

burnable absorber. The Th-Pu and Th-Pu-U fuels were found to give significant reductions in core decay heat compared to UO₂ and MOX fuel. The Th-Pu-U fuel was also found to give the greatest denaturation of the plutonium isotopic vector [369].

A more recent paper proposed a seed-blanket BWR core, with a metallic ²³⁵U-Zr alloy as the seed and a ThO₂ blanket, where concentric rings of seed and blanket are arranged within 8x8 fuel rod sub-assemblies, without the moderating water tubes used in standard BWR fuel. These assemblies are irradiated for four cycles, with more burnt fuel generally towards the core centre. The neutron flux in the proposed fuel is approximately 50% of that in the UO₂ fuel, although power distributions are much more variable, with maximum power peaking factor of 2.81. The plutonium isotopic vector and concentration of ²³³U with irradiation history were reported [370].

2.9.2.3 THO₂ FUELS IN HIGH TEMPERATURE REACTORS

Some work has been carried out into the use of thorium in high temperature reactors (HTRs), both as prismatic block and pebble bed fuel forms.

A helium-cooled HTR with a prismatic block core was considered for operation with ²³³U-Th fuel. A high conversion ratio could be achieved over an 18-month irradiation cycle with high thorium loading, an increased MFR and removal of the inner reflector. Both seed and blanket fuels were placed within each 36 cm wide graphite block, with seed in the inner region of the block and blanket in the outer region giving better performance than the reverse, or a homogeneous mixture. The addition of ²³⁸U to denature of uranium isotopic vector for non-proliferation was again found to significantly reduce conversion and cycle length [371].

In the same reactor another study considered a thorium fuel with 19% weapons-grade plutonium as the fissile driver, finding that this enabled a doubling of cycle length and discharge burnup [372].

Another HTR study considered Pu-Th quadruple isotropic (QUADRISO) fuel particles embedded in graphite prismatic blocks [373]. Similarly to another study by Lau [353], thorium oxide was used to replace burnable poison in order to breed ^{233}U . A 300-day fuel cycle could be achieved using this fuel with a 5% packing fraction, after which 65% of the loaded ^{239}Pu is consumed, and of which $\sim 23\%$ is replaced by ^{233}U . It was observed that the reduced capture cross section of ^{240}Pu are greater in homogeneous fuel than in microheterogeneous QUADRISO fuel due to reduced self-shielding, leading to greater production of ^{241}Pu in the homogeneous fuel. It was again found that the addition of ^{238}U to the fuel as a proliferation resistance measure significantly decreased cycle length, produced additional ^{239}Pu and increased spent fuel radiotoxicity [373].

The in-reactor performance of thorium TRISO fuels have been studied to determine gaseous fission product release rates and historical manufacturing defect rates. It was found that Th fuel performance was equal to or better than uranium fuel performance [374].

A pebble bed reactor was studied with simultaneous thorium conversion and minor actinide irradiation using two fuels, a 30%:70% Pu-Th fuel and a 50%:50% thorium and mixed minor actinide fuel. Both fuels had greater discharge burnups and cycle lengths than 9.6% enriched UO_2 . The isotopic vector change with burnup in the fuels was calculated [375].

2.9.3 THORIUM IN PRESSURISED HEAVY WATER REACTORS

Pressurised heavy water reactors for power generation were first operated in Canada, in order to be able to irradiate uranium without enrichment after the Second World War. The use of heavy water as moderator and coolant means that the loss of neutrons through absorption by non-fuel materials is very low, and thus these reactors are very flexible in terms of the fuels they can accept, requiring much lower fuel reactivity than LWRs to be operable [20].

Different terminology is used to refer to similar components of LWR and CANDU PHWR fuels, and it is necessary to define these terms in order to clarify the discussion which follows. An annotated diagram of key CANDU fuel and core terminology is presented in Figure 2.23.

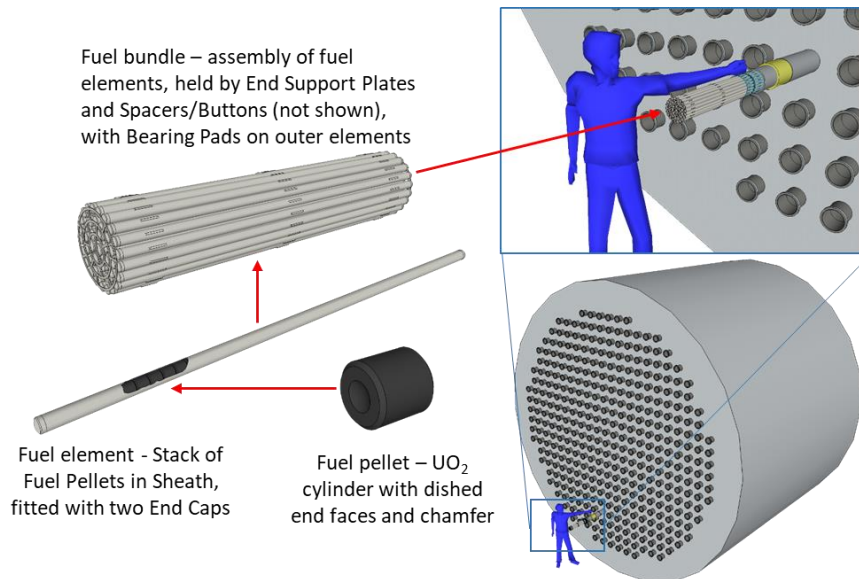


FIGURE 2.23 – DIAGRAM SHOWING KEY COMPONENTS OF CANDU NUCLEAR REACTORS WITH PHWR NOTATION (LEFT). CALANDRIA WITH EXTENDED FUEL CHANNEL (RIGHT).

Thorium was under consideration as a PHWR fuel from at least as early as 1976 in the proposed Self Sufficient Equilibrium Thorium (SSET) fuel cycle, which used uranium separated from irradiated thorium fuel elements as the fissile driver. The isotopic mix of the irradiated uranium was 61% ²³³U, 6% ²³⁵U, and the remainder even-numbered isotopes [376].

CANDU reactors are refuelled almost daily, at full power, with spent fuel bundles being ejected from the core and fresh bundles introduced to 2-3 fuel channels/day on average. Which channels are refuelled, when, and with how much fresh fuel, are decisions made based on the current status of the core and fuel, and any planned transients, in order to manage the core power and reactivity distributions and respect fuel burnup limits [20, 68]. The optimisation of the core loading and management is complex, and the relatively slow decay of ²³³Pa to ²³³U, compared to ²³⁹Np to ²³⁹Pu, adds

additional complications, particularly when it is desirable to minimise ^{232}U generation [377].

Recent work has studied fuelling configurations for CANDU reactors in order to give fuel breeding while respecting constraints on power limits and profiles. Homogeneous ^{233}U -Th fuels were found to only give fuel breeding at very low burnups, meaning that the refuelling frequency had to be very high. Cores with an inner seed region and outer blanket (ISOB) region have been studied in detail, but have been shown not to be operable without reducing reactor power significantly due to power peaking in the seed region. Therefore cores with an outer seed and inner blanket (IBOS), as well as an annulus of seed fuel with inner and outer blankets (IOBMS), were studied, with 1.0-1.6% ^{233}U in 37-element CANDU fuel bundles. In steady state these core configurations performed very well, but during refuelling unacceptable reactivity swings were observed. The IBOS fuel was found to allow operation at greater power than natural uranium fuel due to an improved power profile, but suffered from neutron leakage issues. The IOBMS fuel improved on this, reducing the refuelling rate and increasing core reactivity. Power peaking was observed at the seed-blanket interfaces due to the ^{233}U fraction mismatch [136].

This work was further developed in a study into the effect of reducing fuel bundle sub-division, using 24 annular fuel elements per seed bundle and 28 solid elements per blanket bundle in an IBOS concept. The annular elements were internally cooled, and a large central ZrO_2 element was used to reduce the coolant void coefficient of reactivity and give improved margin to the critical heat flux. The 28-element bundle gave improved breeding. It was found to still be necessary to reduce the core power to 60% of the natural uranium fuelled value for the ISOB concept in order to respect channel power limits, which also brought the core to just below net breeding. The IBOS concept was also just below net breeding, but did not require power reduction. It is suggested that net breeding could be achieved through

further reduction of neutron absorption in non-fuel materials, although such absorbers are already at a very low level in CANDU reactors. Alternatively, the blanket thorium content could be increased and these channels could be more regularly refuelled [378].

The effect of multiple seed and blanket annular regions in CANDU reactors has been studied, as well as the variation in seed-blanket ratio, with 3%Pu-Th and 4%Pu-Th fuels in 35-element fuel bundles with a large ZrO₂ rod in the centre. A large range of performance data were measured and it was found that burnups of up to 31 GWd/t were achievable, consuming 60% of the initial plutonium load. However, all cases required derating of the reactor, with the 75% blanket core requiring a reduction to 35% of rated power. A figure of merit was defined taking account of conversion ratio, fissile utilisation, burnup and power rating, and it was found that one seed region with two blanket regions and 4% plutonium was the most highly performing core, operating at 65% of full power and a burnup of 31.11 GWd/t, with 1.25 times the fissile utilisation of a standard CANDU reactor and a conversion ratio of 0.56 [379].

A variety of ²³³U-Th fuel compositions with up to 3% initial ²³³U have been investigated in order to determine the optimum seed and blanket fuel, based on minimal refuelling rate for the proposed two coaxial core zones while respecting power distribution and criticality criteria. The previously discussed SSET fuel of separated ^{233/232}U and Th was found to correspond approximately to a fuel containing 1.6% pure ²³³U in thorium, and that the ²³⁵U in the separated uranium compensates for the presence of even isotopes. As SSET fuel contains 1.6% ²³³U there is little value in performing isotopic separation on the uranium recovered from its spent fuel, as the impact of other isotopes was very low. It was further found that at low ²³³U fractions (<1.8%) the refuelling rate is heavily dependent on the initial ²³³U fraction. 2.4% pure ²³³U was found to best respect the defined operating constraints [377].

Another study found that PHWRs fuelled with thorium and using former weapons materials as fissile drivers could achieve high conversion factors. Several PHWR and PWR fuels were compared in terms of separative work units and fuel materials requirements, power and conversion ratio, and spent fuel fissile composition [115].

A study was conducted into the use of Pu-Th in PHWRs with MFRs of 1.0 and 1.2, including a suggested fuel cycle deployment scenario. In agreement with other studies, changing from light to heavy water, other things being equal, hardens the neutron spectrum, which with high ^{239}Pu fractions increases the coolant void reactivity. Fuel breeding ratio is highest for low fuel burnups and low power density. Heavy water was a better moderator for breeding than light water. Both MFRs gave positive void coefficients, but this allowed large burnups to be achieved with an almost negligible reduction in core multiplication factor k_{eff} [380].

Further work following from the previous study by Mardiansah and Takaki [380] considered Pu-Th fuels in PHWRs for the production of ^{233}U with a variety of MFRs over five 1000-day irradiation cycles. It was found that MFR = 0.6 gave fuel breeding, despite a lower initial core reactivity than MFR = 1.0, which did not breed fuel. However, the lower MFR gave a positive void coefficient, while the higher MFR did not. The annual yield of ^{233}U from the core is 800-900 kg. This was then suggested for use in a second PHWR fuelled with a closed ^{233}U -Th fuel cycle over a 1300 day irradiation cycle and 8% ^{233}U loading. An MFR of 0.6 again gave good breeding performance and was found to give minimal reactivity swing with irradiation while retaining k_{eff} slightly greater than unity [363].

A series of thorium fuels were studied in a theoretical PHWR consisting of oxide fuel rods with zircaloy cladding, in heavy water moderator/coolant with a BeO outer reflector. Three fuels consisting of thorium oxide with 4% of either ^{233}U , ^{235}U or ^{239}Pu were modelled for k_{eff} , neutron flux, fissile mass

variation with burnup, fission product poison concentration and ^{233}Pa concentration as a function of irradiation time. Coolant void reactivity and temperature effects was also reported. Following an initial reduction the multiplicity factors and fluxes of uranium driven fuels stabilised above unity after 150 days of irradiation. The ^{233}U -Th fuel was found to breed, and had the lowest fission product poison production (considering ^{135}Xe and ^{149}Sm only). The Pu-Th fuel was found to have a positive moderator temperature coefficient of reactivity [381].

The most modern reactor design from CANDU Energy is the 700 MWe Advanced CANDU Reactor (ACR-700), an evolution of the currently operating CANDU-6 reactor. In a comparative study of the CANDU 6 and ACR-700 reactors several core management schemes with LEU-Th fuels were suggested, these being seed and blanket in separate fuel channels, seed and blanket in separate fuel rods of each fuel bundle, and homogeneous LEU-Th oxide. It was found that as the thorium fraction in the homogeneous fuel is increased, the uranium enrichment must also increase in order to achieve equivalent fuel burnup, resulting in greater natural uranium requirements overall. Increasing the burnup however gives reductions in natural uranium requirements compared to natural uranium or LEU fuels. Polynomials are fitted which allow the calculation of discharge burnup in each reactor as a function of uranium enrichment and thorium mass fraction [382].

Another study looked at the evolution of k_{eff} for four thorium fuels in CANDU reactors: a 4% reactor-grade PuO_2 in ThO_2 fuel, a 3% weapons-grade PuO_2 in ThO_2 fuel, and the addition of 5% natural UO_2 to each of these. Eight years of operation was determined to be neutronically feasible with each fuel, although the study only reported on the evolution of k_{eff} [383].

A new concept reactor was analysed for thorium fuel irradiation, which is proposed to be moderated by heavy water but cooled by a molten salt. A full

fuel cycle is proposed with Pu-Th fuel in both the proposed PHWR and existing LWRs, along with partial core loads of slightly reprocessed LWR fuel in the proposed PHWR. The extent to which the fuel cycle is implemented can reduce plutonium production from natural uranium by up to a factor of ten. Reactivity and power are reported as a function of irradiation cycle length. The design is at a very early stage, and even early conceptual work remains to be done, such as considerations of how heavy water and molten salts may be used safely together in adjacent sections of the fuel channels [384].

As well as oxide fuels, carbide TRISO fuels have been investigated for use in PHWRs, using particles of 10%, 30% and 50% reactor-grade plutonium carbide in thorium carbide, with 60% packing fraction in graphite [385].

2.9.4 SUMMARY OF PRIOR RESEARCH INTO SOLID THORIUM FUELS

It has been seen that thorium oxide fuels have been studied in detail for light water reactors, heavy water reactors and gas-cooled high temperature reactors. The conclusions reached have been variable, depending on diverse factors such as the type and amount of fissile driver, and the reactor geometry, materials and operation. The exact fuel composition, target burnup, reactor power and other factors such as fuel cycle integration will define the behaviour of the individual thorium-fuelled reactor. As has been seen in this literature review, a reactor constructed with the aim of maximising ^{233}U breeding and a reactor which seeks to maximise energy output per unit of loaded fissile material will likely be very different machines.

In general terms, it has been shown that thorium oxide fuels are capable of fuel breeding, or at least very high conversion factors, in a number of reactor types. Homogeneous fuels were found to be feasible, but the advantages were limited. Heterogeneous fuels gave better performance in a range of metrics, although care had to be taken to ensure that power limits were

respected through the core, as power peaking was found to be a recurring issue. A number of burnable poisons in various configurations were investigated for flux flattening, including rare earth elements and neutron absorbing actinide isotopes such as ^{231}Pa and ^{237}Np .

A relatively poorly studied fuel group overall was three-component fuel, consisting of plutonium, uranium and thorium used together. Such fuels were studied in VVER reactors with mixed light and heavy water coolant/moderator [365], in BWRs [369] and in PHWRs [383].

The UK has large inventories of separated plutonium and uranium from many years of reactor operations, and it is currently proposed that the plutonium be irradiated in a fleet of Enhanced CANDU-6 reactors as a MOX fuel with depleted uranium, using dysprosium oxide as a burnable poison. A set of alternative fuel compositions was investigated for these reactors, using inventory U and Pu supplies as well as reprocessing products of a UK nuclear new build reactor as fissile drivers for thorium oxide. These studies are outlined in Chapter 4 of this thesis, with more detailed neutronic analysis being reported in Chapter 5.

2.10 NOVEL RESEARCH AREAS IDENTIFIED AND DEVELOPED IN THIS THESIS

In this literature review three areas were identified for further research as part of this work.

2.10.1 THORIUM SOLVENT EXTRACTION FROM MONAZITE

In the front end of the thorium fuel cycle it was seen that the purification of a thorium concentrate produced from monazite by solvent extraction has received attention in the scientific literature. A large number of potential extractants have been investigated, in a range of hydrocarbon and ionic

liquid diluents, from a number of aqueous media. In addition some binary mixtures of extractants have been studied as potential synergic mixtures.

Many synergic mixtures remain to be studied for thorium separation.

Currently, the only industrial recovery of thorium from monazite is by the Indian THRUST process, using PC-88a to separate thorium from rare earth elements. However, uranium and iron must be separated from the mineral mineral PLS before PC-88a can be used to recover thorium. The established extractant HDEHP has been shown to separate uranium and thorium, and to not substantially extract iron. Therefore, a study was carried out into this extractant mixture, with the aim of determining the distribution ratios and separation factors, the extracted complexes, and the number of extraction stages required to recover 99% of thorium from aqueous solution.

2.10.2 THORIUM-URANIUM-PLUTONIUM FUELS IN PRESSURISED HEAVY WATER REACTORS

The first deployments of thorium in the fuel cycle will likely be within light and heavy water reactors as thorium oxide, using separated plutonium or enriched uranium as a fissile driver. A number of reactors have been studied with such fuels for the purposes of increased power output, flux profile shaping, increasing fuel discharge burnup or fuel cycle length, reducing natural resource utilisation, actinide transmutation and ^{233}U breeding.

In this work a particular example is considered of a PHWR with a uranium-plutonium MOX as the fissile driver for thorium, with thorium replacing the proposed dysprosium burnable absorber. Such a reactor is proposed for the UK in order to irradiate the national separated civil plutonium inventory in a standard MOX fuel. It is anticipated that the addition of thorium may be able to increase achievable fuel burnup, thus giving greater conversion of plutonium and increased energy production per unit of Pu irradiated, while fuels with U, Pu and Th have been considered for use in PHWRs.

2.10.3 RECOVERY OF THORIUM AND URANIUM FROM SPENT FUELS

The rate of publication of studies into thorium spent fuel reprocessing and separations is much less than that of thorium separations from minerals, which is unsurprising given the economic drive to be able to recover valuable rare earth elements without radioactive contamination by thorium, which commonly accompanies rare earths in minerals. However, future thorium fuel cycles may require the recovery of uranium and thorium from spent thorium fuels. The Acid THOREX process has a number of issues due to the use of TBP, such as third phase formation, limited solubility of thorium, and radiolytic solvent degradation, which could be resolved by a different extractant or mixture of extractants. Mixtures of established extractants can offer advantages in terms of cost, development time, and technological maturity.

In order to identify possible promising extractant mixtures from the large range of possible extractant pairings to a reasonable number for investigation, a primary extractant was selected for use alongside ten different potential synergists from three different acidic aqueous media. PC-88a was retained as the primary extractant, with secondary extractants selected across a range of types and extraction mechanisms. The aim was to determine the distribution ratios and separation factors for thorium, uranium, iron and zirconium, in order to be able to identify the most promising systems for further development. Zirconium was of interest as it can give useful information for processes used in back end nuclear fuel reprocessing. It is possible to make semi-quantitative assumptions about the behaviour of plutonium by studying the behaviour of both zirconium and thorium [75], and although thorium irradiation produces only very small quantities of plutonium, plutonium is often suggested as a fissile driver for thorium nuclear fuels [334, 346, 352, 369, 372, 386]. Zirconium itself is present in many nuclear fuels, either as a component of the fuel itself [378],

or more often as the main component of Zircaloy fuel cladding materials, which are often dissolved along with the fuel and must be separated [204].

2.11 CHAPTER SUMMARY

In this chapter a review of the scientific literature related to thorium solvent extraction and thorium use in Generation III+ reactors has been considered. Based on this review, gaps in the literature was identified for a synergic process capable of separating thorium from other monazite components, for a solid thorium oxide fuel for use in pressurised heavy water reactors with traditional MOX fuels and for the identification of possible solvent extractant mixtures for the recovery of uranium and thorium from spent nuclear fuel.

Each of these areas will be addressed in the following chapters. Chapter 3 will cover the front end separation of thorium from minerals. Chapters 4 and 5 discuss the application of nuclear-grade thorium in nuclear power reactors. Chapter 6 will cover the back end processing of thorium spent fuel.

3 DEVELOPMENT OF THE PC-88A/ HDEHP/HCl SOLVENT EXTRACTION SYSTEM

In this chapter a study is presented into the separation of thorium from uranium and iron in 3.0 M HCl media by PC-88a/HDEHP in *n*-dodecane. The extraction mechanisms are determined and a possible flowsheet is suggested.

3.1 INTRODUCTION

As was discussed in Chapter 2, the currently used industrial process for the separation of thorium from monazite solutions is the THRUST process, developed and applied in India. PC-88a is used in a solvent extraction system to selectively extract thorium from rare earth elements in an acidic chloride solution [34]. However, before this can be done, a first solvent extraction must be carried out with Alamine-336 in order to extract uranium and iron. As HDEHP was not observed extract uranium or iron strongly from concentrated hydrochloric acid media [87, 325], it was postulated that the addition of HDEHP to the organic phase would suppress the extraction of uranium and iron by PC-88a while still recovering thorium, and thus might allow thorium to be recovered directly from the monazite hydroxide cake dissolved in hydrochloric acid.

In order to determine the optimum operating conditions for the system, it is necessary to understand the metal extraction behaviour and how it is affected by various parameters, such as acidity and extractant

concentration. Separation system optimisation is rarely performed at the bench-scale due to changes in operating conditions introduced at the plant-scale [387]. However, it is still necessary and valuable to investigate and characterise the behaviour of the system in response to a number of basic parameters [77]. The aim of the work presented in this chapter was to determine the extraction mechanisms for Th, U and Fe by slope analysis [388], as well as the number of contact stages required for 99% thorium recovery in a counter-current solvent extraction system based on a predicted McCabe-Thiele extraction isotherm (see Section 3.2.7 below and Appendix B) [79, 389]. From this a process flowsheet for thorium separation was suggested.

3.1.1 PROPERTIES OF PC-88A AND HDEHP

PC-88a and HDEHP are dialkyl phosphorous acids with equivalent alkyl groups (2-ethylhexyl), with the difference being that one is phosphoric (having two alkoxide ester groups) and the other phosphonic (having one alkoxide ester group and one alkyl group). The phosphonic acid, PC-88a, is more basic and more resistant to hydrolysis, typically giving it greater metal bonding strength and affinity for H^+ [76]. Both are typically cation exchange extractants [220]. Both of these extractants aggregate to form cyclic dimers, as shown in Figure 3.1, being $(HEHEHP)_2$, $(HDEHP)_2$ and $(HEHEHP.HDEHP)$ [248, 390, 391]. Acidity constants, dimerisation constants and other selected data for PC-88a and HDEHP are given in Table 3.1. It can be seen that PC-88a and HDEHP are similarly acidic and have a similar tendency to dimer formation.

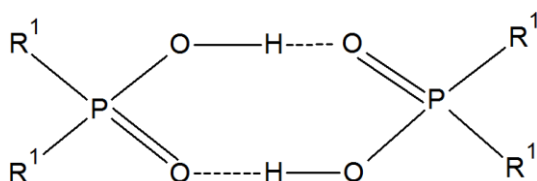


FIGURE 3.1 – FORM OF THE PC-88A AND HDEHP DIMERS, WHERE R^1 REPRESENTS THE ALKYL OR ALKOXIDE ESTER GROUP.

TABLE 3.1 – pK_a AND pK_{dimer} DATA FOR PC-88A AND HDEHP [391, 392].

EXTRACTANT	PC-88A	HDEHP
Acidity constant in water pK_a	3.30-3.42	2.75-2.79
Acidity constant in 75% ethanol pK_a	4.53-4.85	3.45-3.49
Dimerisation constant in kerosene pK_{dimer}	4.33-4.42	4.18-4.53
Distribution ratio into Solvesso #150 pK_D	2.99	2.74
Molecule volume /Å ³ [217]	429.65	421.30

The logarithmic dimerisation constant pK_{dimer} is given by Equation (3.1).

$$pK_{dimer} = \log_{10} K_{dimer} = \log_{10} \frac{[(HA)_2]}{[HA]^2} \quad (3.1)$$

Where K_{dimer} is the dimerisation constant,

$[(HA)_2]$ is the concentration of the extractant dimer in the organic phase, and

$[HA]$ is the concentration of the extractant monomer in the organic phase.

PC-88a forms dimers readily in octane [392], heptane, kerosene, benzene [391], and toluene [393]. It also readily dissociates to give a proton and the associated extractant ligand [391]. The common mechanism of extraction for thorium by PC-88a is cation exchange, but mixed cation exchange/solvation has also been observed [85, 251, 252, 394].

The difference in acidity constant is due to the greater amount of oxygen in HDEHP for two otherwise identical extractant structures. The lower acidity constant of HDEHP means that a greater proportion of the extractant is partially deprotonated at low value of pH in solution, thus making it more available for metal complexation than PC-88a.

Both extractants strongly partition into organic media over aqueous media, as shown by their pK_D values with Solvesso #150 (petroleum naphtha), also in Table 3.1.

THE PREPARATION AND APPLICATION OF THORIUM-BASED NUCLEAR FUELS

Some selected thorium distribution ratio results for PC-88a extraction are presented for three common mineral acid aqueous media in Figure 3.2, Figure 3.3 and Figure 3.4. It can be seen that all three acids will give thorium extraction under the correct conditions.

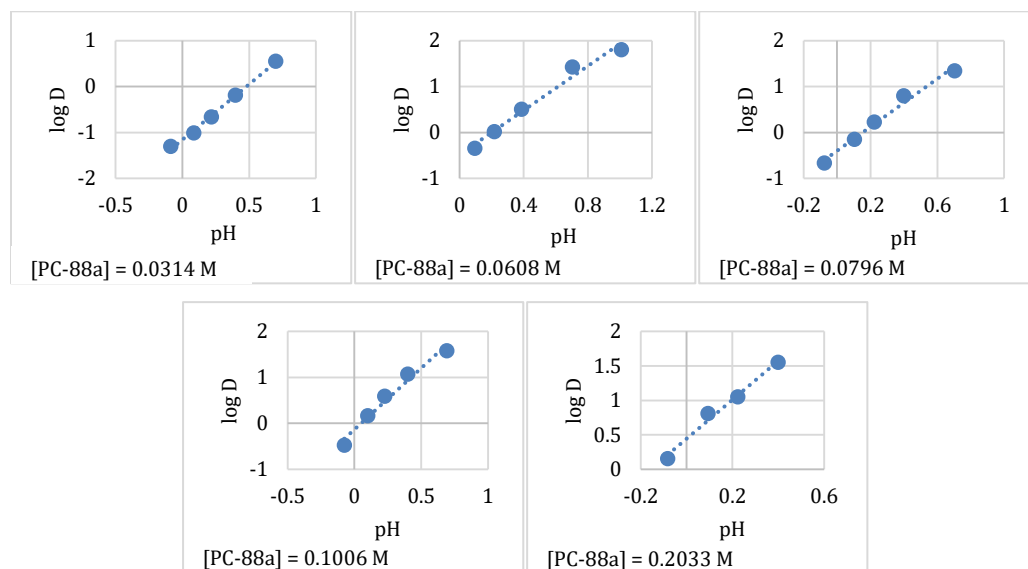


FIGURE 3.2 – DISTRIBUTION RATIO FOR THORIUM AS A FUNCTION OF pH UNDER EXTRACTION BY SEVERAL CONCENTRATIONS OF PC-88A IN KEROSENE FROM SULFURIC ACID MEDIA. IMAGE REPRODUCED FROM DATA PUBLISHED IN [255].

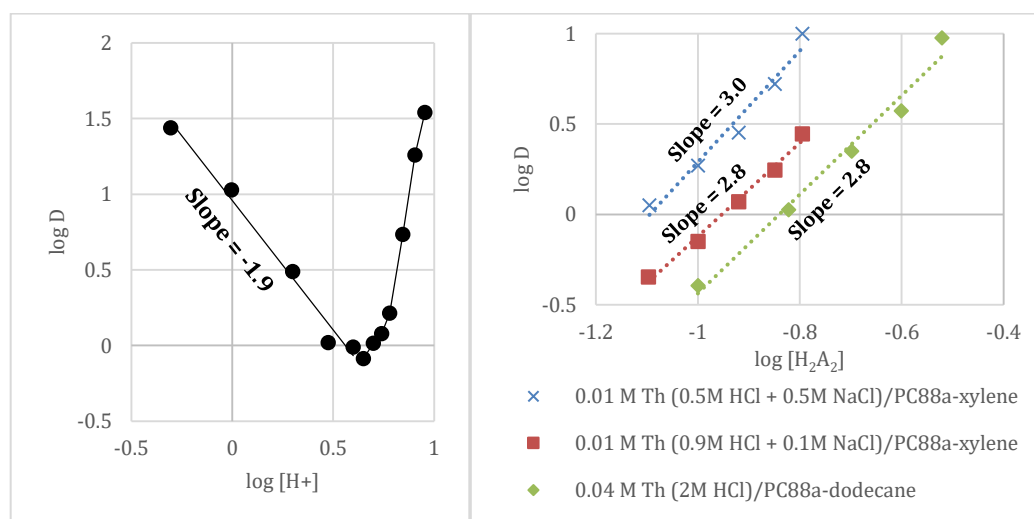


FIGURE 3.3 – DISTRIBUTION RATIO FOR THORIUM AS A FUNCTION OF ACIDITY AND PC-88A CONCENTRATION IN DODECANE WHEN BEING EXTRACTED FROM HYDROCHLORIC ACID (LEFT) AND MIXED HCl/NaCl SOLUTIONS (RIGHT). IMAGES REPRODUCED FROM DATA PRESENTED IN [251].

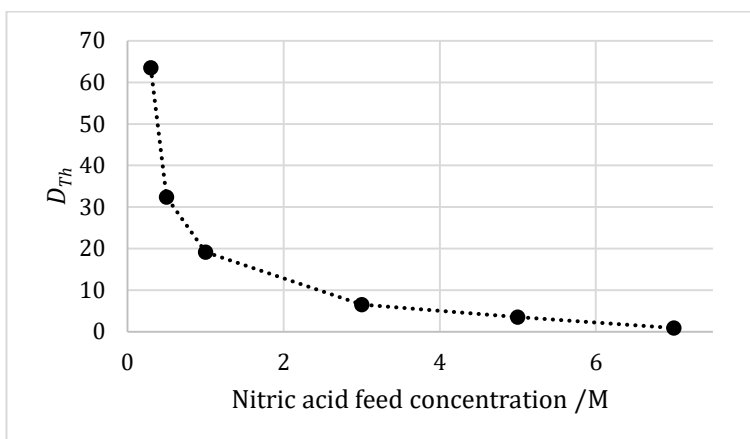


FIGURE 3.4 – DISTRIBUTION RATIO FOR THORIUM AS A FUNCTION OF NITRIC ACID CONCENTRATION WHEN EXTRACTED BY 0.75M PC-88A IN *n*-DODECANE. IMAGE REPRODUCED FROM DATA PUBLISHED IN [253].

3.1.2 SELECTION OF ORGANIC DILUENT

It was decided to use *n*-dodecane as the hydrocarbon diluent in this screening study. *N*-dodecane is a long-chain alkane. The density of *n*-dodecane is 0.7495 g.cm⁻³, with low solubility in water and low viscosity [395]. Several PC-88a diluents have previously been tested, and *n*-dodecane was found to give the strongest thorium extraction [253]. It is also the diluent used in the THRUST process [34].

No PC-88a dimerisation constant data were available for *n*-dodecane, but based on the strong tendency to form dimers in other alkyl diluents it is assumed that this behaviour will be similar in *n*-dodecane.

3.1.3 LITERATURE REVIEW ON THE EXTRACTION OF TH, U AND FE BY PC-88A AND HDEHP

3.1.3.1 THORIUM EXTRACTION

No published data could be found on the extraction of thorium by mixtures of PC-88a and HDEHP. However, some work has been carried out into the separation of thorium by the extractants individually, as well as in combination with other extractants.

As was discussed in Chapter 2, thorium is extracted from acidic media by PC-88a. A number of cation exchange extraction complexes and mixed cation exchange/neutral adduct complexes have been reported. PC-88a extraction of thorium from hydrochloric acid has shown slopes of 2 for pH dependence and 3 for extractant dependence, suggesting the complex $\text{ThCl}_2(\text{HA}_2)_2(\text{H}_2\text{A}_2)$, where the extractant is binding to a thorium chloride species as both a partially deprotonated molecule through cation exchange and as a the fully protonated dimer through solvation [251]. However, the acid dependence slope for PC-88a extraction from HCl has also been reported as -3 [252, 394] and -4 [85], suggesting that the extracted species may be Th^{4+} , $(\text{ThCl})^{3+}$ or $(\text{ThCl}_2)^{2+}$, with a similar set of species also formed with nitrate [394]. In the extraction of Th by PC-88a from nitric acid, pH dependence and PC-88a dependence slopes of 4 have been found, with the reported extraction complex being $\text{Th}(\text{H}(\text{EHEHP})_2)_4$ [85]. Thorium is also extracted from sulfuric acid in the presence of fluoride ion as a ThF^{3+} complex by PC-88a as a mixed cation exchange/solvation complex [255]. The kinetics of thorium extraction from nitrate media with PC-88a have been studied [84]. The nitrate extraction complex was found to be effectively back-extracted by sulfuric acid [83], although sodium and ammonium carbonates were found to give greater back-extraction [253].

Several HDEHP complexes are formed with tetravalent cations [87]. HDEHP extracted Th from HCl in the literature with a slope of 3 for both pH and PC-88a dependence. A slope of 0.8 was found for chloride dependence, leading to two suggested complexes: $\text{Th}(\text{DEHP})_2(\text{H}(\text{DEHP})_2)_2$ and $\text{ThCl}(\text{DEHP})(\text{H}(\text{DEHP})_2)_2$ [394]. Another study found that thorium is well extracted from 0.5 M hydrochloric acid by 0.1 M HDEHP and less well by 0.05 M HDEHP in kerosene diluent. The extracted complex was suggested to be the polymeric species $\text{Th}_2(\text{DEHP})_{10}\text{H}_2$. Four protons are released per thorium atom, with 5 extractant molecules complexed. Mixed cation exchange and neutral complexes are also presented for Th with HDEHP

from hydrochloric acid, and it is suggested that the neutral ThCl_4 species may be extracted by HDEHP as a pure neutral adduct at high aqueous acidities [88]. Another study from nitrate media reported the complex to be $\text{ThNO}_3(\text{H}(\text{DEHP})_2)_3$ [243].

3.1.3.2 URANIUM EXTRACTION

No previous work could be found on the extraction of uranium by mixtures of PC-88a and HDEHP.

Uranium is extracted by HDEHP from dilute hydrochloric acid, sulfuric acid and their mixtures by cation exchange, with two protons exchanging for two HDEHP dimers, as shown in Figure 3.5 [87]. The extraction decreases with increasing acidity, while the extraction of thorium remains strong. The uranyl complex extracted from nitrate media was also reported to be $\text{UO}_2(\text{H}(\text{DEHP})_2)_2$ [243]. At low nitrate concentrations the favoured extracted complex was also found to be $\text{UO}_2(\text{H}(\text{DEHP})_2)_2$. Numerical modelling has been used to study uranyl-HDEHP complexes, and it was found that HDEHP often binds as a bidentate ligand in nitrate systems [396].

The reported complex of uranium with PC-88a is very similar, being $\text{UO}_2(\text{H}(\text{EHEHP})_2)_2$, produced by cation exchange with the release of two protons [251, 397]. Uranium is extracted from acids by PC-88a in a range of conditions [216]. The metal may be extracted from phosphoric acid solutions by PC-88a in xylene, with decreasing extraction at higher acidity [398]. When extracted from hydrochloric acid media, U(VI) has been observed to form a 1:2 complex with PC-88a [399]. The extraction of uranium from nitric acid media is shown in Figure 3.6 [400].

3.1.3.3 IRON EXTRACTION

Iron was found to be quantitatively extracted from 0.15 M hydrochloric acid by 0.1 M PC-88a in five contact stages. However, at 3-5 M HCl the extraction was very low. Iron extraction with PC-88a is quantitative or very high above

pH 0.75, in the cation exchanged complex $\text{Fe}(\text{PC-88a})_3$, but falls to almost nil at higher acidities [401]. PC-88a in toluene diluent was found to extract iron from hydrochloric acid with a loading capacity of 1.3 g/l [402]. The extraction of Fe^{3+} by PC-88a from hydrochloric acid media is shown in Figure 3.7. It also extracts iron well from sulfuric acid [401] and nitric acid [253].

With HDEHP, a range of extracted iron complexes from hydrochloric acid have been reported to occur in parallel [403]. The extraction of iron from hydrochloric acid is shown in Figure 3.8, and it can be seen that D_{Fe} is low at high acidity [403]. 40% HDEHP in a benzene diluent was found to poorly extract iron from hydrochloric acid media via a cation exchange mechanism forming $\text{FeCl}(\text{DEHP})_2$, with $D_{\text{Fe}} \sim 0.3$ for 2.7 M HCl [404]. Stripping could be performed with concentrated HCl [325] or H_2SO_4 solutions [405].

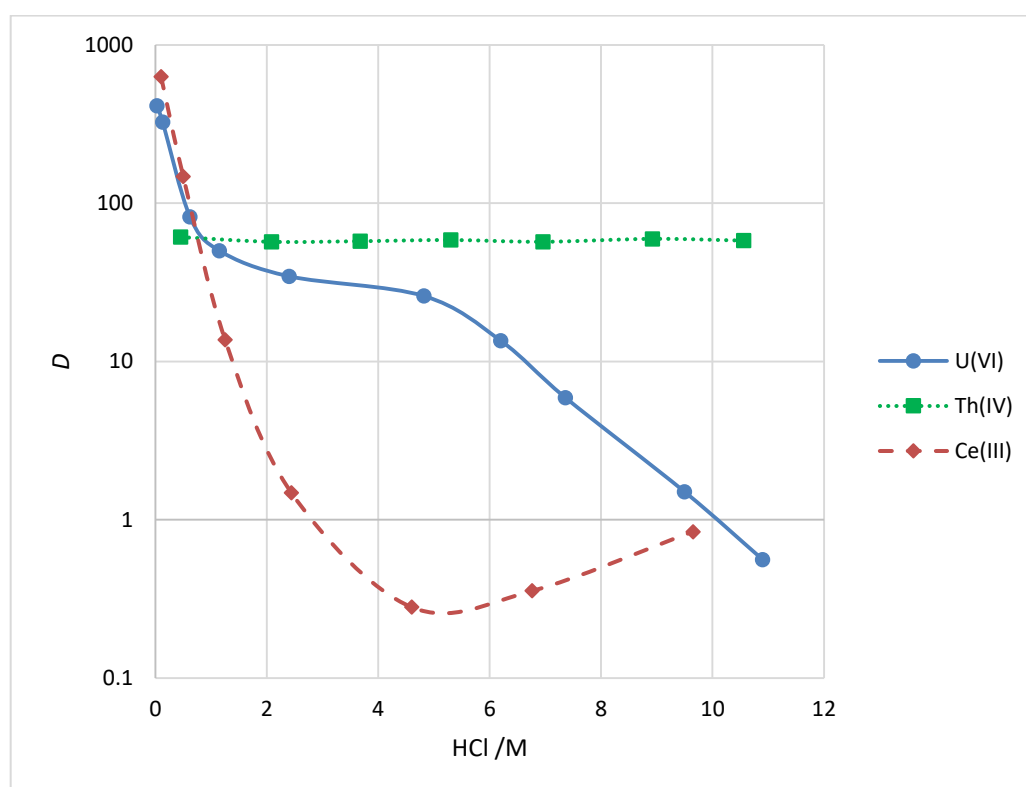


FIGURE 3.5 – DISTRIBUTION RATIOS FOR THORIUM, URANIUM AND CERIUM FROM ACIDIC CHLORIDE MEDIA BY 0.7 M HDEHP IN XYLENE DILUENT. IMAGE REPRODUCED FROM DATA PUBLISHED IN [87].

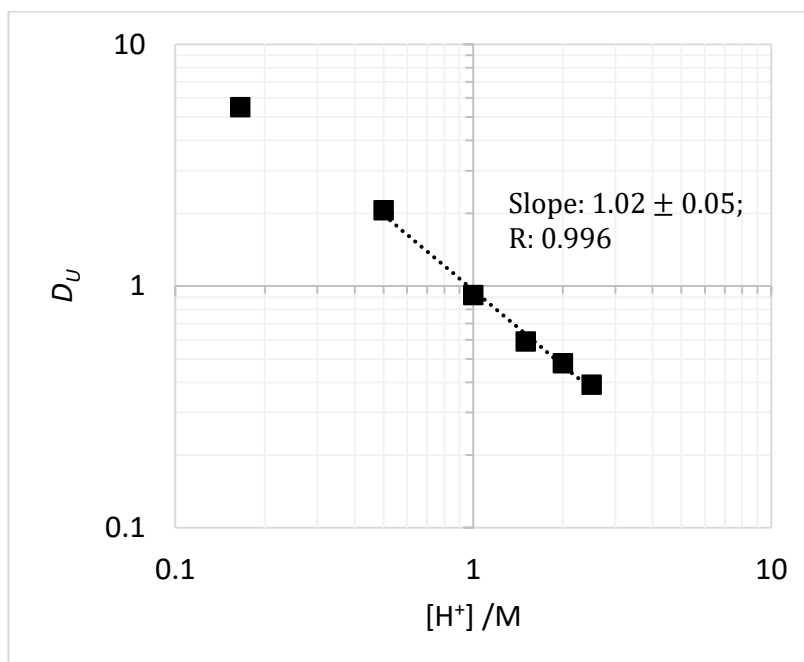


FIGURE 3.6 – EXTRACTION OF URANIUM FROM NITRIC ACID MEDIA AS A FUNCTION OF ACIDITY AT CONSTANT NITRATE CONCENTRATION. 0.005 M PC-88A, 3 M NITRATE, 25°C. IMAGE REPRODUCED FROM DATA PUBLISHED IN [400].

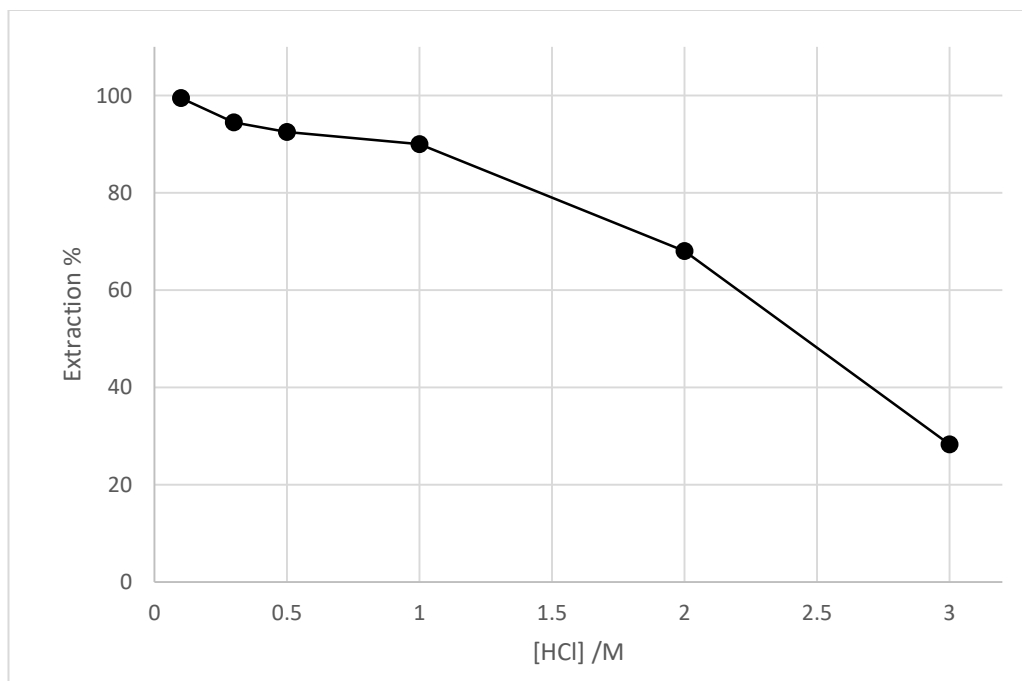


FIGURE 3.7 – EXTRACTION EFFICIENCY OF IRON(III) FROM HYDROCHLORIC ACID MEDIA BY 30% PC-88A (AQUEOUS:ORGANIC RATIO 2, 25°C, CONTACT TIME 15 MINS. IMAGE REPRODUCED FROM DATA PUBLISHED IN [406].

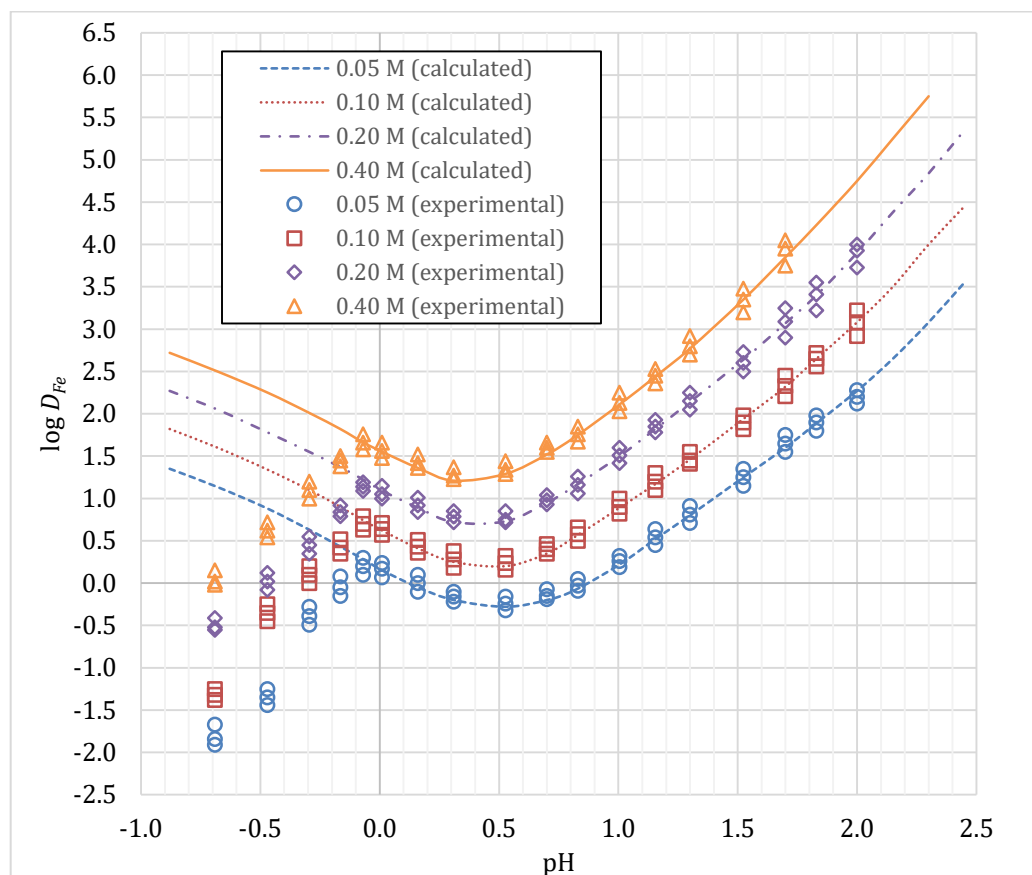


FIGURE 3.8 – EXTRACTION OF IRON(III) BY FOUR CONCENTRATIONS OF HDEHP FROM HYDROCHLORIC ACID MEDIA. [HDEHP] LEVELS ARE 0.05 M, 0.1 M, 0.2 M AND 0.4 M, BOTTOM TO TOP (30°C, ONE HOUR CONTACT TIME). IMAGE REPRODUCED FROM DATA PUBLISHED IN [403].

3.1.3.4 MIXTURES OF PC-88A AND HDEHP FOR SEPARATION OF OTHER METALS

Mixtures of PC-88a and HDEHP have been studied for the extraction of other metals besides thorium, uranium and iron.

The separation of rare earth elements has been studied by several researchers. The trivalent rare earths are extracted by cation exchange from sulfate media, forming rare earth sulfate complexes with HDEHP or PC-88a individually, or the mixed complex $RE(H(DEHP)_2)_2(H)EHEHP)_2$ with the synergic mixture of 0.06 M PC-88a, 0.04 M HDEHP [407]. Another study considered cerium(IV) separation from sulfuric acid media, and confirmed the maximum synergism at the same extractant ratio and at 0.5 M acidity.

The extracted complex was determined to be $\text{Ce}(\text{SO}_4)_{0.5}\text{H}(\text{EHEHP})_2(\text{DEHP})_2$ [408].

Vanadium(IV) was extracted as the VO^{2+} vanadyl species from sulfuric acid by the synergic mixture of 0.8 M PC-88a, 0.2 M HDEHP, with the extracted species being $\text{VO}(\text{H}(\text{EHEHP})_2)(\text{H}(\text{DEHP})_2)$, with a possible small amount of $\text{VO}(\text{H}(\text{EHEHP})_2)(\text{H}(\text{EHEHP})(\text{DEHP}))$ [390].

3.1.4 EXTRACTION STUDIES PERFORMED

There are many parameters in a given solvent extraction system that may be modified in order to alter the extraction behaviour and equilibrium distribution ratios of the metals to be separated. These changes may be separated according to whether they occur in the aqueous phase, in the organic phase, or are related to the overall solvent extraction contact (i.e. temperature and contact time).

The variables studied in this work are illustrated in Figure 3.9.

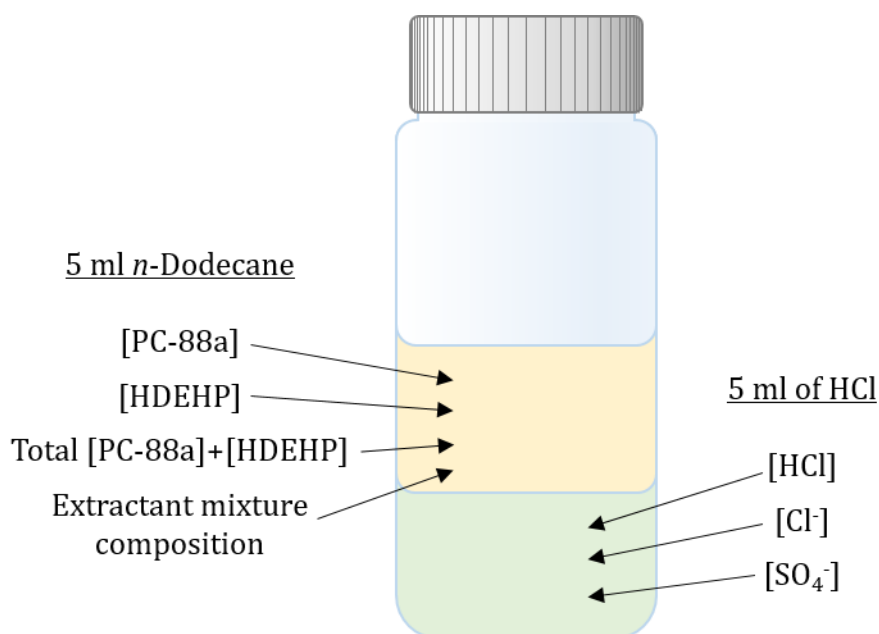


FIGURE 3.9 – THE EXPERIMENTAL VARIABLES STUDIED IN THIS ASSOCIATED WITH EACH PHASE.

In the aqueous phase, the acid concentration, ionic strength and metal concentration will have an effect on extraction behaviour [77]. In the organic phase, the concentration of the extractants may be varied, both independently and together. Two experiments were performed where the concentration of one extractant was held fixed while the other was varied, in order to determine the individual contribution to extraction behaviour of each extractant in the mixture.

Job's method of continuous variation [409-411] was used to determine the presence or absence of synergic/antagonistic effects related to the use of multiple extractants [79, 412]. The total extractant concentration was held to a fixed value, but the relative concentrations of PC-88a and HDEHP were varied. Finally, an experiment was performed with a fixed extractant ratio but variable total extractant concentration in order to determine the extraction constant K_{ex} of the system.

3.2 METHODS

3.2.1 REAGENTS AND STOCK SOLUTIONS

Unless otherwise stated, all organic chemicals and metal salts were ACS Reagent Grade, and were purchased from Sigma Aldrich. PC-88a ($C_{16}H_{35}O_3P$) was supplied by BOC Sciences, USA. The organic reagents were used as supplied without further purification. Two organic stock solutions were prepared, one with 0.2 M PC-88a in *n*-dodecane and the other with 0.1 M HDEHP in *n*-dodecane, standardised by mass. The organic solutions, and a stock of *n*-dodecane, were pre-equilibrated with 3 M HCl. In addition, an unequilibrated mixed organic solution of 0.1 M PC-88a and 0.05 M HDEHP was also prepared.

Thorium chloride octahydrate ($ThCl_4 \cdot 8H_2O$) and uranyl nitrate hexahydrate ($UO_2(NO_3)_2 \cdot 6H_2O$) salts were taken from in-house stocks originally supplied

by British Drug Houses. The initial purity of these aged materials was unknown. Reagent grade iron(III) chloride hexahydrate ($\text{FeCl}_3 \cdot 6\text{H}_2\text{O}$) was used as the iron salt, supplied by Sigma Aldrich. Reagent Grade 37% hydrochloric acid and Analytical Grade 70% nitric acid were purchased from Fisher Scientific.

Hydrochloric acid solutions were prepared at a range of concentrations from 0.05 – 4.0 M, and standardised against a calibration curve using a Mettler Toledo FiveGo pH meter with Ag-AgCl glass electrode. A mixed metal synthetic pregnant liquor solution (PLS) with 100 ppm of each metal and a thorium-only PLS with 100 ppm Th were prepared in 3.0 M HCl. In addition, a 5 M HCl solution was prepared with 12.5 g/l of each metal, as a mixed metal spike solution. The mixed metal PLS and spike were used in the majority of studies performed in order to economise on analytical instrument usage time and costs. This also allows studies to be made on the competition between metals for the available extractant.

3.2.2 ANALYTICAL INSTRUMENTS AND TECHNIQUES

Metal concentrations in aqueous solution were determined by Inductively Coupled Plasma Mass Spectroscopy (ICP-MS) or Inductively Coupled Plasma Mass Spectroscopy (ICP-OES). ICP-MS was the technique used unless otherwise stated.

3.2.2.1 INDUCTIVELY COUPLED PLASMA MASS SPECTROSCOPY

A diagram showing the functional components of a modern type of ICP-MS system is presented in Figure 3.10. Details of the ICP-MS technique and systems are available in many literature sources [413-415].

In this work ICP-MS was performed by an external service, using a Perkin Elmer Elan DRC II, which uses a quadrupole detector and includes a reaction cell for removing species which cause iron interferences [416, 417]. Results were reported as the average of three replicate runs, and the instrument

was flushed with nitric acid between runs. Calibration standards were supplied by Merck (U and Fe in Merck VI) and PerkinElmer (Th in Calibration standard 2), and diluted using 1% analytical grade nitric acid.

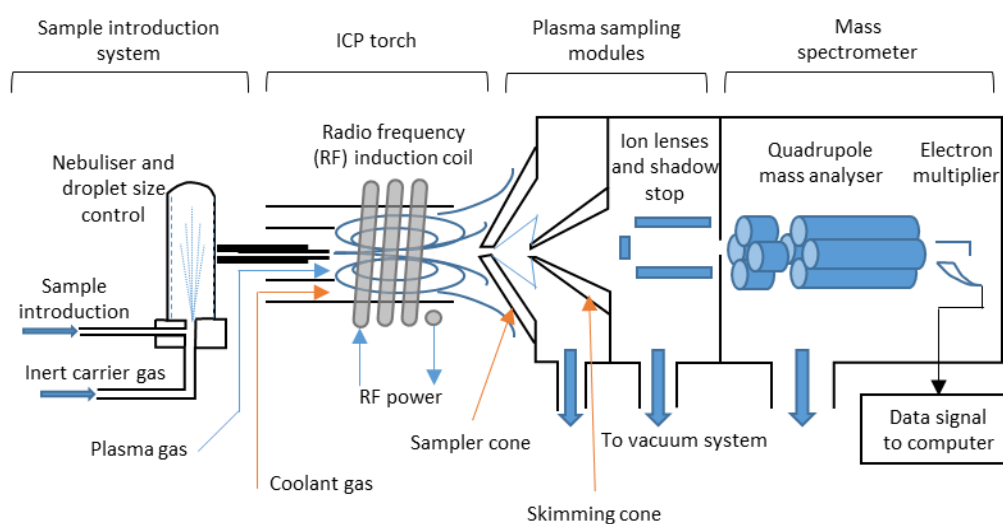


FIGURE 3.10 – DIAGRAM OF MAIN FUNCTIONAL COMPONENTS OF A MASS SPECTROMETRY SYSTEM WITH INDUCTIVELY COUPLED PLASMA ION SOURCE AND QUADRUPOLE MASS ANALYSER.

3.2.2.2 INDUCTIVELY COUPLED PLASMA OPTICAL EMISSION SPECTROSCOPY

ICP-OES differs from ICP-MS in the property of the analyte sample which is measured. Both techniques use an inductively coupled plasma torch to atomise and ionise the introduced analyte. However, where ICP-MS differentiates atoms and ions based on the difference in their mass, ICP-OES measures the energy of the characteristic photons emitted as electrons recombine with the ions in the plasma and give up their excess energy. Fuller details of the ICP-OES technique have been widely published, and will not be discussed further in this thesis [418-420].

The ICP-OES instrument used was a Thermo Fisher iCAP 6000. ICP-OES analyses were performed using a thorium standard produced by Inorganic

Ventures, purchased from ESSLabs. Standards were diluted using 1% analytical grade nitric acid.

3.2.3 EXPERIMENTAL TECHNIQUE

For the solvent extraction contacts 5 ml volumes of both organic and aqueous phases were used in all cases. In this sub-section the general methodology used is described. However, certain experiment specific variations were included, and these are described below in Section 3.2.4.

For a “standard” experiment, 2.5 ml of the 0.2 M PC-88a solution and 2.5 ml of the 0.1 M HDEHP solution were added to a glass liquid scintillation vial, and shaken well by hand to combine the solutions. Then, 4.96 ml of 3.0 M hydrochloric acid was added to the vial, and the phases were again manually shaken to pre-equilibrate the acidity of the organic and aqueous phases. Following this, 0.04 ml of the mixed metal spike was added and the vial was vigorously shaken manually for five minutes to perform the contact, which was enough time for the bulk of the thorium to be extracted, based on literature data [253]. The strength of agitation was judged sufficient to fully inter-disperse the phases, and phase separation was rapid (< 10 s). A 1 ml aliquot of the post-contact aqueous raffinate was taken and diluted with 1% analytical grade nitric acid for ICP analysis.

3.2.3.1 PRESENTATION OF RESULTS

Results are presented as values of distribution ratio D_M , where subscript M is the chemical symbol of the metal of interest, being Th, U or Fe. The formula for D_M was presented in Equation (2.8). If the volumes of the two phases are equal, and it is assumed that all of the initial solute is partitioned into either the aqueous or organic phase (i.e. none precipitates, is volatilised or forms a third phase), then Equation (3.2) may be used [77].

$$D_M = \frac{[M]_0 - [M]}{[M]} \quad (3.2)$$

Where $[M]_0$ is concentration of metal in the aqueous phase before contact with the organic phase, which is the total metal volume in the system.

Values for $[M]_0$ for each metal were taken as the average measured metal concentrations of three identical samples of 40 μl of the mixed metal spike solution (for ICP-MS) or the thorium spike solution (for ICP-OES) added into 4.96 ml of 3 M HCl. 1 ml aliquots were taken and diluted 10x with 1% analytical grade nitric acid and the concentrations of each metal were determined using the standard operating procedure for the instrument. Values for $[M]$ were measured by ICP-MS analysis as described above.

In synergism studies it is also useful to define the synergic factor for each metal ψ_M is a measure of synergic effects, and is given by Equation (3.3) [421].

$$\psi_M = \frac{D_{M,mixture}}{D_{M,PC-88a} + D_{M,HDEHP}} \quad (3.3)$$

Where $D_{M,mixture}$ is the distribution ratio for metal M with the mixture of extractants (0.1 M PC-88a, 0.05 M HDEHP),

$D_{M,PC-88a}$ is the distribution ratio for metal M with 0.1 M PC-88a alone, and

$D_{M,HDEHP}$ is the distribution ratio for metal M with 0.05 M HDEHP alone.

Diluted samples for ICP-MS analysis were expected to have approximately 10 ppm of each metal. Due to the limit of detection for the instrument being 0.001 ppm, the maximum D_M which can be reported is $\sim 10^4$. This was taken to indicate quantitative extraction of the metal in question.

3.2.4 VARIATIONS IN METHODOLOGY

In order to study the impact of variables such as reagent concentration it is necessary to vary the method described above. These modifications are described below according to the independent variable under consideration.

3.2.4.1 ACID CONCENTRATION

The effect of acid concentration was examined by varying the [HCl] concentration in the range 0.02 M – 2.1 M (equilibrium acidity post-contact).

For each sample, 5 ml of the prepared, unequilibrated mixed organic solution was shaken with 4.96 ml of acid of the appropriate concentration. 0.04 ml of mixed metal spike was added and the phases were manually shaken to perform the extraction contact. pH measurements of the aqueous raffinate were taken to determine the equilibrium acidity and aliquots were diluted for ICP-MS analysis.

3.2.4.2 CALCULATION OF SYNERGIC FACTOR AS A FUNCTION OF ACID CONCENTRATION

An experiment was performed following the method of Section 3.2.3 to determine the synergic factor for the extraction. The extraction of each metal was measured by each extractant individually (0.1 M PC-88a and 0.05 M HDEHP) and in the mixture, following the previously described method, from two acid concentrations, being 3.0 M, and a more dilute solution of 0.5 M HCl to determine whether the synergic factor changes significantly when the acidity is varied between these extremes.

3.2.4.3 EFFECT OF IONIC STRENGTH

The effect of added chloride and added sulfate concentrations of up to 100 g/l were tested separately. The base chloride concentration in the aqueous solution, without added chloride, was calculated to be 107 g/l (3.02 M).

Chloride and sulfate were added as their sodium salts, standardised by mass after drying at 80°C for 48 hours. The required masses of the salts were added to scintillation vials with 4.96 ml of 3 M hydrochloric acid and the vials were shaken as required to dissolve the salt. The mixed organic solution was then added and the pre-equilibration and solvent extraction contacts were performed as previously described.

3.2.4.4 ORGANIC PHASE COMPOSITION

Three experiments were performed into variable organic phase composition. In the experiments with variable PC-88a:HDEHP ratio the pre-equilibrated solutions of PC-88a and HDEHP were combined in various ratios to produce a range of mixed organic phases. An equal volume of the mixed metal PLS was added and shaking was applied to contact the phases. An aqueous aliquot was taken for ICP-MS analysis as described previously. Job's method was employed to identify synergic ratios for the extraction of each metal.

For the fixed ratio experiment, a 0.1 PC-88a/0.05M HDEHP organic phase was prepared from the pre-equilibrated solutions, and diluted with the pre-equilibrated *n*-dodecane to a range of concentrations. An equal volume of the thorium only PLS was contacted with the organic phase, and aliquots were taken for ICP-OES analysis.

3.2.5 ERROR CALCULATION

The errors in D_M were calculated based on the three samples used in determining $[M]_0$ in Section 3.2.3.1. The standard error was calculated across the three metal concentration measurements to give the error in metal concentration.

When calculating values of D_M the analytical errors must be combined to determine the errors in distribution ratio. Quotient errors are determined using Equation (3.4).

$$\frac{\delta Q}{|Q|} = \sqrt{\left(\frac{\delta a}{a}\right)^2 + \left(\frac{\delta b}{b}\right)^2 + \left(\frac{\delta c}{c}\right)^2 + \dots} \quad (3.4)$$

Where Q is the result of a quotient, and
 $a, b, c \dots$ are variables in the quotient equation.

Applying this to the calculation of D_M in Equation (3.2) gives Equation (3.5).

$$\frac{\delta D_M}{|D_M|} = \sqrt{\left(\frac{\delta[M]}{[M]}\right)^2 + \left(\frac{\delta[\bar{M}]}{[\bar{M}]}\right)^2} \quad (3.5)$$

As the concentration of metal in the organic phase was determined by subtracting the aqueous concentration from the total concentration, as in Equation (3.2), this error must also be accounted for. When data with errors are summed or subtracted, the errors are also summed or subtracted, as shown in Equations (2.6) and (3.7).

$$R \pm \delta R = (A \pm \delta A) + (B \pm \delta B) \quad (3.6)$$

$$\delta R = \delta A + \delta B \quad (3.7)$$

Where R is the result of a summation/subtraction, and
 A and B are variables in the summation/subtraction equation.

Thus, the error in D_M may be calculated according to Equation (3.8).

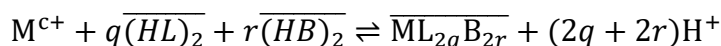
$$\frac{\delta D_M}{|D_M|} = \sqrt{\left(\frac{\delta[M]}{[M]}\right)^2 + \left(\frac{2\delta[M]}{[M]}\right)^2} \quad (3.8)$$

The absolute errors measured by ICP-MS and calculated percentage errors in D_M are given in Table 3.2. These were used to calculate the error bar magnitudes presented in the results plots.

3.2.6 DATA ANALYSIS

PC-88a and HDEHP extracted U and Fe in the literature by cation exchange, and so a cation exchange mechanism was supposed here. The general

formula for solvent extraction of metals by a pair of dimeric cation exchangers is given by



The equilibrium extraction constant K_{ex} for this reaction is given by Equation (3.9). $(HL)_2$ and $(HB)_2$ are the two protonated acid extractants.

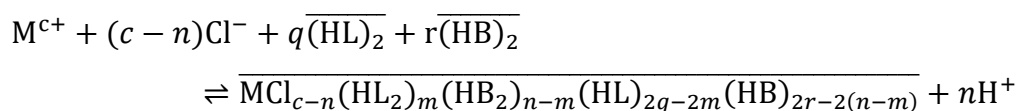
$$K_{ex} = \frac{[\overline{ML}_{2q}\overline{B}_{2r}][H^+]^{2q+2r}}{[M^{c+}][\overline{(HL)}_2]^q[\overline{(HB)}_2]^r} \quad (3.9)$$

When the extraction mechanism is purely cation exchange the metal charge c will be equal to the number of protons released from the extractants $(2q + 2r)$.

TABLE 3.2 – CONCENTRATION OF EACH METAL ACROSS THREE REPLICATES FOR DETERMINATION OF EXPERIMENTAL ERRORS, DETERMINED BY ICP-MS. SAMPLES PREPARED BY ADDING 0.04 ml OF METAL SPIKE SOLUTION TO 4.95 ml OF 3 M HYDROCHLORIC ACID. ALSO GIVEN ARE THE CALCULATED PERCENTAGE ERRORS IN THE METAL DISTRIBUTION RATIOS.

METAL	SAMPLE 1 /PPM	SAMPLE 2 /PPM	SAMPLE 3 /PPM	MEAN OF REPLICATES /PPM	% ERROR IN D_M FROM EQUATION (3.8)
Th	74.712	68.759	63.554	69.008	8.53%
U	94.960	82.034	74.448	83.814	13.04%
Fe	133.84	126.57	119.43	126.61	6.00%

It is possible that the extracted species may be a metal chloride. Thorium was often observed in the literature to be extracted by neutral adduct formation in addition to cation exchange. The extraction mechanism for a metal M of charge c by mixed cation exchange and adduct formation with two dimerised extractants $(HL)_2$ and $(HB)_2$ from chloride media may be characterised by the general reaction



This reaction was adapted from similar general reactions in the literature [88, 253, 422]. Complete deprotonation of the extractants has also been suggested in the literature, which would slightly modify the reaction above. The equilibrium extraction constant K_{ex} for the reaction is given in Equation (3.10).

$$K_{ex} = \frac{[\overline{\text{MCl}_{c-n}(\text{HL}_2)_m(\text{HB}_2)_{n-m}(\text{HL})_{2q-2m}(\text{HB})_{2r-2(n-m)}}][\text{H}^+]^n}{[\text{M}^{c+}][\text{Cl}^-]^{c-n}[(\text{HL})_2]^q[(\text{HB})_2]^r} \quad (3.10)$$

The extraction mechanism and the nature of the extracted complexes were determined by slope analysis [388]. Slope analysis methods are commonly used in the solvent extraction literature, being used in most of the studies cited in this chapter and in Section 2.8.

Slope analysis methods are based on taking the logarithm of extraction constant equations, such as Equation (3.10). The equation is then arranged such that when it is plotted on a set of logarithmic axes, the slope of the resulting straight line gives information on the nature of the extracted complex. In this case, to begin a rearrangement of Equation (3.10) is required. First, the distribution ratio is defined as in Equation (3.11).

$$D_M = \frac{[\overline{\text{M}}]}{[\text{M}]} = \frac{[\overline{\text{MCl}_{c-n}(\text{HL}_2)_m(\text{HB}_2)_{n-m}(\text{HL})_{2q-2m}(\text{HB})_{2r-2(n-m)}}]}{[\text{M}^{c+}]} \quad (3.11)$$

Using Equation (3.11), it is possible to restate Equation (3.10) as shown below in Equation (3.12).

$$D_M[\text{H}^+]^n = [\text{Cl}^-]^{c-n}[(\text{HL})_2]^q[(\text{HB})_2]^r K_{ex} \quad (3.12)$$

Taking the logarithm of Equation (3.12) gives Equation (3.13).

$$\begin{aligned} \log_{10} D_M - n \cdot \text{pH} &= (c - n) \log_{10} [\text{Cl}^-] \\ &+ q \log_{10} [(\text{HL})_2] + r \log_{10} [(\text{HB})_2] + \log_{10} K_{ex} \end{aligned} \quad (3.13)$$

On the basis of Equation (3.13), experiments may be carried out which allow the determination of n , q and r . In an experiment, the values of two

independent variables from the set of pH, $[(\text{HL})_2]$ and $[(\text{HB})_2]$ are fixed, the third is varied, and the impact on D_M is measured. The value of $[\text{Cl}^-]$ should also be fixed. Fixing some variables allows Equation (3.13) to be reduced to three simplified forms, which can be used for the determination of n , q and r by slope analysis.

$$\log_{10} D_M = n \cdot \text{pH} + z \quad (3.14)$$

$$\log_{10} D_M - n \cdot \text{pH} = q \log_{10} [(\text{HL})_2] + z \quad (3.15)$$

$$\log_{10} D_M - n \cdot \text{pH} = r \log_{10} [(\text{HB})_2] + z \quad (3.16)$$

Where z is a constant from the remaining terms of Equation (3.13).

Thus, assuming that a single extraction complex is formed, on a log-log plot of D_M versus the selected independent variable, the experimental data points will lie along a straight line, whose slope is given by n , q or r , based on the independent variable under consideration. To determine the number of protons released in complex formation, the concentration of the extractants is fixed and the pH is varied, while to determine the number of extractant molecules complexed the concentration of that extractant is varied, while the pH and concentration of the other extractant are fixed.

The experiments as described in Sections 3.2.3 and 3.2.4 are designed in order to allow the application of the slope analysis method. Results are plotted in Section 3.3 such that slope analyses could be carried out, where the left hand side of Equation (2.6), (3.15) or (3.16) is used as the y-axis, and the corresponding term from pH, $\log_{10} [(\text{HL})_2]$ or $\log_{10} [(\text{HB})_2]$ is used as the x-axis, such that the data should lie along a straight line of slope n , q or r .

An extended mathematical treatment of slope analysis methods is outlined in Appendix B of this thesis.

3.2.7 PREDICTION OF EXTRACTION ISOTHERMS

The metal concentration in the feed is a key factor in determining the optimum separations conditions. In a thorium fuel cycle front end solvent extraction process plant the metals feed will be determined by the upstream monazite treatment, and the solvent extraction process conditions will be largely determined by the feed composition and the desired thorium product purity. One of the parameters that must be determined in the development of a thorium solvent extraction process is the number of counter-current solvent extraction contact stages required to achieve a given level of thorium recovery, which may be calculated by McCabe-Thiele graphical analysis of an extraction isotherm [77].

An example McCabe-Thiele extraction isotherm is presented in Figure 3.11, in order to explain how this is used to determine the number of stages by a graphical method. The McCabe-Thiele method was originally developed for the design and analysis of binary distillation equipment. However, the method is also applicable to counter-current solvent extraction equipment design.

Two lines are plotted on a set of axes, where the x-axis represents the concentration of metal in the aqueous phase and the y-axis represents the concentration of metal in the organic phase. The first plotted line is the extraction/distribution isotherm. In distillation analysis this would be the equilibrium line. This is a plot of how the metal distributes at equilibrium between the aqueous and organic phases. The second plotted line is the operating line, and represents the concentration of metal which can be complexed by the available free extractant for a given level of aqueous metal concentration. The slope of this line is equal to the slope of a log-log plot of extractant dependence. A line of the aqueous feed concentration is then drawn vertically upwards to meet the isotherm line. The number of stages may then be determined as follows. Where the operating line intercepts the feed concentration, a line is plotted horizontally to the isotherm line, and

then dropped vertically to the operating line. This process is repeated until the concentration in the aqueous phase reaches the desired raffinate concentration. Each horizontal step, moving from the operating line to the isotherm line, represents a single equilibrium contact stage in the counter-current solvent extraction system. Thus, the number of horizontal lines gives the number of equilibrium contact stages required to reduce the concentration in the aqueous phase from the feed concentration to the raffinate concentration.

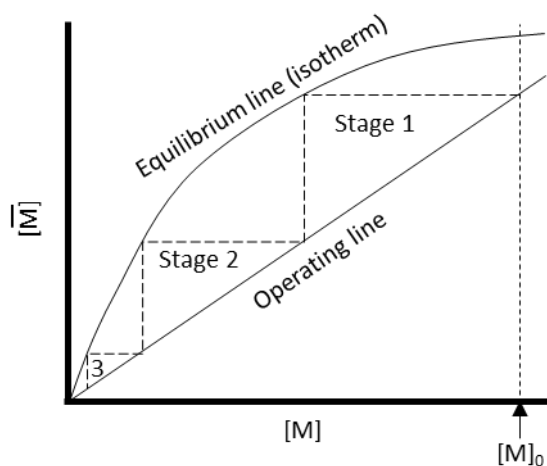


FIGURE 3.11 – EXAMPLE OF A MCCABE-THIELE ISOTHERM AS APPLIED TO SOLVENT EXTRACTION.

Based on the data collected, an isotherm may be predicted for the extraction of thorium, and from this the number of stages required may be estimated by McCabe-Thiele graphical analysis [77, 389]. An aim of the work was to determine the number of stages required for 99% recovery of thorium from the feed, and thus the vertical feed line in Figure 3.11 is set to 99% of the thorium feed concentration.

An extraction isotherm may be predicted for the thorium complex formation reaction, for which the extraction constant is given in Equation (3.10), and reprinted below.

$$K_{ex} = \frac{[MCl_{c-n}(HL_2)_m(HB_2)_{n-m}(HL)_{2q-2m}(HB)_{2r-2(n-m)}][H^+]^n}{[M^{c+}][Cl^-]^{c-n}[(HL)_2]^q[(HB)_2]^r} \quad (3.10)$$

We define two variables, y and x , in Equations (3.17) and (3.18) below respectively.

$$y = \frac{[\text{MCl}_{c-n}(\text{HL}_2)_m(\text{HB}_2)_{n-m}(\text{HL})_{2q-2m}(\text{HB})_{2r-2(n-m)}]}{[\text{M}^{c+}]} \quad (3.17)$$

$$x = [\text{M}^{c+}] \quad (3.18)$$

If it is assumed that the metal is extracted as Th^{4+} , rather than a thorium chloride species, then Equation (3.10) may be simplified to give Equation (3.19).

$$K_{ex} = \frac{y[\text{H}^+]^n}{x[(\text{HL})_2]^q[(\text{HB})_2]^r} \quad (3.19)$$

In order to determine the free quantity of each extractant in the system at equilibrium, as required in the denominator of Equation (3.19), two parameters α and β are defined which represent the total concentration of the extractant dimers L_2 and B_2 respectively. Each total concentration is given by the sum of the free extraction and the complexed ligand.

$$\alpha = [(\text{HL})_2] + y \frac{2m + 2(q - m)}{2} \quad (3.20)$$

$$\beta = [(\text{HB})_2] + y \frac{2(n - m) + 2(r - (n - m))}{2} \quad (3.21)$$

Simplifying the numerators of the fractions in Equations (3.20) and (3.21) and rearranging gives

$$[(\text{HL})_2] = \alpha - qy \quad (3.22)$$

$$[(\text{HB})_2] = \beta - ry \quad (3.23)$$

These can be substituted into Equation (3.19) to give

$$K_{ex} = \frac{y}{x} \frac{[\text{H}^+]^n}{(\alpha - qy)^q(\beta - ry)^r} \quad (3.24)$$

In addition to K_{ex} , the modified extraction coefficient K'_{ex} is defined as

$$K'_{ex} = \frac{K_{ex}}{[H^+]^n} \quad (3.25)$$

Thus, Equation (3.24) may be rearranged to give x as a function of y , as shown in Equation (3.26).

$$x = \frac{y}{K'_{ex}(\alpha - qy)^q(\beta - ry)^r} \quad (3.26)$$

By inserting values of y into Equation (3.26), the corresponding values of x may be determined, allowing the prediction of an extraction isotherm. It can be seen that this equation allows the prediction of an isotherm directly, based on knowledge of the total amount of each extractant, the extraction constant, the acidity of the system and the values of q and r determined from slope analysis.

3.3 RESULTS

3.3.1 DETERMINATION OF EXTRACTION MECHANISM

The extraction mechanisms for each metal were determined by slope analysis of the pH, [PC-88a], [HDEHP] and [Cl⁻] plots presented below.

3.3.1.1 EFFECT OF ACID CONCENTRATION

Figure 3.12 shows the distribution ratios D_M for thorium, uranium and iron, and the fraction of metal extracted as a function of equilibrium acidity. The extraction of all metals increased with increasing pH. Lines of integer slope were fitted through the $\log_{10} D_M$ data, and the resulting slopes are listed in Table 3.3. The increasing extraction with pH indicates a cation exchange mechanism.

TABLE 3.3 – INTEGER SLOPE OF FITTED LINES ON LOG-LOG PLOTS OF D_M AGAINST pH WITH COEFFICIENT OF DETERMINATION R^2 FOR FITTED LINES.

METAL	LOG [H ⁺] SLOPE	R^2
Thorium(IV)	4	0.935
Uranium(VI)	2	0.938
Iron(III)	3	0.946

Thorium extraction is slightly below 100% for the lowest pH level shown. Over 90% of the uranium was extracted from solution for all acidities tested. Iron extraction reduced with increasing acidity, with the $pH_{0.5}$ for iron found to be -0.066 (1.16 M [H⁺]). The trend in extraction was Th > U > Fe, with greatest separation at low acidity.

3.3.1.2 SYNERGIC FACTORS AS A FUNCTION OF ACIDITY

There are indications of synergism for the PC-88a/HDEHP system, as can be seen from the results presented in Table 3.4, as calculated from Equation (3.3). At the higher acidity the extraction of the actinides is synergic, while iron extraction is antagonistic. However, at the lower acidity, while overall distribution ratios are greater, the extraction of thorium switches to become antagonistic, due to extraction by HDEHP alone being quantitative. Uranium extraction remains synergic, and iron extraction becomes synergic at the lower acidity. The large variability in ψ_M for each metal between the two acidities suggests that the extraction mechanism will vary according to the acidity of the system.

3.3.1.3 EFFECT OF EXTRACTANT CONCENTRATION

The distribution ratios for the three metals as a function of [PC-88a] and [HDEHP] are shown in Figure 3.13. Lines of integer slope have been fitted through the data, and these slopes are presented in Table 3.5 with R^2 values.

THE PREPARATION AND APPLICATION OF THORIUM-BASED NUCLEAR FUELS

TABLE 3.4 – SYNERGIC FACTORS FOR THORIUM, URANIUM AND IRON FOR EXTRACTION BY 0.1 M PC-88A AND 0.05 M HDEHP IN *n*-DODECANE FROM HYDROCHLORIC ACID.

PARAMETER	3.0 M HCl			0.5 M HCl		
	Th	U	Fe	Th	U	Fe
$D_{M,mixture}$	68	16	0.22	3800	820	23
$D_{M,PC-88a}$	2.4	3.0	0.14	1500	160	4.2
$D_{M,HDEHP}$	35	6.4	0.12	14000	440	6.9
ψ_M	1.8	1.7	0.85	0.25	1.4	2.1

For uranium and iron the number of protons released was found to equal the number of extractants complexed. However, the number of extractants complexed by thorium was greater than the pH dependence slope, and thus a mixed cation exchange/adduct formation reaction is indicated.

When considering the effect of variable [PC-88a], it can be seen that iron was rejected for most PC-88a concentrations. D_{Fe} was greater than 1 only at 0.2 M PC-88a and 0.05 M HDEHP. Uranium extraction increased with increasing PC-88a, with $1.8 < D_U < 72$. Thorium extraction generally increased with increasing PC-88a concentration, with $D_{Th} = 7.8$ for 0.05 M HDEHP alone, and quantitative extraction at $[PC-88a] \geq 0.167$ M.

The effect of increasing [HDEHP] was to increase extraction for all metals. Thorium and uranium are extracted slightly by 0.1 M PC-88a alone, with D_U greater than D_{Th} . However, increasing [HDEHP] gives increasing distribution ratios for both metals, with D_{Th} increasing by factor 440 and D_U increasing by factor 14 over the range. Iron was found to be partitioned preferentially to the aqueous phase for all levels of HDEHP concentration.

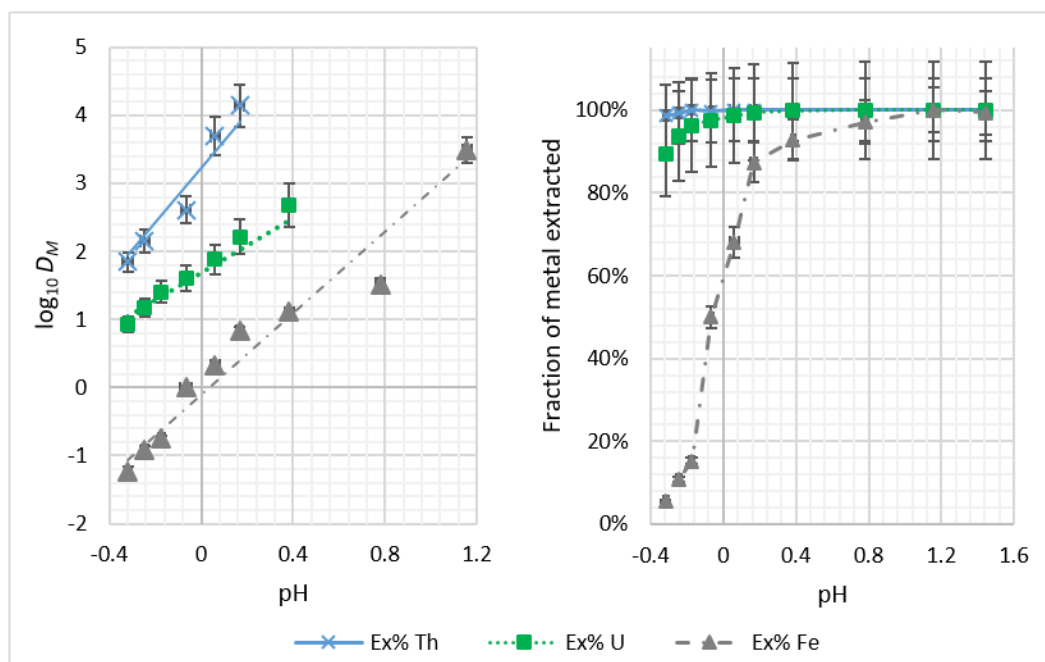


FIGURE 3.12 – Th, U AND Fe DISTRIBUTION RATIOS AS A FUNCTION OF PH, FITTED WITH LINES OF INTEGER SLOPE (LEFT). METAL EXTRACTION FRACTION AS A FUNCTION OF ACIDITY FOR THORIUM, URANIUM AND IRON (RIGHT). EXTRACTION PERFORMED FROM HCl OF VARIOUS CONCENTRATIONS WITH 5 MIN CONTACT TIME AT ROOM TEMPERATURE WITH 100 PPM EACH METAL. EXTRACTANT CONCENTRATIONS WERE 0.1 M PC-88A AND 0.05 M HDEHP.

THE PREPARATION AND APPLICATION OF THORIUM-BASED NUCLEAR FUELS

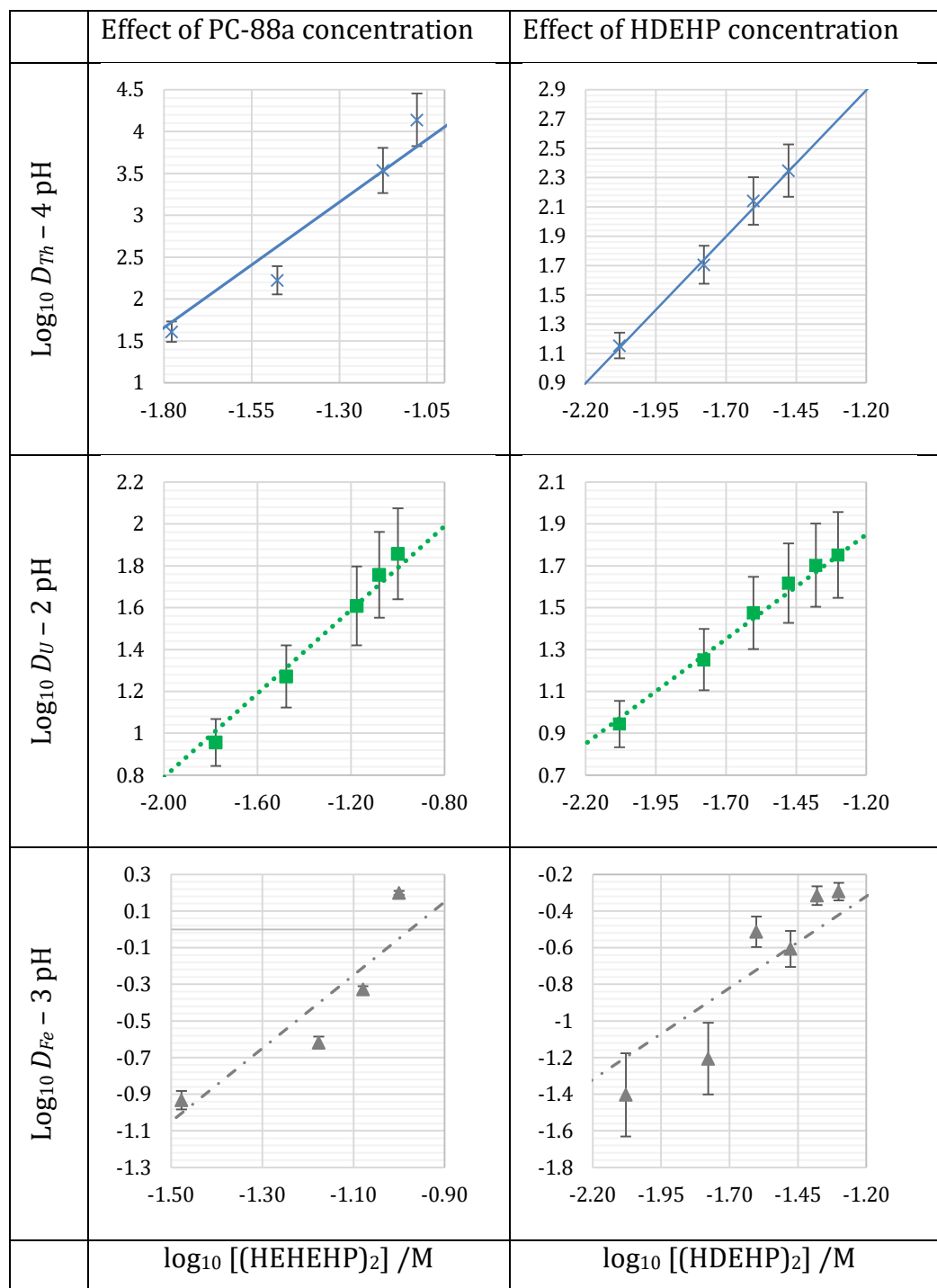


FIGURE 3.13 – DISTRIBUTION RATIO OF TH, U AND FE AS A FUNCTION OF VARIABLE EXTRACTANT CONCENTRATION. TOP: VARIABLE [PC-88A] WITH [HDEHP] = 0.05 M. BOTTOM: VARIABLE [HDEHP] WITH [PC-88A] = 0.1 M. EXTRACTION PERFORMED FROM 3.0 M HCL WITH 5 MIN CONTACT TIME AT ROOM TEMPERATURE WITH 100 PPM EACH METAL.

3.3.1.4 EFFECT OF EXTRACTANT RATIO – JOB'S METHOD

The distribution ratios of thorium, uranium and iron as a function of the fraction of HDEHP in the extractant mixture x_{HDEHP} is shown in Figure 3.14. The fraction of HDEHP is given by Equation (3.27).

$$x_{HDEHP} = \frac{[(HDEHP)_2]}{[(HDEHP)_2] + [(HEHEHP)_2]} \quad (3.27)$$

TABLE 3.5 – INTEGER SLOPE OF FITTED LINES ON LOG-LOG PLOTS OF D_M AGAINST [PC-88A] AND [HDEHP] PLOTTED IN FIGURE 3.13, WITH COEFFICIENT OF DETERMINATION R^2 FOR FITTED LINES.

METAL	LOG [(HEHEHP) ₂] SLOPE q	LOG [(HDEHP) ₂] SLOPE r
Thorium(IV)	3; $R^2 = 0.93$	2; $R^2 = 1.00$
Uranium(VI)	1; $R^2 = 0.98$	1; $R^2 = 0.99$
Iron(III)	2; $R^2 = 0.81$	1; $R^2 = 0.79$

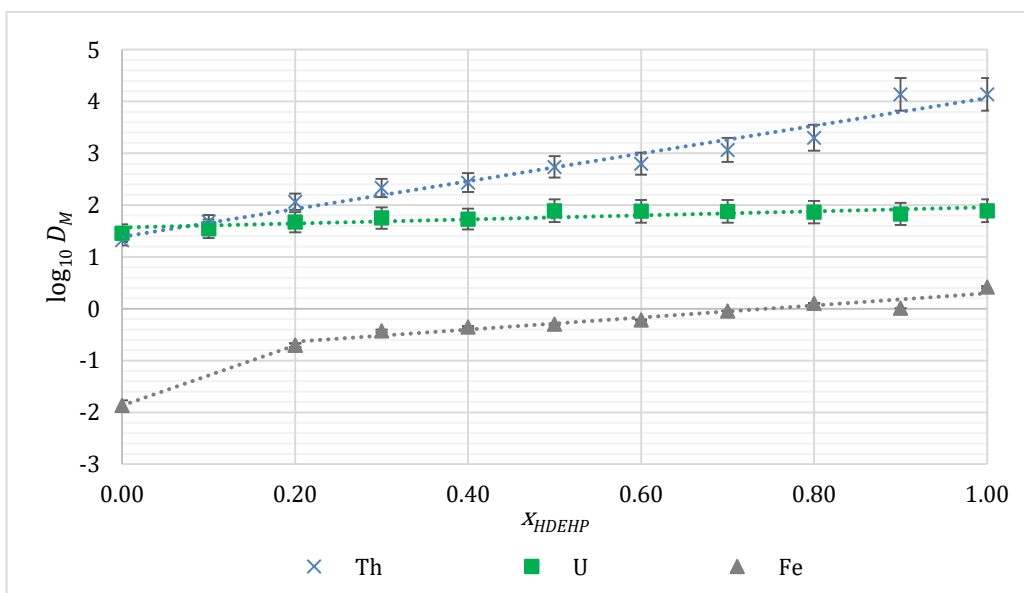


FIGURE 3.14 – JOB'S PLOT SHOWING DISTRIBUTION RATIOS OF FOUR METALS AS A FUNCTION OF THE HDEHP FRACTION IN THE EXTRACTANT MIXTURE. EXTRACTION PERFORMED FROM 3.0 M HCL WITH 5 MIN CONTACT TIME AT ROOM TEMPERATURE WITH 100 PPM EACH METAL, USING 0.15 M TOTAL EXTRACTANT CONCENTRATION. LINES ONLY INTENDED AS A GUIDE TO THE EYE.

Thorium extraction increased with increasing HDEHP fraction, increasing from $D_{Th} = 21$ to quantitative extraction for 100% HDEHP. Uranium extraction increased slightly over the range, with D_U increasing from 29 to 78. The distribution ratio of iron was observed to increase slightly with increasing HDEHP fraction, from 0.01 to 2.6. Given the monotonic trends in distribution ratio for all metals, it is inferred that there is no particular ideal synergic ratio of these extractants under the studied conditions. Assuming that the extractants are behaving through a cation exchange mechanism as would be expected, the fact that HDEHP alone gives stronger extraction than its mixtures with PC-88a is due to the fact that it is a stronger acid due to the presence of the additional oxygen atom in the molecule giving increased electronegativity.

3.3.1.5 EFFECT OF IONIC STRENGTH

Results for D_M as a function of added chloride and added sulfate are presented in Figure 3.15. Linear trend lines have been fitted to each plot. The slope of each line and the associated R^2 is given in Table 3.6.

The slopes are generally negative, indicating that extraction is reduced by increased chloride or sulfate concentration. This is likely due to the formation of relatively poorly extracted metal chloride and metal sulfate species. Sulfate suppresses thorium extraction more strongly than chloride, which is expected given that the stability constants of thorium chloride ThCl_4 and thorium sulfate $\text{Th}(\text{SO}_4)_2$ are 1.57 and 2.34 respectively, as shown in Table 3.7. The slope of iron extraction with sulfate concentration was positive, but due to the magnitude of the errors no reliable conclusion may be drawn from this.

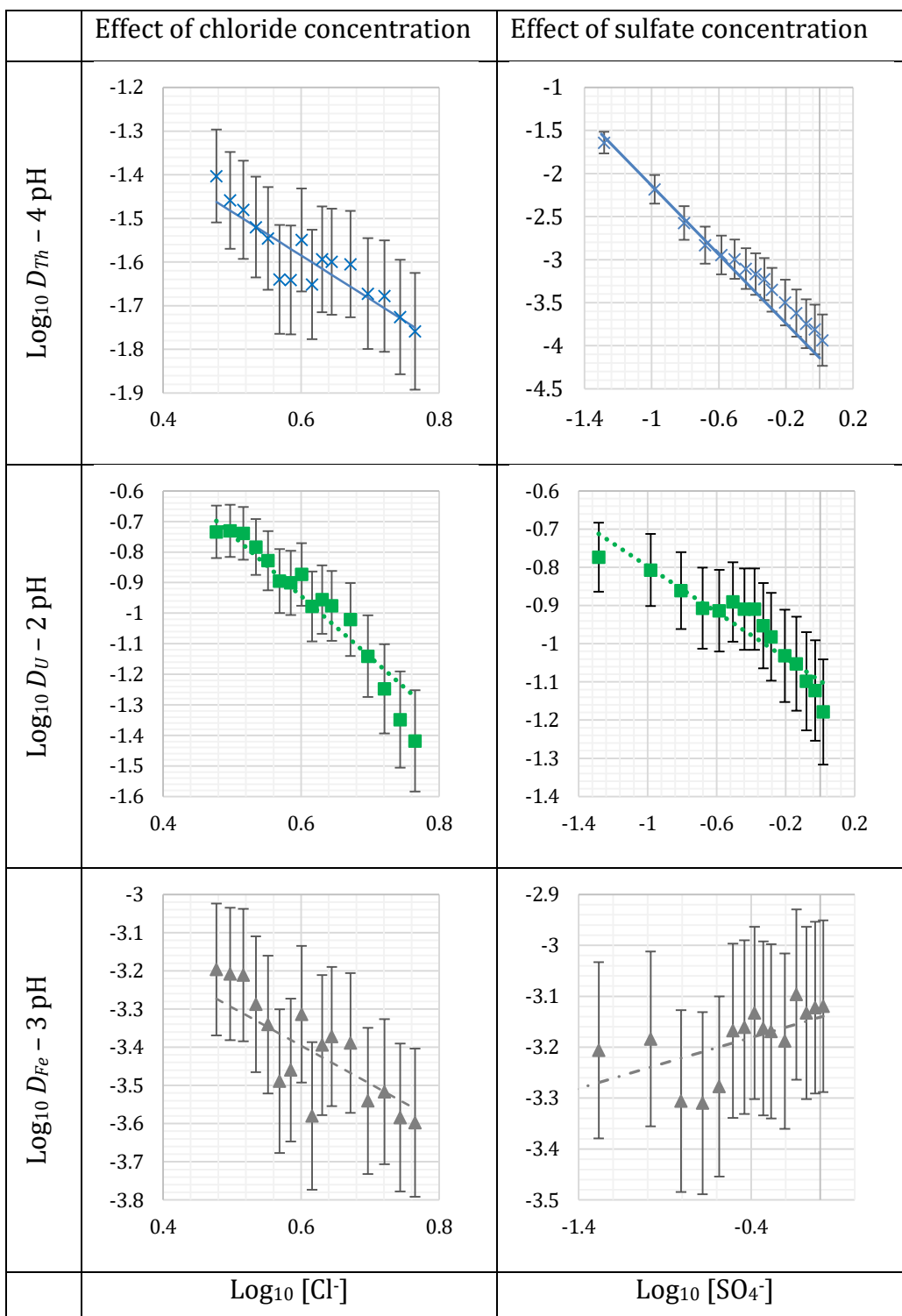


FIGURE 3.15 – DISTRIBUTION RATIO FOR TH, U AND FE AS A FUNCTION OF ADDED CHLORIDE (LEFT) OR SULFATE (RIGHT) IN THE AQUEOUS PHASE. EXTRACTION PERFORMED FROM 3.0 M HCl WITH 5 MIN CONTACT TIME AT ROOM TEMPERATURE WITH 100 PPM EACH METAL, USING 0.1 M PC-88A AND 0.05 M HDEHP IN n-DODECANE AS EXTRACTANTS. NOTE THAT AXIS LABELS ARE IN THE LEFT-MOST COLUMN/BOTTOM ROW OF THE TABLE.

THE PREPARATION AND APPLICATION OF THORIUM-BASED NUCLEAR FUELS

TABLE 3.6 – SLOPE OF FITTED LINES ON LOG-LOG PLOTS OF D_M AGAINST $[Cl^-]$ AND $[SO_4^-]$, WITH COEFFICIENT OF DETERMINATION R^2 FOR FITTED LINES. NON-INTEGER VALUES ARE USED WHERE NO REASONABLE INTEGER SLOPE COULD BE FITTED.

METAL	LOG $[Cl^-]$ SLOPE	LOG $[SO_4^-]$ SLOPE
Thorium(IV)	$-1; R^2 = 0.79$	$-2; R^2 = 0.92$
Uranium(VI)	$-2; R^2 = 0.91$	$-0.3; R^2 = 0.86$
Iron(III)	$-1; R^2 = 0.62$	$0.1; R^2 = 0.37$

TABLE 3.7 – STABILITY CONSTANTS FOR THORIUM CHLORIDE, NITRATE AND SULFATE COMPLEXES IN AQUEOUS SOLUTION [83].

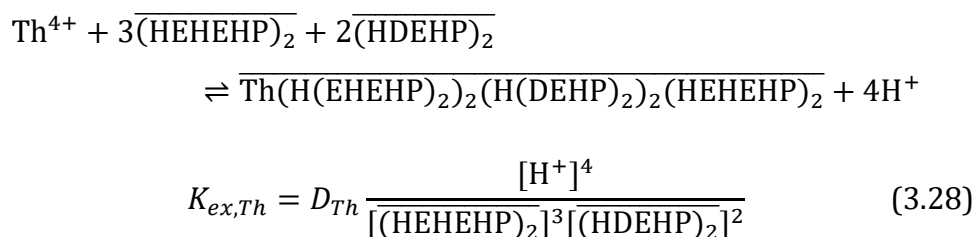
COMPLEX	STABILITY CONSTANT
ThCl ₄	1.57
Th(NO ₃) ₄	0.1
Th(SO ₄) ₂	2.34

When the concentration of added chloride is increased to the level found in sea-water D_{Th} was reduced from 360 to 260, while increasing sulfate to sea-water concentrations reduced D_{Th} from 340 to 280 [423].

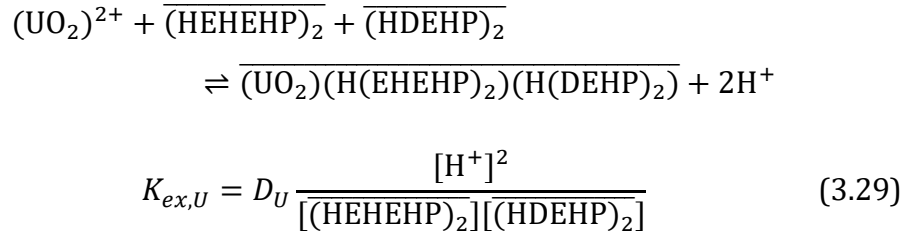
3.3.1.6 REACTIONS DETERMINED FROM SLOPE ANALYSIS

Based on the results presented in Table 3.3 and Table 3.5 the interfacial equilibrium reactions for the formation of the extracted metal complexes are given below, with their associated equilibrium extraction constants.

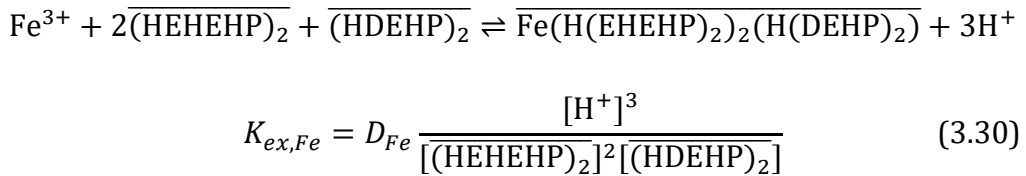
The suggested thorium(IV) reaction, based on a slope of 4 for pH dependence, 3 for PC-88a dependence and 2 for HDEHP dependence is



The suggested uranium(VI) reaction, based on a slope of 2 for pH dependence, and 1 for both PC-88a and HDEHP dependence is



The suggested iron(III) reaction, based on a slope of 3 for pH dependence, 2 for PC-88a dependence and 1 for HDEHP dependence is



3.3.2 CALCULATION OF NUMBER OF REQUIRED EXTRACTION CONTACTS

All solvent extraction experiments performed included data collected at the reference extraction conditions (3 M HCl, 0.1 M PC-88a and 0.05 M HDEHP without added NaCl or Na₂SO₄). The modified extraction constants K'_{ex} for the reactions were calculated for each metal using Equation (3.25), and an average value was calculated. These data are presented in Table 3.8.

The distribution ratio for thorium as a function of free extractant concentration, the denominator of Equation (3.28), is shown in Figure 3.16. The slope of the total extraction plot was found to be 0.66 ($R^2 = 0.983$), which is the overall extractant dependence for the 0.1 M PC-88a, 0.05 M HDEHP mixture. This value was used as the slope of the operating line in the McCabe-Thiele extraction isotherm.

THE PREPARATION AND APPLICATION OF THORIUM-BASED NUCLEAR FUELS

TABLE 3.8 – THORIUM DISTRIBUTION RATIO, THORIUM CONCENTRATION IN THE ORGANIC PHASE AND CALCULATED MODIFIED LOGARITHMIC EXTRACTION CONSTANT FROM EACH EXPERIMENT AT THE REFERENCE EXTRACTION CONDITIONS (3 M HCL, 0.1 M PC-88A, 0.05 M HDEHP).

EFFECT STUDIED	D_{Th}	$\frac{[Th]}{mM}$	$pK_{ex,Th}$	D_U	$\frac{[U]}{mM}$	$pK_{ex,U}$	D_{Fe}	$\frac{[Fe]}{mM}$	$pK_{ex,Fe}$
pH	276	0.297	8.07	25.6	0.0339	3.71	0.181	0.0347	2.57
PC-88a dependence	759	0.296	8.50	29.6	0.0339	3.78	0.179	0.010	2.56
HDEHP dependence	138	0.295	7.76	29.9	0.0341	3.78	0.307	0.0533	2.80
Job Plot	253	0.296	8.03	54.6	0.0346	4.04	0.418	0.0667	2.94
Cl ⁻ ionic strength	395	0.296	8.22	14.4	0.0334	3.46	0.142	0.0881	2.48
SO ₄ ⁻ ionic strength	346	0.297	8.16	33.8	0.0344	3.83	0.140	0.111	2.48
Extractant dependence	234	0.492	8.01	-	-	-	-	-	-
Average pK'_{ex}			8.17			3.80			2.67
Average pK_{ex}			8.77			4.51			3.38

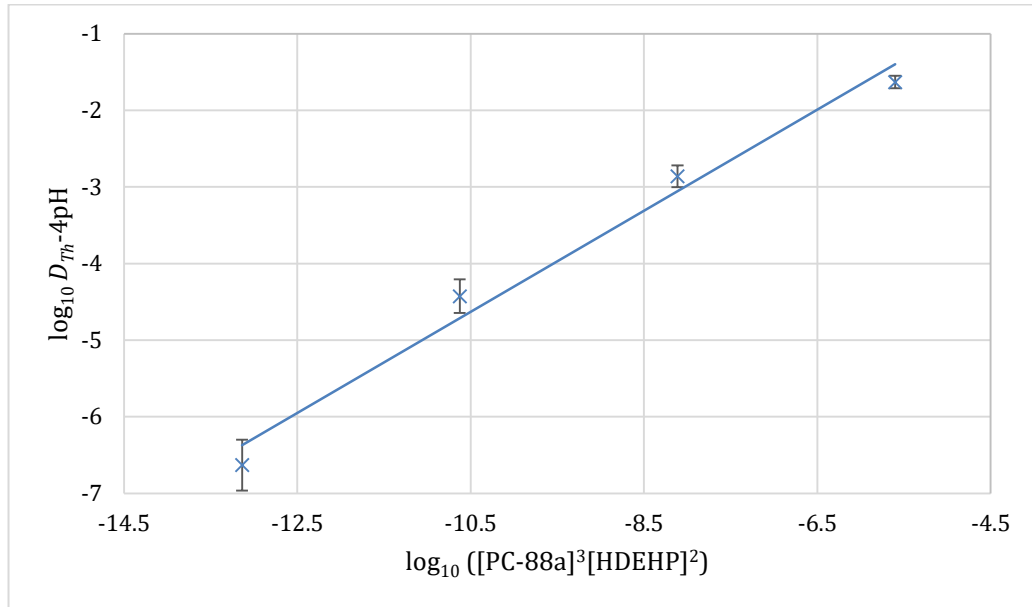


FIGURE 3.16 – DISTRIBUTION RATIO FOR THORIUM AS A FUNCTION OF TOTAL EXTRACTANT CONCENTRATION, WITH PC-88A:HDEHP RATIO 2. EXTRACTION PERFORMED FROM 3.0 M HCL WITH 5 MIN CONTACT TIME AT ROOM TEMPERATURE WITH 100 PPM THORIUM.

TABLE 3.9 – INPUTS REQUIRED FOR PREDICTION OF AN ISOTHERM USING EQUATION (3.25) FOR THORIUM, URANIUM AND IRON, AS USED OR DETERMINED IN THIS WORK.

METAL	Th	U	Fe
K'_{ex}	1.161×10^8	6328	472.2
α	0.10	0.10	0.10
β	0.05	0.05	0.05
q	3	1	2
r	2	1	1

Iron is not well extracted, and it is not useful to plot an extraction isotherm for it. However, an isotherm can be plotted for uranium. The slope of extractant dependence was not experimentally determined for uranium. However, several operating lines were plotted, and the sensitivity of the required number of stages to the slope of the operating line was determined. Lines of slope 0.667-3.0 are shown with the predicted uranium isotherm in Figure 3.18, with details on the number of extraction stages for each given in table Table 3.10, as determined by McCabe-Thiele graphical analysis.

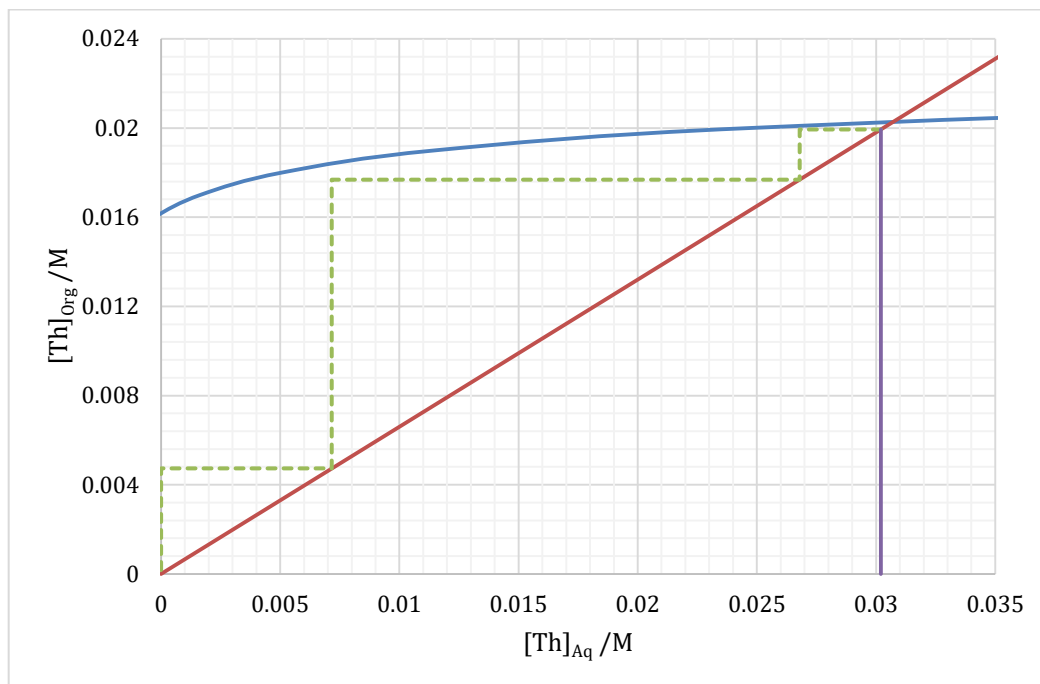


FIGURE 3.17 – PREDICTED MCCABE-THIELE EXTRACTION ISOTHERM, FOR EXTRACTION OF THORIUM FROM HYDROCHLORIC ACID ($[H^+]_{eq} = 1.5 \text{ M}$) USING 0.1 M PC-88A AND 0.05 M HDEHP IN *n*-DODECANE.

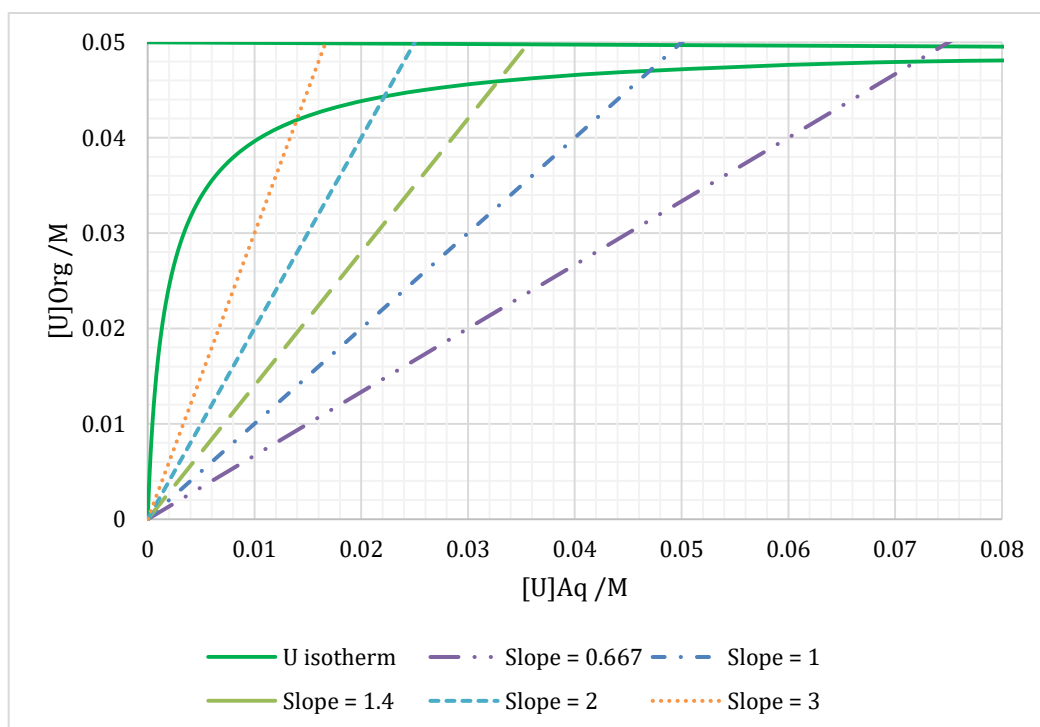


FIGURE 3.18 – URANIUM EXTRACTION ISOTHERM WITH LINES OF VARYING SLOPE THROUGH ORIGIN, REPRESENTING POSSIBLE OPERATING LINES FOR SENSITIVITY ANALYSIS.

TABLE 3.10 – NUMBER OF EXTRACTION STAGES REQUIRED FOR 99% URANIUM RECOVERY FOR DIFFERENT EXTRACTION CONSTANTS. NUMBER OF STAGES FOR AN EXTRACTION CONSTANT OF 2.5 INCLUDED TO INDICATE SENSITIVITY IN THIS REGION.

EXTRACTION CONSTANT LINE SLOPE	NUMBER OF EXTRACTION STAGES
0.67, 1.00, 1.40	3
2.00	4
3.00	5

Given that two extractant ligands bind to each uranium(VI) ion, it is suggested that the extraction dependence slope is likely to be lower than that of thorium(IV), and thus 3-4 extraction stages are likely to be required for 99% uranium recovery.

3.4 DISCUSSION

3.4.1 DETERMINATION OF EXTRACTED COMPLEXES

The suggested thorium(IV) reaction includes neutral adduct formation. In aqueous solutions thorium is known to exhibit 9-, 10- and 11-fold coordination behaviour [424]. 10-fold coordination is suggested here, as four partially deprotonated extractant dimers are binding through two coordination sites each, leaving two sites for the binding of a single PC-88a dimer as a neutral adduct.

The extracted complex identified for thorium based on slope analysis in this work includes features from a number of complexes formed by HDEHP or PC-88a alone. Slopes of pH dependence of 4, without chloride incorporation, have previously been shown [85], as have mixed cation exchange and solvation complexes [88]. Overall the complex is perhaps closest to that identified by Peppard [394]. A previous study into the extraction of thorium from nitrate solutions with PC-88a found an average $pK_{ex} = 3.65 \pm 0.03$ [251], suggesting that the complexation of thorium by mixtures of PC-88a

and HDEHP from chloride media is stronger than PC-88a alone from nitrate media.

Previous studies have shown that uranium is extracted by both PC-88a and HDEHP by cation exchange, with two extractant dimers exchanging for two protons [243, 397]. The slope analysis performed in this work indicated that a similar mixed PC-88a-HDEHP complex was formed with uranium, such as has been seen before with the vanadyl cation [390]. Work into uranium extraction from nitrate solution with HDEHP found $pK_{ex} = 6328$, which is ~ 10 times greater than the value found in this work for synergic extraction from chloride media [243].

Previous work on iron extraction by PC-88a alone from sulfuric acid gave standard cation exchange, forming $\text{Fe}(\text{PC-88a})_3$ [401]. The complex found in this work was similar, with one PC-88a dimer substituted for HDEHP. The iron complex identified is similar to the complex reported for trivalent rare earth elements using a similar PC-88a-HDEHP ratio, although the rare earth complex contained two PC-88a dimers and one HDEHP [407], rather than the one PC-88a to two HDEHP dimers found in this work. No K_{ex} data for iron extraction with PC-88a or HDEHP could be found in the literature.

3.4.2 EXTRACTANT AGGREGATION

From the data collected in this study it was not possible to make inferences about the behaviour of PC-88a and HDEHP in the organic phase. As has been stated, the dimerisation constants in Table 3.1 are large, and many literature sources suggest dimer formation, including between the two extractants [390]. Many suggested extraction mechanisms indicate that a single proton is lost from each dimer during complexation, changing from $(\text{HL})_2$ to HL_2 , where L is (DEHP) or (EHEHP) [403, 407, 421]. However, complete deprotonation has been reported for lanthanum(III) extraction with PC-88a [425].

In this work it was assumed that there was no interaction between PC-88a and HDEHP, and that the extractants in solution formed discrete, non-interacting dimers. However, the possible aggregation of the extractants would reduce their availability for metal complexation, leading to antagonism. The investigation of this aggregation behaviour is a point of recommended future work.

3.4.3 EXTRACTION ISOTHERM AND CONTACT STAGES

The extraction isotherm for thorium showed that the metal is well extracted by mixtures of 0.1 M PC-88a and 0.05 M HDEHP, being able to give 99% thorium recovery in three contact stages.

The acid THOREX process may be used as a basis for comparison. In the original acid THOREX process with TBP, ten extraction stages plus five scrubbing and five stripping stages were required for 99% thorium recovery [201]. Uranium may be > 98% extracted with TBP in only two stages [216]. Modern THOREX processes use 8-12 extraction stages [104]. Iron extraction with TBP in MIBK was possible in three stages, with two stripping stages [426].

Little literature data could be found on the number of stages for thorium extraction with PC-88a or HDEHP for comparison. A study with DEHEHP (di-(2-ethylhexyl) 2-ethylhexyl phosphonate) showed that thorium could be extracted to high purity with six stages each of extraction, scrubbing and stripping, and this extractant was shown to give greater extraction of thorium than TBP [427]. Uranium was found to be extracted in 2-3 stages by mixtures of HDEHP and TOPO [428].

Based on the proposed extraction mechanisms, the predicted maximum loading capacities may be determined for the reference extraction conditions. These are presented in Table 3.11. The iron capacity is slightly reduced due to its relatively low calculated value of K_{ex} .

TABLE 3.11 – LOADING CAPACITIES FOR EACH METAL WITH 0.1 M PC-88A, 0.05 M HDEHP FROM 3.0 M HCl.

METAL	EXTRACTED COMPLEX	LIMITING EXTRACTANT	LOADING CAPACITY /M
Th(IV)	Th(H(EHEHP) ₂) ₂ (H(DEHP) ₂) ₂ (HEHEHP)	HDEHP	0.020
U(VI)	(UO ₂)(H(EHEHP) ₂)(H(DEHP) ₂)	HDEHP	0.050
Fe(III)	Fe(H(EHEHP) ₂) ₂ (H(DEHP) ₂)	PC-88a	0.045

3.4.4 PROPOSED THORIUM SEPARATIONS FLOWSHEET

The work carried out in this chapter indicates that thorium may be separated from uranium and iron in hydrochloric acid media using mixtures of PC-88a and HDEHP. The extraction behaviour of the metals forms one part of the overall separations process. The remaining elements of the process will include back-extraction and possibly washing of the loaded organic phase (“scrubbing”).

This study was carried out with the aim of offering an improvement to the Indian THRUST process, which separates thorium from rare earth elements in an acidic chloride solution using PC-88a in *n*-dodecane as the organic phase. However, uranium and iron must be removed from the feed before the separation of thorium and rare earths can be carried out. A possible system for separation of Th, U and Fe, incorporating PC-88a and HDEHP as the extractants, is suggested in Figure 3.19. It is suggested that the mixed metals are fed in a < 3 M HCl solution between an extraction section and a scrubbing section. The aqueous feed to the scrub solution should be at a higher HCl concentration than the feed, which will strongly reject iron while still extracting uranium and thorium. The acid concentrations of feed and scrub should be set such that the acidity entering the extraction section is 3 M. Care should be taken in selecting conditions such that the equilibrium concentration of iron in the extraction section is not excessive in continuous

operation, and that iron will be rejected with minimal loss of uranium and thorium. The number of stages in the scrub section will be a function of metal distribution ratios at the selected higher acidity.

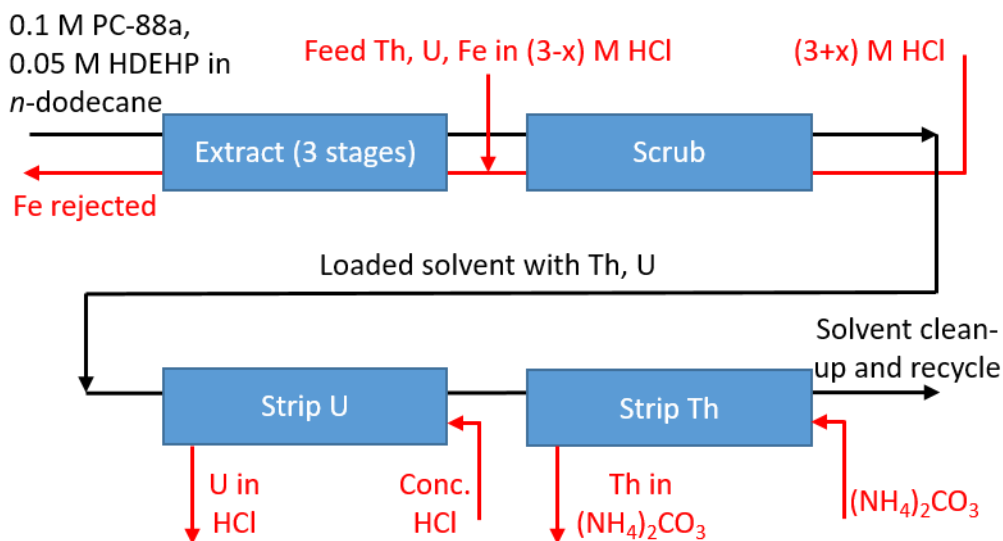


FIGURE 3.19 – SUGGESTED PROCESS FLOWSHEET FOR SEPARATION OF THORIUM, URANIUM AND IRON FROM SALINE HYDROCHLORIC ACID MEDIA. HCl CONCENTRATIONS ARE MARKED AS 3+x AND 3-x M. THE DIFFERENCE IN CONCENTRATION SHOULD BE SET SUCH THAT THE ACIDITY IN THE EXTRACTION SECTION IS 3 M.

In the back-extraction section, two aqueous solutions are suggested. The effects of various stripping agents for thorium and uranium have been tested in the literature, and the stripping efficiencies for each metal are similar across the range of possible stripping agents [253, 429]. For uranium recovery it is suggested that the HCl concentration be increased to very high levels, potentially with the addition of ethanol or acetone to the aqueous phase. For extraction with HDEHP this has been shown to reject uranium while retaining thorium in the organic phase, as shown in Figure 3.5 [87]. Reduced uranium extraction at higher acidities was also observed in this work.

The stripping of both thorium and uranium from HDEHP is effectively accomplished by ammonium carbonate solution [253, 429], and this stripping agent is suggested here. Following separation of the metals the

organic solvent may be cleaned and recycled. Thorium may then be precipitated from the thorium carbonate solution by increasing the pH of the solution, and the precipitate may then be converted to an oxide form for fuel fabrication by direct thermal decomposition.

3.5 CONCLUSIONS ON THE DEVELOPED PROCESS

The aim of the work presented in this chapter was to determine the extracted complexes and the number of contact stages required to extract 99% of the dissolved thorium from a solution of thorium, uranium and iron, and these aims have been accomplished.

The solvent extraction system investigated in this chapter has been shown to be a good system for the extraction of thorium from hydrochloric acid media. The extracted complexes for iron and uranium were found to be formed through a cation exchange mechanism, while the thorium complex was produced through a mixed cation exchange/adduct formation mechanism. Both of these mechanisms have been seen previously in the literature.

The thorium is strongly partitioned into the organic phase, with 99% of the metal extracted in three contact stages. In comparison to currently used TBP-based extraction processes, the PC-88a and HDEHP system offers improved thorium extraction and improved chloride and sulfate tolerance [142]. When compared to the THRUST process, the addition of HDEHP to the organic phase allows good separation of thorium and uranium from iron, but unfortunately offers limited benefits in terms of the separation of thorium from uranium in the extraction step. The low sensitivity of the distribution ratio to up to 20 g/l added chloride and 3 g/l added sulfate suggests that three to four contact stages would even be sufficient to extract 99% of thorium from acidified sea-water [423].

It appears that the addition of HDEHP to PC-88a could give improvements over PC-88a alone for the THRUST process, although separation during the back-extraction step may be required rather than in the extraction step. A concentrated acid scrubbing solution could be used to hold iron down in the aqueous phase, while a concentrated HCl strip could be used to selectively back-extract uranium, leaving thorium in the organic phase. The potential elimination of the Alamine-336 solvent extraction step could lead to significant cost savings in the implementation of the THRUST process.

3.5.1 FUTURE WORK IN THIS AREA

There remains additional experimental work to be carried out to fully define the PC-88a/HDEHP/HCl solvent extraction system with high confidence and allow development to a full process.

3.5.1.1 FURTHER DETAILING OF EXTRACTION SYSTEM

The reliability of the results obtained in this work by calculation would be greatly strengthened by experimental validation. The nature of the extracted complexes and aggregation behaviour may be studied using analytical techniques such as Nuclear Magnetic Resonance (NMR) spectroscopy and Vapour Pressure Osmometry, Fourier Transform Infrared spectroscopy (FTIR) or Extended X-ray Absorption Fine Structure spectroscopy (EXAFS) [393, 430]. The predicted extraction isotherm may be tested by carrying out a series of solvent extraction studies similar to any of those already discussed in this chapter, but with the metal concentration in the feed used as the independent variable, following methods described in the literature [431].

Whether or not the system exhibits synergism is unclear. The Job plot method presented in Figure 3.14 does not show synergism. However, calculation the synergic factor using Equation (3.5) did indicate thorium synergism. The nature of the extraction should be studied further in order to

determine whether a synergic mixture exists, as was indicated by the results in For uranium and iron the number of protons released was found to equal the number of extractants complexed. However, the number of extractants complexed by thorium was greater than the pH dependence slope, and thus a mixed cation exchange/adduct formation reaction is indicated..

Some variables related to the solvent extraction contact were not studied in this work, including temperature, contact duration and choice of diluent. The effect of temperature should be studied, as extraction of iron has been shown to increase with temperature, while extraction of thorium and uranium is decreased at higher temperatures [403, 427, 432]. Based on this it may be that lower temperatures in the extraction and scrubbing sections of the suggested flowsheet will give greater separation of iron from the actinides. The effect of contact time should also be studied. Although five minutes has been shown to be sufficient for metals extraction with the extractants under consideration, this does not necessarily mean that extraction with the mixture will reach equilibrium within the same time period. If the equilibration times for each metal are found to be significantly different this may allow an effective extraction on the basis of kinetic effects. In addition, further studies are suggested to better determine the strength of the synergic effect.

3.5.1.2 BACK-EXTRACTION STUDIES

As was stated in Section 3.4.4, an investigation of suitable stripping solutions and conditions would need to be carried out. Concentrated HCl and ammonium carbonate are a suggested starting point, although oxalic acid also offers an interesting option for the direct precipitation of thorium from the organic phase as a precipitate which may be readily calcined to oxide [433]. For the selected strippants, stripping isotherms and the number of stripping stages required should be determined. From this information a complete picture of the solvent extraction process may be generated for the separation of thorium, uranium and iron.

3.5.1.3 TRANSITIONING TO A REAL FEED

The next stage of process development would be to increase the complexity of the synthetic feed, and eventually test with a “real” feed. The number of metals in solution must be increased to account for other ions in monazite and its residues (Ti^{2+} , Al^{3+} , rare earth elements). Following this, testing with real monazite residues and/or monazite leachate would be required. The composition of monazite is variable, and so a range of monazite feeds should be considered, prioritising those locations with large monazite reserves and/or monazite residue inventories. These might include India, Brazil, Sri Lanka, Indonesia, Malaysia, Australia, South Africa and the United States of America [142].

3.5.1.4 SCALING UP TO PILOT PLANT TESTING

The above represents a more than sufficient body of work to confirm or refute a solvent extraction system for the purification of thorium from monazite using mixtures of PC-88a and HDEHP as an alternative to TBP.

Laboratory-scale testing can only go so far in process development. Assuming success to this point and the availability of a market for the thorium product, process testing must be scaled up, initially to pilot plant scale and eventually to full production scale. Some additional data is required prior to scale-up. The physical behaviour of the system must be studied in order to determine appropriate handling equipment and conditions for continuous operation, including the tendency of the system to form third phases and emulsions at a range of phase ratios, dispersion and phase separation, and the solubility of the organic material in the aqueous phase. The requirements for solvent reconditioning treatment between extraction cycles must also be established [77].

Process modelling work in software packages such as Aspen Plus [434] is recommended prior to investing in a pilot plant. However, additional

experimental studies may be required to provide physicochemical data to the model.

3.6 CHAPTER SUMMARY

This chapter has presented studies into the separation of thorium from uranium and iron in hydrochloric acid media in order to improve upon the Indian THRUST process [34]. It has been shown that thorium may be extracted strongly from aqueous media by a 2:1 ratio of PC-88a and HDEHP in *n*-dodecane, as a mixed cation exchange/neutral adduct complex, with 99% of thorium extracted in three contact stages. However, there is not a specific synergic ratio of extractants which gives optimal extraction, as thorium extraction increases monotonically as the fraction of HDEHP in the extractant mixture increases. The system is highly tolerant of increasing ionic strength of chloride, and is not strongly affected by low levels of sulfate ion. Thus, it is possible that the process will be able to use acidified seawater as the aqueous phase.

Separation from co-contaminant metals may be performed through control of acidity, sulfate ion concentration, and careful selection of extractant concentration. However, other factors, not investigated in this work, such as contact time and temperature, may allow more effective separation. In general, for the process conditions investigated, uranium is extracted into the organic phase, but less well than thorium, while iron tends to distribute across both phases.

Further work remains to be done on this solvent extraction system, including experimental validation of predicted results, additional extraction and stripping testing, and other studies leading to process scale up. Further development of the thorium separations process was not carried out during the work presented in this thesis.

There is already significant published work available in the literature on the latter part of the thorium fuel cycle front end, the conversion of the pure thorium product to an oxide fuel form. Therefore, the focus of the thesis will now turn to an application of separated thorium oxide as a nuclear fuel for pressurised heavy water reactors. Chapter 4 will present a neutronic feasibility study of possible fuels, and Chapter 5 will present a validation study of the Chapter 4 results by computational experiment.

4 PLUTONIUM-THORIUM FUEL OPTIONS FOR IRRADIATION IN HEAVY WATER REACTORS

“And now for something completely different.”

– John Cleese, *“Monty Python”*

The previous chapter of this thesis has shown how thorium may be separated from common co-contaminants using synergic solvent extraction. Having elucidated a promising extraction system for thorium, attention now turns to a possible fuel application for separated thorium, specifically the use of thorium in UK-based pressurised heavy water reactors for plutonium irradiation.

This chapter is based on a paper published by the thesis author [435].

4.1 INTRODUCTION

The primary aim of this chapter was to perform an initial study of alternative fuel compositions for pressurised heavy water reactors that could incorporate thorium alongside plutonium, reprocessed fissile materials and/or depleted uranium. The outcomes of this initial study were used to inform further development work into the feasibility of such thorium-bearing fuels, which are developed in further detail in Chapter 5.

In Chapter 1, four options were described for the management of separated UK plutonium, and it was stated that the work in this thesis would focus on the PHWR option, known as UK CANMOX. The UK CANMOX fuel uses two types of fuel element; these are MOX elements of plutonium and depleted uranium, and elements containing depleted uranium with a dysprosium burnable absorber to flatten the neutron flux across the fuel bundle [68]. This bundle design has some drawbacks. Dysprosium is an expensive rare earth element, which functions by absorbing neutrons. The absorption of neutrons on dysprosium could be considered as a waste of neutron flux. In addition, the neutron captures in the depleted uranium region in the centre pins will produce additional plutonium, which would likely have a high fissile content due to the relatively low burnup of UK CANMOX fuel compared to LWR MOX [63]. Furthermore, the plutonium MOX also uses depleted uranium. Depleted uranium is relatively simple to dispose of as it has not been irradiated in a nuclear reactor [436]. The reuse of previously irradiated uranium could reduce the volume of uranic waste requiring special handling due to its content of ^{234}U and ^{236}U , and this was investigated during the work reported in this chapter.

The use of thorium oxide is proposed as an alternative to the depleted uranium-dysprosium (DU-Dy) mixed oxide in order to address both of these problems. In order to offer an alternative, thorium oxide must be sufficiently close to the DU-Dy oxide in terms of neutronic and thermal-hydraulic behaviour. In order to determine the impact of switching to thorium, and the possibility of using a reprocessed uranium in the U-Pu MOX, it was an aim of this work to calculate the beginning of life neutron multiplication factor and fertile-fissile conversion ratio for a range of possible fuel compositions with three actinide components; thorium, plutonium and uranium. The second aim was to determine whether there would be sufficient quantities of uranium available to irradiate the UK plutonium inventory, based on an equilibrium mass flow assessment.

4.1.1 THE UK CANMOX PROPOSAL

UK CANMOX is the proposal put forward by CANDU Energy Inc. to irradiate the UK's plutonium inventory as part of a MOX fuel with depleted uranium. It is a complete fuel cycle proposal, including the construction and operation of a fuel fabrication facility and sufficient reactors to irradiate the resulting fuel, with consideration also being given to spent fuel management.

4.1.2 THE ENHANCED CANDU 6 REACTOR

The Enhanced CANDU 6 is a Generation III+, 740 MWe (gross) pressurised heavy water reactor. It is a technological evolution of the well-established CANDU 6 reactor, with enhanced safety features and minor design modifications which aims to increase the plant's operating lifetime [437]. The core will be comprised of a tank of heavy water moderator, known as the calandria, surrounding a square lattice of horizontal fuel channels containing fuel bundles cooled by pressurised heavy water [438]. The coolant will flow over and through the fuel bundles within the pressure tubes, removing heat to a steam generator [382]. The pressure tubes will be located within calandria tubes, with the ~ 12 mm annular gap between these concentric tubes being filled with carbon dioxide gas, thermally insulating the coolant from the calandria. A cutaway diagram of the proposed fuel channel is shown in Figure 4.1. A photograph of a CANDU calandria with tubes installed is shown in Figure 4.2, and a diagram showing the fuel channel arrangement within the calandria is shown in Figure 4.3. See also further detail in Figure 2.23 (page 87).

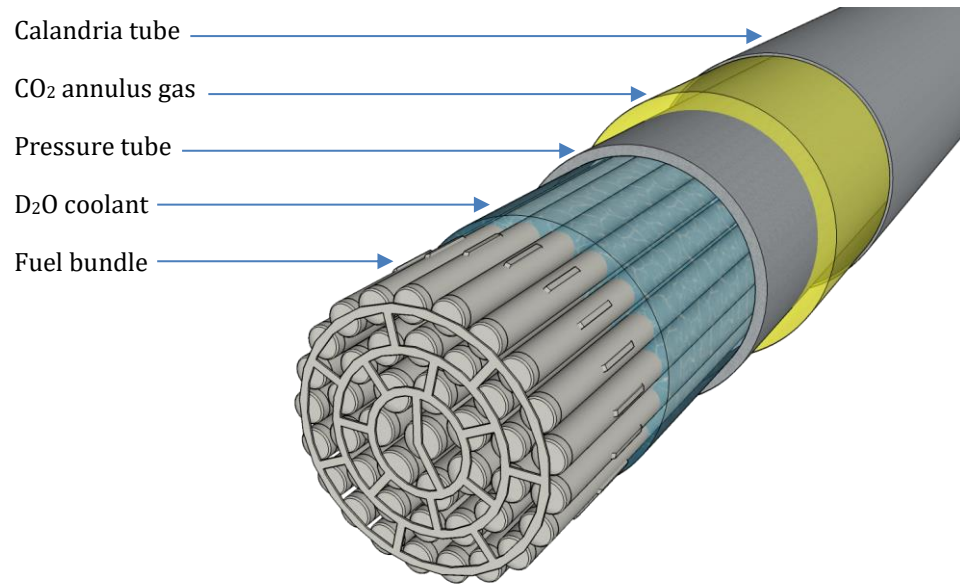


FIGURE 4.1 – CANDU REACTOR FUEL CHANNEL CUTAWAY DIAGRAM. FUEL BUNDLE OUTER DIAMETER IS APPROXIMATELY 10 CM. THE BUNDLE SHOWN IS THE NEW CANFLEX DESIGN.



FIGURE 4.2 – CANDU 6 CALANDRIA WITH PRESSURE TUBES INSTALLED. SCALE OF CORE MAY BE INFERRED FROM WORKERS VISIBLE STANDING AT THE BASE OF THE CALANDRIA VESSEL ON THE LEFT AND ON TOP OF THE VESSEL ON THE RIGHT [439].

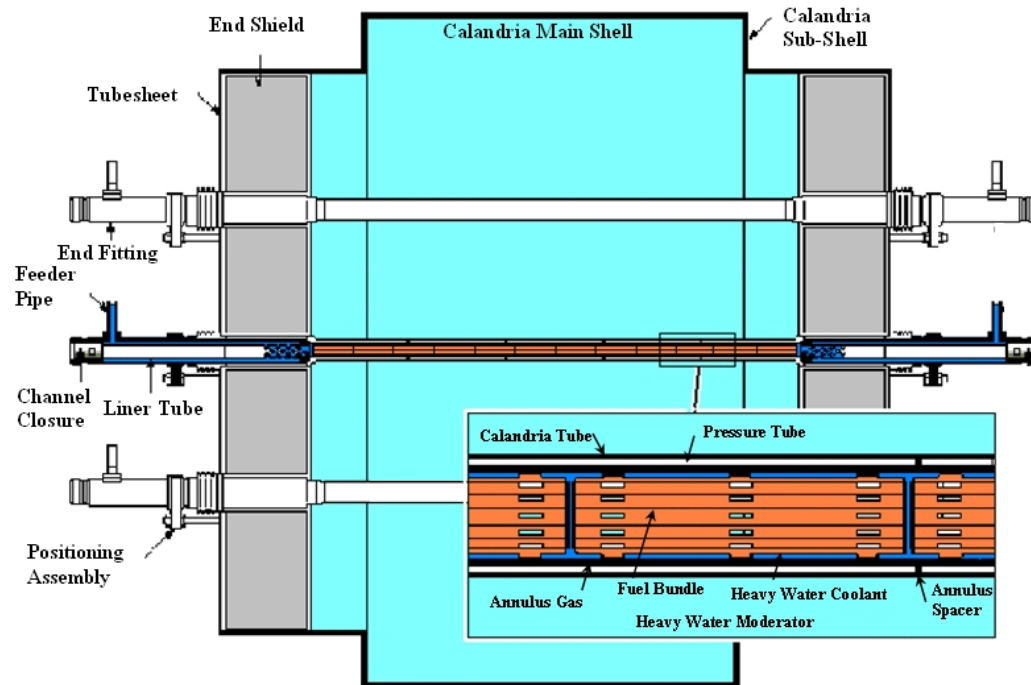


FIGURE 4.3 – FULL CANDU CORE DIAGRAM, SHOWING CALANDRIA VESSEL, THREE FUEL CHANNELS AND COOLANT FEEDERS, AND END SHIELDING ASSEMBLIES. INSET: CLOSE-UP OF FUEL BUNDLES WITHIN FUEL CHANNEL, WITH PRESSURE AND CALANDRIA TUBES AND ANNULUS GAS SPACE. CORE DIAMETER OF EC6 REACTOR IS 7.6 METRES. CORE CONTROL DEVICES OMITTED FOR CLARITY [440].

Due to the insulating annulus gas, most of the core heat will be carried away by the coolant, and only 4% will be transferred to the calandria [68].

Refuelling can be carried out continuously at full power, with an average of 2-3 channels being refuelled daily. In the UK CANMOX reactors, refuelling operations will be carried out by inserting two new fuel bundles and ejecting two spent bundles from each channel being refuelled, with channels to be refuelled selected according to channel burnup, and acceptable power profiles and ramping. Refuelling will be carried out in both directions, with adjacent channels refuelled in opposite directions. Reactivity control will be carried out using a combination of chemical shim control through addition of gadolinium to the moderator, the addition of boron to the coolant, a range

of adjuster and supplemental absorber rods which are lowered vertically into the calandria, and by “liquid zone control” where vertical tubes spaced through the core will be filled with or emptied of light water. Emergency shutdown will be achievable by two mechanisms, either through the use of shut-off rods, or through moderator poisoning by rapid gadolinium injection [68].

The EC6 reactor is designed for an operational lifetime of 60 years, with a mid-life shut down period for refurbishment of key reactor components, most notably the pressure tubes which hold the fuel bundles and carry the pressurised heavy water coolant [441]. During normal reactor operation the pressure tubes undergo thermally induced creep and increase in diameter, leading to bulk coolant flow around the bundles, leading to reduced cooling of the inner fuel elements. Thus they must be replaced to maintain proper coolant flow through the fuel bundles.

Some geometric and operating parameters of the CANDU 6 and Enhanced CANDU 6 are summarised in Table 4.1 [382]. The Enhanced CANDU 6 reactor core design specifications are similar to those of the CANDU 6 reactor, with slight differences in operating power, pressure tube and calandria tube wall thicknesses, and the number and placement of control rods and safety devices.

Further details on CANDU reactor technology are available in a web-based textbook [20].

4.1.3 UK CANMOX FUEL

In the UK CANMOX proposal, each EC6 reactor would consume ~ 1.3 t/yr of plutonium, thus requiring four units running over a 30 year lifetime to consume the UK stockpile [63]. It is anticipated that following mid-life refurbishment the reactor would then be operated for the second 30 years

of its life with a uranium based fuel. The NDA have declared the proposal to be a “credible” option [64].

TABLE 4.1 – MAIN GEOMETRIC AND OPERATING PARAMETERS OF THE CANDU 6 REACTOR [383] AND THE ENHANCED CANDU 6 REACTOR [63, 382, 437, 438, 442].

REACTOR NAME	CANDU 6	ENHANCED CANDU 6
Thermal power P_{th} /MWth	2061	2084
Thermal efficiency η_{th}	34.6%	35.5%
Design lifetime /yr	40	60
Design capacity factor C_f	85%	94%
Core length /mm	5944	5944
Calandria inner radius /mm	3800	3797.5
Calandria outer radius /mm	-	3826.1
Number of fuel channels	380	380
Fuel bundles per channel	12	12
Channel lattice pitch /mm	286	286
Average fuel burnup /MWd.kgU ⁻¹	7.154	7.500
Pressure tube inner radius /mm	51.689	51.689
Pressure tube outer radius /mm	55.879	56.389
Calandria tube inner radius /mm	64.478	64.478
Calandria tube outer radius /mm	65.875	65.998
Number of adjustor rods	21	11
Number of shut off rods	28	32

The proposal suggests the use of two MOX fuels containing approximately 2.5 wt% and 5.0 wt% plutonium, mixed homogeneously with depleted uranium. Such fuel blends would be fabricated into cylindrical pellets and then assembled into 43-element “CANFLEX” fuel bundles, as shown in Figure 4.4. CANFLEX bundles have two different fuel element diameters arranged in three concentric rings surrounding a central element [382]. The key fuel bundle geometric data is presented in Table 4.2.

The smaller diameter, outer fuel elements (35) will contain the MOX fuels, while the larger diameter, inner elements (8) containing dysprosium oxide (Dy_2O_3) dispersed in depleted uranium oxide perform the function of a burnable neutron absorber. The dysprosium provides the necessary neutron flux modification at the beginning of a bundle's irradiation history to ensure equal burnup across the MOX fuels. The exact dysprosium loading data was not available to the author, and will likely be a modified parameter during fuel fabrication based on the isotopic composition of the incoming plutonium.

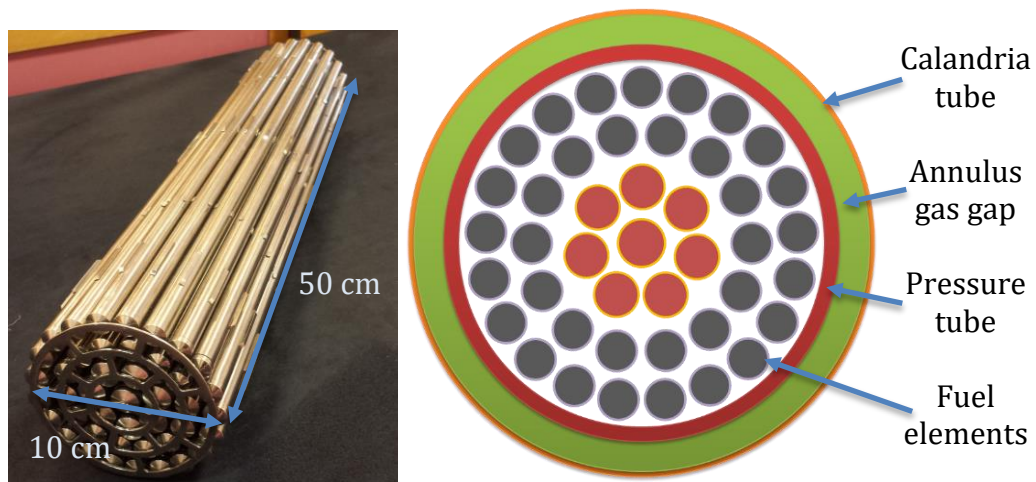


FIGURE 4.4 – LEFT: PHOTOGRAPH OF 43 FUEL ELEMENT CANFLEX FUEL BUNDLE. RIGHT: DIAGRAM SHOWING CANFLEX FUEL ELEMENTS IN PRESSURE TUBE (RED) WITH ANNULUS GAS SPACE (GREEN) CONTAINED WITHIN CALANDRIA TUBE (ORANGE).

In UK CANMOX fuel, the outer ring of 21 elements contains ~ 2.5 wt% Pu within depleted uranium, while the intermediate ring of 14 elements contains ~ 5.0 wt% Pu, again within depleted uranium. As with the dysprosium loading fraction, the actual Pu fractions will be varied according to the isotopic composition of the plutonium used in order to flatten the flux profile across the fuel bundle. The CANFLEX bundle provides more efficient heat transfer to the coolant when compared to the currently used 37-element CANDU fuel bundle [442].

THE PREPARATION AND APPLICATION OF THORIUM-BASED NUCLEAR FUELS

A design discharge burnup of $\sim 16,000 - 20,000$ MWd/tHM has been proposed for UK CANMOX fuel, compared to $\sim 7000 - 7500$ MWd/tHM burnup within natural uranium fuelled CANDU reactors [63]. However, it has also been suggested that the discharge burnup may be $\sim 14,000 - 16,000$ MWd/tHM [68].

TABLE 4.2 – GEOMETRIC PARAMETERS AND MASS DATA FOR A CANFLEX FUEL BUNDLE. A CALCULATED MASS IS GIVEN FOR UK CANMOX FUEL, BASED ON 2.5% DYSPROSIUM LOADING AND 96.6% THEORETICAL DENSITY [382, 443].

PROPERTY	CENTRAL ELEMENT AND INNER RING OF ELEMENTS	INTERMEDIATE AND OUTER RINGS OF ELEMENTS
Number of elements	1 + 7	14 + 21
Fuel pellet diameter /mm	12.58	10.65
Fuel pellet length /mm	16.00	10.60
Fuel element diameter /mm	13.50	11.50
Pellets per fuel element	30	45
Pellet stack length /mm	481.1	481.1
Pitch circle radii /mm (ring radius to element centreline)	17.34, 30.75, 43.84	
Intermediate ring offset rotation	$\pi/14$ rad $\approx 12.857^\circ$	
Fuel bundle length /mm	495.3	
Fuel bundle outer diameter /mm	98.11	
Bundle structural (non-fuel) mass /kg	2.3	
Natural uranium mass in bundle /kgHM	17.98	
UK CANMOX fuel mass in bundle /kgHM	18.47	

Plutonium makes up $\sim 2.4\%$ of the total fuel mass of the mixed oxide in CANMOX fuel, i.e. ~ 480 gHM per fuel bundle. After irradiation the spent fuel from UK CANMOX is expected to still contain 1-2% plutonium. However, irradiation will induce a significant change in the isotopic composition of the plutonium, reducing its fissile quality.

4.1.3.1 SPENT FUEL MANAGEMENT

UK CANMOX spent fuel will not be reprocessed prior to disposal, in order to maximise the proliferation resistance of the material. Spent fuel quantities from heavy water reactors are generally much greater than those from light water reactors for the same power output, as they operate with lower fuel enrichments and thus burn out the fuel fissile component more rapidly, necessitating more frequent refuelling. In comparison, the proposed burnup of MOX fuel in the UK EPR reactor is $\sim 50,000$ MWd/tHM [63, 444]. However, compared to light water reactor spent fuel, a given quantity of heavy water reactor natural uranium spent fuel can often be emplaced within a smaller footprint in a geological repository, as the fuel is less heat generating due to its lower burnup [68]. However, this may not be the case for more highly irradiated mixed oxide fuels containing significant quantities of plutonium. If thorium were to be introduced to this fuel it is likely that the heat generation would be further increased, as thorium spent fuel is more heat generating than uranium spent fuel at the $10^4 - 10^6$ year time-scale [34, 334].

4.1.4 THE UK URANIC MATERIALS INVENTORY

As well as the plutonium inventory built up from used fuel reprocessing, the UK also holds an inventory of uranic materials, including depleted uranium tails from enrichment activities, MAGNOX Depleted Uranium (MDU) from reprocessing of MAGNOX reactor fuels and ThORP Product Uranium (TPU) from reprocessing Advanced Gas-cooled Reactor (AGR) uranium oxide fuels. EDF Energy, the operator of the AGR fleet, also owns a significant quantity of TPU. The inventory is detailed in Table 4.3 [61, 445]. If these inventories were to be used in nuclear fuels the result would be to reduce the overall quantity of natural uranium required per kilowatt-hour of electricity generated in the UK.

4.1.5 USE OF URANIC MATERIALS IN THE EC6

The Enhanced CANDU 6 is described as fuel flexible, and AECL have proposed multiple alternative fuelling regimes suitable for the reactor, including plutonium-thorium MOX fuels and reprocessed uranium fuels [446]. There is also ongoing work into the development of Natural Uranium Equivalent (NUE) fuels which blend depleted and reprocessed uranium stocks to produce a synthetic uranium oxide fuel with similar properties to natural uranium [447, 448]. It is intended that such NUE fuels will be used in the CANDU 6 reactors under construction at Qinshan in China.

TABLE 4.3 – SELECTED DATA ON UK URANIC MATERIALS INVENTORIES AS OF 1 APRIL 2013 [61, 382, 445].

MATERIAL	OWNER	ESTIMATED QUANTITY /t
UF ₆ tails stored at Sellafield and URENCO Capenhurst site	NDA/URENCO	21500
MAGNOX Depleted Uranium stored at Sellafield	NDA	26000
ThORP Product Uranium stored at Sellafield	NDA	300
ThORP Product Uranium stored at Sellafield and reactor sites	EDF Energy	3110
ThORP Product Uranium, predicted future arisings to ThORP closure	EDF Energy	2200

4.1.6 ALTERNATIVE EC6 FUELS

The work described here details initial studies into alternative two- and three-component nuclear fuel concepts for the Enhanced CANDU 6 reactor. Neutronic feasibility studies and nuclear fuel materials availability

assessments have been undertaken regarding the use of U-Pu and U-Pu-Th nuclear fuels in the EC6 PHWR.

Two-component fuels comprise a uranium-plutonium mixed oxide fuel, i.e. traditional MOX. In three-component fuels, thorium fuel elements are proposed to replace the burnable absorber elements as used in UK CANMOX fuel, with U-Pu MOX in the intermediate and outer rings of fuel elements as the fissile driver. In order to do this, thorium in the fuel would have to satisfy two key criteria:

1. Reduce the initial excess reactivity of the fuel bundle due to the uranium and plutonium loading.
2. Undergo conversion over time as the fissile content of the MOX fuel reduces to maintain a suitable reactivity profile over the fuel life in-core.

It is highly desirable that changes required to the fuel bundle and reactor design should be minimal, and that the proposed fuel should operate within the existing UK CANMOX safety case. In particular, the effectiveness of existing control and safety mechanisms should not be diminished, and heat generation limits should not be exceeded.

It is anticipated that the replacement of burnable absorbers by thorium will have a positive impact on the long-term reactivity depletion of the fuel in the core. As the initial fissile content is consumed due to the material absorbing neutrons and undergoing fission, neutron captures on thorium will lead to the production of fissile uranium-233, theoretically reducing the rate of reactivity depletion in the core with burnup relative to two-component U-Pu MOX fuels. However, it may be that the rate of uranium-233 production is too low to have a meaningful effect, and thus the reactivity depletion rate will be similar to that of UK CANMOX. In this case thorium will still have some advantage over depleted uranium in that it will produce a much reduced quantity of additional plutonium.

4.1.7 FUEL MATERIAL RESOURCES

Sources of nuclear fuel materials for the fissile drive elements include both current inventories and projected future reprocessing products from UK LWRs. The isotopic compositions of the various “lots” in the plutonium inventory have been reported as being either suitable for direct use in UK CANMOX fuel, or as able to be blended with other lots in the inventory to produce a fuel suitable for UK CANMOX use [68]. A small amount of the least fissile lots may be used for flux balancing during non-equilibrium operations such as the initial core fuelling or replacement of defective fuel bundles, or may be placed in regions close to the core edge for irradiation [68].

For LWR reprocessing product compositions, it was decided to use the AREVA EPR as the reference LWR. At the time of writing, 4 EPR reactors were planned for the UK, at the existing Hinkley Point and Sizewell sites, with the potential for several more to follow at other EDF-operated sites, particularly Hartlepool and Heysham, notwithstanding project financing and political issues [449].

Six uranium and three plutonium sources were considered. The uranium sources were depleted uranium tails, natural uranium, reprocessed uranium from an EPR with LEU fuel (LEU EPR RepU), reprocessed uranium from an EPR fuelled with U-Pu MOX (MOX EPR RepU), MAGNOX Depleted Uranium (MDU) and ThORP Product Uranium (TPU). The plutonium sources were an average plutonium composition from the UK inventory, reprocessed plutonium from an EPR with LEU fuel (LEU EPR Pu) and reprocessed plutonium from an EPR fuelled with U-Pu MOX (MOX EPR Pu). The isotopic compositions of these uranium and plutonium sources are listed in Table 4.4 and Table 4.5 respectively. Only natural thorium was considered, being 100% Th-232.

The UK inventory plutonium composition listed in Table 4.5 represents only an average value for this material. The plutonium has been produced over a

period of 50 years, from the start of the weapons-grade plutonium production reactors in the 1950s, e.g. the Windscale Piles and the MAGNOX reactor fleet. Thus, this material will have experienced a range of burnup levels, in different reactors and reactor types, and different ageing periods prior to and since separation, giving a range of plutonium isotopic compositions with variable ingrowth of radioactive decay products, most notably americium-241. Of this highly variable material, only a small subset will be available for fuel fabrication at a given time, meaning that the fuel fabrication process must be flexible in order to produce a consistent fuel product [68]. Based on the tentative timescale in construction of EC6 plants in the UK, it is very likely that at least some of the plutonium will have been removed from the reactor more than 100 years prior to its irradiation within CANDU bundles. In this work the average composition from Table 4.5 was used, although it will be necessary in future work to consider a range of Pu isotopic compositions which are representative of the lots in the inventory.

TABLE 4.4 – ISOTOPIC COMPOSITION OF URANIUM SOURCES CONSIDERED [62, 450].

MASS %				
SOURCE	U-234	U-235	U-236	U-238
Depleted uranium	0.001	0.25	0.00	99.75
Natural uranium	0.006	0.72	0.00	99.27
LEU EPR RepU	0.02	0.92	0.70	99.38
MOX EPR RepU	0.00	0.10	0.02	99.88
MDU	0.006	0.303	0.068	99.62
TPU	0.02	0.89	0.25	98.84

TABLE 4.5 – ISOTOPIC COMPOSITION OF PLUTONIUM SOURCES CONSIDERED [451, 452].

MASS % SOURCE	Pu- 238	Pu- 239	Pu- 240	Pu- 241	Pu- 242	Am- 241
UK inventory Pu	0.21	72.0	23.7	1.55	1.08	1.51
LEU EPR Pu	4.37	51.8	24.3	11.5	8.06	0.00
MOX EPR Pu	5.90	33.3	31.3	12.4	16.8	0.00

The concept fuels developed for this study were based on the CANFLEX fuel bundle, shown in Figure 4.4. While these concepts include two-component MOX fuels based on uranium and plutonium for comparative purposes, the larger focus is on the three-component fuels which also include thorium. Radial grading of the plutonium fraction in the intermediate and outer MOX rings will be employed to achieve a suitable flux profile and equivalent burnup in the MOX elements across the outer and intermediate rings. The separation of ThO₂ and U-Pu MOX means the fuel components are neutronicly coupled, but physically and chemically separated, thus minimising complexities in any reprocessing operations, as well as giving the neutronic advantages of heterogeneity in thorium fuels discussed in Chapter 2. If reprocessing were to be carried out it might begin with automated disassembly of the bundles, allowing separate treatment of U-Pu MOX and thorium oxide spent fuel elements. This would be necessary if, for example, the thorium elements were to be subjected to multiple irradiation cycles in order to breed additional U-233 [450].

This separation of the fissile and fertile fuel regions is in-line with other thorium CANFLEX concepts [103]. The thermal neutron flux in the centre of the bundle is reduced due to the shielding provided by the MOX elements. It is anticipated that the neutronic coupling of thorium and plutonium will produce some mutual self-shielding effects. Neutron capture of both ²³²Th and ²³³Pa will be reduced due to captures by isotopes such as ²³⁸U, ²⁴⁰Pu and

^{241}Am present in the MOX, thus increasing the formation of ^{239}Pu and ^{233}U , whilst reducing ^{232}U .

4.2 NEUTRONIC ANALYSIS METHOD

An empirical method was used to perform estimations of the neutronic feasibility in the various two- and three-component fuel combinations. Initially, 36 fuel bundle composition concepts were suggested, based on the various uranium and plutonium sources from Table 4.4 and Table 4.5. For each combination 1%, 2% and 3% plutonium loading fractions were considered in the MOX fuel elements.

Initial analysis showed that reprocessed uranium from MOX-fuelled LWRs would perform less well than depleted uranium tails, and also be more costly to fabricate due to the hazards from its higher U-234 and U-236 content, potentially necessitating the use of more costly radiation protection equipment and systems during fuel handling and fabrication. Natural uranium fuels were only considered as a basis for neutronic comparison, and were not intended as an actual concept for development, as such a fuel would go against the goal of reduced natural uranium resource utilisation. Only two fuels using ThORP Product Uranium were considered initially as it was believed that the available quantity of this material would be insufficient. The list of fuel concepts developed is given in Table 4.6.

THE PREPARATION AND APPLICATION OF THORIUM-BASED NUCLEAR FUELS

TABLE 4.6 – DETAILS OF FUEL CONCEPTS CONSIDERED BY COMPONENTS OF MOX AND WHETHER A THORIUM BLANKET WAS INCLUDED. CONCEPTS 10-18 ARE THE THREE-COMPONENT FUEL VERSIONS OF TWO-COMPONENT FUEL CONCEPTS 1-9 RESPECTIVELY.

Fuel concept #	Uranium Source	Plutonium Source	Includes thorium?
1	Enrichment tails	UK inventory	No
2	Enrichment tails	LEU-fuelled EPR used fuel	No
3	Enrichment tails	MOX-fuelled EPR used fuel	No
4	MAGNOX used fuel	UK inventory	No
5	MAGNOX used fuel	LEU-fuelled EPR used fuel	No
6	MAGNOX used fuel	MOX-fuelled EPR used fuel	No
7	LEU-fuelled EPR used fuel	UK inventory	No
8	LEU-fuelled EPR used fuel	LEU-fuelled EPR used fuel	No
9	LEU-fuelled EPR used fuel	MOX-fuelled EPR used fuel	No
10	Enrichment tails	UK inventory	Yes
11	Enrichment tails	LEU-fuelled EPR used fuel	Yes
12	Enrichment tails	MOX-fuelled EPR used fuel	Yes
13	MAGNOX used fuel	UK inventory	Yes
14	MAGNOX used fuel	LEU-fuelled EPR used fuel	Yes
15	MAGNOX used fuel	MOX-fuelled EPR used fuel	Yes
16	LEU-fuelled EPR used fuel	UK inventory	Yes
17	LEU-fuelled EPR used fuel	LEU-fuelled EPR used fuel	Yes
18	LEU-fuelled EPR used fuel	MOX-fuelled EPR used fuel	Yes
19	AGR used fuel (ThORP product uranium)	UK inventory	Yes
20	Natural uranium	UK inventory	Yes
21	MAGNOX and AGR reprocessed U blend	UK inventory	Yes

4.2.1 NEUTRONIC COMPARISON FACTORS

As the common fuel for CANDU reactors is natural uranium oxide, all fuel concepts studied in this work were compared to natural uranium as the reference fuel. The screening study was performed by comparing the neutron reproduction factor η and fission:capture ratio α^{-1} of each fuel concept to that of the reference fuel. The formula for neutron reproduction factor, which is the number of fast fission neutrons produced per thermal neutron captured in the fuel, is given in equation (4.1) [16].

$$\eta = \nu \frac{\sigma_f^F}{\sigma_a^F} = \frac{\sum_{i=1}^j N_i \nu_i}{\sum_{i=1}^j N_i} \times \frac{\sum_{i=1}^j N_i \sigma_{f,i}}{\sum_{i=1}^j N_i \sigma_{a,i}} \quad (4.1)$$

Where ν is the neutron multiplicity factor, that is the average number of neutrons produced per fission in the fuel,
 σ^F is the microscopic neutron cross section for fission (subscript f) or absorption (subscript a) in the fuel
 j is the total number of fuel isotopes,
 i is an index representing each fuel isotope, and
 N is the atomic density of the isotope in the fuel bundle.

Americium in the plutonium inventory was accounted for in the estimation of neutron reproduction factor, although strictly speaking it should not be, given that it is not a fuel isotope.

The fission:capture ratio α^{-1} , which is the overall ratio of microscopic fission capture cross section to microscopic capture cross section, is calculated using equation (4.2). The difference between the absorption cross section and the fission cross section is the neutron capture cross section.

$$\alpha^{-1} = \frac{\sigma_f^F}{\sigma_c^F} = \frac{\sigma_f^F}{\sigma_a^F - \sigma_f^F} = \frac{\sum_{i=1}^n N_i \sigma_{f,i}}{\sum_{i=1}^n N_i (\sigma_{a,i} - \sigma_{f,i})} \quad (4.2)$$

Where σ_c^F is the microscopic neutron cross section for capture in the fuel.

The calculation method used for the initial screening study does not account for the neutronic contributions of structural materials, moderator or coolant. Only the fuel isotopes themselves are considered. The results of the calculations therefore do not give an absolute value for the whole core reproduction factor or fission:capture ratio. Instead results are presented as comparisons against the reference natural uranium fuel, as well as a number of operating and proposed fuel compositions calculated using the same method. The contribution of non-fuel materials is constant for all fuel compositions, and so at this stage of the work these were ignored. All calculations are for fresh, unirradiated fuel at its beginning of life (BOL) in the core.

4.2.2 HOMOGENEOUS CORE ISOTOPIC ATOMIC DENSITY ESTIMATION

The atomic densities of the atoms of each isotope were estimated as follows. The total mass of each isotope of uranium, plutonium and thorium present in the concept fuel bundle was determined from the geometry of the fuel pellet stacks [447], the material density [453] and isotopic composition data. Pellets were assumed to be idealised uniform cylinders of 95% relative density. The MOX density was estimated by linear interpolation of the densities of its components.

For this screening study it was assumed that the fuel isotopes were homogeneously distributed through the volume of the fuel bundle (3744 cm³). The masses of each isotope were then used to determine an atomic density for each isotope across the fuel bundle volume. Although such a homogeneity assumption will significantly impact the absolute precision of the calculation, the results are presented in relative terms, allowing for comparison only. Further study will be required to determine absolute performance.

4.2.3 NEUTRON INTERACTION DATA LIBRARY

Neutron interaction data libraries contain data collected from a range of analyses, and provide information on a range of nuclear interaction properties and probabilities, such as radiative capture, scattering and fission cross sections and fission yields. The main libraries are JENDL [45], JEFF [454] and ENDF/B [455]. In this work the JENDL-4.0 library was used, as it contains data for all isotopes of interest in the problem, and has been used previously for the analysis of CANDU 6 cores [456]. Previous models using JENDL-4.0 have produced results which fall between those of other data libraries, such as ENDF/B-VI.8, ENDF/B-VII, and JEFF3.1.1 when studying fuel temperature coefficients of reactivity using MCNPX [456]. While other libraries are more commonly used, comparative data for CANDU reactors is lacking in the literature.

4.2.4 ONE GROUP REACTOR THEORY

The initial screening study used a one group reactor assumption, where only thermal neutron interactions were considered, ignoring fast neutron induced fissions or resonant captures. This is not a realistic assumption, but allows for an initial analysis of the core, and should be suitable for a comparison across the different fuel compositions with a well moderated core.

Some additional fissions are caused by fast neutrons, however, the microscopic cross sections for fast fissions are generally much lower [45]. The heavy metal to deuterium ratio of the core was calculated as 1:75-80 (see Table 4.9), and it is generally recommended that the contribution of fast fissions can be ignored for fuel:moderator ratios of 1:50 or greater [457]. In real CANDU reactors, fast neutron induced fissions typically increase the number of fast neutrons in the core by 3% over those from thermal fissions [458]. Thus not including fast fissions will not greatly impact the analysis.

4.3 NEUTRONIC ANALYSIS RESULTS

Thermal neutron interaction data from the JENDL-4.0 data library at 300 K were used to predict the macroscopic cross sections for fission, capture and scattering, the reproduction factor η and fission:capture ratio α^{-1} . These last two are presented in Table 4.7, which shows the calculated neutronic parameters across a range of known fuels.

TABLE 4.7 – CALCULATED NEUTRON REPRODUCTION FACTORS η AND FISSION:CAPTURE RATIOS α^{-1} FOR A SELECTION OF FUELS EITHER PREVIOUSLY REPORTED IN THE LITERATURE OR IN OPERATION. RESULTS ARE ALSO SHOWN NORMALISED AGAINST NATURAL URANIUM FOR COMPARISON WITH THIS REFERENCE FUEL.

FUEL CONCEPT DESCRIPTION	CALCULATED RESULT		NORMALISED TO NATURAL URANIUM	
	η	α^{-1}	η	α^{-1}
Natural uranium	1.35	1.25	1.00	1.00
1.2% enriched UO ₂	1.57	1.82	1.16	1.46
2.5% enriched UO ₂	1.80	2.86	1.33	2.30
2.5% UK inventory Pu in DU host [63]	1.74	1.54	1.29	1.24
1.8% (U-Th)O ₂ [450]	1.49	1.60	1.11	1.28
EPR reprocessed uranium	1.46	1.49	1.08	1.20
0.65% UK inventory Pu in DU host [452]	1.42	1.06	1.06	0.85

Table 4.8 shows the results from the neutronic feasibility assessment for fuel concepts 1-20. The results are normalised to those of natural uranium, and as such values greater than unity are taken to indicate neutronic feasibility for the fresh unirradiated fuel. The effect of thorium can be seen by comparing the three-component fuel of interest to the equivalent MOX two-component fuel. Fuel concept 21 is discussed in Section 4.6.2.

TABLE 4.8 – CALCULATED RELATIVE REPRODUCTION FACTORS AND FISSION:CAPTURE RATIOS FOR TWO AND THREE-COMPONENT MOX CONCEPTS WITH 1%, 2% AND 3% BY MASS PLUTONIUM LOADING IN MOX FUEL ELEMENTS. NORMALISED TO NATURAL URANIUM VALUES.

FUEL CONCEPT DESCRIPTION	CALCULATED RESULT									NORMALISED TO NATURAL URANIUM								
	η			α^{-1}			η			α^{-1}								
	1% Pu	2% Pu	3% Pu	1% Pu	2% Pu	3% Pu	1% Pu	2% Pu	3% Pu	1% Pu	2% Pu	3% Pu	1% Pu	2% Pu	3% Pu			
1 Depleted U, UK Inventory Pu	1.54	1.70	1.76	1.22	1.47	1.60	1.14	1.26	1.31	0.98	1.18	1.28						
2 Depleted U, LEU-EPR Pu	1.49	1.64	1.71	1.15	1.38	1.50	1.10	1.22	1.27	0.92	1.11	1.20						
3 Depleted U, MOX-EPR Pu	1.35	1.49	1.55	1.35	1.49	1.55	1.00	1.10	1.15	1.08	1.19	1.25						
4 MAGNOX Depleted U, UK inventory Pu	1.56	1.70	1.77	1.26	1.50	1.62	1.15	1.26	1.31	1.01	1.20	1.30						
5 MAGNOX Depleted U, LEU-EPR Pu	1.51	1.65	1.71	1.20	1.41	1.52	1.12	1.22	1.27	0.96	1.13	1.22						
6 MAGNOX Depleted U, MOX-EPR Pu	1.37	1.50	1.56	1.00	1.15	1.23	1.02	1.11	1.16	0.80	0.92	0.99						
7 LEU-EPR reprocessed U, UK inventory Pu	1.68	1.76	1.81	1.70	1.79	1.83	1.25	1.31	1.34	1.37	1.43	1.47						
8 LEU-EPR reprocessed U, LEU-EPR Pu	1.65	1.72	1.76	1.65	1.71	1.74	1.22	1.28	1.30	1.32	1.37	1.40						
9 LEU-EPR reprocessed U, MOX-EPR Pu	1.56	1.61	1.64	1.49	1.48	1.48	1.16	1.19	1.21	1.19	1.19	1.19						
10 Th, Depleted U, UK inventory Pu	1.30	1.52	1.62	0.90	1.19	1.37	0.97	1.13	1.20	0.72	0.96	1.10						
11 Th, Depleted U, LEU-EPR Pu	1.26	1.48	1.58	0.83	1.10	1.25	0.94	1.10	1.17	0.67	0.88	1.01						
12 Th, Depleted U, MOX-EPR Pu	1.48	1.61	1.68	1.28	1.47	1.58	1.10	1.19	1.25	1.03	1.18	1.27						
13 Th, MAGNOX Depleted U, UK inventory Pu	1.32	1.53	1.63	0.93	1.22	1.39	0.98	1.14	1.21	0.75	0.98	1.12						
14 Th, MAGNOX Depleted U, LEU-EPR Pu	1.28	1.49	1.59	0.87	1.12	1.27	0.95	1.10	1.18	0.69	0.90	1.02						
15 Th, MAGNOX Depleted U, MOX-EPR Pu	1.14	1.33	1.43	0.72	0.91	1.02	0.85	0.99	1.06	0.58	0.73	0.82						
16 Th, LEU-EPR reprocessed U, UK inventory Pu	1.49	1.61	1.68	1.29	1.47	1.59	1.10	1.20	1.25	1.04	1.18	1.27						
17 Th, LEU-EPR reprocessed U, LEU-EPR Pu	1.46	1.58	1.65	1.23	1.38	1.47	1.08	1.17	1.22	0.99	1.11	1.18						
18 Th, LEU-EPR reprocessed U, MOX-EPR Pu	1.37	1.46	1.52	1.10	1.19	1.24	1.01	1.08	1.12	0.88	0.95	1.00						
19 Th, ThORP Product U, UK inventory Pu	1.48	1.61	1.68	1.28	1.47	1.58	1.10	1.19	1.25	1.03	1.18	1.27						
20 Th, natural U, UK inventory Pu	1.44	1.59	1.67	1.18	1.40	1.53	1.07	1.18	1.24	0.95	1.12	1.23						

4.4 NEUTRONIC ANALYSIS DISCUSSION

As can be seen in Table 4.8, two-component mixed oxide nuclear fuels based on depleted uranium (concepts 1-3) require a minimum loading of ~2-3 wt% Pu to be comparable with natural uranium. Reprocessed uranium from MAGNOX reactors (concepts 4-6) provides a minor neutronic advantage when compared to uranium enrichment tails. In practice such an advantage may not outweigh the costs introduced to fuel fabrication when working with irradiated uranium. The LEU-fuelled EPR reprocessed uranium (concepts 7-9) provides a significant neutronic benefit, allowing lower plutonium fractions when compared to other fuels, potentially maximising the energy value of the plutonium. Three-component fuels (concepts 10-18) suffer significant neutronic penalties due to the replacement of some fissile material by thorium when compared with their equivalent two-component MOX fuels. Thus, they require increased plutonium loading to offset the use of fertile material. At 1% plutonium loading only fuels 16, 17 and 19 have both normalised neutronic values greater than or equal to unity, suggesting a requirement for enriched uranium if comparable performance levels are desired with such loading. Conversely, higher plutonium fractions allow the use of lower quality fissile uranium resources.

Some three-component fuels are comparable with the 2.5% UK plutonium MOX fuel, specifically fuel concepts 16, 17, 19 and 20. However, ~ 5% Pu would be required to match the calculated reproduction factor and fission:capture ratio of the UK CANMOX mimic.

As would be expected the isotopic composition of plutonium used has a large impact on neutronic performance. Variation in the input plutonium will require the fraction of plutonium used to be altered to maintain consistency in the fuel product.

4.4.1 CONCEPTS FOR DEVELOPMENT

Fuel concepts 17 and 19 are of interest for further development as they both provide options for management of separated nuclear materials, including the UK's plutonium inventory. Fuel concept 19 can allow the reuse of reprocessed uranium stocks from AGR reactors while irradiating separated UK plutonium, whereas fuel concept 17 gives an alternative option to LWR MOX where closed fuel cycles are used. Two other concepts which have neutronic feasibility, although more limited utility, are fuel concept 16, as it requires reprocessing of EPR spent fuel but does not manage the produced plutonium, and fuel concept 20, as it uses natural uranium, thus requiring additional natural uranium resources.

4.5 MULTIPLICATION FACTOR CALCULATION

The neutron reproduction factor and fission:capture ratio do not give a complete representation of homogeneous reactor neutron multiplication. To estimate the impact of other reactor materials and the moderator on neutronic performance, a more in-depth calculation has been performed on selected fuels to estimate their effective neutron multiplication factor, as was first discussed in Section 2.1.2. The studied fuels consisted of 2.5% UK plutonium MOX fuel with a range of dysprosium burnable absorber loadings and fuel concepts 17 and 19 with a range of plutonium loadings, with natural uranium in a 37-element CANDU bundle used as a reference. The reproduction factor is one of the factors in the estimation of the effective neutron multiplication factor within a reactor k_{eff} , as given in equation (4.3) [17, 19].

$$k_{eff} = \eta \epsilon p f P_{FNL} P_{TNL} \quad (4.3)$$

Where k_{eff} is the effective neutron multiplication factor,

ϵ is the fast fission factor,

η is the neutron reproduction factor,

- p is resonance escape probability,
- f is the thermal utilisation factor,
- P_{FNL} is the fast neutron non-leakage probability, and
- P_{TNL} is the thermal neutron non-leakage probability.

The calculation of the parameters in Equation (4.3) requires information on the mass of moderator and coolant, structural zircaloy-4, fuel and carbon dioxide annulus gas in the core. These have been estimated from data in Table 4.1 and are presented in Table 4.9. The structural materials considered are the pressure and calandria tubes, the fuel bundle structures, but not the calandria vessel or other components such as control rods or dissolved gadolinium in the moderator. The mass of carbon dioxide depends on the annulus gas system operating pressure, typically 25-100 kPa [459]. The gas temperature was set to 179°C, the average of the coolant and moderator temperatures [438, 460]. The sensitivity of the neutronic results to the annulus gas pressure is expected to be negligible, given the small interaction cross sections and the low mass fraction in the core of this material.

TABLE 4.9 – MASS OF MATERIALS IN HOMOGENEOUS CORE.

MATERIAL	MASS /t
Heavy water moderator	263
Heavy water coolant	7.13
Carbon dioxide annulus gas	~3-12
Structural Zircaloy-4	19.47
Fuel	~100 (varies by composition)

Thermal neutron cross sections and resonance capture integrals were taken from the JENDL-4.0 library [45] and used to determine the thermal utilisation factor f , resonance escape probability p , thermal non-leakage probability P_{TNL} and fast non-leakage probability P_{FNL} , as defined in the literature [16, 17, 19].

The fast fission factor ε was set to unity, although in most reactors it is slightly greater than unity [17, 461]. The atomic moderator-to-fuel ratio for the core has been estimated as 75-80:1, based on the calculated masses of fuel and moderator in the core. For such high ratios of moderator-to-fuel it can be assumed that neutrons are rapidly brought to thermal energies, and fast fissions are sufficiently rare to take $\varepsilon = 1$ [457]. The tendency towards unity with increasing moderator-to-fuel ratio may be estimated empirically, and it can be seen that even at ratios of 5:1, it is approximately 1.03 for heavy water moderated systems [461].

The calculation of neutronic factors here is conducted for a complete core of unirradiated plutonium-containing fuel bundles. However, in operation the core will contain fuel bundles with a full range of burnup levels. Less fissile plutonium bundles will also be used during the core life, as a means of irradiating low quality plutonium which cannot by itself sustain a critical chain reaction [68].

4.5.1 NATURAL URANIUM REFERENCE FUEL

Calculations of k_{eff} , p , f , η , P_{FNL} and P_{TNL} were carried out for natural uranium fuel within a standard 37-element CANDU fuel bundle. The results for the natural uranium fuel are shown in Table 4.10. Typical values for these values from the literature are also presented.

There is some significant divergence between calculated and typical values, with the greatest variation being between the values for the reproduction factor. This variation may be due to the one group neutron energy approximation, as all neutron interactions are assumed to occur at thermal energy, or the idealized cylinder approximation applied to the fuel pellets, although this approximation should only reduce the overall fuel mass in a bundle by approximately 2% [462]. In addition, the reported typical values may be average values over the core life, rather than for a core of fresh fuel.

THE PREPARATION AND APPLICATION OF THORIUM-BASED NUCLEAR FUELS

TABLE 4.10 – CALCULATED INITIAL EFFECTIVE MULTIPLICATION FACTOR AND CONTRIBUTING VARIABLES FOR NATURAL URANIUM FUEL IN A 37-ELEMENT CANDU BUNDLE [331]. FAST FISSION FACTOR ε ASSUMED TO EQUAL UNITY. ALSO SHOWN ARE TYPICAL VALUES FOR NATURAL URANIUM-FUELLED CANDU REACTORS [431].

FACTOR	CALCULATED VALUE	TYPICAL VALUE	$\frac{\text{CALCULATED}}{\text{TYPICAL}}$
k_{eff} multiplicity factor	1.131	1.03	1.10
η reproduction factor	1.349	1.2	1.12
ε fast fission factor	<i>Assumed 1.00</i>	1.03	0.97
p resonance escape probability	0.875	0.9	0.97
f thermal utilisation factor	0.977	0.95	1.03
P_{TNL} thermal non-leakage probability	0.991	0.98	1.01
P_{FNL} fast non-leakage probability	1.000	0.995	1.01

4.5.2 UK CANMOX MIMIC REFERENCE FUEL

As the proposed dysprosium burnable absorber loading in the UK CANMOX fuel was not known, calculations were undertaken to determine the effect of Dy loading on neutronic parameters for the 2.5% UK plutonium MOX fuel. The mass fraction of dysprosium in the inner eight fuel elements was varied, and the neutronic parameters were calculated for each loading level. The results are presented in Figure 4.5. The assumption of $\varepsilon = 1$ was used in all cases, and as such this factor is independent of dysprosium loading in this model.

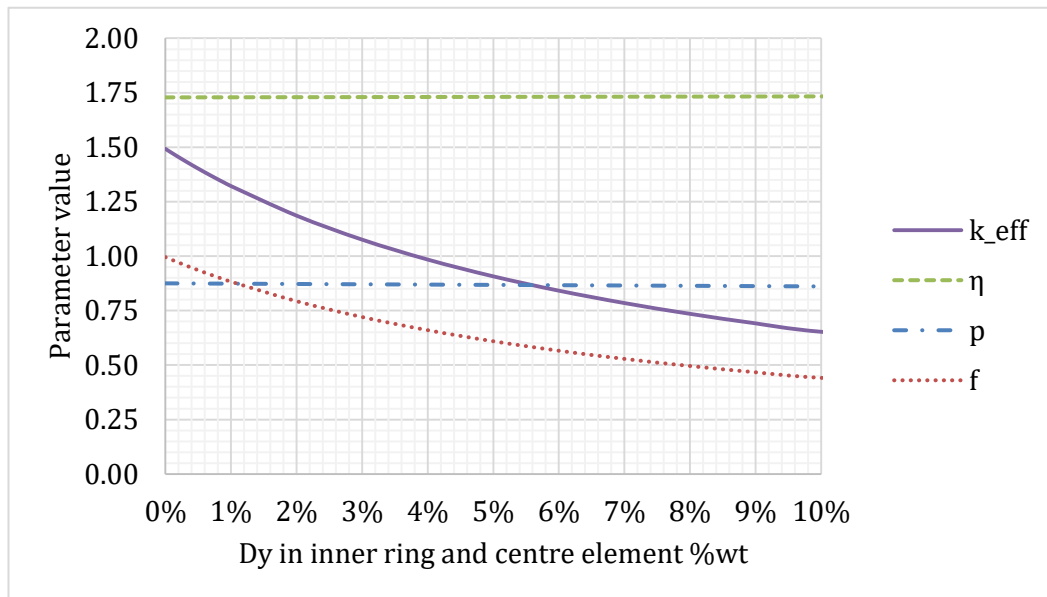


FIGURE 4.5 – EVALUATED VALUES OF NEUTRONIC FACTORS AS AFFECTED BY DYSPROSIUM BURNABLE ABSORBER LOADING IN UK CANMOX FUEL. FAST FISSION FACTOR AND LEAKAGE FACTORS WERE VERY CLOSE TO UNITY FOR ALL Dy LOADING FRACTIONS, AND SO ARE NOT SHOWN.

In the empirical model used it was found that most parameters are little affected by the dysprosium loading fraction. With increasing Dy fraction:

- η slightly increases as the amount of depleted uranium decreases, due to the depleted uranium having a very low fissile fraction.
- P_{FNL} and P_{TNL} were expected to increase with increasing dysprosium loading, as thermal neutrons (with energy 0.0253 eV) are more likely be absorbed by dysprosium ($\sigma_a = 942.4$ barn) than by depleted uranium ($\sigma_a = 4.427$ barn) [45], thus increasing overall thermal neutron absorptions with increased dysprosium loading. However, the leakage parameters were found to be close to unity for all examined dysprosium loadings. This is because the thermal non-leakage probability approximation used is a function of the core geometry and moderator material only, and is therefore not affected by the Dy fraction.
- ϵ was taken as unity throughout.

- p slightly decreases, due to the large resonance capture integral (1401 barn) of natural dysprosium.
- f decreases strongly, due to the increasing absorption of thermal neutrons in the burnable absorber.
- k_{eff} decreases strongly being driven by decreasing thermal utilisation, and was found to equal unity when dysprosium was set to 3.815wt%.

As can be seen in Figure 4.5, the 2.5% UK plutonium MOX fuel has an initial k_{eff} that is heavily dependent upon the level of loaded burnable absorber. With no initial dysprosium k_{eff} can be up to 1.49, falling to a value of 1.00 with 3.815% Dy loading. An equivalent initial multiplication factor to the reference fuel may be achieved with 2.367% Dy. While the actual fraction of Dy loading is unknown, it can be assumed that the loading is unlikely to be greater than 4% Dy metal by mass in the eight central fuel elements.

Over the course of the fuel irradiation, it is anticipated that the plutonium and dysprosium will both deplete and fission product poisons will build up, gradually reducing fuel reactivity until it reaches the point where it must be removed from the core.

4.5.3 BUCKLING CONSTANT METHOD

An alternative approach to determine criticality in nuclear systems is based on the calculation of buckling constants. This is also used here, as a comparison to the method described in Section 4.2. The method is based on an analytical solution of the Helmholtz Equation, of which full derivations are available in the literature [17]. A reduced derivation is provided here.

Neutron diffusion may be expressed through Fick's diffusion law. When applied to neutron diffusion, the law is given by Equation (4.4).

$$\mathbf{J} = -D\nabla\phi \quad (4.4)$$

Where \mathbf{J} is the neutron density vector, or neutron current,
 D is the neutron diffusion coefficient,
 ∇ is the gradient vector operator, and
 ϕ is the neutron flux.

The diffusion coefficient is approximated from the mass number of the scattering nucleus, as shown in Equation (4.5). Note that the approximation of $\bar{\mu}$ is valid for atoms of mass greater than carbon-12 [17], although a more complex expression can be used which is valid for lighter nuclei [16].

$$D = \frac{1}{\Sigma_s(1 - \bar{\mu})} = \frac{1}{\Sigma_s \left(1 - \frac{2}{3A}\right)} \quad (4.5)$$

Where Σ_s is the macroscopic scattering cross section of the target
 $\bar{\mu}$ is the average cosine of the neutron scattering angle, and
 A is the mass number of the scattering atom.

Neutron leakage from a system may be calculated based on Equation (4.4) by multiplying by the rate of change of neutron flux across the reactor volume, as given in Equation (4.6).

$$l = \text{div } \mathbf{J} = -D\nabla^2\phi \quad (4.6)$$

Where l is the neutron leakage rate from an element volume.

The rate of generation of thermal neutrons from fission in an infinite reactor is given by Equation (4.7).

$$s = \Sigma_f\phi \times \varepsilon p v = k_{inf}\Sigma_{aR}\phi \quad (4.7)$$

Where s is the thermal neutron production rate,
 Σ_f is the macroscopic fission cross section,
 k_{inf} is the infinite neutron multiplication factor, and
 Σ_{aR} is the macroscopic absorption cross section of the reactor.

In an infinite nuclear reactor, the rate of change of the neutron population over time is as given by Equation (4.8), where the first term on the right hand side is the rate of thermal neutron production, the second term is the rate of thermal neutron absorption and the third term is the rate of thermal neutron leakage

$$-\frac{1}{v} \frac{\delta n}{\delta t} = D \nabla^2 \phi - \Sigma_a \phi + k_{inf} \Sigma_{aR} \phi \quad (4.8)$$

Where n is the neutron population in the system, and
 t is time.

Under critical conditions where the neutron population is time independent the left hand side of Equation (4.8) equals zero. This is known as the steady state diffusion equation.

$$\frac{\Sigma_a}{D} = \frac{1}{L^2} \quad (4.9)$$

Where L is the thermal neutron diffusion length in the moderator.

Using Equation (4.9), when in steady state Equation (4.8) may be rearranged to give

$$\frac{s}{D} = \nabla^2 \phi - \frac{1}{L^2} \phi \quad (4.10)$$

If it is assumed that all neutrons in the core are at thermal energy and that the core is homogeneous, the definition of s from Equation (4.7) may be used with Equation (4.10) to give Equation (4.11). The ratio of thermal diffusion length to slowing down length in heavy water is 15.1, compared to 0.55 for light water [17, 20]. For a CANDU reactor neutrons have long mean free paths and are rapidly thermalised in the calandria between fuel tubes. Thus these assumptions are respected for CANDU-type PHWRs.

$$0 = \nabla^2 \phi + \left(\frac{k_{inf} - 1}{L^2} \right) \phi \quad (4.11)$$

The bracketed fraction in Equation (4.11) gives the reactor materials buckling constant B as shown in Equation (4.12).

$$B^2 = \frac{k_{inf} - 1}{L^2} \quad (4.12)$$

Substituting Equation (4.12) into Equation (4.11) gives the reactor flux equation, also known as the Helmholtz equation, Equation (4.13).

$$0 = \nabla^2 \phi + B^2 \phi \quad (4.13)$$

The solution of the Helmholtz equation relates geometry of the core to the properties of the core materials, creating a link between the length and radius of the Enhanced CANDU 6 core and the fuel composition which influences k_{inf} .

The CANDU core is cylindrical. Under the assumptions taken in this model, the core is homogeneous, and thus all azimuthal positions are equivalent. The core shape is annotated in Figure 4.6. The dimensions H and R are the geometric boundaries of the core. In addition it is necessary to consider the “extrapolated” flux boundaries, where the neutron flux falls to zero beyond the geometric boundaries. These extrapolated boundaries are denoted as H' and R' respectively.

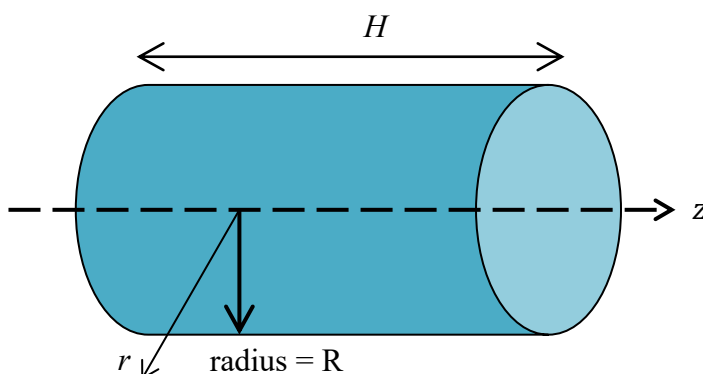


FIGURE 4.6 – CYLINDRICAL CORE SHAPE LABELLED WITH GEOMETRIC ANNOTATIONS AS USED IN BUCKLING CONSTANT DERIVATION.

The first term of Equation (4.13) may be expressed in cylindrical coordinates to yield Equation (4.14).

$$0 = \frac{\delta^2 \phi}{\delta r^2} + \frac{1}{r} \frac{\delta \phi}{\delta r} + \frac{d^2 \phi}{dz^2} + B^2 \phi \quad (4.14)$$

It may be assumed that the flux shape is a product of two functions $F(r)$ and $G(z)$, each of which is a function of one geometry component only, as given in Equation (4.15).

$$0 = \frac{1}{F} \frac{\delta^2 F}{\delta r^2} + \frac{1}{Fr} \frac{\delta F}{\delta r} + \frac{1}{G} \frac{d^2 G}{dz^2} + B^2 \phi \quad (4.15)$$

It is assumed that the functions $F(r)$ and $G(z)$ are independent of one another and equal to two constants, $-\alpha^2$ and $-\beta^2$ respectively. Thus the geometric buckling constant of the core is given in Equation (4.16).

$$B_g^2 = \alpha^2 + \beta^2 \quad (4.16)$$

The general solution of function $G(z)$ is given by

$$G(z) = A \sin \beta z + C \cos \beta z \quad (4.17)$$

As the flux shape must be symmetrical about the core centre plane where $z = 0$, and the flux must equal zero at the extrapolated boundaries of the core where $z = \pm \frac{H'}{2}$,

$$G(z) = C \cos \frac{\pi z}{H'} \quad (4.18)$$

Thus,

$$\beta = \frac{\pi}{H'} \quad (4.19)$$

In the radial direction, considering only function $F(r)$ and defining $x = \alpha r$ allows Equation (4.15) to be rewritten as

$$x^2 \frac{d^2 F}{dr^2} + x \frac{dF}{dr} + x^2 F = 0 \quad (4.20)$$

This equation is Bessel's ordinary function of zero order, of which the solution has two components, denoted J_0 and Y_0 , of which only the J_0 component is meaningful in reactor flux theory, as the Y_0 component approaches negative infinity at $r = 0$. The J_0 component has a zero at $\alpha r = 2.405$. Thus,

$$F(r) = J_0\left(\frac{2.405r}{R'}\right) \tag{4.21}$$

Therefore,

$$\alpha = \frac{2.405}{R'} \tag{4.22}$$

From Equations (4.19) and (4.22) the overall geometric buckling constant of the core may be calculated using Equation (4.16). The reactor geometric buckling constant B_g^2 was thus calculated to be $6.8 \times 10^{-5} \text{ cm}^{-2}$.

According to the Helmholtz Equation, Equation (4.13), criticality is given by the condition where $B_g = B$. When not accounting for the impact of reactivity control systems, and for a reactor core loaded with fresh fuel, one would expect the materials buckling constant $B > B_g$. A plot of B/B_g as a function of dysprosium loading is presented in Figure 4.7.

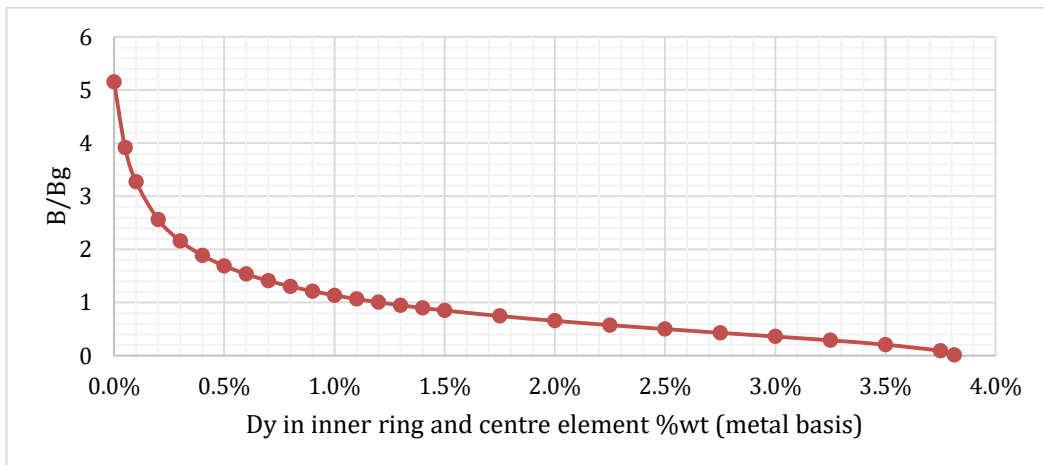


FIGURE 4.7 – RATIO OF MATERIALS BUCKLING CONSTANT TO GEOMETRIC BUCKLING CONSTANT IN UK CANMOX FUEL AS A FUNCTION OF BURNABLE ABSORBER LOADING.

During irradiation within the core, the dysprosium will capture neutrons and thus reduce neutron absorption by fissile/fertile isotopes, lowering the thermal utilisation factor of the core and reactivity of the fuel bundle.

Correct selection of the dysprosium loading fraction will reduce reactivity swing over the course of the bundle irradiation history.

In order to determine whether a proposed three-component fuel can operate under the same conditions as UK CANMOX fuel, further work will be required to determine the relationship between fuel burnup, fertile conversion and reactivity depletion. The evolution of reactivity with fuel burnup will determine the initial plutonium loading and design discharge. The replacement of burnable absorber fuel elements by thorium elements will have a strong impact on these factors, and in particular it will be necessary to determine the rate of thorium conversion to uranium-233.

Fuel composition as a function of burnup may be calculated by analytical methods [463], by time stepping through the burnup history while solving the neutron transport equation and the burnup equation cyclically [464]. Such approaches are mathematically onerous, and are now regularly carried out by numerical simulation methods, which are highly suited to the rapid evaluation of large matrices as encountered in solving the burnup equations. Such a numerical analysis is reported in Chapter 5 of this thesis.

In order to gain an indication of an appropriate dysprosium loading as suggested by the buckling constant method, some points can be noted from Figure 4.7. When comparing buckling constants, the critical reactor condition where $B = B_g$ is given when the dysprosium loading is 1.21%, for 2.5% Pu MOX fuel. Higher dysprosium fractions would suggest a sub-critical initial core. An indicative operating point is given by normalising against the buckling constant of a core of natural uranium fuel, in which case B should be set to $1.61B_g$. For this condition, the dysprosium loading fraction should be 0.55%.

Under both studied methods, the maximum dysprosium fraction has been found to be less than or equal to 4%, and may be significantly lower. The required fraction is however much more dependent on how the fuel composition evolves with burnup than the initial state, and only a burnup analysis of the type reported in Chapter 5 may give a definitive value for the dysprosium fraction. The range of values calculated here gives a useful starting point for this analysis.

4.5.4 CONCEPT FUELS 17 AND 19 RESULTS

The neutronic factors for fuel concepts 17 and 19 were found to be very similar. Those for concept 19 are presented in Figure 4.8. Only those factors which vary visibly as a function of plutonium loading are presented. As with the UK CANMOX mimic fuel, the fast non-leakage probability was found to be very close to unity, the thermal non-leakage probability was found to be 0.99, and the fast fission factor was assumed to be 1.00. The thermal utilisation factor was found to be > 0.985 for all plutonium fractions.

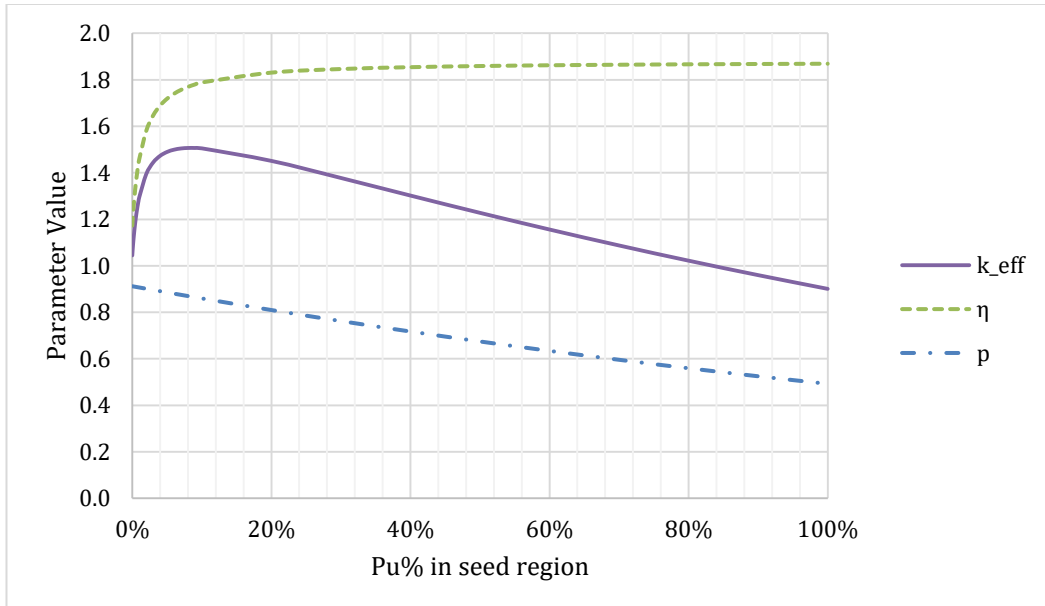


FIGURE 4.8 – EVALUATED VALUES OF NEUTRONIC FACTORS AFFECTED BY PLUTONIUM LOADING IN PROPOSED FUEL CONCEPT 19. VARIABILITY BETWEEN CONCEPT 19 AND CONCEPT 17 IS MINIMAL. FAST FISSION FACTOR, THERMAL UTILISATION FACTOR AND LEAKAGE FACTORS WERE ALL CLOSE TO UNITY.

The proposed three-component fuel concepts have a highly variable k_{eff} which reaches a maximum value at approximately 8.8% plutonium loading, although it remains within 90% of this maximum value over the range 2-30% plutonium loading. Below approximately 4% Pu the reproduction factor reduces rapidly as the Pu fraction tends to zero. At high plutonium fractions additional plutonium has little impact on the reproduction factor, but resonance absorption has an increasingly negative impact on the k_{eff} .

The impact of very high plutonium loading may also be observed in the variation of the buckling constant with plutonium loading, as shown in Figure 4.9. The ratio B/B_g has a maximum at 16.4% plutonium loading, and decreases at higher plutonium fractions. The core is at least critical, that is $B \geq B_g$, over the range 0.1 – 83.9% Pu loading in fuel concept 17, and $B \geq 1.61B_g$ over the range 0.1 – 81.1%.

The change in B/B_g is very rapid for low plutonium fractions, further confirming that the initial reactivity of the fuel is highly sensitive to the plutonium fraction.

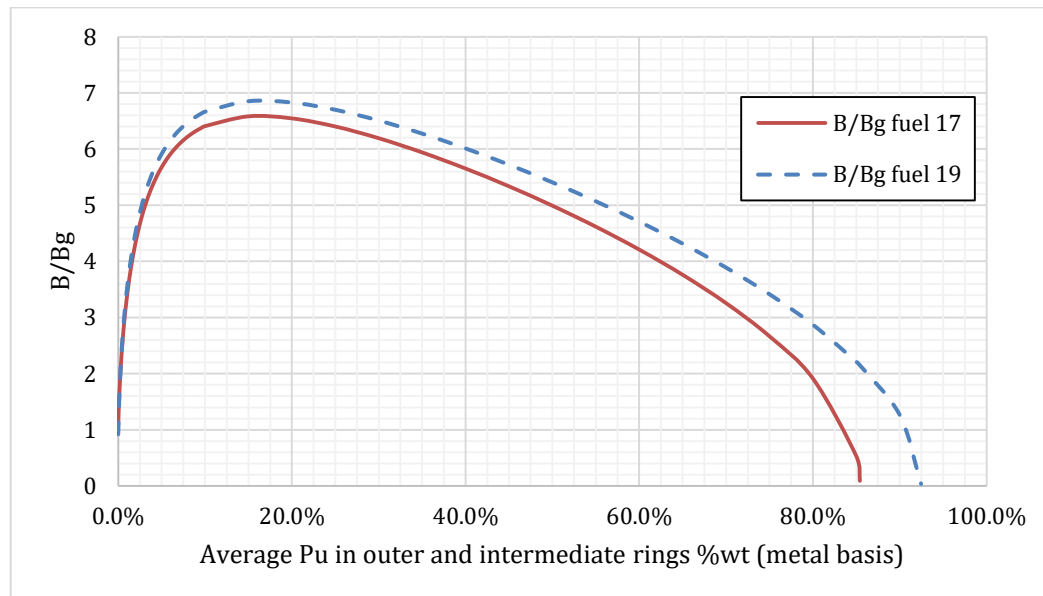


FIGURE 4.9 – VARIATION IN RATIO OF MATERIALS BUCKLING CONSTANT TO GEOMETRIC BUCKLING CONSTANT AS A FUNCTION OF AVERAGE PLUTONIUM LOADING IN OUTER AND INTERMEDIATE FUEL ELEMENTS.

High values of plutonium loading are presented for completeness, but these are not suggested for actual fabrication or reactor use, as high plutonium fuel would be more difficult to fabricate due to criticality safety requirements. There could also be a greater proliferation risk; 80% plutonium loading in a UK CANMOX bundle is 11.4 kgHM of plutonium, potentially a critical mass when assembled as a bare metal sphere [465]. The mass and geometry of a single bundle could make this a feasible target for theft. With 3.5% average loading as in UK CANMOX fuel, 23 bundles would be required for the same mass of plutonium, a much more difficult proposition.

4.6 NUCLEAR MATERIALS AVAILABILITY FOR FUEL CONCEPTS

In addition to neutronic feasibility, calculations were undertaken to determine whether there would be sufficient nuclear material to fuel one or more EC6 plants over the 30-year MOX operational period, in-line with the proposed timescale for UK CANMOX operation prior to the mid-life refurbishment of the reactors, after which they would be fuelled by uranic materials. It would be beneficial to perform the mid-life refurbishment after all MOX has passed through the plant, as the extended shutdown period would allow for an easier transition to uranium fuel.

For fuels based on UK inventory materials, calculations were undertaken to determine the number of EC6 reactors required to consume the UK plutonium inventory over the course of the 30 year period, whilst ensuring the availability of sufficient uranium to produce the desired MOX component of the fuel.

For fuels based on EPR reprocessing products an LWR:EC6 support ratio has been determined, based on the lifetime spent fuel production from an EPR and the EC6 fuel requirements. The LWR:EC6 calculations are for fuel

production/use in equilibrium, and do not take into account the transient availability of spent nuclear fuel from LWRs. In reality this may delay the operation of the UK CANMOX plant. As of March 2015, the first loading of MOX fuel was scheduled for 2028 [68]. At the time of writing it was projected that the first UK EPR operation would be in 2026 [466], with the first fuel being removed from the core approximately 18-24 months later. Allowing time for post-irradiation cooling (nominally 5 years) and reprocessing operations, it is unlikely that any reprocessed EPR materials would be available for fabrication into CANMOX fuel bundles before the mid-2030s.

4.6.1 PLUTONIUM INVENTORY UTILISATION

When producing fuels based on spent fuel and inventory material, the availability of material in sufficient quantity must be determined. The annual fuel requirement for an EC6 is calculated using equation (4.23) [467]. Values for P_{th} and C_f were taken from Table 4.1.

$$F = \frac{P_{th} \times C_f}{B_U \times \left[\frac{1 \text{ year}}{365.24 \text{ days}} \right]} \quad (4.23)$$

Where F is the annual fuel requirement in tHM,
 P_{th} is the reactor thermal power in MW
 C_f is the reactor design capacity factor, and
 B_U is the fuel burnup at discharge in MWd/tHM.

Under the UK CANMOX proposal, 1.3 t of plutonium would be irradiated per reactor.year in four EC6 units. [68]. The mass of plutonium in a UK CANMOX bundle has been calculated as 480 g, thus giving 2690 fuel bundles/reactor.year which corresponds to a fuel burnup of 15,000 MWd/t calculated over a period of 30 years, the lower end of the burnup range quoted in the literature. When calculated over a period of 27 years, this burnup decreases to 13,300 MWd/tHM. The calculated burnup is sensitive,

however, to the quantity of plutonium irradiated per year. A change of 0.05 tPu/reactor.year alters the burnup by ± 510 MWd/tHM when calculated over 27 years.

Three levels of plutonium fraction and discharge burnup were selected for initial investigation as three component fuels.

- 1.0% Pu, irradiated to 7000 MWd/t. Mimic for natural uranium fuel.
- 3.4% Pu, irradiated to 16,000 MWd/t. Mimic for UK CANMOX fuel.
- 8.4% Pu, irradiated to 20,000 MWd/t. Selected as giving the approximately the maximum value of k_{eff} for three-component fuels, using the highest cited value for burnup [63].

These were based on an assumption of equivalent reactivity depletion rate to the fuels they mimic. Whether the fuels can reach this level of burnup in a critical core was not determined at this stage, but three-component fuel reactivity depletion is studied in Chapter 5. Plutonium loading fractions were altered slightly to give complete utilisation of the UK plutonium inventory over 30 years in a fleet of EC6 units.

Assuming equivalent reactivity depletion with natural uranium, for a fuel with similar neutronic parameters to natural uranium with 1.0%Pu and 7000 MWd/t burnup, 102,200 kg/reactor.year of three-component fuel will be required, equivalent to 5760 fuel bundles per reactor.year, in six EC6 reactors.

For a fuel similar to the proposed UK CANMOX fuel with 3.4% Pu and 16,000 MWd/t burnup, 44,800 kg/reactor.year of fuel (2520 fuel bundles) will be required, in four EC6 reactors.

A three-component fuel with 8.4% average plutonium loading irradiated to 20,000 MWd/t would require 35,900 kg/reactor.year of fuel (2010 fuel bundles), in two EC6 reactors.

4.6.2 URANIUM INVENTORY UTILISATION

Many of the proposed two- and three-component fuel concepts make use of reprocessed and depleted uranium stocks. Before developing any of these concepts further, it should be ensured that sufficient stocks of these materials are available. A fuel concept which could utilise significant quantities of the UK uranic materials inventory would give advantages in terms of maximising the energy value of this material and reducing the requirement for fresh uranium fuel.

It may be necessary that some fraction of the uranic inventory be retained for use in an NUE fuel over the second 30 years of the EC6 fleet life. An EC6 operating at 7000 MWd/t will consume 173,000 fuel bundles over a 30 year period, equivalent to 3110 t uranium. Blending of TPU and MDU to achieve the same reproduction factor as natural uranium fuel would require 71% TPU and 29% MDU, this being 2210 t TPU and 900 t MDU to produce 3110 t NUE fuel.

The single reactor unit annual fuel requirements and 30 year fleet fuel requirements, broken down by element, for each of the three fuels discussed in Section 4.6.1 are displayed in Table 4.11.

The data in Table 4.3 show that there will be 5600 t of TPU, 21,500 t DU tails and 26,000 t MDU available. The 1.0% Pu fuel cannot be produced from TPU; under this regime enough fuel could be produced for two EC6 units, irradiating only one third of the UK plutonium inventory. Tripling the plutonium fraction to 3% would naturally reduce the number of units by a factor of three at the same discharge burnup, bringing the TPU lifetime fleet requirement to 4620 t. However, this will lead to a greatly reduced plutonium isotopic conversion, again assuming that the rate of reactivity depletion between the three component MOX and natural uranium fuel is the same.

TABLE 4.11 – FUEL MATERIALS REQUIREMENTS WITH PROPOSED THREE-COMPONENT FUELS. REQUIRED MASSES GIVEN PER REACTOR.YEAR AND FOR A FLEET OF UNITS CAPABLE OF IRRADIATING THE WHOLE PLUTONIUM INVENTORY OVER 30 YEARS.

Pu%, BURNUP, NUMBER OF EC6 UNITS IN FLEET	ANNUAL MASS PER UNIT /tHM			30-YEAR MASS OVER FLEET /tHM		
	U	Pu	Th	U	Pu	Th
1.0% Pu 7000 MWd/tHM 6 EC6 units	78.5	0.793	23.0	14100	143	4140
3.4 % Pu 16,000 MWd/tHM 4 EC6 units	33.5	1.18	10.1	4020	142	1210
8.4% Pu 20,000 MWd/tHM 2 EC6 units	25.5	2.34	8.04	1530	140	483

The higher Pu fraction fuels as described in Table 4.11 could be fabricated with TPU. However, if TPU is required to be set aside for NUE fabrication for 30 years in a single EC6, only 3400 t of TPU will available. From this material high Pu, high burnup fuels may be manufactured. However, the 3.4% Pu fuel will not be able to be produced. The total amount of uranium may be made to 4020 t by blending 3400 t TPU with 610 t MDU, to give a slightly enriched uranium oxide with 0.8% uranium-235. For a 3.4% Pu fuel, this blending gives an overall reduction in k_{eff} of 0.33% compared to the use of unblended TPU. The reduction in B was 0.92%. Fuels prepared from a blend of TPU and MDU are given the fuel concept number 21, as listed in Americium in the plutonium inventory was accounted for in the estimation of neutron reproduction factor, although strictly speaking it should not be, given that it is not a fuel isotope.

The fission:capture ratio α^{-1} , which is the overall ratio of microscopic fission capture cross section to microscopic capture cross section, is

calculated using equation (4.2). The difference between the absorption cross section and the fission cross section is the neutron capture cross section..

4.6.3 EPR REPROCESSING PRODUCT AVAILABILITY AND SUPPORT RATIO

If three-component fuels were to be fabricated from EPR spent fuel as in the case of fuel concept 17, a support ratio of the number of EPR units per EC6, or vice versa, should be calculated. The various options for fuel plutonium fraction, composition, burnup, and the number of reactors of each type define a large envelope within which any real support ratio will be found. However, some possible scenarios with associated ratios are defined here.

The concept of using LWR spent fuel to operate pressurised heavy water reactors is not new. The DUPIC (Direct Use of Used PWR fuel in CANDU) process, as its name suggests, consists of the refabrication of LWR spent fuel into CANDU bundles, with very little chemical separation; either the volatile fission products are removed, as a result of opening the fuel cladding and grinding the fuel pellets to powder for repressing as CANDU pellets, or alternatively LWR rods could be simply cut to length, have their ends capped or be placed into a CANDU sheath, and reassembled in CANDU bundles [468]. The work described here did not consider this direct use or dry reprocessing, and instead is based on a complete separation of the fission products and minor actinides from the uranium and plutonium. However, separation of uranium and plutonium from one another is not necessarily required, in-line with the aim of several advanced hydrometallurgical reprocessing cycles which do not separate completely U and Pu [74].

An EPR fuelled by 5% enriched UO_2 over its life will produce 3400 spent fuel assemblies [469], giving a lifetime spent fuel production of 22.5 t Pu and 1650 t U [451]. Currently, four EPR units are planned for the UK, giving a total fleet lifetime production of 90 t Pu and 6600 t U. If this fuel were to be reprocessed, EC6 plants with three-component MOX fuels might form a

route for the management of the plutonium and reprocessed uranium. Some fleet and fuelling options are presented in Table 4.12. It can be seen that the full-life EPR:EC6 support ratio is between 2:1 and 1:1.

In EPR spent fuel, plutonium makes up 1.4% of the total mass of plutonium and uranium. Thus, the 1.4% Pu three-component fuel is of particular interest, in that it can be produced by complete use of all plutonium and uranium from the EPR units, in a DUPIC-like fuel. It is highly desirable to determine the achievable discharge burnup of this fuel, as it could provide a method of increasing the energy value of EPR fuel while irradiating thorium to produce a supply of U-233 for use in starting a dedicated thorium fuel cycle.

The higher plutonium enrichment levels are more likely to allow higher burnups to be achieved. However, some fraction of the uranium will be left over after MOX irradiation, although it could be dealt with as reprocessed uranium or natural uranium equivalent fuel.

TABLE 4.12 – POTENTIAL FUELLING OPTIONS FOR AN EC6 REACTOR FLEET BASED ON REPROCESSING PRODUCTS FROM FOUR EPR UNITS.

PU FRACTION IN MOX	BURNUP /MWd.t⁻¹	NUMBER OF EC6 UNITS PER EPR	60 YEAR FLEET U USAGE /t	60 YEAR FLEET PU USAGE /t	60 YEAR FLEET TH USAGE /t
1.4%	10,000	2	6570	93.2	1930
4.4%	16,000	1	1990	91.7	603
5.4%	20,000	1	1580	90.0	483

4.7 CONCLUSIONS

Three-component U-Pu-Th fuels have been studied using a simplified model, giving early indications of their potential feasibility for use in the Enhanced CANDU 6 reactor using the CANFLEX 43-element fuel bundle. Although the method is based on significant assumptions, results can be considered as at least indicative, as they are presented as relative to other fuels which have been studied previously in more detail, specifically the currently used natural uranium fuel, the proposed UK CANMOX fuel [63], low Pu-DU MOX fuels [452] and Pu-Th fuels [450].

Two possible operation modes have been suggested. In “Inventory Management” mode, a fleet of two to six EC6 units would irradiate a three-component U-Pu-Th oxide fuel over a 30-year period, where the uranium and plutonium would be taken from the existing UK inventory, while thorium would be supplied from either existing international inventories or through setting up the necessary nuclear fuel cycle facilities to supply primary thorium. Following an 18-month mid-life refurbishment, the plants would then be fuelled with a uranic fuel, which could be natural uranium, although the use of a blended NUE fuel based on UK reprocessed uranium stocks would be more advantageous from the perspective of natural resource utilisation and maximising energy value per unit of primary uranium. Conceivably, some partially converted thorium fuel elements could be recycled into these fuel bundles, potentially allowing a thorium fuel cycle to be developed in the UK, depending on the degree of conversion that could be achieved in the thorium fuel elements.

In “LWR Spent Fuel Management” mode, the used fuel from UK new build light water reactors could be reprocessed to separate the uranium and plutonium, which could then be refabricated into a MOX for use in a three-component fuel. Nominally the light water reactor type would be the AREVA EPR, although other LWR LEU fuels could potentially also be used, such as

the Westinghouse AP1000, Hitachi-GE ABWR, or China General Nuclear HPR1000. Sizewell B fuel could also be reprocessed and used, although the reduced burnup and enrichment in this older reactor would give a significantly different used fuel isotopic breakdown. The three-component fuel would be irradiated over the full 60-year life of the EC6, following the full 60 year design life of modern Generation III+ LWRs such as the EPR. Plant Lifetime Extension (PLEx) of both plant types might occur, although given the requirement for mid-life refurbishment of EC6 plants it may be deemed uneconomical to refurbish a second time. If LWR PLEx is foreseen, the EC6 fuel characteristics may be altered to allow >60 years' worth of LWR MOX to be irradiated within the EC6 lifetime. Currently the UK is moving away from nuclear fuel reprocessing, towards an open fuel cycle where spent fuel is disposed of directly, with the closure of existing reprocessing facilities between 2018 and 2020 and no plans for replacement facilities. However, the option to transition back to a closed fuel cycle remains open [53].

It is worth noting that both operation modes can run simultaneously in two sets of reactors, or sequentially within the same fleet, with 30 years of Inventory Management and 30 years of LWR Spent Fuel Management. Furthermore, blending of inventory materials with LWR spent fuel reprocessing products may also present further fuel options for development.

Calculations indicate that, from a neutronic perspective, there are several feasible three-component fuel concepts which will allow operation of these fuel regimes. Based on these a recommendation is made to further develop fuel cycle options for a three-component fuel in the Enhanced CANDU 6 reactor. The calculations were performed under assumptions of a homogeneous reactor core and equivalent reactivity depletion with other fuels in CANDU reactors, using only initial, unirradiated fuel compositions.

Heavy water reactors have a number of disadvantages when compared to light water reactors, including the greater production of spent fuel, the cost of the heavy water and the possibility of licensing difficulties due to their positive void coefficient [470]. However, the Enhanced CANDU 6, at low plutonium loading levels, should produce a large quantity of energy per unit mass of plutonium fuel and is a complete proposal for plutonium disposition based on generally very mature technologies. UK CANMOX will be a strong option for NNL when selecting an option for UK plutonium disposition if energy value is an important criterion. Three-component fuels can provide benefits over the proposed UK CANMOX fuel in terms of nuclear materials inventory utilisation, and the use of a thorium region in the fuel may be beneficial in terms of extending fuel lifetimes in the core as the thorium is converted to fissile uranium-233, while providing seed material for a thorium fuel cycle in the UK.

4.7.1 RECOMMENDATION

Of the various fuelling options discussed in this chapter, it is the author's recommendation at this stage that both the Inventory Management and LWR Spent Fuel Management Options be further developed. The rapid disposition of inventory plutonium should be prioritised, and high burnup operation solely using inventory materials for the first 30 years of the EC6 operation cycle will be effective in achieving this. If a suitably high discharge burnup can be achieved and other fuel performance and safety parameters respected, fuel concept 21 with ~3.4% Pu appears to be a very promising fuel option. For the second 30 years of operation, an NUE fuel is suggested based on the use of the remaining ThORP Product Uranium and a small amount of MAGNOX Depleted Uranium. A fleet of four EC units would be required for this. This would allow the use of all inventory plutonium as fuel, all ThORP Product Uranium and ~1500 t of MAGNOX Depleted Uranium. ~1200 t of thorium could also be irradiated in this fuel.

With regards to LWR Spent Fuel Management, it is recommended to further develop fuel concept 17, based on a support ratio of one EC6 unit per two EPR units, operating with ~1.4% plutonium. While fuel burnup is expected to be low compared to the Inventory Management fuels, such a fuel would allow further energy value to be extracted from each unit of LWR fuel, while producing a quantity of partially converted thorium. Whether to implement such a reactor and fuel programme would depend upon the costs and benefits of using fresh uranium fuel in an LWR open fuel cycle versus the costs and benefits of reprocessing spent LWR fuel and using it in an EC6, when selecting nuclear generating capacity options to meet the energy needs of the UK.

4.8 FUTURE WORK

A significant amount of development work remains to be carried out before the most promising three-component fuel options from this screening study may be considered as a feasible option for use in a reactor core.

4.8.1 NEUTRONIC INTERACTIONS IN A HETEROGENEOUS CORE

The neutronic behaviour of the various fuel components with one another and with the other materials within the core must be studied. In particular it is anticipated that the use of multiple fuel materials together may produce complex neutronic interactions that cannot be easily predicted from the homogeneous simulations conducted here. Heterogeneous features of the fuel bundle and core will also have significant impacts which this study cannot foresee. These features have significant impacts on the core, and cannot be ignored, as was discussed in Section 2.9.1.

4.8.2 IMPACT OF IRRADIATION HISTORY ON REACTIVITY AND POWER

The irradiation history impacts on the fuel composition must be established with various levels of burnup, as well as the impact of burnup on fuel

reactivity. The EC6 reactor is refuelled continuously at full power, with several refuelling operations carried out per week according to the power profile and actual burnup of individual channels and bundles in the core. It will be necessary to determine if and how a core composed of multiple three-component fuel bundles can be operated. Linear fuel element power ratings are expected to be a strong limiting factor when determining plutonium loading limits, and thorium conversion may also drive increases in the element power. The neutronic parameters calculated in this work must be validated by a robust calculation. For these purposes a Monte Carlo neutronics simulation is suggested, using a stochastic modelling code such as MNCP [471], or alternatively a set of deterministic codes suitable for pressurised heavy water reactors, such as WIMS-AECL [472] and RFSP [473] or a combination of DRAGON [474] and DONJON [475].

A Monte Carlo neutronic analysis is presented in Chapter 5 of this thesis, in order to determine the behaviour of a heterogeneous fuel bundle with burnup.

4.8.3 FUEL CYCLE INTEGRATION

Additional studies would also need to consider fuel cycle options for such fuels – how they may be manufactured and handled before irradiation and how operators might deal with spent fuel bundles according to their heat generation and radiation field. Dynamic analyses of strategies for how such fuels might fit into the existing nuclear energy systems of the United Kingdom are suggested, using scenario assessment modelling tools such as DANESS [476].

4.9 SUMMARY AND DEVELOPMENT

This work has suggested that there may be feasible EC6 reactor fuel compositions based on a reprocessed plutonium and uranium mixed oxide

fissile driver operating with a thorium oxide fertile region within CANFLEX fuel bundles. The necessary quantities of suitable plutonium and uranic materials to produce these fuels appears to be available in the United Kingdom nuclear materials inventory. Such fuels may also be produced from reprocessed LWR spent fuel, allowing additional energy per unit mass to be extracted from uranium fuel irradiated in UK new build light water reactors.

This work represents a first step in the exploration of these fuel options, and further work is required before such fuels might be deemed to be feasible. In the following chapter, a neutronic simulation is performed to study the transient evolution of reactivity and fuel isotopics with burnup, while dispensing with the homogeneous fuel bundle assumption.

5 THREE-COMPONENT NUCLEAR FUEL SIMULATION IN THE ENHANCED CANDU 6 REACTOR

In this chapter the most promising U-Pu-Th fuel concepts are simulated using a Monte Carlo neutronics package. The reactivity behaviour, element power distribution and isotopic composition are reported as a function of fuel burnup. Scenarios are suggested to incorporate the MOX into the UK fuel cycle.

5.1 INTRODUCTION

In the previous chapter a number of U-Pu-Th mixed oxide fuels were considered for use in the Enhanced CANDU 6 reactor. The calculation methods used were quite limited, considering one neutron energy group in a homogeneous reactor, and only the fuel composition at beginning of life (BOL). In this chapter these issues and others are addressed through a computational simulation. The aim was to determine the following:

- The rate of reactivity depletion with burnup, in particular the average burnup at which fuel should be discharged from the core. This allows the refuelling rate and thus the annual and lifetime fuel requirements to be determined.
- The relative power distribution in each ring of the fuel bundle, in order to better understand how the element power peaking is likely to vary over the irradiation history. Ideally all fuel elements would generate equal power, as this allows the average bundle power to be

higher without breaking power limits on individual elements, but this is not realistic in a real, dynamic core with multiple fuel materials, a non-flat power profile, and on-power refuelling. Thus, it is important to understand the power peaking across the bundle.

- The evolving isotopic composition of the plutonium, uranium, thorium and dysprosium in UK CANMOX fuel and three-component fuel concepts 17 (LWR used fuel management), and 19 and 21 (existing U/Pu inventory management). It is important to understand the rate of plutonium fission and conversion, and the plutonium isotopic vector in the final product. Likewise, the production and fission of ^{232}U and ^{233}U need to be analysed. This information will be a useful starting point in any future work on spent fuel handling and waste disposal.

From the information above, the materials flow analyses from Chapter 4 were further developed, and suggested fuel cycle options were analysed from the perspective of uranium and plutonium resource availability.

5.1.1 NUCLEAR REACTOR CORE BEHAVIOUR SIMULATION

The behaviour of operating nuclear reactors can be broken down into two major aspects: thermal-hydraulic behaviour, concerning heat transfer, temperature distribution and fluid dynamics, and neutronic behaviour, concerning criticality, power production, and fuel composition evolution with burnup. These two aspects are very much interlinked.

The design of nuclear energy systems makes great use of numerical simulation in order to predict reactor behaviour. A variety of simulation codes have been produced which may be used for this purpose. Thermal-hydraulic behaviour may be modelled by general computational fluid dynamics codes such as ANSYS Fluent, OpenFOAM, STAR-CD or Comsol CFD, although a large number of other codes are available, both commercial and open source.

Neutronic behaviour may be modelled deterministically or probabilistically. Probabilistic models use the Monte Carlo method, tracking a population of neutrons within a modelled reactor geometry and using statistical techniques to generalise the behaviour of this neutron population to the whole modelled system. Some examples of stochastic Monte Carlo codes are MCNP, KENO, TRIPOLI, SERPENT and OpenMC. Deterministic models predict the behaviour of the system by solving a discretised form of the neutron transport equation, often based on a reduced set of neutron interaction data, known as group constants. Some examples of deterministic codes are DRAGON/DONJON, PANTHER and APOLLO.

In the modelling of CANDU reactors commonly used deterministic codes are combinations of WIMS-AECL [472] and RFSP [473] or DRAGON [474] and DONJON [475], as these codes were developed with such reactors in mind, although their capabilities are quite general, particularly those of DRAGON 4.0. Probabilistic models have been studied in the literature, but no particular code stands out for use with CANDU/PHWR reactors, as the Monte Carlo method is not reactor specific. In this work a Monte Carlo lattice physics code was used to simulate the behaviour of three-component fuels, as the Monte Carlo method does not depend on the availability of suitable neutron group constant data, which was not readily available for the proposed fuels. Neutron group constants are used to reduce the large amount of neutron interaction spectra data into a small number (usually two or four) or energy groups, with averaged cross sections for all neutrons whose energies fall within a given energy range.

5.1.2 THE MONTE CARLO METHOD

The basis of the Monte Carlo technique is that the behaviour of a system may be determined by studying a large number of simple elements within the system, and then using statistics to generalise their behaviour in order to predict whole system behaviour. In neutronics, the simple elements are

individual neutrons. A reactor geometry is defined, and material properties applied to each element of the geometry. A population of neutrons is then randomly distributed over the geometry, the fate of each neutron is calculated, and a new generation of neutrons is generated. This process is repeated over a number of cycles, converging to the equilibrium state of the core, given the geometry and materials used.

The greater the population of neutrons and number of iteration cycles for a given reactor geometry, the more accurate the converged solution. However, both of these parameters are proportional to the computational time required, and increasing the number of neutrons also increases the computer memory requirements. It is important that the number of neutrons and cycles run is sufficient to give an acceptably accurate solution, but not so high that calculation time and resources are used excessively.

5.1.3 FUEL AND CORE PARAMETERS CALCULATED

5.1.3.1 MULTIPLICATION FACTOR AND CONVERSION FACTOR EVOLUTION

The infinite multiplication factor k_{inf} given by each fuel composition will evolve with fuel burnup, tending towards zero as burnup increases and the fissile components of the fuel are depleted. The depletion rate is related to the fuel conversion ratio C_r . The addition of thorium to a fuel may allow thermal fuel breeding, a condition which would be characterised by the level of ^{233}U reaching equilibrium and thus allowing a critical chain reaction to be maintained without the need for the addition of a fissile driver. At this point the depletion rate would be tied to the mass of thorium in the core, and not the mass of fissile driver.

The evolution of multiplication factor and conversion ratio with fuel irradiation were crucial parameters to study, as they indicate the amount of time the fuel may spend in the reactor and whether breeding is taking place.

Many operational parameters, including refuelling rate, spent fuel properties and required soluble absorber levels in the calandria, are tied to k_{inf} and C_r .

5.1.3.2 FUEL COMPOSITION EVOLUTION

The evolution of the fuel isotopic and chemical composition with burnup is vital information for the three-component fuel, as the main aim of the UK CANMOX programme is the irradiation of inventory plutonium. The ideal used fuel would contain no fissile material, thus making it useless for nuclear weapons fabrication. However, this is not realistic in a critical reactor system, and thus instead it is aimed to reduce the amount of fissile ^{239}Pu and ^{241}Pu , while increasing the isotopic fraction of the even-numbered, neutron capturing isotopes of plutonium.

In the three-component fuels it is also important to consider the conversion of thorium to ^{233}U , as this will provide additional fissile material as the fissile isotopes in the driver MOX are burnt out. The production of ^{232}U should also be considered, as this will reduce k_{eff} while increasing the decay heat and activity of the spent fuel.

5.1.3.3 POWER DISTRIBUTION OVER FUEL BUNDLE

The distribution of power across the elements of the fuel bundle is an important parameter to consider. In UK CANMOX fuel dysprosium is used as a burnable neutron absorber in the inner fuel elements in order to flatten the flux profile over the fuel bundle. Without burnable absorber the burnup in the intermediate and outer fuel elements is very different, and this was found to give an unacceptable plutonium product [68].

In addition the permitted power in a given fuel element and fuel bundle is limited. In this work the absolute power generated by individual elements was not determined; instead a power distribution across the elements of the bundle was calculated, normalised to the core average power density. The

power shape could be compared between fuels, but actual fuel element powers were not determined and as such could not be compared to the reactor power limits. This was a necessary limitation due to the 2D infinite lattice approach used, as described in Section 5.2.2.

5.1.3.4 VOID COEFFICIENT OF REACTIVITY

While CANDU reactors are both cooled and moderated by heavy water, the segregation of the coolant from the calandria means that the pressure tube may be voided while the calandria remains liquid. While safety systems are in place to prevent this, the effect of pressure drops in the coolant must be considered. As was shown in the literature review, CANDU reactors are prone to having positive coolant void reactivity, and this is worsened by the increased plutonium fraction, due to the increase in ^{239}Pu fission cross section and reduction in ^{238}U capture cross section in the epithermal neutron energy range [363, 380]. Most of the moderation comes from the calandria. The coolant volume is 3.4% of the total heavy water volume in the core, meaning that fuel remains well moderated even if coolant is completely lost. Coolant voiding is a highly coupled neutronic and thermal-hydraulic effect, and detailed study of the phenomenon is beyond the scope of this work. However, coolant void reactivity is a particular concern in heavy water reactors, and as such a simplified analysis is undertaken.

5.2 METHODOLOGY

In this work the selected Monte Carlo code for the computational experiments was Serpent [477]. The latest version of the code at the time of writing was used, being version 2.1.27.

5.2.1 THE SERPENT NEUTRONICS CODE

Serpent began development in 2004 in Finland, originally being developed as a simplified Monte Carlo code specifically for reactor lattice physics

modelling. An alternative neutron tracking routine and a reduced neutron energy grid are used to decrease the computational effort required compared to older Monte Carlo neutronics packages, particularly MCNP. The code uses standard format neutron interaction data libraries, including ENDF-B [455] and JEFF [454]. Serpent also includes an integrated burnup calculation routine. A description of Serpent's development and methodology is outlined in a recent paper [478], and in the user's manual [479].

The fact that Serpent was constructed for the purpose of reactor lattice physics simulation gives it a number of advantages over other Monte Carlo codes, not least the optimisation for minimal computational time. The inbuilt burnup routine means that no coupling to external codes is necessary in order to solve the Bateman equations, thus greatly simplifying operation and optimising the calculation.

A comparison of SERPENT with WIMS-AECL in PHWRs found good agreement for the calculation of core reactivity as a function of burnup for ^{233}U -Th fuels, and a slightly worse agreement for Pu-Th fuels. Serpent was found to underestimate achievable discharge burnup by $\sim 10\%$, and also to underestimate reactivity compared to WIMS-AECL. Researchers from Canadian Nuclear Laboratories have stated that the agreement between the two packages is sufficiently close to allow survey comparisons between different fuel and core types [379].

5.2.2 GEOMETRY SIMPLIFICATION

Simulation of complete core behaviour, taking account of coupled neutronic and thermal-hydraulic behaviour over the core life, is extremely computationally expensive, and could not be reasonably carried out with the resources available. It was instead necessary to carry out a reduced analysis at the fuel channel level.

The EC6 core comprises a square lattice of 380 fuel channels within the calandria. Analysis of a single channel can be carried out with periodic boundary conditions at the half-lattice pitch distances such that neutrons leaving the simulated geometry are reintroduced at the opposite side of the geometry, effectively simulating an infinite lattice of equivalent fuel channels. In real CANDU cores there is a flux and power distribution across the calandria, reducing away from the core centre, and the power distribution between adjacent bundles may be large given the different refuelling rates of each channel. In addition, CANDU reactors are refuelled from both sides, with adjacent channels being refuelled in opposite directions in order to give a balanced axial flux profile, meaning that adjacent fuel channels will have very different fuel compositions. Simulation of the channel at a range of power densities can mimic some of these effects.

The geometry may also be simplified in the axial direction, reducing to a two-dimensional geometry. This effectively simulates a core of infinite length with equivalent fuel at all axial points, as if refuelling of all channels were continuous at the same rate and in the same direction. Real CANDU cores have neutron leakage from their end faces, and have complex axial core and channel power profiles due to different burnup levels in each bundle and channel. Again, simulation of several power densities can provide some information on the effect of localised power variation.

This work will simulate a 2D infinite lattice. The geometry used is pictured in Figure 5.1, as plotted by Serpent. The geometry was set up as a square cell of heavy water, with width and height equal to the core lattice pitch. Within this were placed the calandria tube and pressure tube, with carbon dioxide gas between the two tubes. Fuel elements were arranged within the pressure tube according to their placement and diameters in the CANDU 37-element or CANFLEX 43-element fuel bundles. Fuel elements consisted of fuel pellets of the appropriate diameters surrounded by the fuel sheath. The

boundary conditions at the outer edge of the moderator region were set to periodic.

A correction to the calculated infinite multiplication factor may be made to account for neutron leakage by reducing its value by a factor of 0.0625, taken as an average of literature values [380, 382]. This factor is the combined fraction of all neutrons which escape from the core. As such the effective multiplication factor is assumed to be given by Equation (5.1).

$$k_{inf} = \frac{k_{eff}}{P_F P_T} = (1.0625)k_{eff} \quad (5.1)$$

Where k_{inf} is the infinite multiplication factor over the core,

k_{eff} is the infinite multiplication factor for the 2D, infinite lattice,

P_F is the probability of non-leakage for fast neutrons, and

P_T is the probability of non-leakage for thermal neutrons.

Some small or inconsistent geometric features were neglected, for example the small gap between the fuel pellets and sheath at BOL, and structural and heat transfer features of the fuel bundles. The effect of reactivity control devices, including control rods and soluble chemical shim, was not considered in this work.

5.2.3 NEUTRON POPULATION AND ITERATION NUMBER INDEPENDENCE

As was discussed in Section 5.1.2, it is important to ensure that a sufficient number of neutrons and active cycles are run to give sufficient accuracy. In order to avoid running simulations which are unnecessarily computationally expensive it is important to optimise the number of neutrons and cycles.

A series of BOL simulations were run using natural uranium oxide in the CANFLEX bundle. Simulations were performed with either a fixed number of neutrons and a variable number of active cycles, or a fixed number of a

cycles and variable neutron population. The results of this analysis are presented in Figure 5.2.

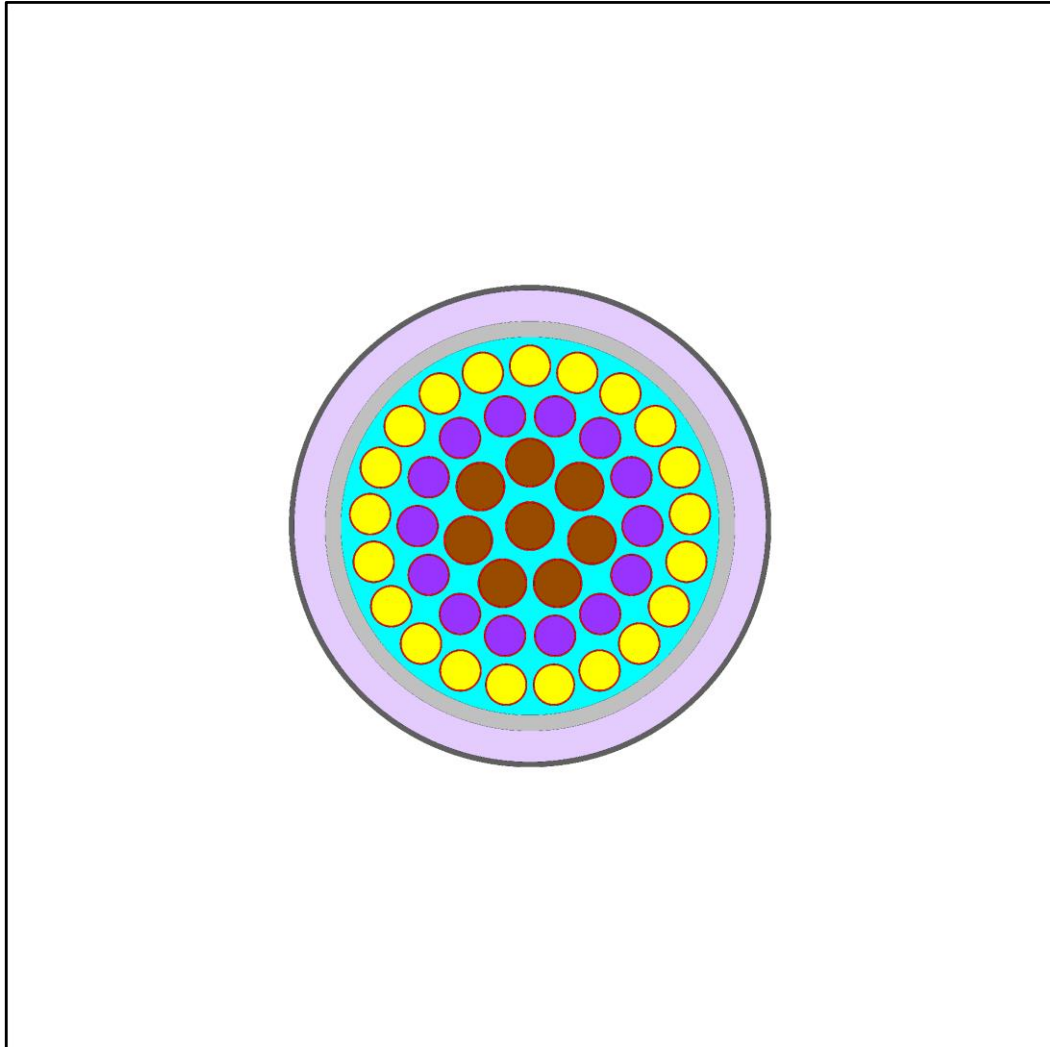


FIGURE 5.1 – FUEL CHANNEL GEOMETRY USED IN COMPUTATIONAL EXPERIMENTS. CORE IS CONSIDERED TO BE AN INFINITE LATTICE OF INFINITELY LONG FUEL CHANNELS, CONTAINING EQUIVALENT FUEL THROUGHOUT. FOR SCALE, CALANDRIA TUBE OUTER DIAMETER IS 66 mm.

It can be seen that with increasing neutron population and number of cycles, the computational errors are reduced and the reported value of k_{eff} converges to a stable result. However, the time required to perform the simulation increases. When fuel burnup is also calculated the number of cycles and hence time required is multiplied by the number of burnup steps

considered. Burnup also increases the amount of memory required for the simulation in line with the number of depletion zones considered.

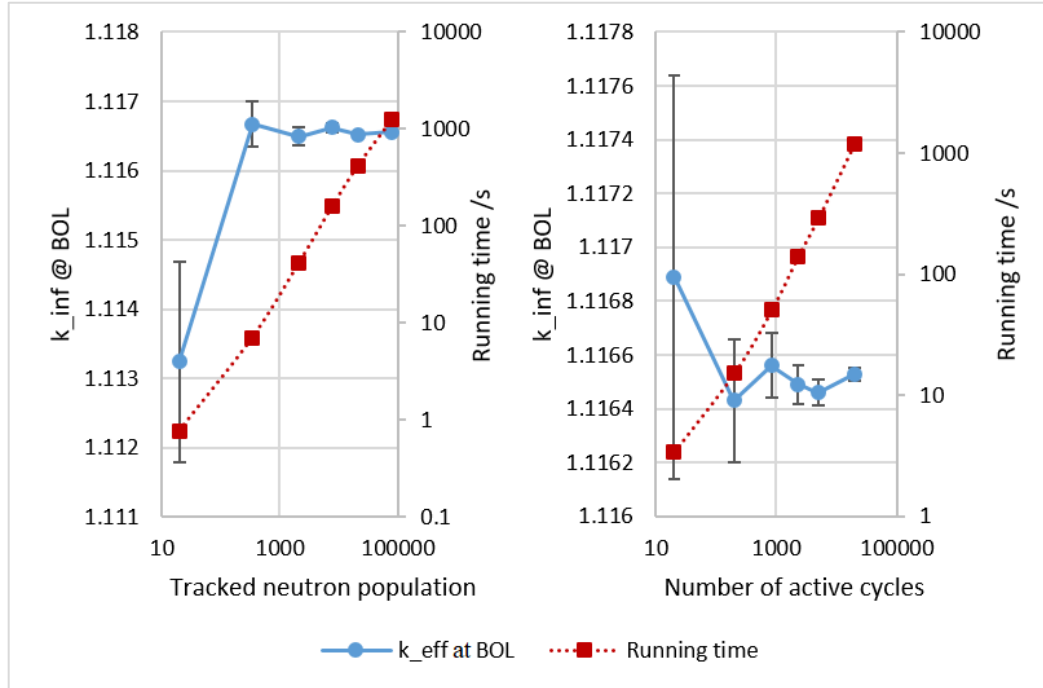


FIGURE 5.2 – EFFECT OF NEUTRON POPULATION SIZE (LEFT) AND NUMBER OF CYCLES (RIGHT) ON EFFECTIVE MULTIPLICATION FACTOR AND CALCULATION RUNNING TIME.

In order to minimise computational requirements while retaining sufficient accuracy it was decided that for the experimental simulations the neutron population would be fixed as 2000, and the number of active cycles would be set to 500. The number of inactive cycles, used for initial convergence of the solution, was set to 20, and this was found to allow solution convergence during the active cycles. In any case, given that the geometry is neutronicly small and simple the risk of false convergence should be low.

5.2.4 FUEL CONCEPTS ANALYSED

A number of fuel compositions were analysed, including current CANDU natural uranium oxide fuels, UK CANMOX fuel, and U-Pu-Th fuel concepts 17, 19 and 21 from Chapter 4.

5.2.4.1 NATURAL URANIUM REFERENCE CASES

Natural uranium oxide fuel was tested in both the operating 37-element fuel bundle and the planned CANFLEX bundle. The discharge burnup of the 37-element fuel bundle is ~ 7.5 MWd/kgHM, and it is anticipated that this will be similar for the 43-element bundle, despite the 5% reduction in fuel mass, as the greater subdivision of the fuel allows a 5-8% increase in fuel element power [68, 442]. The value of k_{inf} at this burnup was taken to represent the reference infinite multiplication factor of discharged CANDU fuel, and was used in the study of other fuel concepts to suggest the burnup at which they would be discharged from the core.

5.2.4.2 UK CANMOX FUEL

The UK CANMOX fuel was tested in the CANFLEX fuel bundle with a range of dysprosium burnable absorber loadings in the inner eight fuel elements. The proposed burnup of the fuel has been suggested to be anywhere between 14 and 20 MWd/kgHM, which is understandable given the variability in plutonium composition as different fuel bundles will likely achieve differing levels of discharge burnup. In this work the uranium and plutonium isotopic compositions were taken from Table 4.4 and Table 4.5 respectively, and several dysprosium fractions were tested to determine the burnup at which k_{inf} fell below the value found for natural uranium fuel. The target discharge burnup was set to the average value of 18 MWd/kgHM.

5.2.4.3 THREE-COMPONENT FUEL CONCEPTS

Three of the three-component fuel concepts from Chapter 4 were taken for further testing in this chapter. These were fuel concept 19 (inventory plutonium, ThORP product uranium, natural thorium), fuel concept 21 (inventory plutonium, mixed ThORP product uranium, MAGNOX depleted uranium, natural thorium) and fuel concept 17 (EPR reprocessed plutonium and uranium, natural thorium). Fuel concepts 17 and 19 were tested with a range of plutonium compositions, and fuel concept 21 was tested with a

fixed plutonium fraction and a range of TPU/MDU blends. As in UK CANMOX fuel two plutonium fractions were used about an average value, with the intermediate ring fraction double the outer ring fraction, as shown in Equation (5.2).

$$Pu\%_{average} = \frac{7}{5} Pu\%_{outer} = \frac{7}{10} Pu\%_{intermediate} \quad (5.2)$$

Where $Pu\%_{average}$ is the average Pu fraction in the MOX fuel,

$Pu\%_{outer}$ is the Pu fraction in the bundle outer ring, and

$Pu\%_{intermediate}$ is the Pu fraction in the bundle intermediate ring.

5.2.5 ANALYSIS CASE SET-UP

The analyses in Serpent were run using almost identical conditions in all cases, with alterations made for the specific cases only as required.

The density of materials was set on the mass basis, with fuel pellet densities assumed to be 95% of their theoretical values [480]. The densities of mixed oxide fuels were calculated by linear interpolation of the densities of their metal oxide components. An annulus gas pressure of 1 bar was used, with the temperature of the gas assumed to be 150°C. Coolant and moderator densities were set according to their reference temperatures [438, 460]. Dysprosium containing fuel elements were divided into ten annular depletion zones for the purposes of burnup calculations, in line with the recommendation given in the Serpent user's manual, in order to account for the high capture cross section of dysprosium leading to differing radial depletion in the inner fuel elements of UK CANMOX fuel.

The JEFF-3.1.1 nuclear interaction data library [454] was used as the standard library for all experiments. The power density in the core was set as 26 kW/kgHM, calculated from a thermal power of 2084 MWt and the calculated mass of uranium, plutonium and thorium in the core at BOL.

An example input case file for 3% Pu in fuel concept 19 is presented in full in Appendix C.

5.2.6 VOID COEFFICIENT OF REACTIVITY

As was stated in Section 5.1.3.4, a full thermal-hydraulic study into void reactivity is beyond the scope of this initial computational experiment. Instead a simplified study is carried out where the coolant is modelled as homogeneous with reduced density representing voiding. This should be acceptable given neutrons have a large mean free path in the coolant. The coolant void reactivity may be calculated using Equation (5.3) [379].

$$CVR = \frac{k_{inf-void} - k_{inf-cool}}{k_{inf-void} \times k_{inf-cool}} \quad (5.3)$$

Where CVR is the coolant void reactivity,
 $k_{inf-void}$ is the infinite multiplication factor in the 99% voided condition, and
 $k_{inf-cool}$ is the infinite multiplication factor in the unvoided condition.

5.3 NEUTRONIC SIMULATION RESULTS

Results are presented here by fuel type. In general error bars are not shown in the plots of k_{inf} , but were of the order of 10^{-4} .

5.3.1 NATURAL URANIUM FUELS

The evolution of the infinite neutron multiplication factor and conversion ratio with fuel burnup for natural uranium oxide in each bundle is presented in Figure 5.3. It can be seen that at the discharge burnup of 7.5 MWd/kgHM the infinite multiplication factors were $k_{inf} = 0.989$ for the 37-element bundle and $k_{inf} = 0.983$ for the CANFLEX bundle. A full core study will be required to determine actual discharge burnups, as higher BOL k_{inf} will

likely allow lower discharge k_{inf} . However, a value of 0.986 will be used to define an assumed discharge burnup for fuels in this study, as the average of the values found for the natural uranium fuels.

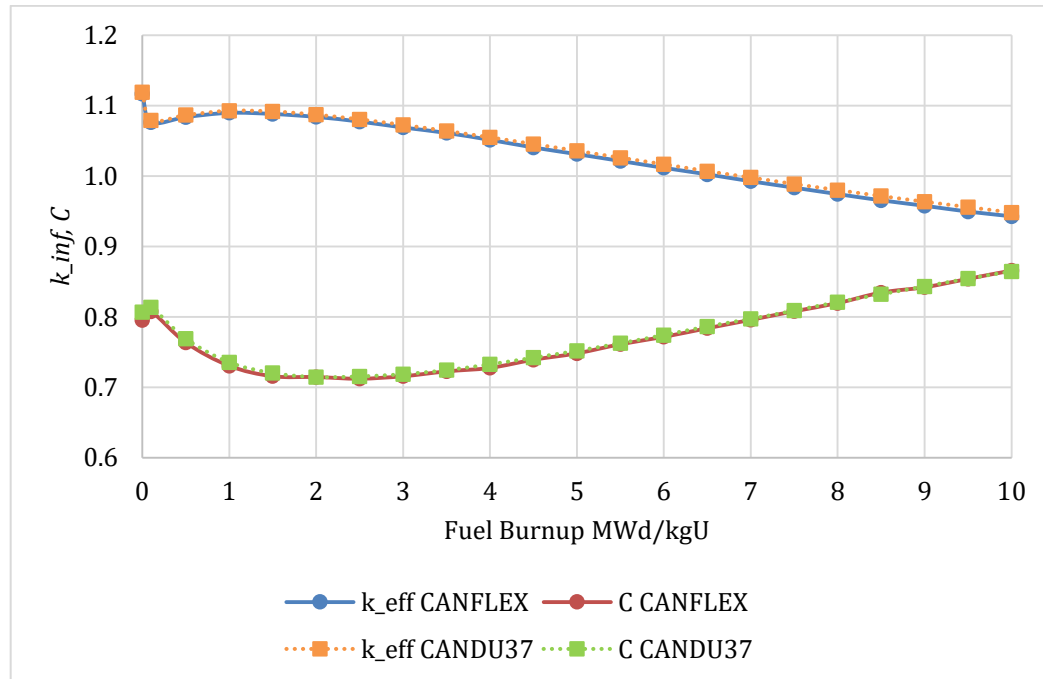


FIGURE 5.3 – EVOLUTION OF INFINITE MULTIPLICATION FACTOR k_{inf} AND CONVERSION RATIO C WITH NATURAL URANIUM OXIDE FUEL IN THE ENHANCED CANDU 6 REACTOR.

The initial conversion ratio of 0.8 is in agreement with the value reported in the literature [20]. The difference in k_{inf} and C_r between the 37-element and CANFLEX bundles was minimal, although it was found to be greater than the reported numerical uncertainty.

The power profiles across the bundles was calculated, and these are presented in Figure 5.4. It can be seen that the shape of the power profiles does not alter significantly over the irradiation cycle. As fuel burnup increases the power peaking increases slightly in the outer pins relative to the BOL, while at discharge the power peaking factors are reduced slightly compared to BOL. The overall power peaking factors in the CANFLEX bundle are slightly reduced compared to the 37-element bundle, and the overall profile is flatter. The reduced power in the intermediate ring compared to its

neighbours is due to the use of different pin diameters. Similar power profiles are reported in the literature for 37-element fuel bundles [481] and for CANFLEX bundles [482].

The effect of coolant voiding was studied for natural uranium fuel in CANMOX fuel bundles. The results are plotted in Figure 5.5. It was found that as the coolant density is reduced there is an increase of 1.6% in k_{inf} , with the maximum increase found between 0% and 99% voiding. CVR was calculated to be $+12.5 \pm 0.3$ mk (1 mk = $0.001 \Delta k_{inf}/k_{inf}$). This was expected, as CANDU reactors are well known to exhibit slight positive void coefficients [20, 470].

The depletion of some key isotopes in the CANFLEX bundle over the burnup cycle is presented in Figure 5.6. It can be seen that 60% of the initial ^{235}U is converted or undergoes fission. Additionally, 0.5% of the initial ^{238}U is converted to plutonium.

5.3.2 UK CANMOX FUEL

UK CANMOX fuels were studied with a range of dysprosium fractions in the inner eight fuel elements, from 0% to 6% Dy. As has been discussed, two plutonium fractions are used in the outer two rings in order to flatten the flux profile across the fuel bundle.

The variation in k_{inf} and C for each dysprosium fraction with burnup is shown in Figure 5.7. The values of burnup at which $k_{inf} = 0.986$ for each dysprosium fraction are given in Table 5.1. It can be seen that 2.5% dysprosium loading in the inner fuel elements gave a burnup of 18.25 MWd/kgHM, which was close to the target discharge burnup. As such 2.5% dysprosium loading in UK CANMOX fuel was taken as the reference value.

Some power profiles across the bundle are presented in Figure 5.8. Profiles are given for 2.5% Dy, as well as 0% and 10% Dy for comparison.

THE PREPARATION AND APPLICATION OF THORIUM-BASED NUCLEAR FUELS

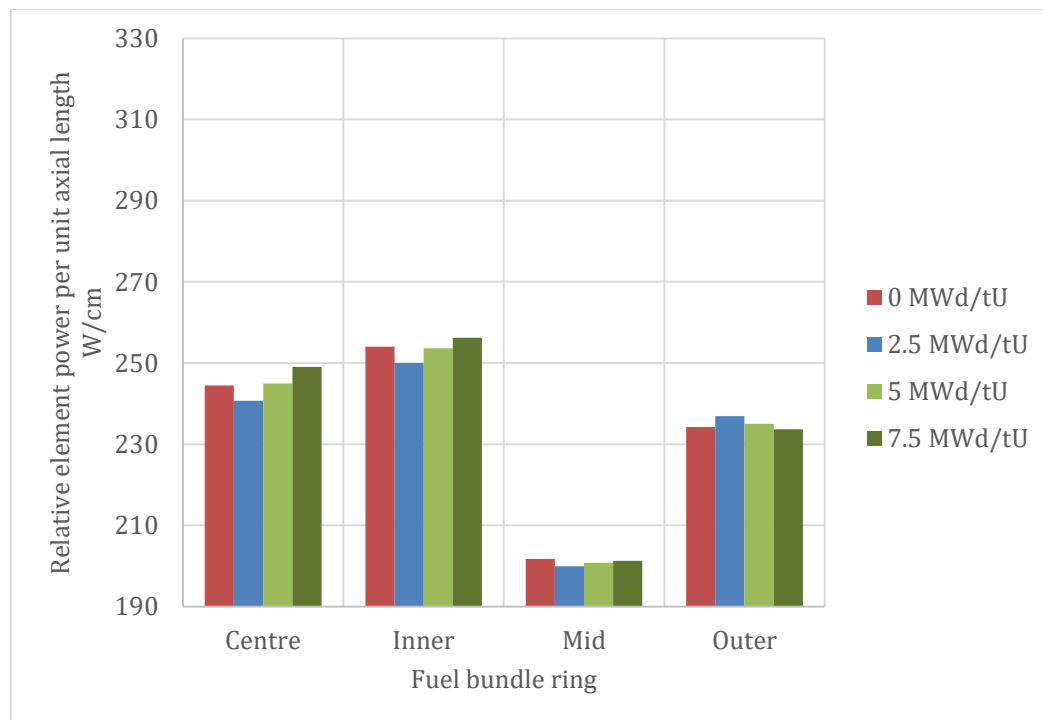
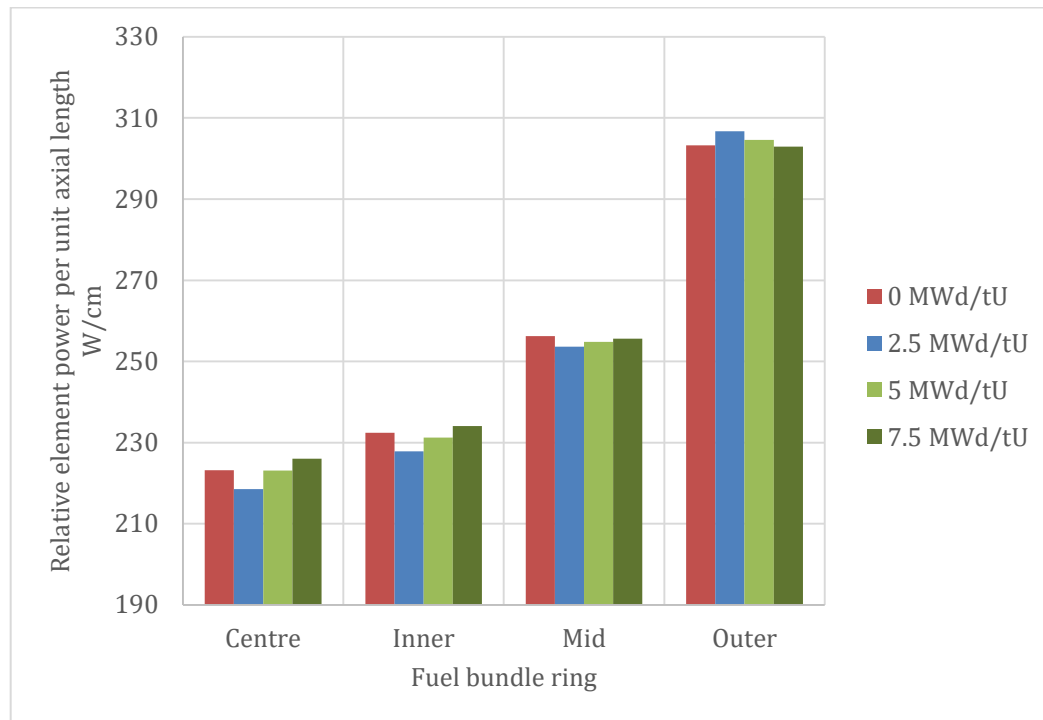


FIGURE 5.4 – EVOLUTION OF NORMALISED POWER PROFILE IN NATURAL URANIUM FUEL IN 37-ELEMENT BUNDLE ELEMENTS (TOP) AND CANFLEX BUNDLE ELEMENTS (BOTTOM) WITH BURNUP. VALUES AVERAGED OVER ALL ELEMENTS IN EACH RING, NORMALISED RELATIVE TO AVERAGE POWER OF A BUNDLE IN THE CORE.

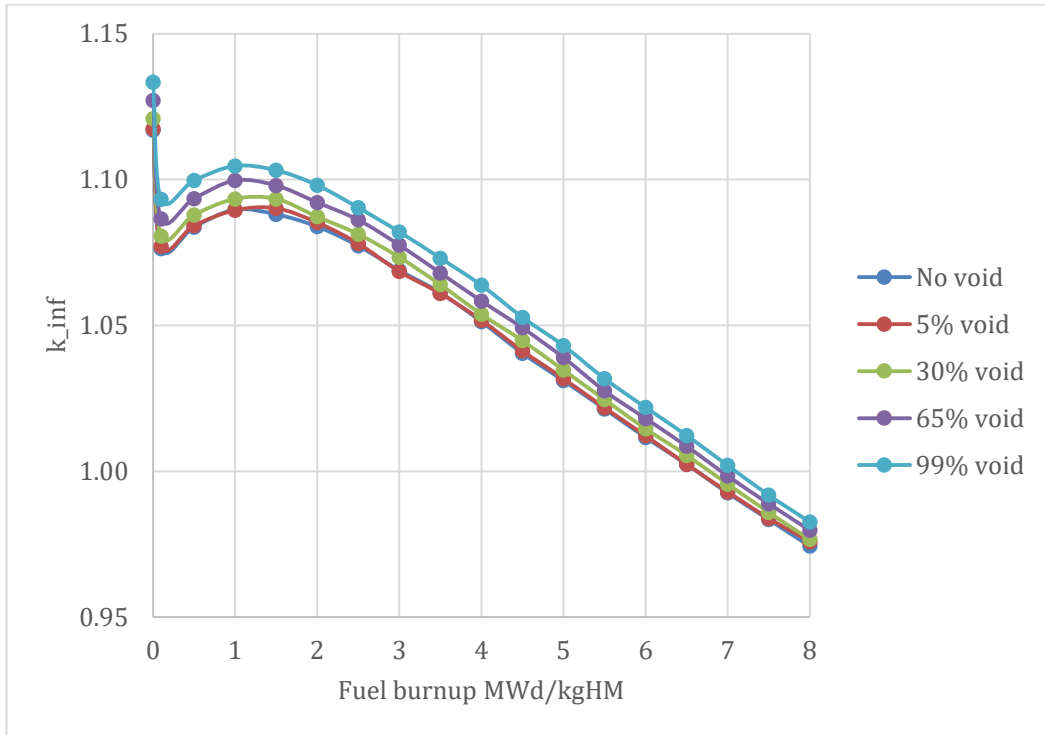


FIGURE 5.5 – EFFECT OF REDUCED COOLANT DENSITY ON k_{inf} FOR NATURAL URANIUM FUEL IN THE CANFLEX FUEL BUNDLE.

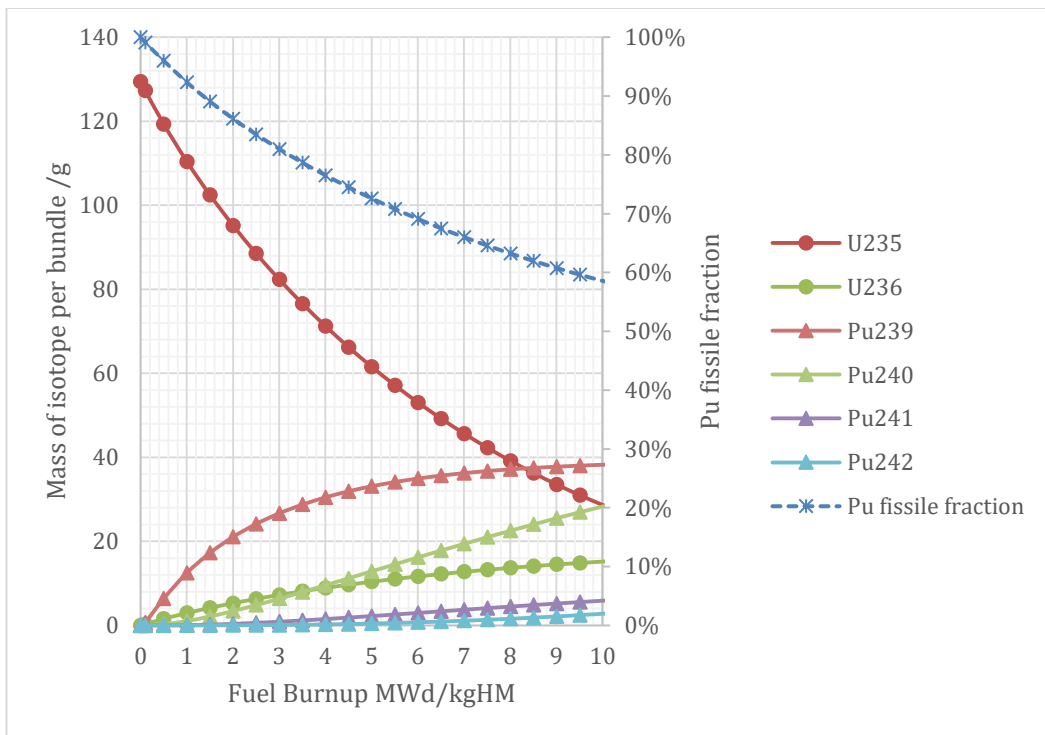


FIGURE 5.6 – ISOTOPIC DENSITY OF SELECTED U AND Pu ISOTOPES IN FUEL BUNDLE AS A FUNCTION OF BURNUP FOR NATURAL URANIUM FUEL IN THE CANFLEX BUNDLE.

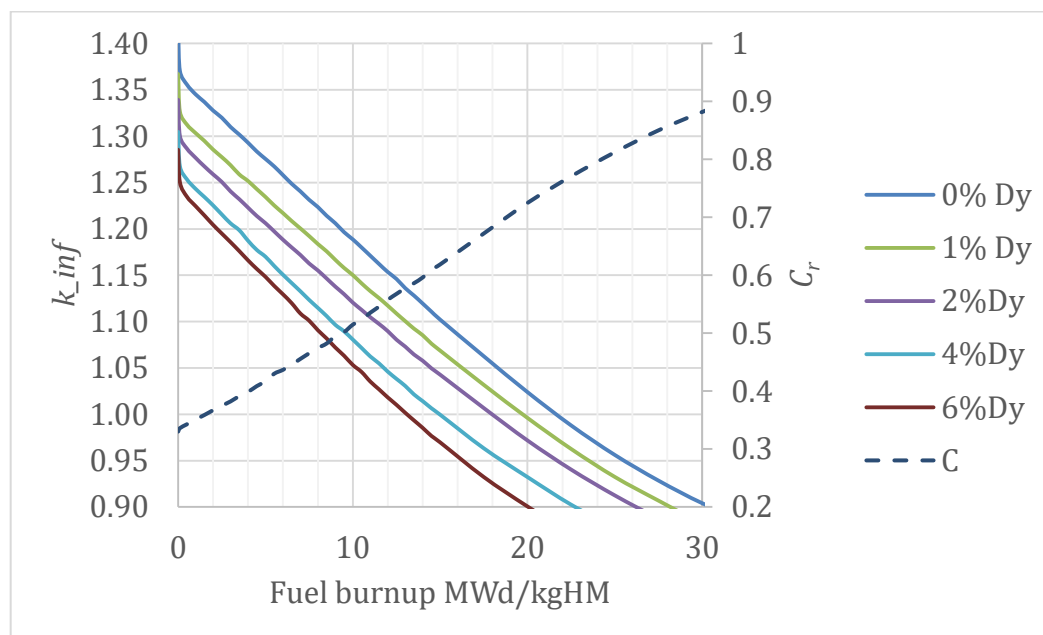


FIGURE 5.7 – EVOLUTION OF k_{inf} WITH BURNUP FOR UK CANMOX FUELS WITH DIFFERENT DYSPROSIUM FRACTIONS. ALSO SHOWN IS THE CONVERSION RATIO, WHICH WAS FOUND TO BE ALMOST IDENTICAL FOR ALL DYSPROSIUM FRACTIONS.

TABLE 5.1 – BURNUP AT WHICH $k_{inf} = 0.986$, THE AVERAGE VALUE AT WHICH NATURAL URANIUM FUELS ARE DISCHARGED FROM CANDU 6 REACTORS.

Dy ATOMIC FRACTION IN INNER FUEL ELEMENTS	BURNUP AT WHICH $k_{inf} = 0.986$ /MWd.kgHM ⁻¹
0.0%	22.75
1.0%	20.75
2.0%	19.00
2.5%	18.25
3.0%	17.25
4.0%	16.00
5.0%	14.75
6.0%	14.00

For the 2.5% Dy fuel, the masses of key isotopes of interest as a function of burnup are given in Figure 5.9. It can be seen that the plutonium isotopic composition is altered significantly, with the overall fissile fraction being

reduced from 74% to ~41%. Of the total plutonium mass loaded, 35.6% is consumed. This performance sets the benchmark against which three-component fuels with thorium must be compared. Of the initially loaded mass of dysprosium-160, -161 and -164 isotopes, ~60% is consumed.

As with natural uranium fuel, coolant voiding leads to a uniform increase in k_{inf} at all burnup levels. The effect of coolant voiding at 1 MWd/kgHM in both natural uranium and UK CANMOX fuels is presented in Figure 5.10. It can be seen that in UK CANMOX fuel 5% voiding (coolant at 95% of reference density) gives rise to a large increase in reactivity. However, the additional increase in reactivity at higher void fractions is not as great. CVR for the 2.5% Dy CANMOX fuel was calculated to be $+9.7 \pm 0.3$ mk, slightly lower than in natural uranium fuel.

5.3.3 PLUTONIUM LOADING IN THREE-COMPONENT FUEL

The effect of varying the plutonium fraction in fuel concept 19 (inventory Pu, TPU, Th) was studied to determine the evolution of k_{inf} and C with fuel burnup. The results are presented in Figure 5.11. It can be seen that at 0% Pu (TPU seed, Th blanket), a critical chain reaction cannot be sustained. Increasing the plutonium fraction increases the initial k_{inf} and reduces the reactivity depletion rate, allowing greater discharge burnups to be achieved. As burnup increases so does the conversion ratio, reaching 0.70-0.83 at the discharge burnup for each fuel.

THE PREPARATION AND APPLICATION OF THORIUM-BASED NUCLEAR FUELS

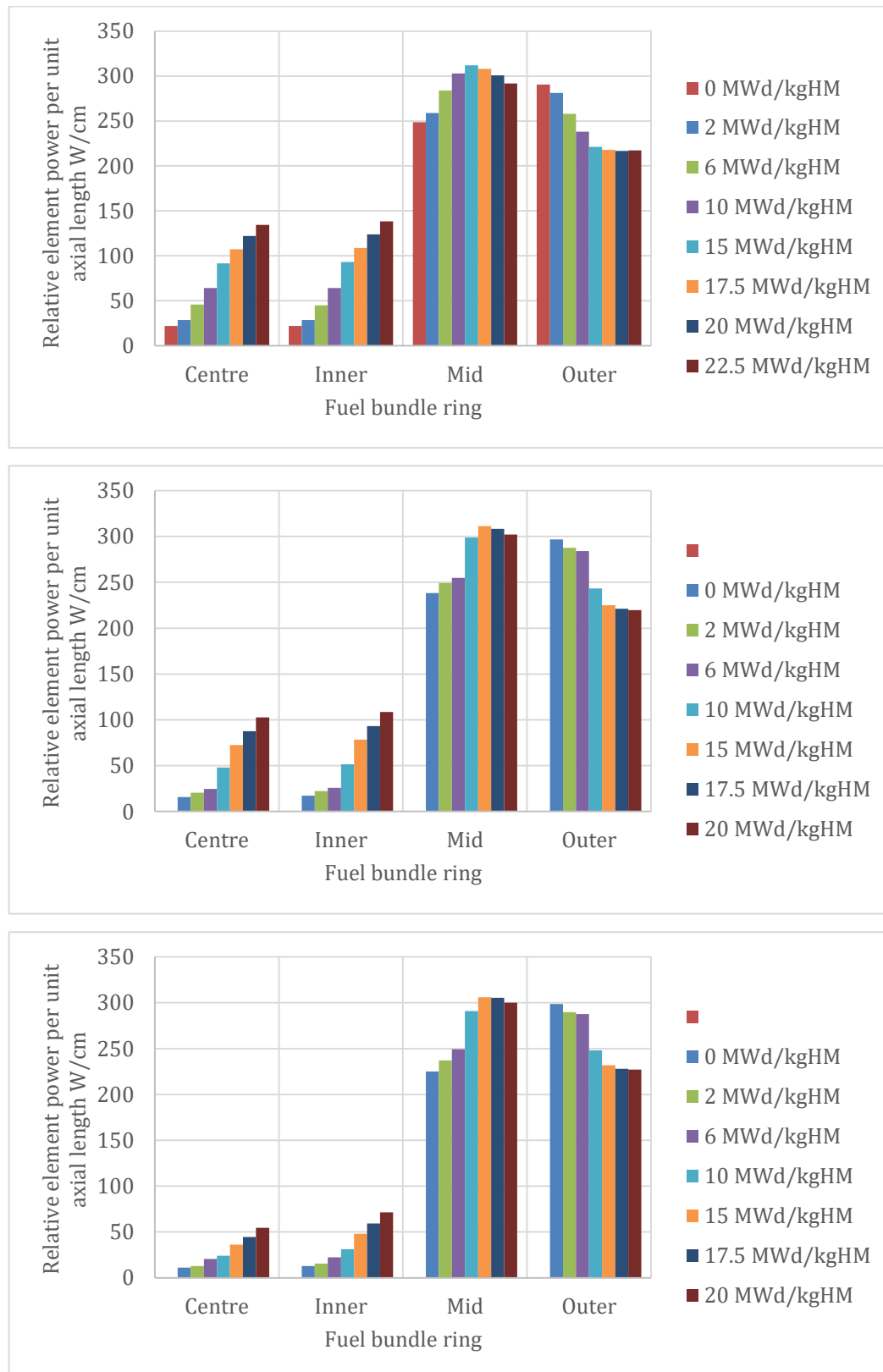


FIGURE 5.8 – POWER PROFILES ACROSS THE UK CANMOX FUEL ELEMENTS AT 0%Dy (TOP), 2.5%Dy (MIDDLE) AND 10%Dy (BOTTOM). POWER DENSITY SET TO 25.8 kW/kgHM.

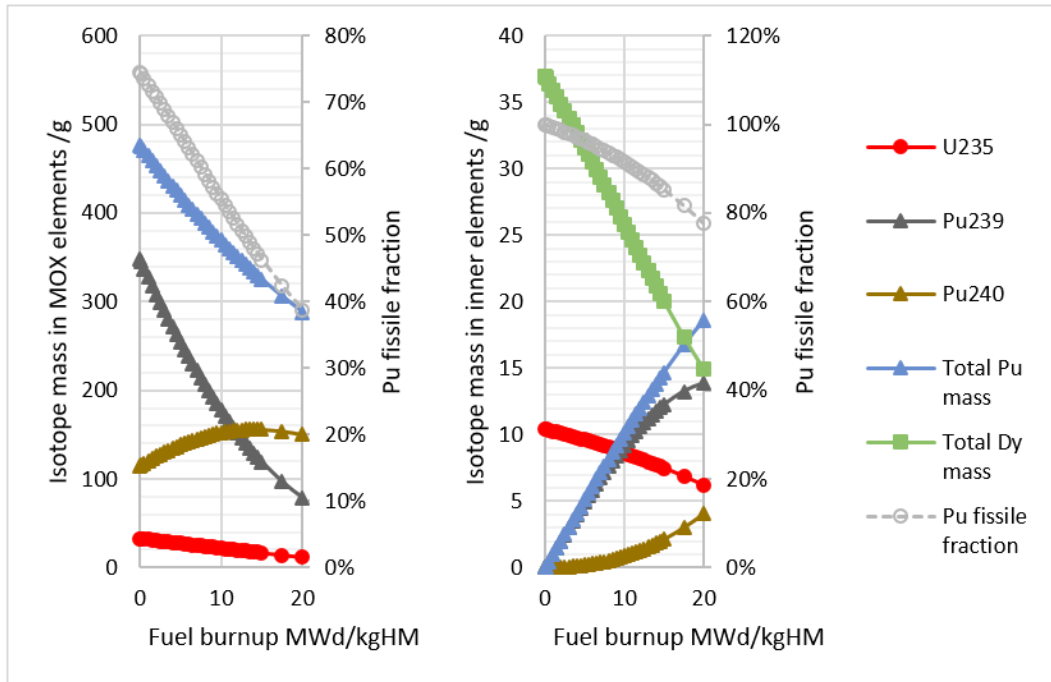


FIGURE 5.9 – EVOLUTION OF PLUTONIUM ISOTOPIC VECTOR, CONSUMPTION OF ^{235}U , AND DEPLETION OF KEY DYSPROSIUM ISOTOPES IN UK CANMOX BUNDLE WITH 2.5% DYSPROSIUM LOADING. LEFT: OUTER AND INTERMEDIATE RINGS WITH MOX. RIGHT: INNER RING AND CENTRE ELEMENTS WITH DYSPROSIUM AND DEPLETED URANIUM.

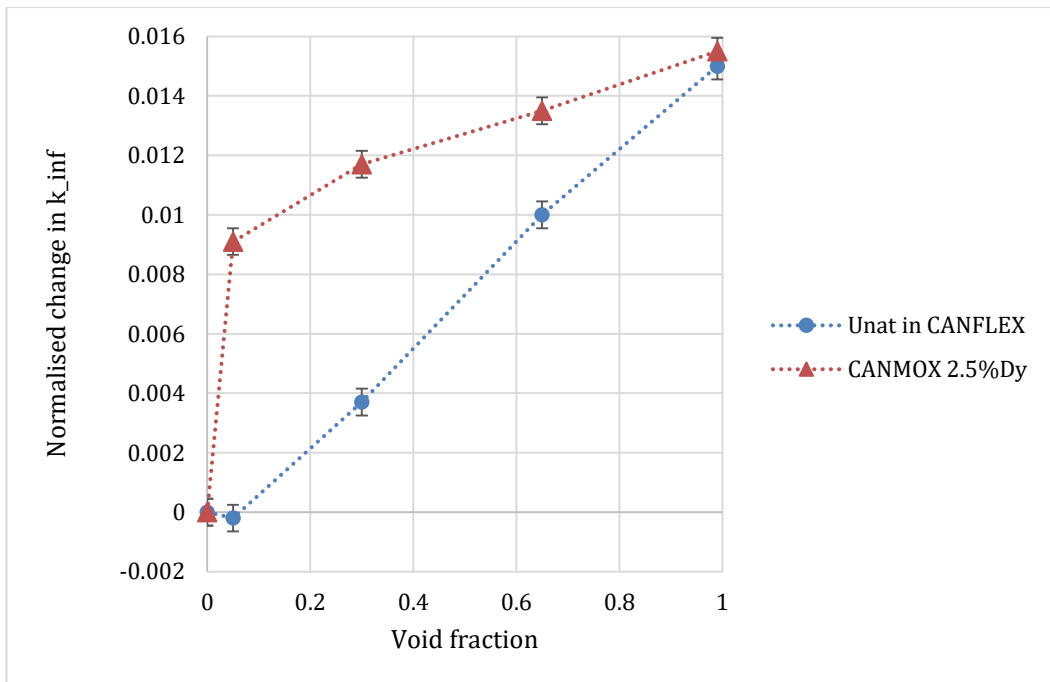


FIGURE 5.10 – NORMALISED CHANGE IN k_{inf} AT 1 MWd/kgHM UK CANMOX FUEL WITH 2.5% Dy AS A FUNCTION OF FUEL BURNUP FOR SEVERAL COOLANT DENSITIES.

Power profiles for three plutonium fractions are shown in Figure 5.12. It can be seen that with 1% plutonium loading the power in the intermediate and outer rings is almost equal over the whole irradiation to discharge.

Increasing the plutonium fraction causes greater power difference between the intermediate and outer rings, with the highest power in the outer ring early in the irradiation history, with the highest power in the intermediate ring at higher burnup. Table 5.2 shows the normalised power distribution in UK CANMOX fuel with 2.5% dysprosium loading compared to the distribution in fuel concept 19 with 3% Pu loading. It can be seen that the power profiles are broadly similar. The intermediate ring power is slightly higher in UK CANMOX fuel, but the outer ring power is higher in the three-component fuel. In addition the difference in power between the rings is lower for the three-component fuel, giving more equal power and burnup across the two MOX enrichments.

The material composition evolutions in the intermediate and outer plutonium MOX regions of fuel concept 19 are shown in Figure 5.13. It can be seen that despite different initial plutonium loadings, the fraction of fissile ^{239}Pu and ^{241}Pu in the final plutonium is almost identical across the two rings, and slightly below the level achieved in UK CANMOX fuel with 2.5% dysprosium loading.

TABLE 5.2 – COMPARISON OF NORMALISED POWER DISTRIBUTIONS IN INTERMEDIATE AND OUTER RINGS OF UK CANMOX FUEL AND THREE-COMPONENT FUEL CONCEPT 19.

		ELEMENT POWER PER UNIT LENGTH W/cm		
		BOL	MID-LIFE	EOL
Intermediate ring	UK CANMOX	237	300	302
	3%Pu in fuel concept 19	245	290	285
Outer ring	UK CANMOX	297	245	220
	3%Pu in fuel concept 19	300	260	225

The evolution of the material composition in fuel concept 19 is presented in Figure 5.14. It can be seen that the fissile fraction of plutonium is halved over the burnup to 22.5 MWd/kgHM. The quantity of ^{239}Pu is reduced by 80% over the irradiation cycle. In the thorium blanket region a total of 38 g of ^{233}U and 0.05 g of ^{232}U are produced, in addition to 3.6 g of ^{233}Pa which will decay to ^{233}U . Of the initially loaded thorium, 61.4 g are consumed. In addition to the plotted radionuclides, at EOL the thorium rods also contain 2.36 g of ^{234}U and 0.15 g of ^{235}U . The shortfall between thorium lost and other actinides produced suggests that approximately 17 g of ^{233}U have already undergone fission at EOL, which accounts for the power gain in the inner fuel elements with increasing burnup.

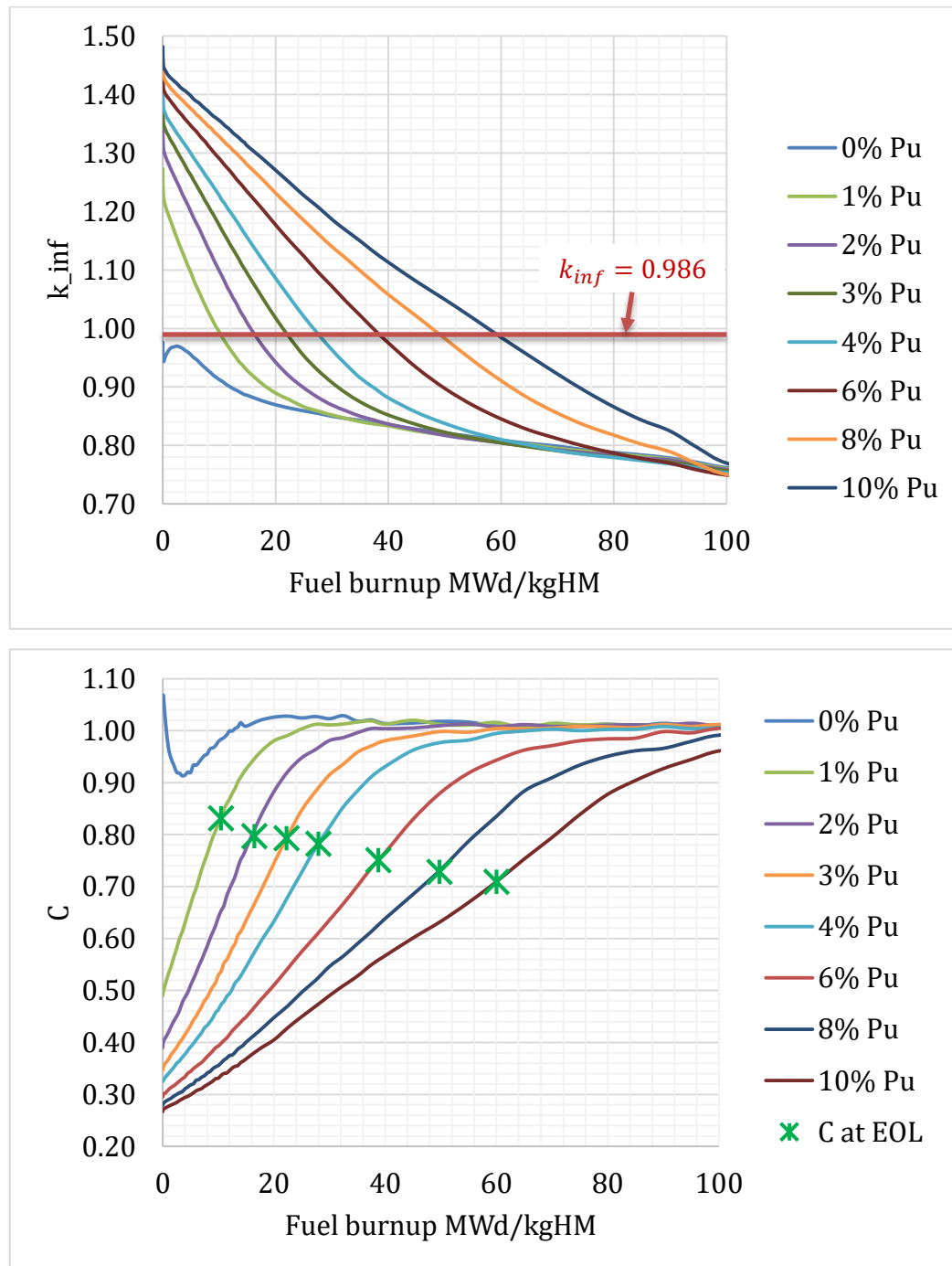


FIGURE 5.11 – EVOLUTION OF k_{inf} (TOP) AND C (BOTTOM) WITH BURNUP FOR FUEL CONCEPT 19 WITH DIFFERENT AVERAGE PLUTONIUM FRACTIONS IN THE MOX SEED REGION. MARKED ON GRAPHS ARE THE ASSUMED MULTIPLICATION FACTOR AND CALCULATED CONVERSION RATIO AT DISCHARGE.

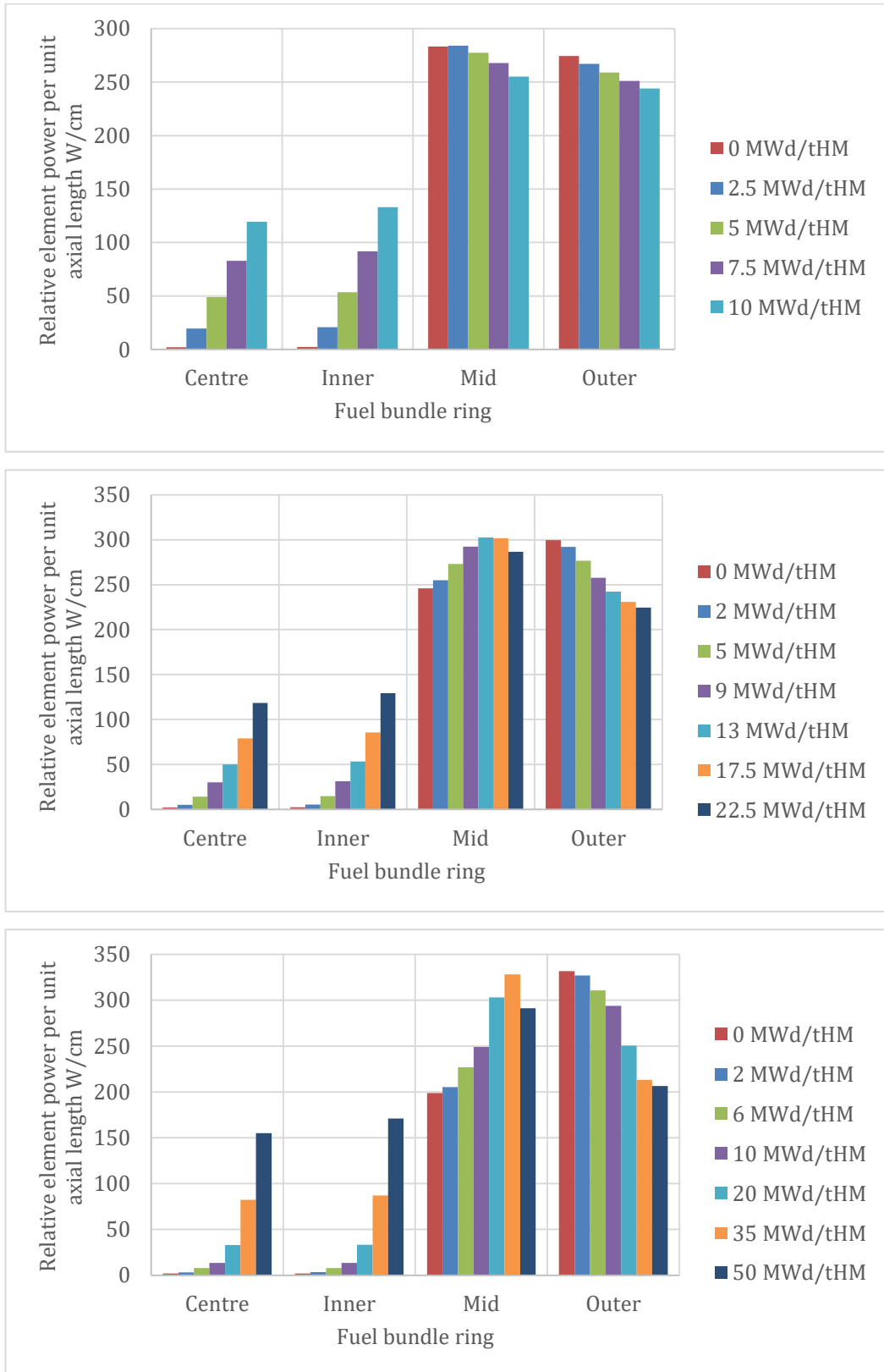


FIGURE 5.12 – POWER PROFILES ACROSS THE BUNDLE IN FUEL CONCEPT 19. PLUTONIUM FRACTIONS IN THE MOX DRIVER ARE 1% (TOP), 3% (MIDDLE) AND 6% (BOTTOM).

THE PREPARATION AND APPLICATION OF THORIUM-BASED NUCLEAR FUELS

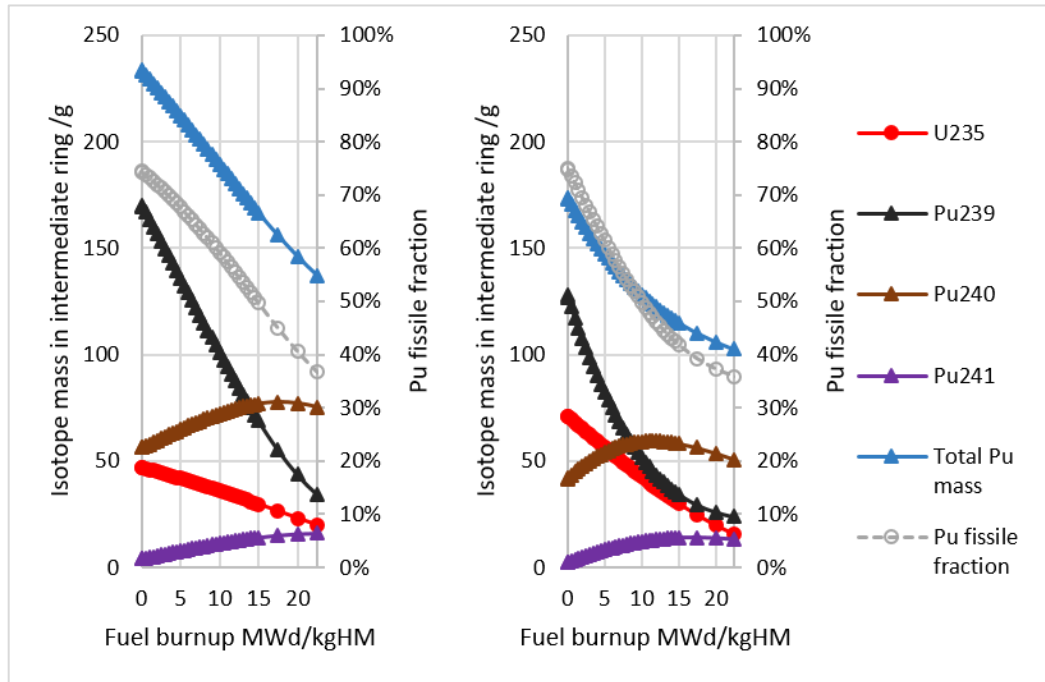


FIGURE 5.13 – ISOTOPE MASS VARIATION WITH BURNUP IN FUEL CONCEPT 19 WITH AVERAGE PU FRACTION OF 3%. INTERMEDIATE RING WITH 4.29% INITIAL PLUTONIUM LOADING (LEFT) AND OUTER RING WITH 2.14% INITIAL PLUTONIUM LOADING (RIGHT).

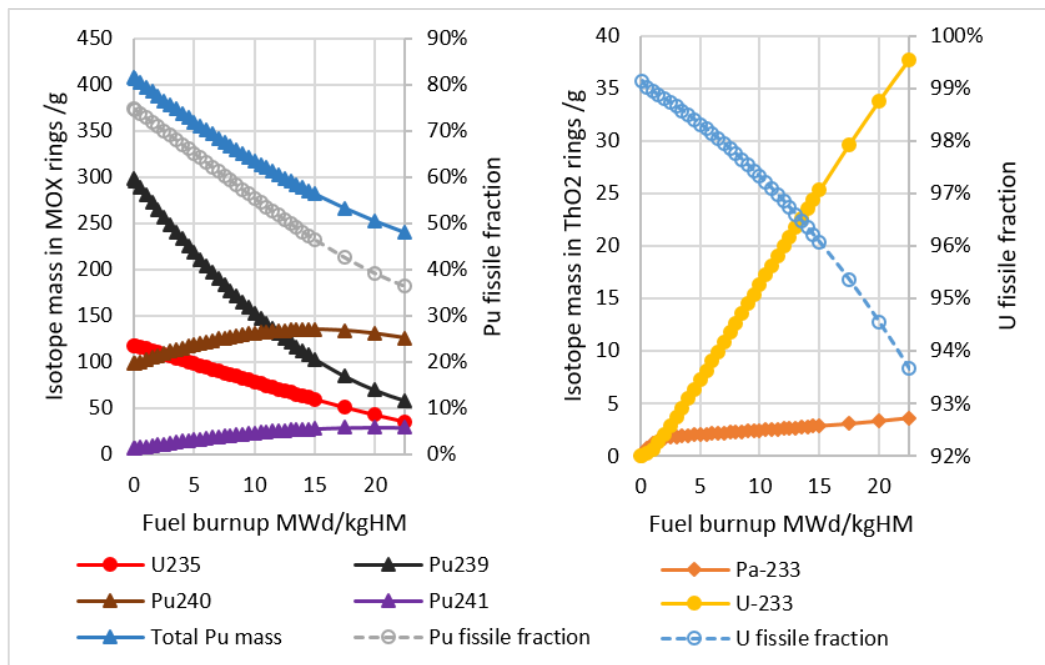


FIGURE 5.14 – EVOLUTION OF SELECTED ISOTOPE MASSES IN FUEL CONCEPT 19 WITH 3% INITIAL PLUTONIUM LOADING. TOTAL ACROSS INTERMEDIATE AND OUTER RINGS WITH U-Pu MOX (LEFT), AND INNER RING AND CENTRE PIN WITH ThO₂ (RIGHT).

5.3.3.1 EFFECT OF COOLANT VOIDING

The impact of coolant density reduction on fuel concept 19 is shown in Figure 5.15. It can be seen that similarly to natural uranium and UK CANMOX fuels, fuel concept 19 with 3% plutonium loading gives an increase in k_{inf} with reduced coolant density for a full range of burnups. The coolant void reactivity was found to be slightly positive from 0.1 to 22.5 MWd/t, with an increasing trend in CVR with burnup due to the increasing fraction of ^{233}U in the central fuel elements.

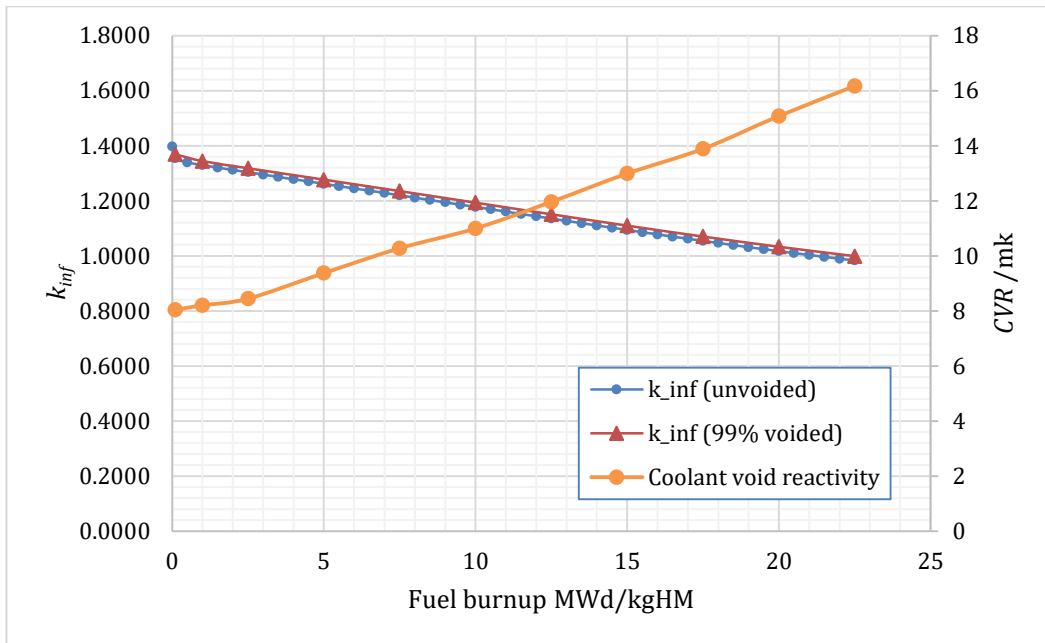


FIGURE 5.15 – EFFECT OF VOID FRACTION ON k_{inf} FOR FUEL CONCEPT 19 WITH 3% AVERAGE PLUTONIUM LOADING AT 1 MWd/kg, PRESENTED AS CHANGE IN k_{inf} FROM UNVOIDED CONDITION.

5.3.4 FUEL CONCEPT COMPARISON – USE OF EPR REPROCESSED MOX

Fuel concept 17, produced from the reprocessed uranium and plutonium of modern LWR fuels, was studied to determine its performance in comparison to fuel concept 19.

The variation in k_{inf} and C_r for two plutonium fractions in fuel concepts 17 and 19 can be seen in Figure 5.16. It can be seen that switching to fuel

concept 17 gives a reduction in k_{inf} compared to concept 19. Fuel concept 17 with 3% plutonium loading will only reach 20 MWd/kgHM when k_{inf} reaches the discharge level. A similar reduction is seen with the greater average plutonium loading, reducing from 43 to 37 MWd/kgHM. Conversion factors in fuel concept 17 are greater across the range of burnup, and the concept reaches similar EOL conversion factors to fuel concept 19. Based on the results presented in Figure 5.11, it is projected that an increase in average initial plutonium loading to approximately 4% in fuel concept 17 will compensate for the difference in k_{inf} against fuel concept 19.

The power profile for 3% plutonium in fuel concept 17 is presented in Figure 5.17. When comparing this to the 3% plutonium plot in Figure 5.12 the power profile is not appreciably different, and the power distribution is therefore expected to be similar across the two bundles.

The isotopic composition with burnup is plotted in Figure 5.18. The general change in composition is similar to fuel concept 19. In the MOX fuel elements the final Pu fissile fraction is slightly lower, although the amount of fissile isotope is very similar, with the change in fissile fraction instead being due to greater quantities of the even-numbered isotopes. In the thorium fuel elements, the fissile uranium fraction is greater in concept 17 than concept 19. Slightly less ^{233}U and slightly more ^{233}Pa are produced.

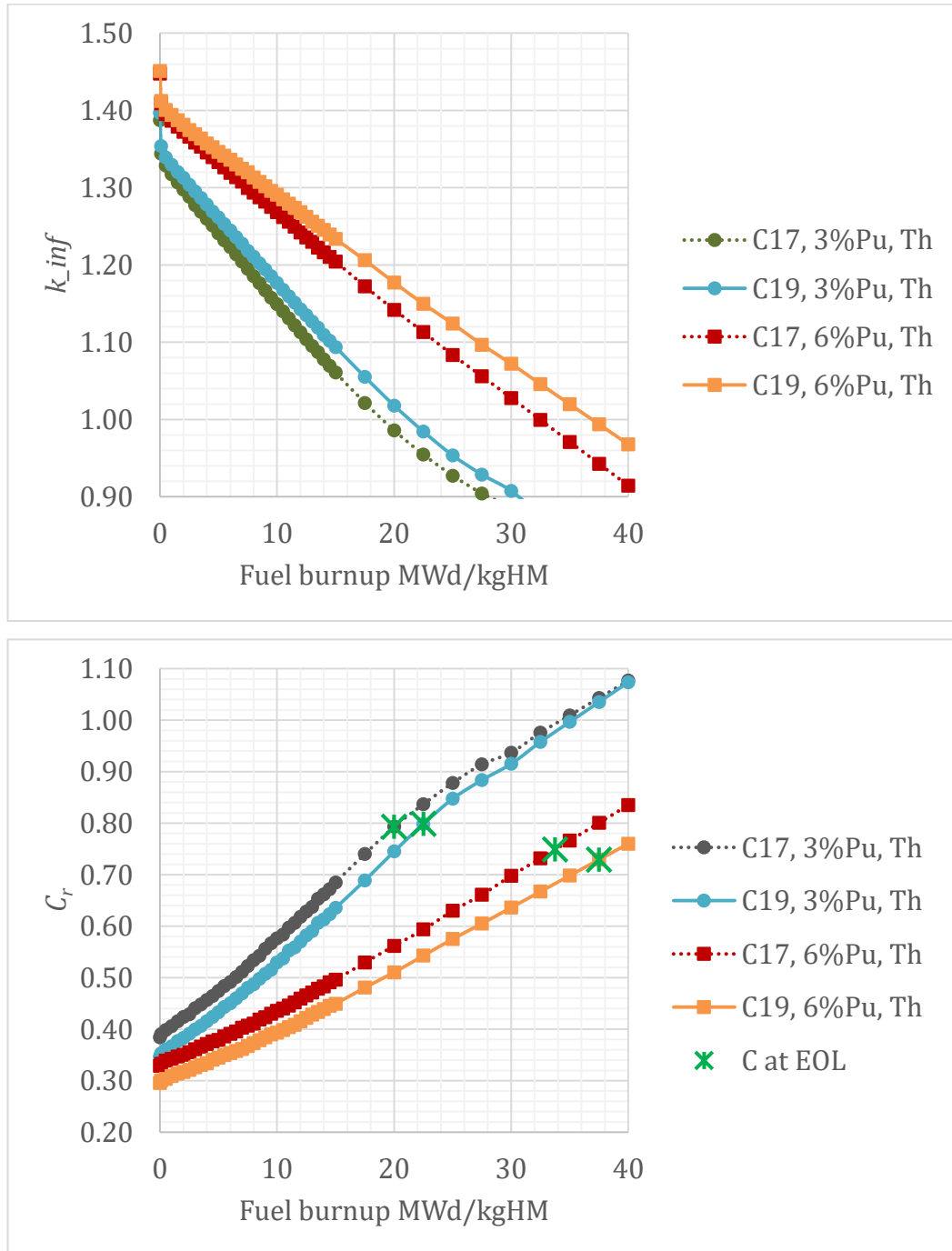


FIGURE 5.16 – EVOLUTION OF k_{inf} AND C WITH BURNUP IN TWO THREE-COMPONENT FUEL CONCEPTS 17 (REPROCESSED EPR MOX) AND 19 (INVENTORY MOX) WITH TWO PLUTONIUM LOADING FRACTIONS.

THE PREPARATION AND APPLICATION OF THORIUM-BASED NUCLEAR FUELS

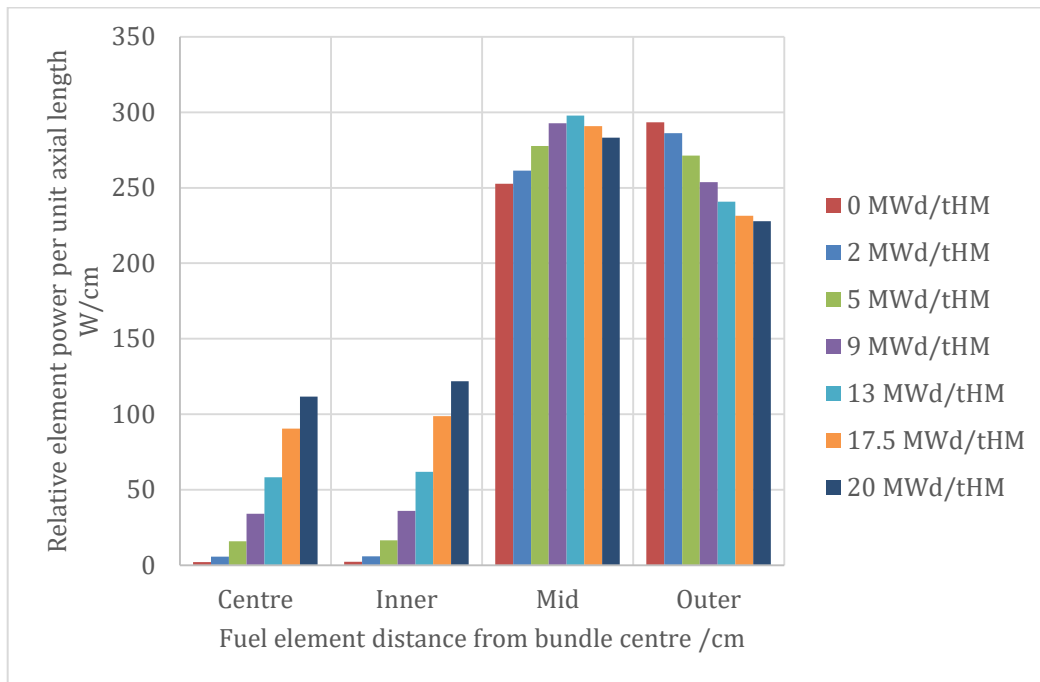


FIGURE 5.17 – POWER PROFILES ACROSS THE BUNDLE IN FUEL CONCEPT 17 WITH 3% AVERAGE PLUTONIUM LOADING.

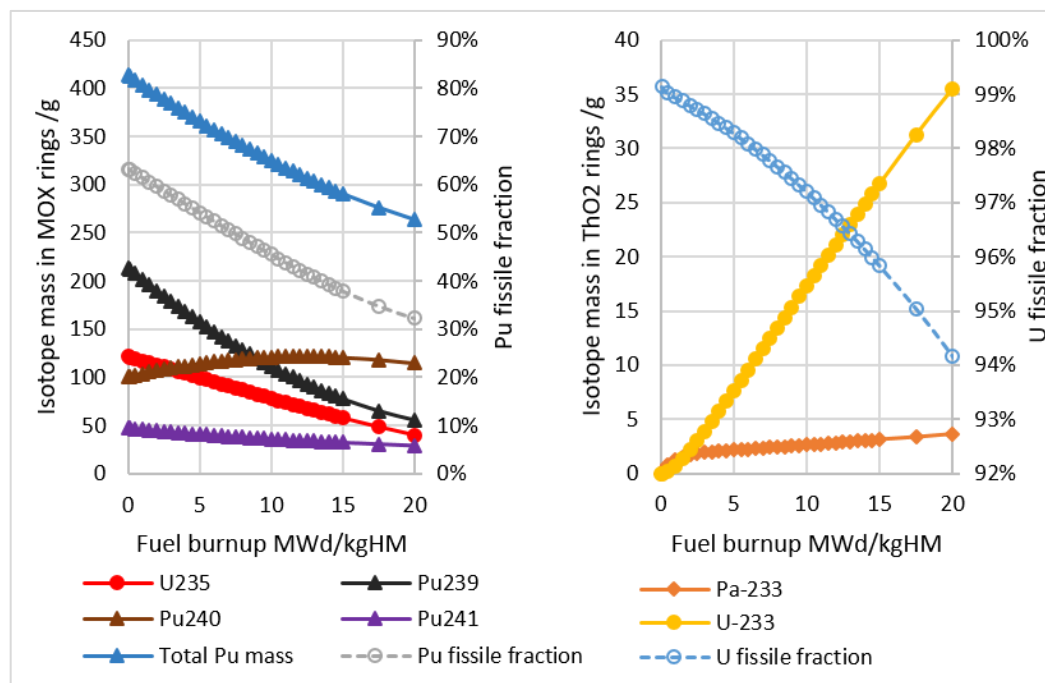


FIGURE 5.18 – EVOLUTION OF SELECTED ISOTOPE MASSES IN FUEL CONCEPT 17 WITH 3% INITIAL PLUTONIUM LOADING. TOTAL ACROSS INTERMEDIATE AND OUTER RINGS WITH U-Pu MOX (LEFT), AND INNER RING AND CENTRE PIN WITH ThO₂ (RIGHT).

5.3.5 EFFECT OF MDU-TPU BLENDING

As was discussed in Chapter 4, depending on the quantity of reprocessed uranium necessary for fuel concept 19, it may be necessary to blend in a fraction of MDU with the TPU, giving fuel concept 21. The effect of this blending on achievable discharge burnup is shown in Figure 5.19. The greater the fraction of MDU the lower the achievable discharge burnup, although the overall reactivity depletion slope is very similar.

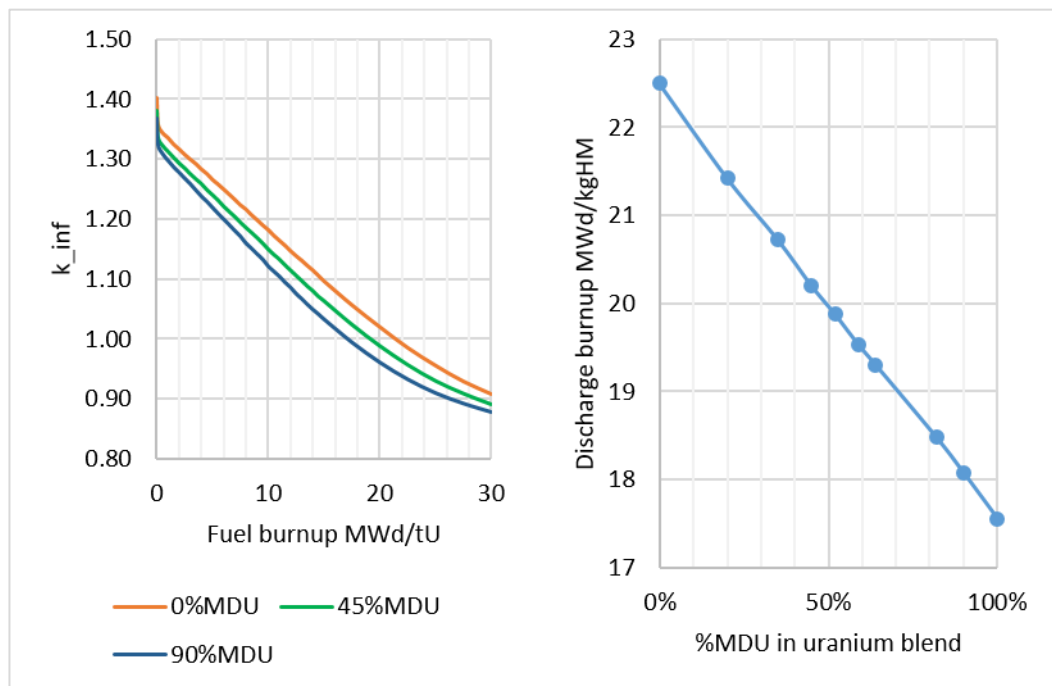


FIGURE 5.19 – REDUCTION IN k_{inf} WITH FUEL BURNUP FOR FUEL CONCEPT 21 WITH 3% PLUTONIUM LOADING WITH 3 LEVELS OF MDU BLENDING FRACTION (LEFT). VARIATION IN BURNUP AT WHICH $k_{inf} = 0.986$ (RIGHT).

5.4 DISCUSSION AND MATERIALS REQUIREMENTS

5.4.1 VALIDATION AGAINST NATURAL URANIUM CANDU FUELS

The results of the numerical simulation for natural uranium fuel are in good agreement with operational data from CANDU 6 reactors with natural uranium oxide fuel. The conversion ratio at BOL and EOL was found to be

0.8, which is the quoted typical value for CANDU reactors [20]. The multiplication factor fell to unity at $\sim 7 - 7.5$ MWd/kgHM. Additionally, the power profile shapes across the fuel bundles were in good agreement with literature data. These results give confidence in the accuracy of the simulation, and increase the confidence in the results generated for UK CANMOX and three-component fuel concepts.

5.4.2 UK CANMOX FUELS

Given that UK CANMOX is not fully defined in the literature and that it was desirable to use this fuel as the baseline for comparison of three-component fuels, it was necessary to study the impact of dysprosium loading within the fuel bundle.

It was found that the 2.5% Dy loaded fuel reached the assumed discharge multiplication factor at the average level of discharge burnup stated for UK CANMOX fuel in the literature, and on this basis 2.5% was set as the reference dysprosium fraction. Upon discharge the fissile fraction of plutonium in the MOX elements was reduced to an average value of 40%, with the total Pu mass reduced from 477 g to 300 g. However, in the burnable absorber bundles 17.5 g of plutonium are produced by ^{238}U conversion, and this plutonium is 80% fissile at EOL. If the 140 t plutonium inventory were to be irradiated in this fuel, this would lead to the production of 5.1 t of this highly fissile plutonium in the burnable absorber elements, which could be recovered if these elements were to be reprocessed.

In order to fabricate sufficient fuel bundles to irradiate 140 tHM plutonium, each containing 477 g plutonium metal, there would be a requirement for 11 tHM of dysprosium and 3910 tHM of depleted uranium, to be irradiated in 222,800 fuel bundles. Using Equation (5.4) it can be shown that for a burnup of 18.25 MWd/kgHM, an EC6 will require 39.2 tHM of fuel per reactor year.

5.4.3 THREE COMPONENT FUELS

The three-component fuels show good neutronic behaviour and offer a range of advantages over UK CANMOX fuel. The discharge burnup of the fuel is greater, giving transmutation of the loaded plutonium to a lower fissile fraction of 36% and reducing the overall plutonium mass per bundle from 407 g to 240 g, a 41% mass reduction compared to the 37% reduction offered by UK CANMOX. Furthermore no additional plutonium is produced in the inner fuel elements. The three component fuel also has a positive coolant void reactivity, as is normally the case for CANDU fuels. While it would be an advantage to have a negative CVR for reactor safety and stability [20], positive void coefficients are within the scope of existing CANDU safety cases.

The power distribution across the bundle is comparable to that of UK CANMOX, but the distribution was calculated for a fixed overall power density and further studies must be carried out to determine the actual power in each fuel element and ensure that power limits are not exceeded.

5.4.3.1 INVENTORY MANAGEMENT WITH FUEL CONCEPT 19

The annual quantity of fuel required for an EC6 irradiating fuel to 22.5 MWd/kgHM was calculated to be 31.8 tHM/reactor.year, equivalent to 1787 CANFLEX bundles. Irradiation of 140 t Pu in fuel concept 19 with 3% plutonium loading could be carried out over 48.4 years in four EC6 units or 27.6 years in seven EC6 units. Also required would be 4520 t TPU and 1490 t Th. This would leave enough TPU to fabricate 4435 t NUE fuel, sufficient for 10 reactor.years of operation. Alternative fuel sources would be required following depletion of the Pu and TPU inventories.

The use of irradiated thorium elements within NUE bundles is suggested as a potential option to increase NUE operation time. Following ~ 30 years of post-irradiation cooling when the ^{233}Pa will have decayed to ^{233}U , concept 19 thorium elements will contain 1% ^{233}U by mass. Additionally a portion of

the short-lived fission products will have decayed. If the thorium elements can provide similar performance to NUE fuel, the 1490 tHM of irradiated thorium elements could be used to increase the NUE operation time to ~22.5 years. Based on this, the three-component fuel and NUE+Th fuels could provide 216 reactor.years of EC6 operation, equivalent to 160 GW.years of electrical power over the plant’s 60-year lifetime. An EPR produces 96 GW.years of electrical power and requires 1785 tHM LEU [444]. If the EPR total power is scaled to match that of the EC6 units with three-component and NUE+Th fuel, it is found that 30,000 tHM of natural uranium resources could be saved through the use of the proposed three-component fuel and Th+NUE fuel in four EC6 reactors, while managing the UK plutonium inventory and breeding ²³³U.

Three plutonium loadings were investigated for fuel concept 19 in Chapter 4, being 1%, 3.4% and 8.4% Pu. Simulation of fuels of these compositions gave discharge burnups as shown in Table 5.3.

TABLE 5.3 – DISCHARGE BURNUPS ACHIEVABLE WITH FUEL CONCEPT 19 PLUTONIUM LOADINGS SUGGESTED IN CHAPTER 4.

PLUTONIUM LOADING IN FUEL CONCEPT 19 MOX ELEMENTS	DISCHARGE BURNUP FROM SERPENT MODEL MWd/kgHM
1.0%	10.5
3.4%	24.6
8.4%	47.8

If it is deemed acceptable to operate an EC6 with three-component fuel both before and after mid-life refurbishment, it is suggested that four EC6 units be constructed. All units would operate with fuel concept 19 with 3% plutonium loading for 30 years and then undergo refurbishment. In the second half of life two units would continue to irradiate fuel concept 19 for 30 years. One unit would irradiate fuel concept 19 for ~15 years and then

switch to NUE fuel. The fourth unit would irradiate natural uranium in the second half of life. This fuel cycle seeks to strike a balance between the level of investment required in EC6 plant and the use of natural uranium while irradiating all plutonium and TPU.

There will likely be some range of flexibility in the selected plutonium fraction, thus allowing some variation in the time required to irradiate the plutonium in the EC6 reactors. However, based on the results generated here it is strongly indicated that four reactors will be able to irradiate the plutonium inventory in four EC6 units over a 45-50 year period (not including mid-life refurbishment), or that seven reactors could irradiate the fuel over a 25-30 year period.

5.4.3.2 EXTENDING THORP PRODUCT URANIUM RESOURCES WITH MAGNOX DEPLETED URANIUM IN FUEL CONCEPT 21

For fuel concept 21, it was shown in Figure 5.19 that blending MDU and TPU reduces the achievable discharge burnup of the core, in line with the expectation from Chapter 4. The potential need for such blending was outlined in Section 4.6.2. If necessary the multiplication factor reduction due to the use of a TPU-MDU blend could be compensated by increasing the plutonium fraction, although additional work would be required to confirm the behaviour of fuels with higher plutonium in less fissile uranium.

5.4.3.3 LWR USED FUEL URANIUM AND PLUTONIUM IRRADIATION IN FUEL CONCEPT 17

For fuel concept 17, it was seen that the reduced plutonium quality is not compensated by the slightly higher fraction of ^{235}U in EPR used fuel. The fuel composition and power profile are slightly modified compared to those of fuel concept 19, but overall these changes are minor. For LWR spent fuel management, it was stated in Chapter 4 that a fuel with 1.4% plutonium could manage all U and Pu produced from EPR reactors. An EPR produces

115 tHM of uranium and plutonium per year in used fuel, of which 1.4% is plutonium.

A simulation of fuel concept 17 with 1.4% plutonium loading showed that the achievable discharge burnup was 12 MWd/kgHM. The evolution of the composition of this fuel with burnup is shown in Figure 5.20, showing that the plutonium composition is 39% fissile upon discharge.

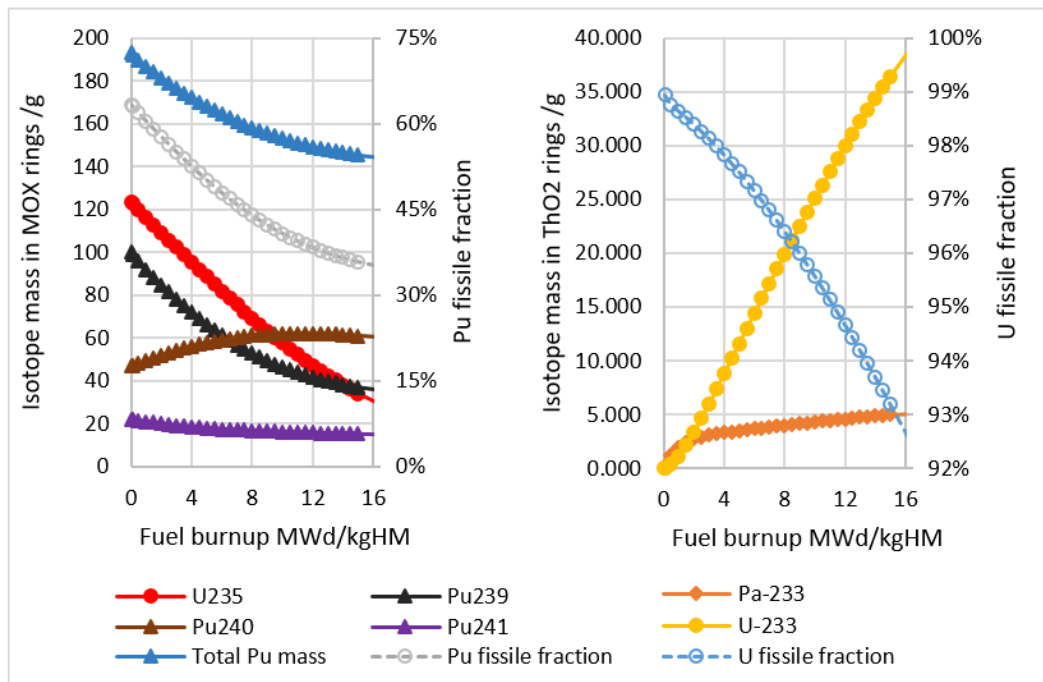


FIGURE 5.20 – EVOLUTION OF SELECTED ISOTOPE MASSES IN FUEL CONCEPT 17 WITH 1.4% INITIAL PLUTONIUM LOADING. TOTAL ACROSS INTERMEDIATE AND OUTER RINGS WITH U-Pu MOX (LEFT), AND INNER RING AND CENTRE PIN WITH ThO₂ (RIGHT).

The annual fuel requirement was calculated to be 59.6 tHM, of which 45.2 tHM is uranium and plutonium. As such an EC6:EPR support ratio of 5:2 is indicated, meaning that ten EC6 units would be required for the UK if both the Hinkley Point C and Sizewell C EPR plants were to be constructed. A lower support ratio is expected for other LWRs planned for the UK, as these are less powerful and are thus expected to produce less used fuel. The addition of ten EC6 reactors to the UK would add 7.4 GWe of generating

capacity, in addition to the 6.4 GWe from the four EPRs, with the only additional required fuel resource being 8640 t Th.

Higher plutonium fraction options from Chapter 4 for concept 17 fuels had 4.4% and 5.4% plutonium loading, and would be capable of managing all separated LWR plutonium but only a fraction of the uranium, the remainder of which might be re-irradiated as an NUE fuel by blending with MDU. The discharge burnups for these fuels are shown in Table 5.4.

TABLE 5.4 – DISCHARGE BURNUPS ACHIEVABLE WITH FUEL CONCEPT 17 PLUTONIUM LOADINGS SUGGESTED IN CHAPTER 4.

PLUTONIUM LOADING IN FUEL CONCEPT 19 MOX ELEMENTS	DISCHARGE BURNUP FROM SERPENT MODEL MWd/kgHM
1.4%	11.0
4.4%	26.8
5.4%	31.25

5.5 FUTURE WORK

The next stage of the three-component fuel development work is to carry out further neutronic analysis. A range of power densities may be used to further inform fuel behaviour in low and high power core regions. The feasibility of incorporating irradiated thorium fuel elements into NUE fuel bundles is also an appealing area of further study that can be carried out at the 2D infinite lattice level. The extension of this work would be to carry out further 2D infinite lattice simulations, but on a set of nine fuel elements in a three-by-three “supercell” configuration, where the outer eight bundles have a fixed composition, and the composition of the inner bundle is variable as a function of fuel burnup. This will allow the use of more realistic neutron energy spectra to be used. Varying the composition of the outer

bundles will allow the determination of sensitivity of the fuel reactivity to the neutron energy spectrum, a vital parameter towards understanding the core behaviour, and a first step towards the generation of appropriate core management schemes.

The impact of reactivity devices must be studied. This is commonly carried out in PHWR cores by a reduced 3D simulation of the effect of introducing a single control rod vertically between two horizontal fuel channels, as shown in Figure 5.21. A range of fuel burnups should be used to determine the relative negative reactivity insertion compared to natural uranium fuels, and whether the rods can still provide sufficient shutdown margin for UK CANMOX and three-component fuels, or whether the rod composition must be altered.

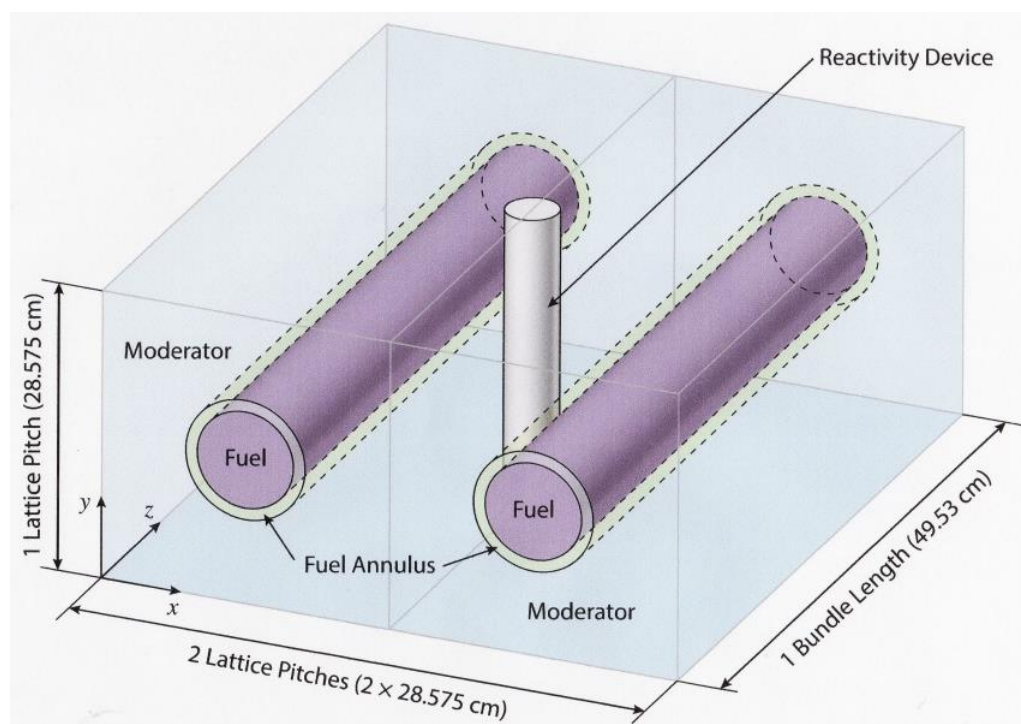


FIGURE 5.21 – SUGGESTED SIMULATION GEOMETRY FOR INITIAL STUDIES INTO THE EFFECT OF CONTROL RODS IN PHWR CORES [483].

Eventually the analysis must transition into a coupled neutronic and thermal-hydraulic model, with a full core being simulated. Determination of actual fuel power profiles within a core, temperature effects and heat

transfer to the coolant must be analysed in order to ensure that the fuel may operate safely within the reactor limits. It is suggested that a deterministic neutron transport model is used for this purpose in order to manage the high computational cost of such a simulation in a Monte Carlo model. However, Monte Carlo modelling will be useful in providing group constant data to the deterministic package.

The effect of reactivity control devices in the full core simulation must particularly be considered, as the effectiveness of control rods is often reduced with Th-Pu and Th-U fuels [366]. Furthermore, the large excess of fuel reactivity at beginning of life will require the use of high soluble absorber concentrations, which can lead to a positive moderator temperature coefficient [484].

Transients within the core must also be considered. In CANDU reactors the most common transients occur during refuelling operations. CANDU reactors are also designed to cope with a range of potential accident scenarios. The response of an EC6 with three-component fuel to a range of fault conditions such as coolant loss, fuel failure, pressure/calandria tube leakage, station blackout and others must be established.

A wide range of fuel cycle analyses are required to supplement the reactor operation studies. Spent fuel management will be a major work area, to consider how the fuel might be safely either disposed of in a deep geological formation, or otherwise managed in the back end of the fuel cycle. This might include hot cell disassembly of the highly active bundles for thorium fuel element recovery and reassembly into other bundles. In the fuel cycle front end studies into fuel fabrication would be required, although the fabrication of U-Pu mixed oxide fuels and thorium oxide fuels are ongoing work areas, already with a significant literature work, and industrial experience in the case of U-Pu MOX. As has been discussed at length in

Chapters 2 and 3 of this thesis, work remains to be done in the separation and purification of nuclear-grade thorium suitable for fabrication.

An economic and market analysis must be carried out to determine whether there will be sufficient demand for three-component fuels. For inventory management, three-component fuel must be able to compete with and offer value over the reference UK CANMOX fuel to be realised. For LWR used fuel irradiation, it would have to be shown that the value of the additional energy per unit of EPR fuel was greater than its generation cost.

5.6 CONCLUSIONS AND CHAPTER SUMMARY

Overall, three-component fuels with thorium present a suite of advantages over UK CANMOX fuel. The final plutonium product is less fissile, and no plutonium is bred in the inner fuel elements. Irradiated uranium is reused rather than unirradiated depleted uranium, and no additional natural uranium is required. As with natural uranium and UK CANMOX fuels, three component fuels give positive coolant void reactivity. Power profiles between the three-component and UK CANMOX fuels are comparable, and the final plutonium composition in the intermediate and outer rings is very similar.

Two three-component fuel concepts have been studied, one for plutonium inventory management (fuel concept 19), and the other for re-irradiation of modern LWR spent fuel (fuel concept 17). Fuel concept 19 with 3% plutonium loading in the MOX was able to irradiate the 140 t of inventory plutonium to 22.5 MWd/kgHM in four Enhanced CANDU 6 reactors over 45-50 years, achieving a 50% reduction in the fissile fraction of the plutonium while also irradiating reprocessed uranium from AGR reactors. If EPR used fuel is re-irradiated then 1.4% plutonium loading fuel is recommended, with five EC6 units required per two EPRs.d

It is suggested for future work that Serpent or another package be used to generate few group constant data suitable for coupled neutronic-thermal-hydraulic full core simulations with three-component fuels. Equilibrium and transient studies will be required to confirm the feasibility of EC6 operation with three component fuels. Following this studies into the potential fuel cycle options and its economics are recommended.

The physical separation of the thorium fuel elements and the plutonium-containing fuel elements in the three-component fuel concept means that the irradiated fuel bundles could be disassembled in order to recover the thorium elements by cutting the endplates. The plutonium-uranium MOX elements could be placed into waste containers and prepared for long-term interim storage prior to geological disposal. The thorium elements could then be reprocessed to recover the uranium and thorium.

In the next chapter, a study is presented into the use of synergic mixtures of PC-88a and other extractants from three different aqueous phases, in order to identify possible systems for the separation of thorium and uranium from zirconium and iron. The distribution ratios and separation factors are determined for these systems, and the most promising systems for thorium spent fuel reprocessing are identified.

6 COMPARISON OF THORIUM SEPARATION BY TEN SOLVENT EXTRACTION MIXTURES

In the previous chapter it was shown that, from the neutronics perspective, three component nuclear fuels with reprocessed uranium, plutonium and thorium appear to be feasible for use in pressurised heavy water reactors. As the thorium fuel elements do not contain plutonium or reprocessed uranium, they may be reprocessed to recover the uranium-233 for use in starting a full thorium-²³³U fuel cycle. In this chapter is presented a screening study into the separation of thorium and uranium from zirconium and iron by PC-88a with ten different potential synergists. The aim was to determine promising extractant pairings which might form the basis of a solvent extraction system for further development.

6.1 INTRODUCTION

As was shown in Chapter 2, the number of possible synergic thorium solvent extraction systems which may be assessed is very large, considering many aqueous media, a large number of possible extractants and diluents, and a large range of extraction conditions. Very few of these studies, however, were aimed at spent fuel reprocessing, focussing instead on front end separation of thorium from minerals, normally to recover rare earth elements. To test the whole range of possible synergic extraction systems for a reprocessing application, even those which had not previously been considered in the literature, would be a very large task. As such it was

deemed necessary to narrow down to a subset of potential systems to examine, from which the most promising could be selected. In order to do this, a screening study was planned to investigate a range of systems for further development.

6.1.1 AQUEOUS PHASE SELECTION

In order to prepare spent fuel for separation of the recyclable components, it must first be dissolved. Thorium oxide spent fuel is much more resistant to dissolution than uranium spent fuel, necessitating the use of hot, concentrated nitric acid with an amount of hydrofluoric acid added as a catalyst [485]. However, it is not necessarily the case that nitric acid will be the best acid from which to extract thorium and uranium. Hydrochloric, nitric and sulfuric acids are all commonly used process acids, and so all three were investigated as potential aqueous media. Two levels of concentration were investigated for each acid in order to determine the impact of high and low acidity in solution, these being 0.5 M and 3.0 M. While a lower level of acidity could have been used, 0.5 M was selected to prevent the possibility of thorium hydroxide precipitation in less acidic conditions [486-488].

The use of strong acids, particularly hydrochloric acid, will need to be considered during process scale-up and process plant design, due to the potential for corrosion of metallic materials used in reaction vessels, pipework, and so on. The corrosion induced by HF in the Acid THOREX process is managed by the addition of aluminium nitrate [104].

6.1.2 METALS OF INTEREST IN THE AQUEOUS FEED

The metals selected for the simulated spent fuel liquor were Th(IV), U(VI), Fe(III) and Zr(IV). The concentration for each element was set to 100 mg/l. This low concentration was selected in order to avoid competition between metals for the available extractant, allowing each metal in the PLS to complex with the extractant quasi-independently. It also means that the

concentration of free extractant in the system will be little changed by complexation of the available metal.

Zirconium was found to be extracted quantitatively by PC-88a in xylene from hydrochloric acid at a range of acidities [489]. It is also extracted strongly when kerosene is used as the diluent, with greater extraction at higher acidities [490]. The extracted complex was found to be $ZrO(H_2O)_nCl_2.(PC-88a)_2$ [491]. As such, it might be advantageous to identify a secondary extractant which would be antagonistic with PC-88a for zirconium.

6.1.3 SELECTION OF ORGANIC EXTRACTANTS FOR SYNERGISM TESTING

In this study the aim was to identify potential synergic mixtures for thorium and uranium recovery from spent fuel based on well-established extractants, and determine the distribution ratios for thorium, uranium, iron and zirconium and to determine the separation factors for uranium and thorium against one another and against iron and zirconium. Ten extractant mixtures were tested to determine thorium extraction and separation behaviour, using a single primary extractant in all tests and ten secondary extractants for screening as potential synergists. As a mixture of PC-88a and HDEHP in *n*-dodecane was found to extract both thorium and uranium while rejecting iron in the work presented in Chapter 3, it was decided to retain PC-88a as the primary extractant and *n*-dodecane as the diluent. However, the use of other diluents might give improved separation of the metals.

The secondary extractants were selected across three broad types: other phosphorous-based extractants, amine/ammonium extractants, and room temperature ionic liquids. The selected secondary extractants are listed in Table 6.1, with their structures shown in Figure 6.1 (b)-(k). Other secondary extractants were tested at the same concentration as HDEHP in Chapter 3, in order to compare distribution and separation behaviour for each metal. In addition, 0.1 M PC-88a alone, without secondary extractant, was also tested.

6.2 MATERIALS AND METHODS

6.2.1 REAGENTS AND STOCK SOLUTIONS

Unless otherwise stated, all organic chemicals and metal salts were ACS Reagent Grade, and were purchased from Sigma Aldrich. PC-88a was supplied by BOC Sciences, USA. The *n*-dodecane diluent was supplied by Sigma Aldrich. All organic reagents were used as supplied without further purification, with the exception of TBP which was washed with 0.1 M sodium bicarbonate solution and deionised water to remove degradation products. An organic stock solution was prepared with 0.2 M PC-88a in *n*-dodecane, standardised by mass.

Thorium chloride octahydrate ($\text{ThCl}_4 \cdot 8\text{H}_2\text{O}$) and uranyl nitrate hexahydrate ($\text{UO}_2(\text{NO}_3)_2 \cdot 6\text{H}_2\text{O}$) salts were taken from in-house stocks originally supplied by British Drug Houses. The initial purity of these aged materials was unknown. Reagent grade iron(III) chloride hexahydrate ($\text{FeCl}_3 \cdot 6\text{H}_2\text{O}$) and zirconyl chloride octahydrate ($\text{ZrOCl}_2 \cdot 8\text{H}_2\text{O}$) were used as the inactive metal salts. Reagent Grade stock acids and Analytical Grade 70% nitric acid were purchased from Fisher Scientific.

Stock acid solutions were prepared at 0.5 M and 3.0 M concentration, standardised using a Mettler-Toledo FiveGo pH meter with Ag-AgCl glass electrode. Individual metal spike solutions were prepared in 5.0 M HCl containing Th(IV), U(VI), Fe(III) and Zr(IV) from the metal salts. These were then combined to produce a mixed metal spike with 12.5 g/l of each metal. Mixed metal studies were performed, rather than single metal studies, in order to economise on analytical instrument usage time and costs. This also allows studies to be made on the competition between metals for the available extractants.

THE PREPARATION AND APPLICATION OF THORIUM-BASED NUCLEAR FUELS

TABLE 6.1 – SELECTED EXTRACTANTS EXAMINED IN THIS THESIS.

TYPICAL EXTRACTION MECHANISM	EXTRACTANT TYPE	ABBREVIATED FORM	CHEMICAL FORMULA	EXTRACTANT
Cation exchange	Phosphonic acid	PC-88a	$(C_8H_{17}O)(C_8H_{17})POOH$	2-ethylhexylphosphonic acid mono-2-ethylhexyl ester
	Phosphoric acid	HDEHP	$(C_8H_{17}O)_2POOH$	Di-(2-ethylhexyl) phosphoric acid
Solvation	Phosphorous ester	TBP	$(C_4H_9O)_3PO$	Tributyl phosphate
	Phosphine oxide	TOPO	$(C_8H_{17})_3PO$	Trioctylphosphine oxide
Anion exchange	Long chain amine	MOA	$(C_8H_{17})NH_2$	Octylamine
		DOA	$(C_8H_{17})_2NH$	Dioctylamine
		TOA	$(C_8H_{17})_3N$	Trioctylamine
	Branched amine	TertOA	$C(CH_3)_3(CH_2)(CH_3)_3NH_2$	<i>tert</i> -octylamine
	Quaternary ammonium salt	A336	$(C_8H_{17})_3NCH_3Cl$	Aliquat-336 (tricaprylmethylammonium chloride)
	Room temperature ionic liquid (RTIL)	C101	$(C_6H_{13})_3(C_{14}H_{29})PCl$	Cyphos 101 (trihexmethyltetradecyl phosphonium chloride)
		BMIM	$C_8H_{15}ClN_2$	BMIM chloride (1-butyl-3-methylimidazolium chloride)

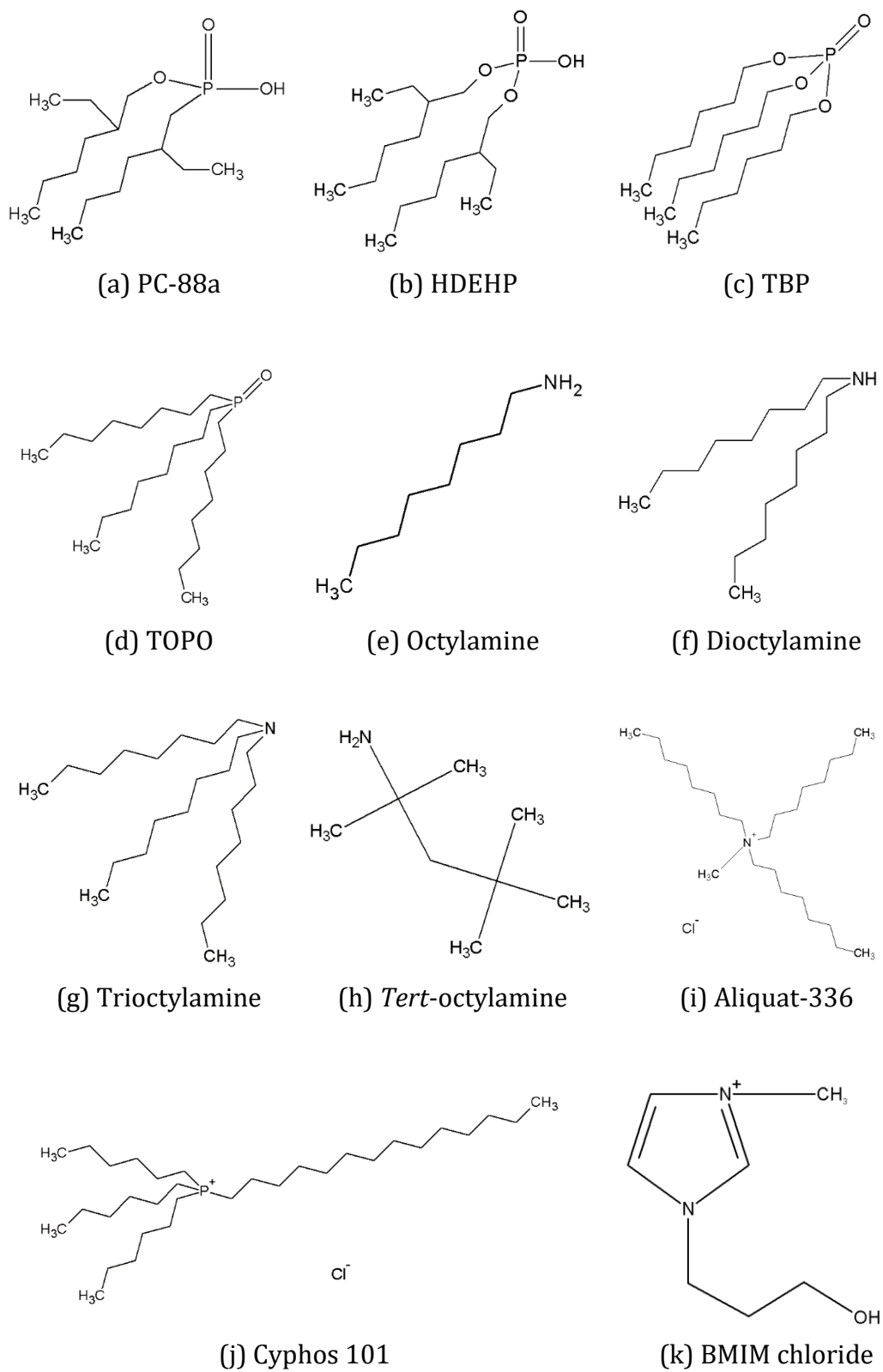


FIGURE 6.1 – CHEMICAL STRUCTURES OF ORGANIC EXTRACTANTS USED IN THE STUDY.

6.2.2 EXPERIMENTAL TECHNIQUE

For the solvent extraction contacts 5 ml volumes of both organic and aqueous phases were used in all cases. The organic phase was prepared as 0.1 M PC-88a and 0.05 M secondary extractant by taking 2.5 ml of the previously prepared 0.2 M PC-88a solution, adding 0.25 mmol of the secondary extractant by mass, and making the volume to 5 ml with *n*-dodecane. 4.96 ml of the required acid was added and the phases were manually shaken to pre-equilibrate the acidity of the phases. 0.04 ml of the mixed metal spike was then added and the contact vial was manually shaken for five minutes to perform the contact, which was enough time for the bulk of the thorium to be extracted, based on literature data [253]. The strength of agitation was judged sufficient to fully inter-disperse the phases, and phase separation was rapid (< 10 s). 1 ml aliquots of the post-contact aqueous phase were taken and diluted with 1% analytical grade nitric acid for ICP-MS analysis.

Diluted samples for ICP-MS analysis were expected to have approximately 10 ppm of each metal. Due to the limit of detection for the instrument being 0.001 ppm, the maximum D_M which can be reported is $\sim 10^4$. This was taken to indicate quantitative extraction of the metal in question.

In addition to the distribution ratio D_M , it is also useful to present the separation factors against thorium $\alpha_{M,Th}$ and uranium $\alpha_{M,U}$, which represents the separation of thorium or uranium from another metal M. The formula for separation factor is given in Equation (6.1).

$$\alpha_{M,Th} = \frac{D_M}{D_{Th}} \quad (6.1)$$

The error in separation factor may then be calculated using Equation (6.2), following the method described in Section 3.2.5.

$$\frac{\delta\alpha_{M,Th}}{|\alpha_{M,Th}|} = \sqrt{\left(\frac{\delta D_M}{D_M}\right)^2 + \left(\frac{\delta D_{Th}}{D_{Th}}\right)^2} \quad (6.2)$$

From the errors measured in Table 3.2 the errors in the separation factor can be calculated. These are presented in Table 6.2.

TABLE 6.2 – CALCULATED PERCENTAGE ERRORS IN METAL SEPARATION FACTORS.

METAL	% ERROR IN D_M FROM EQUATION (3.8)	% ERROR IN $\alpha_{M,Th}$ FROM EQUATION (6.2)	% ERROR IN $\alpha_{M,U}$ FROM EQUATION (6.2)
Th	8.53%	N/A	15.58%
U	13.04%	15.58%	N/A
Fe	6.00%	10.43%	14.35%
Zr	2.63%	8.93%	13.30%

6.3 RESULTS

Distribution ratio data are presented by aqueous phase in Figure 6.2 (hydrochloric acid), Figure 6.3 (nitric acid) and Figure 6.4 (sulfuric acid). Two graphs are presented per acid, one for each aqueous acidity level. Abbreviated names as given in Table 6.1 are used to refer to the extractants in these figures. "PC-88a" indicates that no secondary extractant was added, thus giving a total extractant concentration in these samples of 0.1 M, as opposed to 0.15 M in the mixed samples. Lines between data points are a guide to the eye only.

Numerical results of D_M are tabulated in Appendix D to this thesis.

6.3.1 ERROR CALCULATION

The errors in metal concentration measurements were determined according to the method outlined in Section 3.2.2.

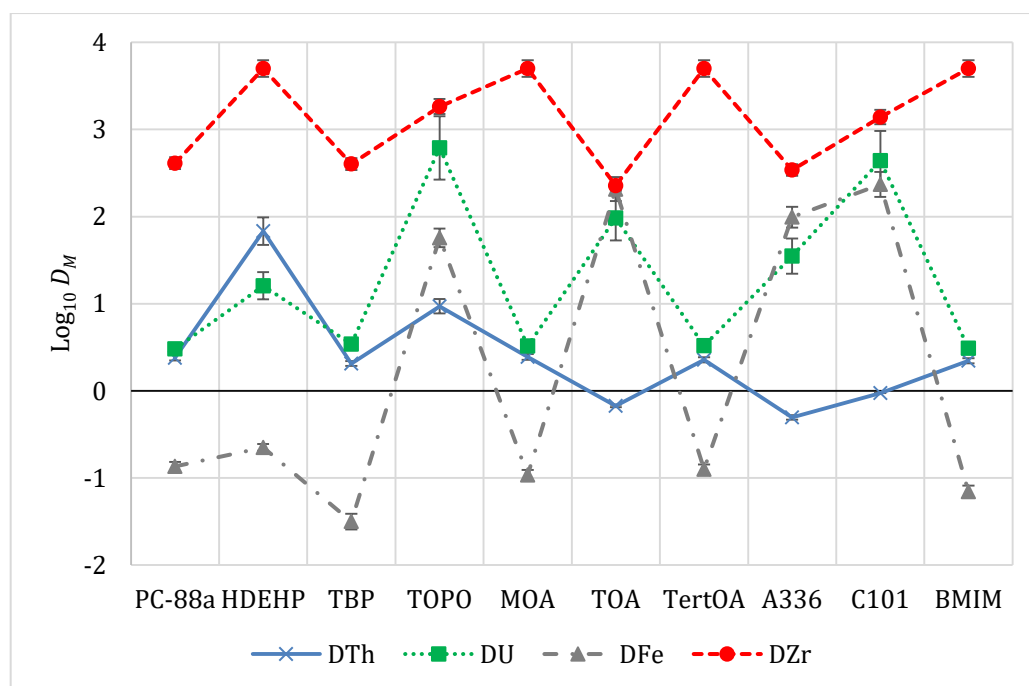
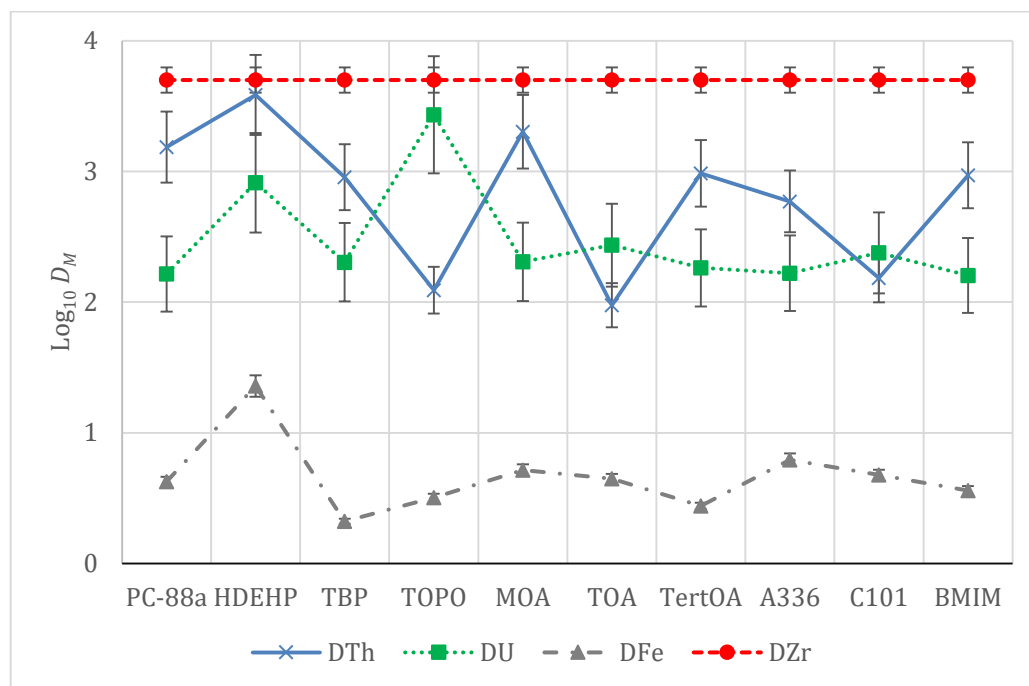


FIGURE 6.2 – LOGARITHMIC DISTRIBUTION RATIOS WITH 0.5 M HYDROCHLORIC ACID (TOP) AND 3.0 M HYDROCHLORIC ACID (BOTTOM) AS THE AQUEOUS PHASE. RESULTS FOR 5 ML ACID WITH 100 PPM EACH METAL AGAINST 5 ML OF 0.1 M PC-88A AND 0.05 M OTHER EXTRACTANT IN *N*-DODECANE, WITH 5 MIN CONTACT TIME AT ROOM TEMPERATURE.

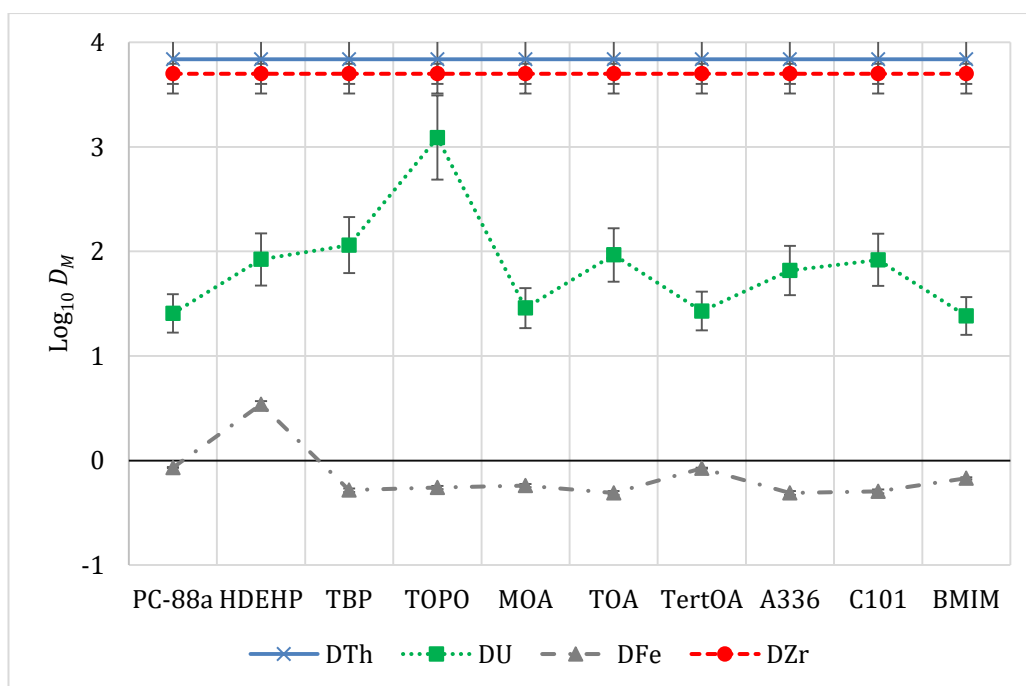
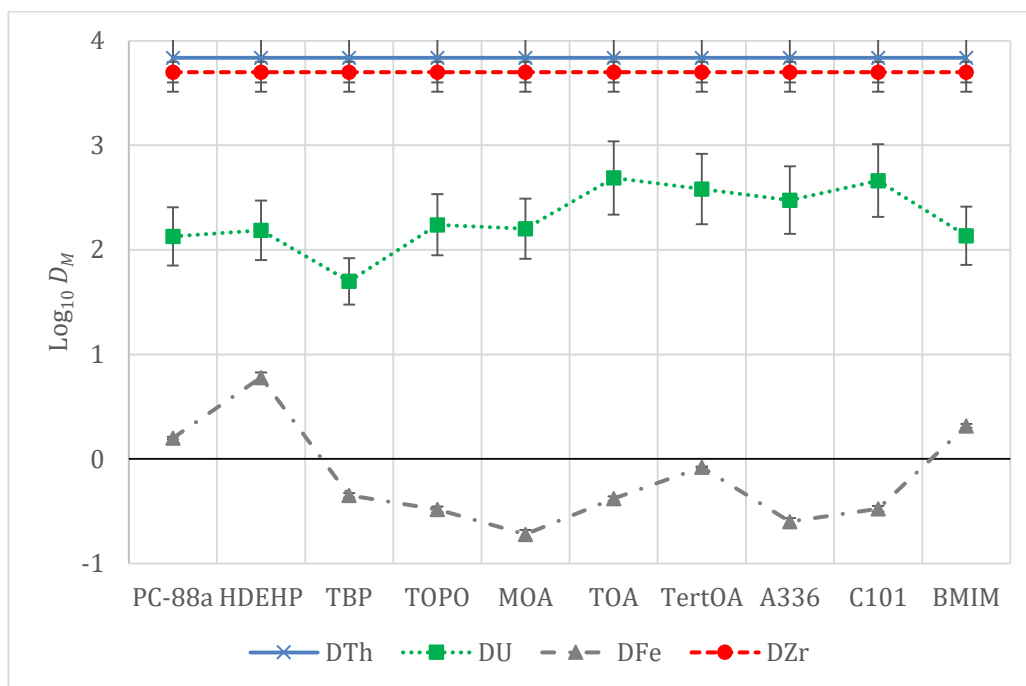


FIGURE 6.3 – LOGARITHMIC DISTRIBUTION RATIOS WITH 0.5 M NITRIC ACID (TOP) AND 3.0 M NITRIC ACID (BOTTOM) AS THE AQUEOUS PHASE. RESULTS FOR 5 ML ACID WITH 100 PPM EACH METAL AGAINST 5 ML OF 0.1 M PC-88A AND 0.05 M OTHER EXTRACTANT IN *n*-DODECANE, WITH 5 MIN CONTACT TIME AT ROOM TEMPERATURE.

THE PREPARATION AND APPLICATION OF THORIUM-BASED NUCLEAR FUELS

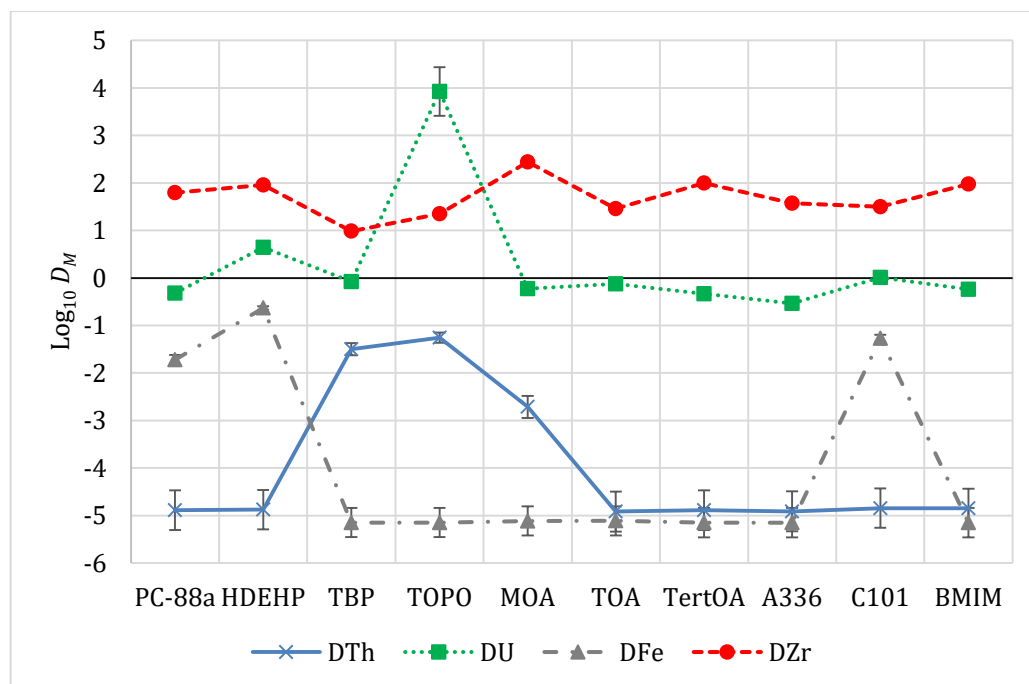
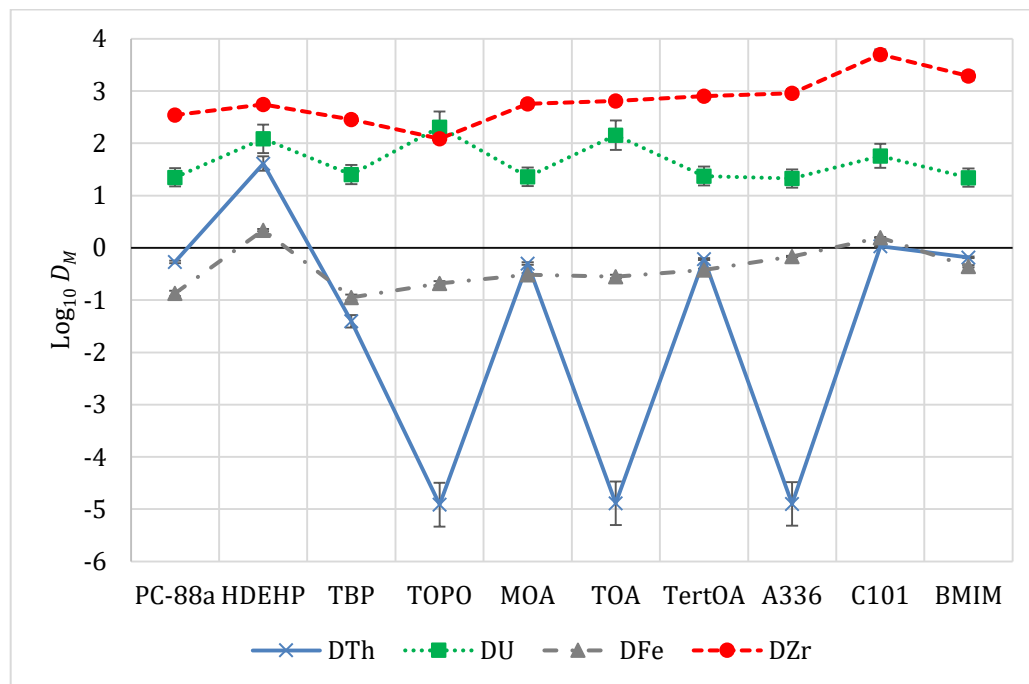


FIGURE 6.4 – LOGARITHMIC DISTRIBUTION RATIOS WITH 0.5 M SULFURIC ACID (TOP) AND 3.0 M SULFURIC ACID (BOTTOM) AS THE AQUEOUS PHASE. RESULTS FOR 5 ML ACID WITH 100 PPM EACH METAL AGAINST 5 ML OF 0.1 M PC-88A AND 0.05 M OTHER EXTRACTANT IN *n*-DODECANE, WITH 5 MIN CONTACT TIME AT ROOM TEMPERATURE.

6.3.2 THIRD PHASE FORMATION BY DIOCTYLAMINE

Dioctylamine is not presented in the results, as when exposed to acidic aqueous media a white, solid third phase was formed, which originally formed as a dispersion throughout the sample contact vial. High speed centrifugation of the vial compacted the third phase into a brittle, solid disc at the aqueous-organic phase interface. The third phase also occurred when dioctylamine in *n*-dodecane was exposed to acid in the absence of PC-88a or added metals, indicating that the third phase is a product of some interaction of the dioctylamine and the acid. No literature information could be found regarding this behaviour, and no other secondary extractant gave this behaviour, including the other amines. As a result no further study of dioctylamine was carried out in this work.

6.4 DISCUSSION

As can be seen from the results presented above, there is a significant variation in extraction of the four metals between different aqueous and organic phases. The results are discussed first for a given aqueous phase, and then comparisons will be drawn across the three aqueous phases.

6.4.1 IDENTIFICATION OF POTENTIAL SEPARATION SYSTEMS

Indicators of a good solvent extraction system for the separation of thorium or uranium from other metals may be characterised by one of three sets of distribution/separation data. These are expressed below for thorium, but the similar form exists for uranium (i.e. high $\log_{10} D_U$ with $\log_{10} \alpha_{Fe,U}$, $\log_{10} \alpha_{Zr,U}$ and $\log_{10} \alpha_{Th,U}$ all significantly below zero).

- High $\log_{10}(D_{Th})$, with $\log_{10} \alpha_{Fe,Th}$, $\log_{10} \alpha_{Zr,Th}$ and $\log_{10} \alpha_{U,Th}$ all significantly below zero, indicating extraction of thorium into the organic phase with rejection of other elements – thorium is extracted with high selectivity.

THE PREPARATION AND APPLICATION OF THORIUM-BASED NUCLEAR FUELS

- Low $\log_{10}(D_{Th})$ with $\log_{10} \alpha_{Fe,Th}$, $\log_{10} \alpha_{Zr,Th}$ and $\log_{10} \alpha_{U,Th}$ all significantly above zero, indicating rejection of thorium by the organic phase which accepts other elements well – thorium is rejected while other elements are extracted.
- $\log_{10}(D_{Th}) \sim 1$ with $\log_{10} \alpha_{Fe,Th}$, $\log_{10} \alpha_{Zr,Th}$ and $\log_{10} \alpha_{U,Th}$ all far from zero, indicating strong separation of thorium from other elements, even if thorium itself distributes relatively evenly across the organic and aqueous phases – other elements are rapidly extracted or rejected, while thorium may be partitioned to one phase with multiple contact stages.

For $\alpha_{M,Th}$ or $\alpha_{M,Th}$ values around unity further processing steps will likely be required to separate the thorium or uranium from the contaminant M.

Multiple contact stages may be able to perform the separation to a satisfactory level, although more stages lead to increased costs. Hence, strong separation factors are desirable.

As two acidities were investigated for each system, it may be apparent that systems exist where the acidity could be varied in order to move from one set of desirable extraction behaviour to another. For example, a system might exhibit strong extraction of all metals at high acidity, and reject thorium and/or uranium at low acidity while retaining other metals. This could form the basis of a promising extraction and back-extraction circuit.

Figure 6.5, Figure 6.6 and Figure 6.7 show the distribution ratio for thorium D_{Th} and the separation factors for other metals against thorium $\alpha_{M,Th}$, for hydrochloric acid, nitric acid and sulfuric acid respectively.

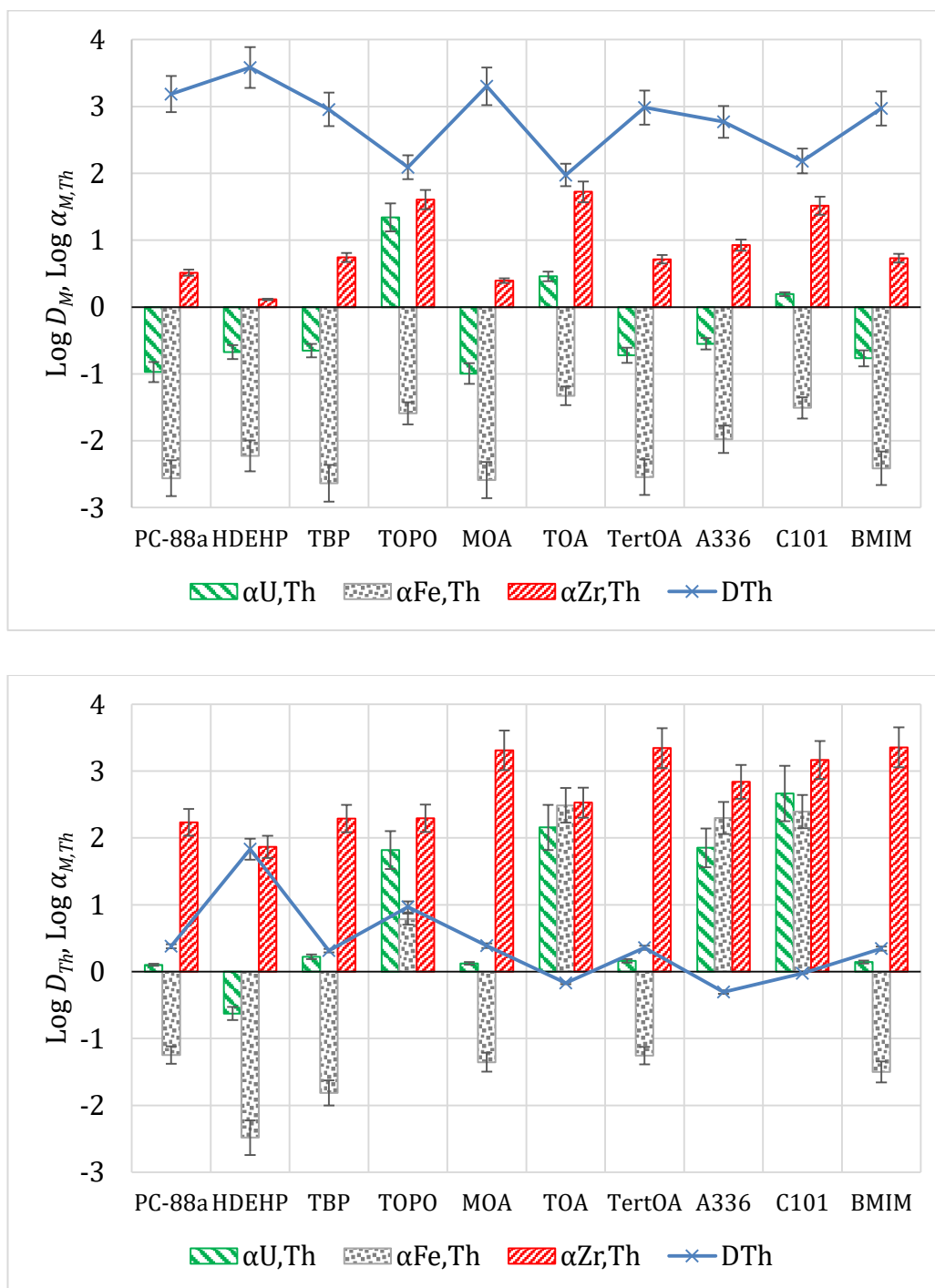


FIGURE 6.5 – LOGARITHMIC DISTRIBUTION RATIO FOR THORIUM (LINE) AND LOGARITHMIC SEPARATION FACTORS FOR CO-CONTAMINANTS AGAINST THORIUM (BARS) WITH 0.5 M HYDROCHLORIC ACID (TOP) OR 3.0 M HYDROCHLORIC ACID (BOTTOM) AS THE AQUEOUS PHASE. RESULTS FOR 5 ML ACID WITH 100 PPM EACH METAL AGAINST 5 ML OF 0.1 M PC-88A AND 0.05 M OTHER EXTRACTANT IN *N*-DODECANE, WITH 5 MIN CONTACT TIME AT ROOM TEMPERATURE.

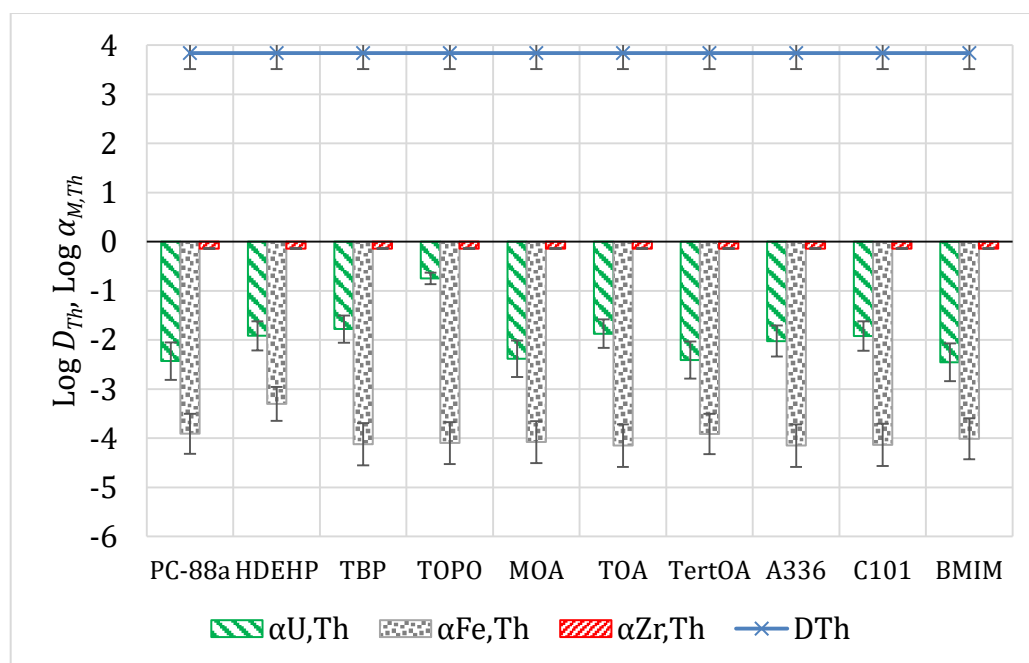
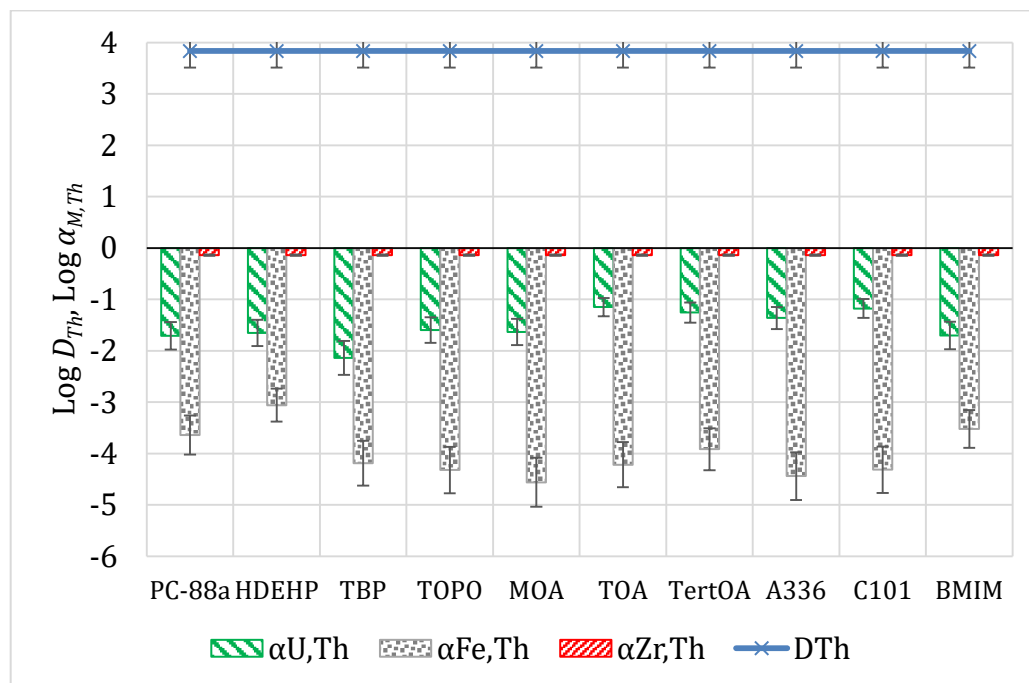


FIGURE 6.6 – LOGARITHMIC DISTRIBUTION RATIO FOR THORIUM (LINE) AND LOGARITHMIC SEPARATION FACTORS FOR CO-CONTAMINANTS AGAINST THORIUM (BARS) WITH 0.5 M NITRIC ACID (TOP) OR 3.0 M NITRIC ACID (BOTTOM) AS THE AQUEOUS PHASE. RESULTS FOR 5 ML ACID WITH 100 PPM EACH METAL AGAINST 5 ML OF 0.1 M PC-88A AND 0.05 M OTHER EXTRACTANT IN *N*-DODECANE, WITH 5 MIN CONTACT TIME AT ROOM TEMPERATURE.

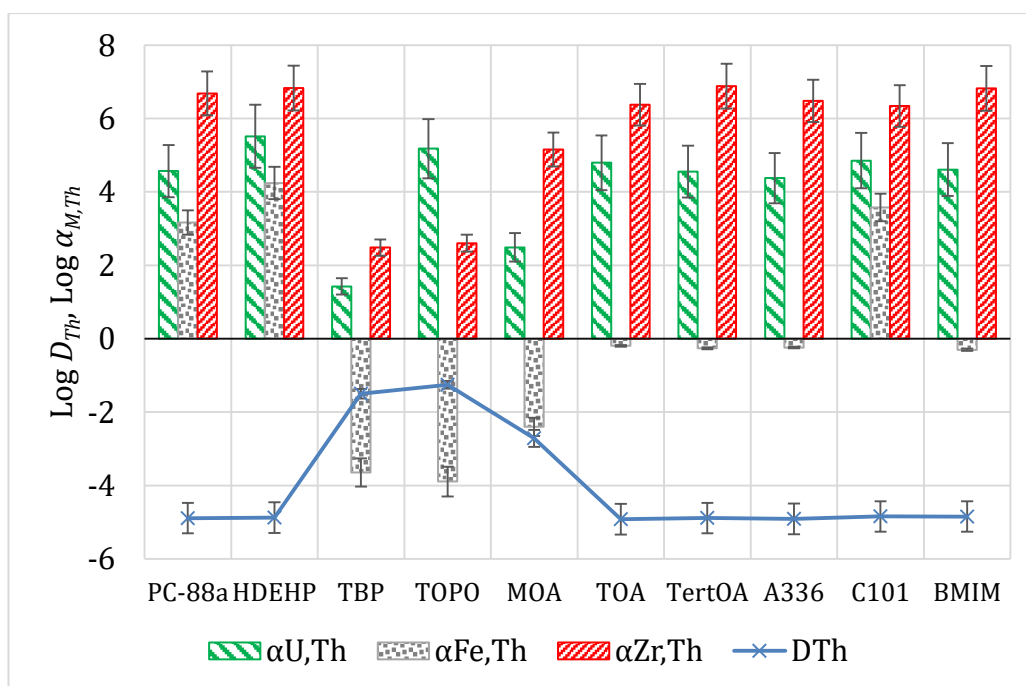
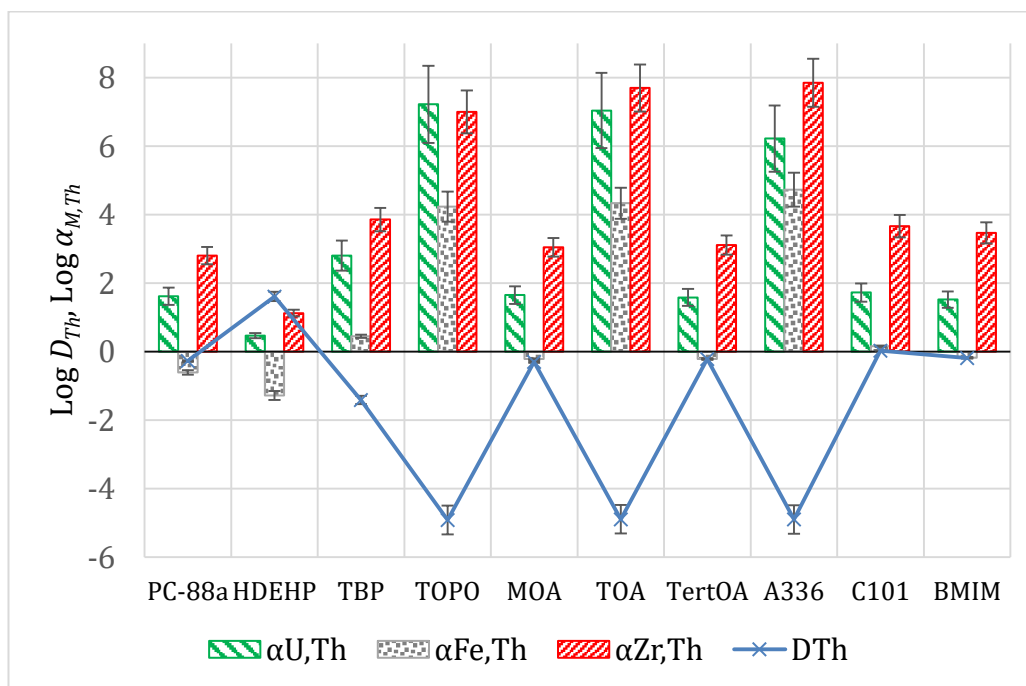


FIGURE 6.7 – LOGARITHMIC DISTRIBUTION RATIO FOR THORIUM (LINE) AND LOGARITHMIC SEPARATION FACTORS FOR CO-CONTAMINANTS AGAINST THORIUM (BARS) WITH 0.5 M SULFURIC ACID (TOP) OR 3.0 M SULFURIC ACID (BOTTOM) AS THE AQUEOUS PHASE. RESULTS FOR 5 ML ACID WITH 100 PPM EACH METAL AGAINST 5 ML OF 0.1 M PC-88A AND 0.05 M OTHER EXTRACTANT IN *N*-DODECANE, WITH 5 MIN CONTACT TIME AT ROOM TEMPERATURE.

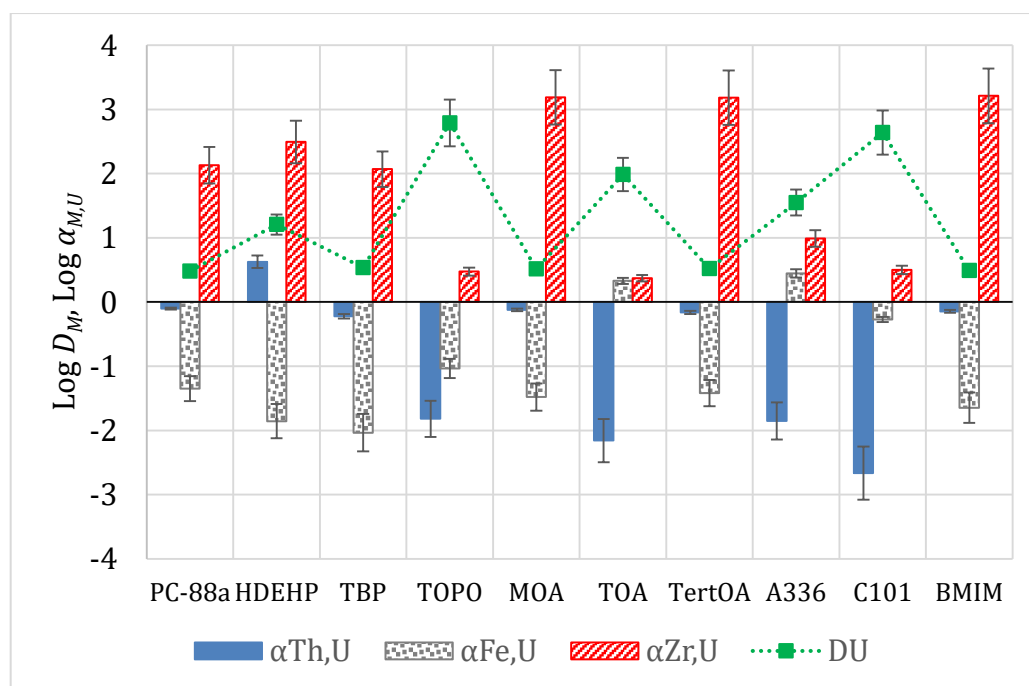
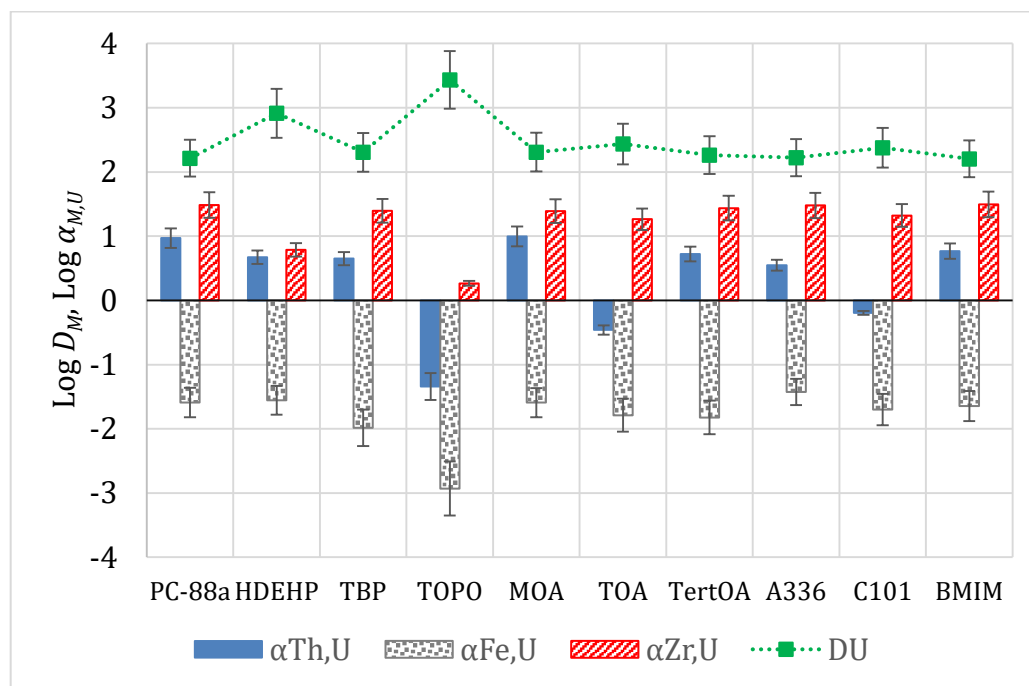


FIGURE 6.8 – LOGARITHMIC DISTRIBUTION RATIO FOR URANIUM (LINE) AND LOGARITHMIC SEPARATION FACTORS FOR CO-CONTAMINANTS AGAINST URANIUM (BARS) WITH 0.5 M HYDROCHLORIC ACID (TOP) OR 3.0 M HYDROCHLORIC ACID (BOTTOM) AS THE AQUEOUS PHASE. RESULTS FOR 5 ML ACID WITH 100 PPM EACH METAL AGAINST 5 ML OF 0.1 M PC-88A AND 0.05 M OTHER EXTRACTANT IN *N*-DODECANE, WITH 5 MIN CONTACT TIME AT ROOM TEMPERATURE.

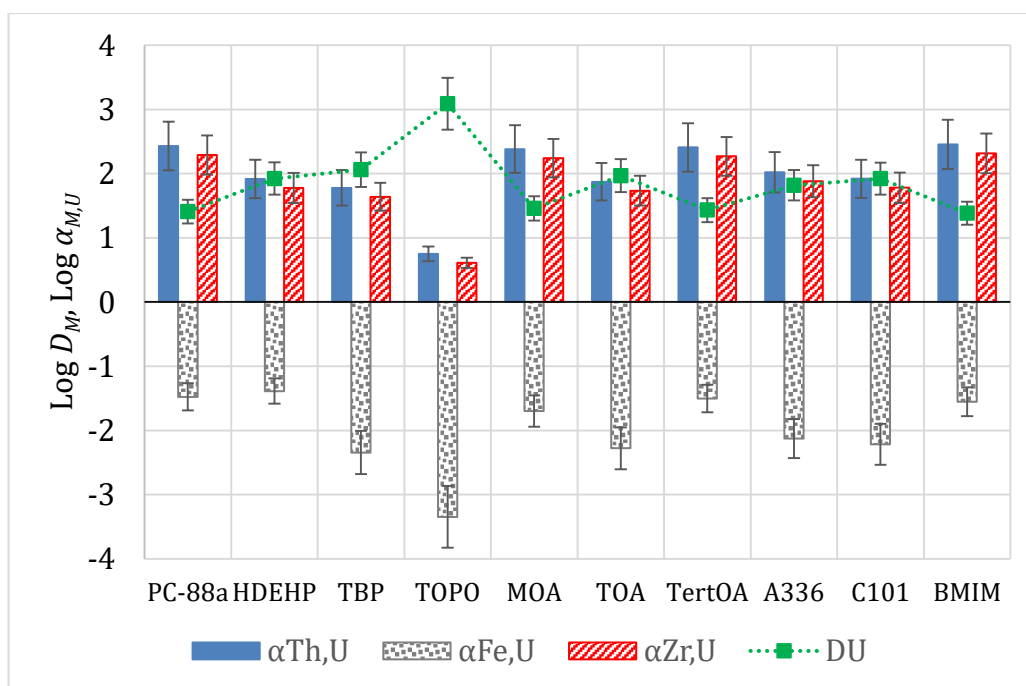
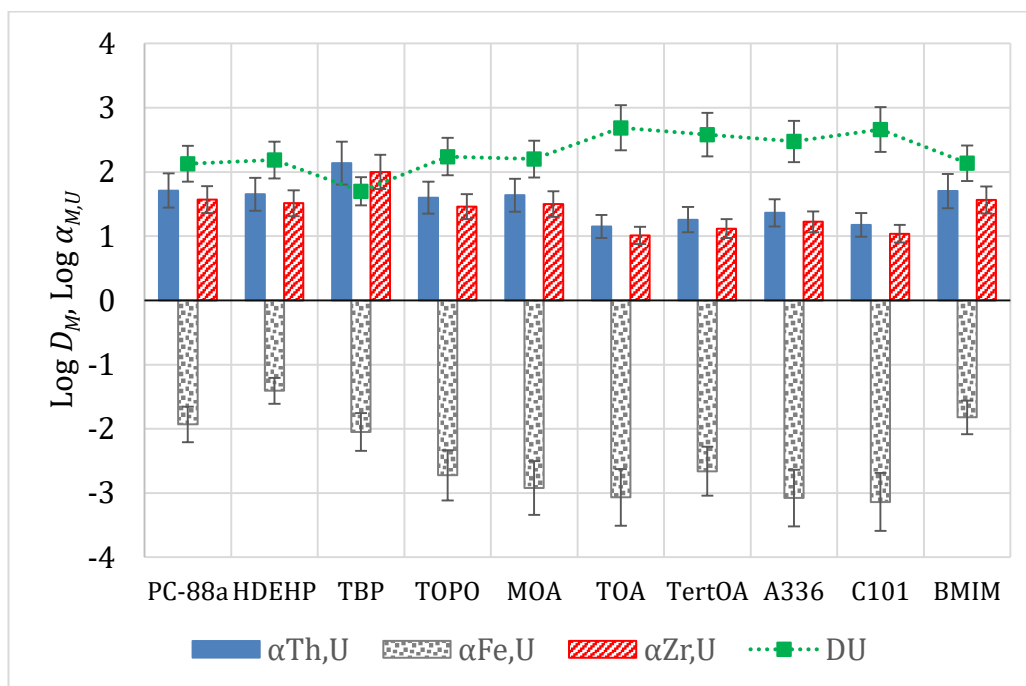


FIGURE 6.9 – LOGARITHMIC DISTRIBUTION RATIO FOR URANIUM (LINE) AND LOGARITHMIC SEPARATION FACTORS FOR CO-CONTAMINANTS AGAINST URANIUM (BARS) WITH 0.5 M NITRIC ACID (TOP) OR 3.0 M NITRIC ACID (BOTTOM) AS THE AQUEOUS PHASE. RESULTS FOR 5 ML ACID WITH 100 PPM EACH METAL AGAINST 5 ML OF 0.1 M PC-88A AND 0.05 M OTHER EXTRACTANT IN *N*-DODECANE, WITH 5 MIN CONTACT TIME AT ROOM TEMPERATURE.

THE PREPARATION AND APPLICATION OF THORIUM-BASED NUCLEAR FUELS

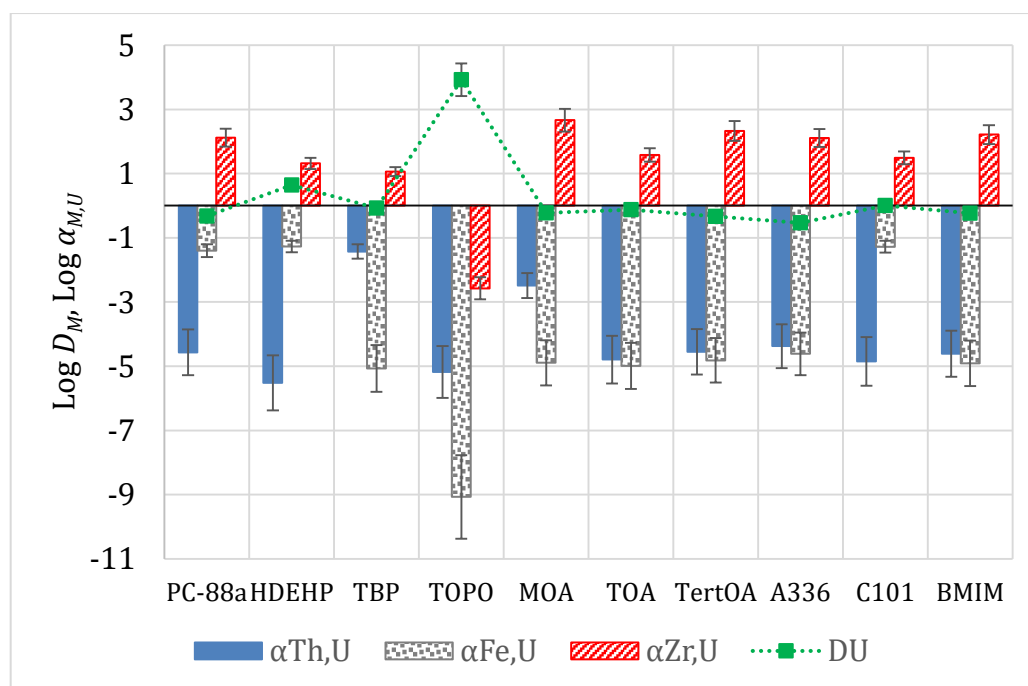
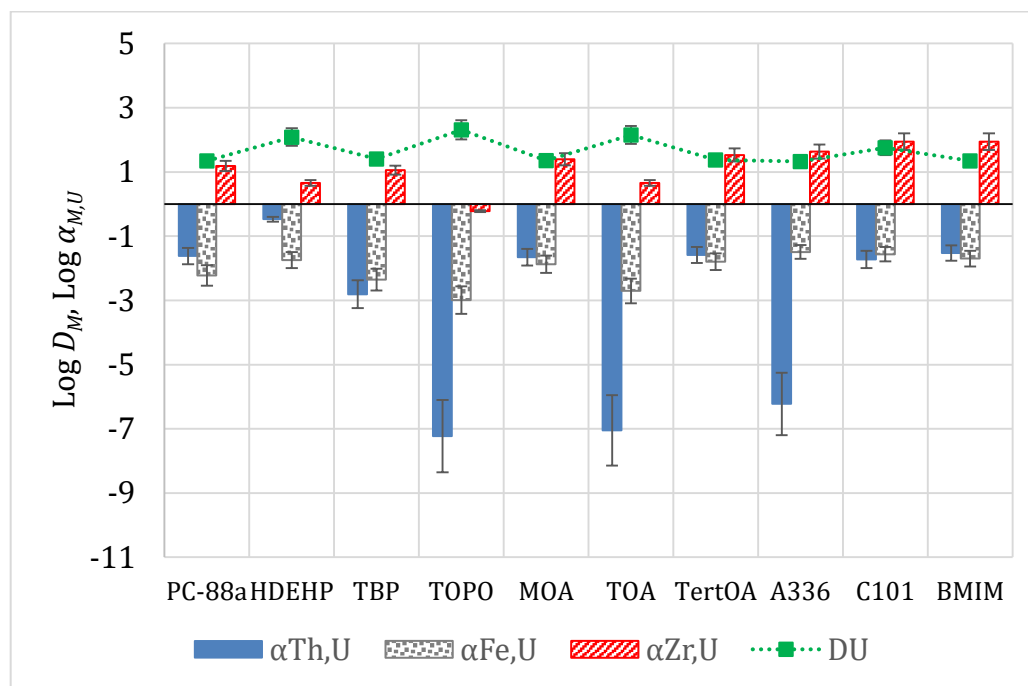


FIGURE 6.10 – LOGARITHMIC DISTRIBUTION RATIO FOR URANIUM (LINE) AND LOGARITHMIC SEPARATION FACTORS FOR CO-CONTAMINANTS AGAINST URANIUM (BARS) WITH 0.5 M SULFURIC ACID (TOP) OR 3.0 M SULFURIC ACID (BOTTOM) AS THE AQUEOUS PHASE. RESULTS FOR 5 ML ACID WITH 100 PPM EACH METAL AGAINST 5 ML OF 0.1 M PC-88A AND 0.05 M OTHER EXTRACTANT IN *N*-DODECANE, WITH 5 MIN CONTACT TIME AT ROOM TEMPERATURE.

Figure 6.8, Figure 6.9 and Figure 6.10 show the distribution ratio for uranium D_U and the separation factors for other metals against uranium $\alpha_{M,U}$, for hydrochloric acid, nitric acid and sulfuric acid respectively.

It should be borne in mind that the total concentration of extractant in the mixed systems was 0.15 M (0.1 M PC-88a + 0.05 M synergist), while the in PC-88a alone system the total extractant concentration was 0.1 M. As such, care should be taken in comparing the results for PC-88a alone to those for a secondary extractant, as differences between these may be due to the different extractant concentration rather than the use of different extractants. Unfortunately, as can be seen from the results presented in Chapter 3, it is not possible to simply extrapolate the impact of increased extractant concentration on distribution ratio.

6.4.2 EXTRACTION FROM HYDROCHLORIC ACID

6.4.2.1 THORIUM EXTRACTION FROM HYDROCHLORIC ACID

When extracting from 0.5 M hydrochloric acid, D_{Th} ranges from 100 to 4000 for all extractant combinations. HDEHP and MOA as secondary extractants give greater extraction than PC-88a alone. Other secondary extractants reduce the extraction of thorium compared to PC-88a alone, with TOPO, TOA and C101 giving the lowest extraction, although D_{Th} remains above 100.

Increasing the acidity greatly reduces extraction. The secondary extractants TOPO and HDEHP give good extraction, with D_{Th} of 10-100. For PC-88a alone and the other secondary extractants thorium distributes relatively evenly across the two phases.

6.4.2.2 URANIUM EXTRACTION FROM HYDROCHLORIC ACID

Uranium is well extracted from 0.5 M hydrochloric acid by PC-88a alone and all extractant pairings, with D_U of 150 – 280 for most. The use of TOPO or

HDEHP as the secondary extractant gives a stronger extraction than PC-88a alone.

For 3.0 M hydrochloric acid, uranium extraction is reduced overall. PC-88a alone and with TBP, MOA, TertOA and BMIM give $D_U \sim 3.2$, while others give increasing D_U in the order PC-88a < HDEHP < A336 < TOA < C101 \lesssim TOPO.

6.4.2.3 SEPARATION OF URANIUM AND THORIUM IN HYDROCHLORIC ACID

The separation factors for uranium against thorium were rarely greater than one order of magnitude, with TOPO giving the greatest separation due to the strong extraction of uranium and comparatively poor extraction of thorium. Separation factors for uranium in 3 M HCl were variable across the range of secondary extractants. Poor separation of the two actinides is given by PC-88a alone, TBP, MOA, TertOA and BMIM, whereas good separation is given by TOPO, TOA, A336 and C101.

6.4.2.4 SEPARATION OF CONTAMINANTS FROM THORIUM IN HYDROCHLORIC ACID

At 0.5 M HCl, iron is extracted with D_{Fe} in the range 2 – 25, with HDEHP giving the strongest extraction. TBP, TOPO, TertOA and BMIM reduce D_{Fe} below that of PC-88a alone. The separation factors are high across the range of organic phases due to the relatively poor extraction of iron compared to thorium. At 3.0 M HCl, iron is either strongly extracted or moderately rejected depending on the secondary extractant. PC-88a alone gives rejection with D_{Fe} of 0.14, and rejection is also given by TBP, HDEHP, MOA, TertOA and BMIM. However, increasingly strong D_{Fe} was given in the order TOPO < A336 < TOA \lesssim C101. Separation factors were variable, but generally strong, with the lowest being given by TOPO ($\alpha_{Fe,Th} = 6.1$).

Zirconium is extracted strongly from hydrochloric acid into the organic phase by all studied extractant combinations. When the hydrochloric acid

concentration is 0.5 M, zirconium is quantitatively extracted. When 3.0 M hydrochloric acid is used, the zirconium extraction is slightly reduced for many secondary extractants, although D_{Zr} remains very high in all cases. HDEHP, MOA, TertOA and BMIM give quantitative extraction. The lowest extraction is given by TOA ($D_{Zr} = 227$).

6.4.2.5 SEPARATION OF CONTAMINANTS FROM URANIUM IN HYDROCHLORIC ACID

Uranium is extracted more strongly than iron by all extractants from 0.5 M HCl, with TOPO giving the greatest separation due to the strong extraction of uranium given by mixtures of PC-88a and TOPO. Other extractant mixtures gave separation factors of between 26 and 100. From 3.0 M HCl, some extractant mixtures give greater extraction of iron than uranium, being trioctylamine and Aliquat-336. Cyphos 101 gives relatively poor separation of uranium and iron. The remainder give separation factors of 10-110, with uranium extracted more strongly than iron.

Zirconium is always extracted more strongly than uranium from hydrochloric acid solutions due to the strong or quantitative extraction of zirconium. The use of TOPO from the less concentrated acid gives poor separation due to the strong extraction of uranium. The greatest separation is achieved by those extractants which give lower uranium extraction.

6.4.2.6 SUMMARY OF EXTRACTION BEHAVIOUR FROM HYDROCHLORIC ACID

Overall, the correct selection of secondary extractant is vital to ensure separation of uranium and iron from thorium, particularly from 3.0 M HCl for uranium. At 0.5 M, $\alpha_{Fe,Th}$ values are consistently greater than from 3 M, but both uranium and thorium are very well extracted, making extractive separation of the target metals potentially difficult. At 3.0 M HCl, iron may be either moderately extracted or rejected depending on the secondary extractant, while thorium may distribute slightly into either phase and

uranium is either well ($D_U = 16-615$) or slightly ($D_U = \sim 3$) extracted. The distributions of iron and uranium for 3.0 M HCl follow a similar pattern across the range of secondary extractants; if D_U increases, D_{Fe} usually also increases, and this is true for decreases between extractants also. This suggests that PC-88a is dominating the extraction behaviour for these metals from 3.0 M HCl. Due to the strong extraction of zirconium, separation from thorium and uranium would have to be reliant on low values of D_{Th} and D_U , either by extracting all metals and then selectively back-extracting thorium and uranium, or by preferential extraction of zirconium.

6.4.3 EXTRACTION FROM NITRIC ACID

6.4.3.1 THORIUM EXTRACTION FROM NITRIC ACID

Complete extraction of thorium was observed for all studied organic phases from both 0.5 M and 3.0 M nitric acid. As PC-88a alone gave complete extraction, it can be assumed that any antagonism between PC-88a and the secondary extractant was insufficient to reject an observable quantity of thorium from the organic phase.

6.4.3.2 URANIUM EXTRACTION FROM NITRIC ACID

Uranium is well extracted into the organic phase from 0.5 M HNO_3 by all extractant pairings. Compared to PC-88a alone, TOA, TertOA, A336 and C101 give higher D_U , while TBP gives antagonism.

The extraction of uranium from 3.0 M HNO_3 is more variable. Values of D_U range from approximately 25-110 in most cases, with the exception of TOPO as the secondary extractant, which gives $D_U \sim 1000$.

6.4.3.3 SEPARATION OF URANIUM AND THORIUM IN NITRIC ACID

In 0.5 M HNO_3 , values of $\alpha_{U,Th}$ are all at least 10, and that of TBP exceeds 100. A separation of thorium and uranium from this aqueous medium would be therefore best achieved by the use of TBP as the secondary extractant to

minimise simultaneous extraction of uranium, although $D_U = 50$ for TBP. Values of $\alpha_{U,Th}$ are generally better for 3.0 M HNO₃ than for 0.5 M HNO₃.

6.4.3.4 SEPARATION OF CO-CONTAMINANTS FROM THORIUM IN NITRIC ACID

For 0.5 M HNO₃, PC-88a alone gives $D_{Fe} \sim 1$. Most secondary extractants are antagonistic, and give a slightly greater rejection of iron. The greatest rejection is given by MOA, with D_{Fe} of 0.2. HDEHP and BMIM are exceptions to this, extracting iron with D_{Fe} of 6.0 and 2.1 respectively. The fact that thorium is completely extracted across the range of extractants means that $\alpha_{Fe,Th}$ values are always very high. For 3.0 M HNO₃, a similar set of results is given. A slight tendency towards iron rejection is observed for all extractant pairings, with the exception of HDEHP as secondary extractant, which extracts with $D_{Fe} = 3.4$. As with $\alpha_{U,Th}$, strong separation is observed due to the complete extraction of thorium by all extractants.

6.4.3.5 SEPARATION OF CO-CONTAMINANTS FROM URANIUM IN NITRIC ACID

Across all extractant pairings and for both acid concentrations, the distribution ratio of uranium lies between those of iron (generally rejected except for with HDEHP) and zirconium (quantitatively extracted). Separation factors for iron are always >10 , and are >100 for seven of the secondary extractants. HDEHP gives the lowest separation, due to iron being extracted by this mixture.

The separation of uranium and zirconium is based on the non-quantitative extraction of uranium. For those mixtures which extract uranium strongly, the separation against zirconium will be reduced. Across both acid concentrations, the lowest separation factor is given by mixtures of TOPO and PC-88a from 3.0 M nitric acid, due to the strong extraction of uranium.

6.4.3.6 SUMMARY OF EXTRACTION BEHAVIOUR FROM NITRIC ACID

Overall, the extraction behaviour from nitric acid is characterised by quantitative extraction of the more charge dense metals, zirconium and thorium, across all studied organic phases. Selective extraction appears unlikely to deliver an effective separation of these two metals, and instead it may be necessary to rely on selective back-extraction. Uranium separation may be effected by using an extractant which gives slight uranium extraction which may be readily stripped of uranium while retaining thorium and zirconium in the organic phase. Iron is generally slightly rejected, allowing relatively easy separation of this metal.

6.4.4 EXTRACTION FROM SULFURIC ACID

6.4.4.1 THORIUM EXTRACTION FROM SULFURIC ACID

For 0.5 M H₂SO₄, thorium tends to either have complete rejection or a relatively even distribution. A slight rejection is observed for PC-88a alone and with MOA, TertOA and BMIM as secondary extractants. TOPO, TOA and A336 give complete rejection, and TBP gives moderate rejection.

Distribution is even between the phases for C101. HDEHP does not follow the other secondary extractants, giving a reasonably strong extraction. For 3.0 M H₂SO₄, thorium is rejected by all organic phases. PC-88a alone and many secondary extractants give complete rejection. MOA, TBP and TOPO give some measurable thorium extraction, but overall the great majority of the thorium still remains in the aqueous phase.

6.4.4.2 URANIUM EXTRACTION FROM SULFURIC ACID

For 0.5 M H₂SO₄, uranium is extracted well by all tested extractant pairings, with D_U in the range 20 – 200. TOPO gives the strongest extraction.

For 3.0 M H₂SO₄, D_U is close to unity, with slight rejection, for most extractant pairings. The main exception is when TOPO is used as the secondary extractant, which gives quantitative extraction of uranium.

6.4.4.3 SEPARATION OF URANIUM AND THORIUM IN SULFURIC ACID

From 0.5 M H₂SO₄, the extraction of thorium is much more variable as a function of secondary extractant choice than that of uranium. Thus, the distribution ratio of thorium dominates the separation factor. TOPO, trioctylamine and Aliquat-336 give the greatest separation as these secondary extractants give quantitative thorium rejection. Uranium is always more strongly extracted than thorium.

From 3.0 M H₂SO₄, again uranium is more strongly extracted than thorium across all extractants, with most mixtures giving strong or quantitative rejection of thorium, while uranium distributes quite evenly across the phases. Values of $\alpha_{U,Th}$ are strong across the range of extractants, although less so for TBP and MOA due to the weaker rejection of thorium.

6.4.4.4 SEPARATION OF CO-CONTAMINANTS FROM THORIUM IN SULFURIC ACID

For 0.5 M H₂SO₄, D_{Fe} is slightly below unity for most extractants. PC-88a alone and with TBP have D_{Fe} values of ~0.12. Other secondary extractants increase the overall extraction of iron, although slight rejection remains the trend. HDEHP and C101 give D_{Fe} greater than unity, although the maximum distribution ratio achieved is only 2.2, which is for HDEHP. Values of $\alpha_{Fe,Th}$ vary considerably, mainly as a function of D_{Th} . For 3.0 M H₂SO₄, iron rejection is even stronger. PC-88a alone has $D_{Fe} = 0.02$, but most secondary extractants give complete rejection. HDEHP and C101 give a comparatively minor rejection of iron, although D_{Fe} is greater than for PC-88a alone. Good $\alpha_{Fe,Th}$ values can be achieved except for with TOA, TertOA, A336 and BMIM, which reject both thorium and iron.

Zirconium is well extracted from sulfuric acid at both acidities, although overall extraction is stronger from the less concentrated acid. For 0.5 M H₂SO₄, the use of TBP or TOPO reduces D_{Zr} compared to PC-88a alone. Other extractants give slightly increased D_{Zr} , and C101 gives quantitative

extraction of zirconium. This strong extraction gives high $\alpha_{Zr,Th}$ for all systems except with HDEHP, due to it extracting both thorium and zirconium, as well as uranium and to a lesser extent iron. For 3.0 M H₂SO₄, D_{Zr} ranges from 10 – 280. Many secondary extractants show antagonism for zirconium, as can be observed by the reduced D_{Zr} relative to that of PC-88a alone. MOA gave the strongest D_{Zr} . Values of $\alpha_{Zr,Th}$ are strong across the range of extractants, and strongest for those which reject thorium.

6.4.4.5 SEPARATION OF CO-CONTAMINANTS FROM URANIUM IN SULFURIC ACID

As iron is generally rejected from the organic phase into sulfuric acid, the separation of iron and uranium in 0.5 M sulfuric acid media is quite achievable. Separation factors were found to lie between 30 (Aliquat-336) and 1000 (TOPO). From 3.0 M acid separation factors were generally much stronger, due to the quantitative rejection of iron for most secondary extractants. The greatest separation is again given by TOPO, due to it also strongly extracting uranium while rejecting iron.

Strong sulfuric acid was observed to reduce the distribution ratio of zirconium. While the metal is still extracted, the extraction is no longer quantitative. TOPO as the secondary extractant actually gives a strong negative value of $\log_{10} \alpha_{Zr,U}$, with uranium being quantitatively extracted while $D_{Zr} = 22$, and iron and thorium are rejected. Uranium extraction is also stronger than zirconium extraction from 0.5 M H₂SO₄, but the separation factor is very small (0.6). For other secondary extractants the separation factor varies in the range 11 (TBP) to 460 (octylamine) for 3.0 M acid and in the range 5 (TBP) to 88 (BMIM chloride) for 0.5 M acid.

6.4.4.6 SUMMARY OF EXTRACTION BEHAVIOUR FROM SULFURIC ACID

Thorium exhibits quite different behaviour depending on the concentration of H₂SO₄. Sulfuric acid appears to be the most difficult aqueous medium of

those studied from which to extract thorium with the studied organic media. However, the extraction of co-contaminants is much greater than that of thorium, and thus selective extraction of co-contaminants might form the basis of a successful separation flowsheet. In contrast, the distribution of uranium from sulfuric acid media is generally only slightly affected by the secondary extractant, with TOPO being the major exception. TOPO gives good separation of uranium from iron and thorium, but unfortunately this results in a poor separation factor against zirconium.

6.4.5 SUMMARY OF EXTRACTION BEHAVIOURS

Across the various aqueous and organic phases studied, some general observations may be recorded. This section presents a summary of the extraction behaviour of the four metals of interest reported in detail above.

Thorium extraction is highly variable depending on the selection of aqueous and organic phase. For hydrochloric acid, extraction at 0.5 M is strong, but this is reduced at 3.0 M HCl, often to the point of equal thorium distribution between phases. Nitric acid gives complete extraction into all organic phases at either of the studied acidities. Sulfuric acid at 0.5 M may either slightly or completely reject thorium, although HDEHP gives quite strong extraction from this medium, while 3.0 M H₂SO₄ reduces D_{Th} across the range, giving complete rejection in most cases. In general, thorium is most easily extracted from nitric acid, followed with hydrochloric acid and then sulfuric acid. This follows the order of decreasing thorium species stability constants, as was shown in Table 3.7 (page 130), indicating that the extractant is competing with the anions in solution for the metal.

Uranium is extracted well from most aqueous media, with the exception of 3.0 M sulfuric acid, in which case it gives even distribution across the phases. Hydrochloric acid gives $D_U > 100$ for all secondary extractants at low acidity, and while this reduces at higher acidity the general trend remains towards extraction. Extraction was stronger from nitric acid at each

concentration, with mixtures of PC-88a and TOPO extracting particularly strongly from 3.0 M nitric acid. From sulfuric acid, the extraction of uranium is more dependent on acid concentration. At low acidity, uranium is well extracted by mixtures of PC-88a and the secondary extractants, with $D_U > 10$ for all mixtures. However, increasing the acidity to 3.0 M leads to a reduction in extraction, with uranium distribution evenly across the phases. This is with the exception of TOPO as secondary extractant, which gives increased uranium extraction.

Uranium and thorium separation factors are highly variable across the range of studied systems. Uranium is never strongly rejected by the organic phase, and is often well extracted, although 3.0 M hydrochloric or sulfuric acid can give a relatively even distribution between phases with the use of some secondary extractants.

Iron often distributes equally between the phases. Nitric acid and 0.5 M sulfuric acid gave mostly equal distributions, but 3.0 M sulfuric acid often led to iron being strongly rejected. 0.5 M hydrochloric acid generally gives extraction with D_{Fe} between 2.1 and 6.2. However, 3.0 M HCl produced a set of either moderate rejections or strong extractions.

Zirconium is extracted well from all acids by all organic phases, and thorium/zirconium separation will likely best be done by selective back-extraction of thorium, leaving zirconium in the organic phase. If extractive separation of zirconium and thorium were required, this would likely need to be accomplished at plant scale either by a rapid contact to remove the bulk of the zirconium from the feed, followed by thorium extraction in later steps, or by some variation in extraction conditions beyond the scope of the work presented in this chapter.

6.4.6 SUGGESTED SEPARATIONS SYSTEMS FOR FURTHER DEVELOPMENT

6.4.6.1 THORIUM SEPARATIONS FROM HYDROCHLORIC ACID MEDIA

Thorium is extracted well by PC-88a and HDEHP from both concentrations of hydrochloric acid, being quantitatively extracted from 0.5 M acid. When searching for a simultaneous separation of thorium from the three co-contaminants, an effective system will be to begin with 0.5 M hydrochloric acid, using PC-88a and A336 as the extractants. Zirconium is loaded completely, thorium and uranium are loaded strongly, and iron is loaded moderately. Back-extraction could then be performed by increasing the acid concentration to 3.0 M. The co-contaminants will remain in the organic phase, but thorium will be rejected to an aqueous product stream. However, a large number of back-extraction stages may be required due to the relatively weak rejection of thorium under these conditions. More concentrated HCl is predicted to further reduce D_{Th} , which may optimise this process. Additionally, suitable back-extraction processes must be devised for Fe, U and Zr in order to allow the organic phase to be recycled.

6.4.6.2 THORIUM SEPARATIONS FROM NITRIC ACID MEDIA

Based on the data presented in this chapter, it is difficult to recommend a promising separation system for thorium in nitric acid based on PC-88a and a secondary extractant. Across the range of extractants and at both acidities, thorium and zirconium are both quantitatively extracted, and uranium extraction is strong at all tested conditions. At either of the tested acidities, MOA would give iron rejection, as the secondary extractant with the lowest value of D_{Fe} at low acidity, and on par with a number of others at the higher acidity. The greatest uranium separation is given by PC-88a alone from 3.0 M HNO_3 . Nitric acid systems are not recommended for further development.

6.4.6.3 THORIUM SEPARATIONS FROM SULFURIC ACID MEDIA

The most effective separation of thorium from co-contaminants in sulfuric acid media is likely to be based on selective rejection or back-extraction of thorium, while the co-contaminants are largely partitioned to the organic phase. The use of Aliquat-336 as the secondary extractant at low acidity gives strong extraction of uranium and zirconium while thorium is rejected. Iron is slightly rejected, but multiple extraction stages could be used to extract the iron. Alternatively, some variation in extraction conditions may be able to increase iron extraction per stage.

If HDEHP were to be used as the secondary extractant at low acidity all four metals are extracted to some degree. If back-extraction were to be performed at high acidity thorium would then be completely rejected and iron slightly rejected, while uranium and zirconium would remain largely in the organic phase. More precise pH control between these two extremes may find a condition where the separation factors can be further increased, allowing iron to be retained in the organic phase while thorium is back-extracted.

The decrease in D_{Th} is greater than the decrease in D_{Fe} between 0.5 M and 3.0 M acidity, and if the relationship between D and acidity is assumed to be constant then the point where $D_{Th} = D_{Fe}$ is at 1.077 M, as shown in Figure 6.11. The required acidity to give extraction of thorium but rejection of iron is between 1.122 M and 1.375 M. The condition for equal extraction of thorium and rejection of uranium, where D_{Th} and D_{Fe} are equidistant from unity, is given by Equation (6.3).

$$\log D_{Th} + \log D_{Fe} = 0 \quad (6.3)$$

This condition is given by an acid concentration of 1.161 M, which gives a separation factor of 0.65.

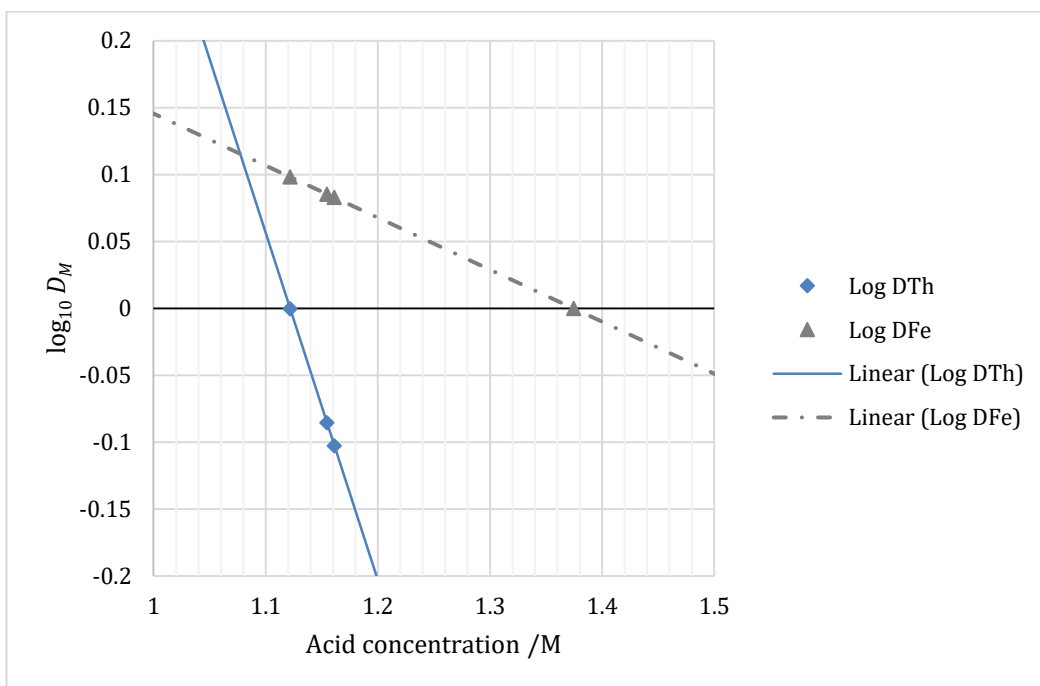


FIGURE 6.11 – INTERPOLATION OF DISTRIBUTION RATIOS FOR THORIUM AND URANIUM EXTRACTED FROM SULFURIC ACID AT ACIDITIES 0.5 M AND 3.0 M BY A MIXTURE OF 0.1 M PC-88A AND 0.05 M HDEHP IN *n*-DODECANE.

6.4.6.4 URANIUM SEPARATIONS FROM HYDROCHLORIC ACID OR NITRIC ACID

For both concentrations tested of hydrochloric acid and nitric acid, uranium was found to be extracted well. As such, back extraction of uranium by these acids is not possible at 0.5 M or 3.0 M acidity. Other concentrations or the addition of counterions such as sulfate may be used to strip uranium with these acids. With sulfuric acid, a high acid concentration may be used to strip uranium, although it appears that acid concentrations of greater than 3.0 M are required for effective stripping.

The use of a different loading acid and stripping acid might be used to give effective separation of uranium from hydrochloric or nitric acid media. However, this is likely to lead to contamination of the strip solution by unwanted ions carried over from the aqueous feed, particularly if the extracted complex includes anions from the acid, as is common for solvation and anion exchange mechanisms. For example, if uranium were to be

extracted as an organic uranyl nitrate complex, the back extraction would lead to nitrate addition to the stripping solution, likely resulting in reduced stripping efficiency.

6.4.6.5 URANIUM SEPARATIONS FROM SULFURIC ACID MEDIA

The use of sulfuric acid as both aqueous feed and stripping solution prevents contamination of the stripping solution by anions from the feed. As thorium is poorly recovered from sulfuric acid due to formation of relatively stable thorium sulfate sulfuric acid offers good opportunities to recover uranium only, leaving thorium in the aqueous raffinate, as is performed with the Interim-23 process. Trioctylamine offers a system which can strongly load uranium and zirconium from a dilute sulfuric acid feed, leaving iron and particularly thorium in the raffinate. Increasing the acidity then allows uranium to be selectively stripped, retaining zirconium in the organic phase. Use of acidities > 3.0 M should allow greater uranium back-extraction. This gives advantages over the use of PC-88a alone, which does not reject thorium very strongly at 0.5 M. Aliquat-336 gives greater uranium rejection at 3.0 M, but iron is not so strongly rejected during the extraction from 0.5 M acid. Overall, some further detail of the relationship between acidity and distribution ratio is required to make good recommendations about these systems.

For recovery of both uranium and thorium, the PC-88a/HDEHP mixture is recommended, either loading all metals at 0.5 M acid, and then selectively rejecting thorium at ~1.16 M and iron at ~3.0 M. It is believed that uranium may be then rejected at higher acidities, although further experimental work would be required to determine whether uranium is stripped by strong acid, or possibly by increasing the concentration of sulfate anion.

6.5 CONCLUSIONS

The screening study presented in this chapter was useful in determining promising systems from a range of aqueous and organic phases, and based on these results the next step was to select one or more systems for further detailed development.

The chosen system should ideally strongly extract thorium and/or uranium and reject other metals, or strongly extract other metals while rejecting thorium and/or uranium. It can be seen from the results of the screening experiments that no such system was found among those tested. However, a number of systems do exist where the target metals are not strongly partitioned into either phase but the co-contaminants are, and the results suggest several systems where slight modifications to the system acidity will yield such conditions.

6.6 FUTURE WORK

Any of the systems discussed in Section 6.4.6 could be further developed, and these represent areas of further work beyond the scope of this thesis. These selected systems may undergo an initial round of further development to gather additional information on their behaviour over a range of acidities, organic mixture concentrations and extractant ratios, and the impact of anion concentration, in order to determine whether these systems do provide promising options for detailed investigation. Following from this, the most promising systems should undergo detailed development, potentially following the methodology and results described in Chapter 3, and the further work described for the system detailed in that chapter.

6.7 CHAPTER SUMMARY

In this chapter a number of aqueous and organic media have been considered for thorium and uranium separation from iron and zirconium. By performing a screening study it has been possible to select the most interesting aqueous and organic solutions for further development and study. The most promising systems may now undergo further development beyond the work presented here.

7 OVERALL CONCLUSIONS AND FUTURE WORK

This thesis has presented novel work in three areas. This closing chapter reviews the motivations and aims of the research, what was found during the work, and summarises that which remains to be done.

7.1 MOTIVATION FOR WORK AND AIMS

As was discussed in Chapter 1, there is an increasing need for energy which can be met effectively by nuclear power. Thorium can supplement natural uranium resources as an alternative fertile material, and can bring its own unique advantages, such as fuel breeding in a thermal neutron spectrum, minimal transmutation to plutonium and improved fissile conversion as a component of mixed oxide fuels compared to ^{238}U .

The main source of thorium beyond existing inventories is likely to be monazite and monazite processing residues. When the literature was investigated it was found that solvent extraction processes for the separation of thorium from contaminants have been investigated over many years, with new extractants and diluents still being produced and studied. These were mainly for the separation of thorium from rare earth elements and other components of monazite and bastnäsite. However, even some of the most well-established extractants have not been fully investigated in binary combinations, and given their availability and relative maturity these extractants may yet deliver highly attractive separations processes through synergic interactions.

This led to the first aim of the work, which was to determine the extracted complexes and number of contact stages required to extract 99% of the dissolved thorium from an acidic monazite leachate using a synergic solvent extraction system. The mixture of PC-88a and HDEHP was selected, as PC-88a is the currently used industrial thorium extractant, but it does not separate thorium well from iron or uranium [34]. HDEHP was selected as an established extractant which extracts thorium more strongly than uranium, particularly from strong acid, and does not extract iron.

While the eventual use of thorium is predicted by many to be in molten salt reactors, it is commonly agreed that the first modern use of thorium for power generation will be as an oxide fuel in current generation LWRs and/or PHWRs. In these reactors an internal neutron source is required to act as a fissile driver. Studies into plutonium and uranium driven thorium oxide fuels within LWRs and PHWRs have shown that these fuels, when correctly implemented, can bring benefits over LEU or U-Pu MOX fuels, even achieving fuel breeding and/or significantly extended fuel lifetimes in the core. The great majority of such studies have looked at single heavy metal element fissile drivers, being either uranium or plutonium. However, the use of U-Pu MOX as a fissile driver has only been slightly studied in the literature, and only a single, limited study could be found into the use of such fuel in PHWRs. Given that an Enhanced CANDU 6 PHWR may be constructed in the UK for plutonium irradiation in the coming years, this reactor was selected for these MOX-driven three-component fuels, in order to determine the potential advantages that such fuels might bring.

This led to the second aim of this work, which was to determine the neutronic feasibility of mixed U-Pu-Th oxide nuclear fuels as an alternative to the proposed UK CANMOX fuel of U-Pu MOX with dysprosium burnable absorber in the Enhanced CANDU 6 reactor. Neutronic feasibility was established by determining the beginning of life infinite multiplication factor relative to that of natural uranium fuel, and the reactivity depletion and

conversion factor with burnup. In order to determine the elimination and isotopic conversion of fissile plutonium, the change in fuel composition was also determined. Furthermore, CANDU reactors are known to operate with a positive void coefficient, but this becomes negative when the central region of the fuel bundle is replaced by a zirconium or graphite “fuel” element [378, 443]. It was postulated that thorium may also offer this advantage, at least early in the irradiation before significant conversion of thorium to fissile ^{233}U , and so this was also examined.

Finally, it was observed in the literature that few studies have reported on the separation of thorium and uranium from spent thorium nuclear fuel. Currently, the main process for reprocessing thorium spent fuel is the Acid THOREX process, which uses solvent extraction with TBP to recover uranium and also possibly thorium. TBP has a number of issues, and the use of a synergic mixture of extractants was proposed as a replacement for TBP. PC-88a was retained as a primary extractant, but a range of ten potential synergists were examined. The aim was to find a synergist which would allow the individual recovery of thorium and uranium from zirconium and iron. The aim was to determine the distribution ratios for the four metals, and the separation factors for uranium and thorium against one another and zirconium and iron.

7.2 THORIUM PURIFICATION FROM MONAZITE AND MONAZITE RESIDUES

A mixture of PC-88a and HDEHP in an *n*-dodecane diluent was used to separate thorium, uranium and iron from 3.0 M hydrochloric acid. The process was found to be tolerant of moderate concentrations of the chloride and sulfate ions. In general, it was found that thorium was extracted more strongly than uranium under a range of conditions, while iron distributed

evenly across the organic and aqueous phases. The extracted complexes of thorium, uranium and iron were determined to be

$\text{Th}(\text{H}(\text{EHEHP})_2)_2(\text{H}(\text{DEHP})_2)_2(\text{HEHEHP})$ for thorium(IV),
 $(\text{UO}_2)(\text{H}(\text{EHEHP})_2)(\text{H}(\text{DEHP})_2)$ for uranium(VI), and
 $\text{Fe}(\text{H}(\text{EHEHP})_2)_2(\text{H}(\text{DEHP})_2)$ for iron(III).

It was found that three contact stages would be sufficient for 99% thorium recovery, and a process flowsheet for metals separation was suggested.

7.3 THREE-COMPONENT U-PU-TH FUELS IN THE EC6 PRESSURISED HEAVY WATER REACTOR

A number of two- and three-component mixed oxide fuels were proposed based on a range of plutonium and uranium isotopic compositions. These compositions were based on materials either already in the UK nuclear materials inventories, or projected to be produced in new build UK LWRs. Based on the assumption of a homogeneous, one-group reactor, neutron reproduction factors were calculated for 20 of these fuels. Two U-Pu-Th fuels were selected from these and the beginning of life effective multiplication factors were estimated. It was indicated that such fuels could be produced in sufficient quantities based on inventory materials, and that a reasonable LWR-PHWR support ratio could be produced for irradiation of LWR reprocessed uranium and plutonium in PHWRs.

These fuels were analysed in a computational simulation using the SERPENT Monte Carlo neutronics package, and the results were compared to natural uranium and proposed "UK CANMOX" fuels. The neutronic analysis showed that three-component fuels could outperform UK CANMOX fuels in a number of areas, including plutonium transmutation and power peaking factors. It was found that a fleet of four EC6 reactors could irradiate all 140 t of UK inventory plutonium to 22.5 MWd/kgHM in 45-50 years, also irradiating 4520 t of separated AGR reprocessed uranium. Such three-

component fuels may also be used to increase the energy value from EPR fuel, allowing an additional 12 MWd/kgHM of irradiation to be carried out on reprocessed LWR uranium and plutonium, saving 30,000 t of natural uranium that would be needed in EPRs to achieve the same capacity increase. A fleet of ten EC6 reactors could irradiate the U and Pu from the used fuel of the four planned UK EPRs over the planned lifetime of both plants.

7.4 RECOVERY OF THORIUM AND URANIUM FROM SPENT THORIUM NUCLEAR FUEL

The well-established alkyl phosphonic acid extractant PC-88a was investigated alongside a set of secondary extractants to determine the extraction behaviour of thorium, uranium, iron and zirconium from hydrochloric, nitric and sulfuric acid media. Three systems were identified as of interest for further development, showing either strong thorium distribution ratios, or the separation of thorium from the other elements when the acidity of the system was altered. There were:

- Extraction of all four metals from 0.5 M HCl by mixtures of 0.1 M PC-88a and 0.05 M Aliquat-336, stripping thorium with 3.0 M HCl. The results suggest that iron could possibly be retained in the raffinate by using a lower extraction acidity, while uranium could be stripped by a higher acidity.
- Extraction of uranium and zirconium only from 0.5 M H₂SO₄ by mixtures of 0.1 M PC-88a and 0.05 M Aliquat-336, stripping uranium only using 3.0 M H₂SO₄. Thorium remains in the raffinate. Iron may be extracted by a slight reduction in the extraction acidity, and selectively rejected at an intermediate acidity between 0.5 and 3.0 M.
- Extraction of all four metals from 0.5 M H₂SO₄ by mixtures of 0.1 M PC-88a and 0.05 M HDEHP, stripping thorium from 3.0 M H₂SO₄. Iron

is also stripped by this acid, but selective stripping of one metal or the other may be accomplished by varying the acidity between the two experimental values. Linear interpolation of the distribution ratios between 0.5 M and 3.0 M shows that an acid concentration of 1.16 M allows thorium to be selectively stripped from the loaded organic phase.

It is suggested that further investigation be carried out into these systems, following the methodology of Chapter 3. Further systems of interest may be identified from the results based on the use of different aqueous media in extraction and stripping.

7.5 MONAZITE REQUIREMENTS FOR UK PLUTONIUM IRRADIATION AND SPENT FUEL PRODUCTION

A number of studies have considered the material flows, processes and economics of full thorium fuel cycles [35, 43, 107, 133, 336, 357, 364, 467, 492-494]. In this section a simple analysis is carried out into the combination of the developed fuel concepts and thorium separations process into a single fuel cycle concept.

The EC6 reactor core produces approximately 720 MWe (net). Using natural uranium fuel this requires an annual loading of 100 tHM, using Equation (4.23). However, with the proposed three-component fuel from Chapter 5, the annual loading becomes 31.8 tHM, of which 7.7 t is thorium, 23.4 t is uranium and 0.72 t is plutonium. If 99% of the thorium is recovered from monazite with an average of 10% thorium by mass, this will require the processing of 77 t of monazite per reactor per year. The irradiation of the UK plutonium inventory of 140 t will require 193.5 reactor.years in fuel concept 19 with 3% plutonium, giving a total requirement of 1490 t thorium and 4530 t ThORP product uranium. This indicates a requirement for 15,000 t of 10%Th monazite to be processed for its thorium content, or 5000 t of

monazite residues with 30% thorium by mass. The annual spent fuel production per reactor will be 31.8 tHM, of which 7.7 tHM of thorium spent fuel which might be reprocessed to recover

7.6 FUTURE WORK

It is recommended that PC-88a/HDEHP mixtures should be further investigated and developed in order to fully determine whether the system is appropriate for the separation of thorium, uranium and iron, with full loading and stripping isotherms produced from experimental data. If the system appears sufficiently promising process scale-up studies might be carried out. Studies into the behaviour of additional metals should also be carried out, including titanium and rare earth elements.

For the three-component fuel concepts, the next major step of work is to perform a coupled neutronics and thermal-hydraulics study at the level of the full core over the full range of fuel loading possibilities at equilibrium, over operating transients, and in fault conditions. A range of supporting fuel cycle studies are also required, into used fuel management and fuel purification and fabrication.

It is recommended that the three extraction systems identified in Chapter 6 be further investigated in order to examine these systems in detail, following the methods of Chapter 3, including determination of the extraction mechanism and complexes, and loading and stripping isotherms. The systems should also be tested for other metals present in spent thorium nuclear fuel, and the effects of a radiation field on the system.

7.7 CONCLUSION

In conclusion, the aims of the work laid out in this thesis have been achieved. The extracted complexes and number of contact stages required

for 99% thorium recovery from 3.0 M hydrochloric acid have been determined, using PC-88a and HDEHP in *n*-dodecane as the organic phase. It has also been shown that U-Pu-Th nuclear fuels can operate in heavy water reactors, giving advantages over the proposed UK CANMOX fuel for plutonium conversion. Much work remains to be done in these areas, but the initial feasibility of both has been demonstrated, and they have been shown to be worthy of further investigation.

Thorium can bring advantages to nuclear energy production and thus global energy security. In the correct applications this alternative nuclear energy resource may offer unique possibilities in improved energy sustainability.

REFERENCES

1. Zhang, X.-P. and X.-M. Cheng, *Energy consumption, carbon emissions, and economic growth in China*. Ecological Economics, 2009. **68**(10): p. 2706-2712.
2. Bloom, D.E., et al., *The contribution of population health and demographic change to economic growth in China and India*. Journal of Comparative Economics, 2010. **38**(1): p. 17-33.
3. Ögütçü, M., *Changing Dynamics and Risks in World Energy: The Way Forward*, in *Perspectives on Energy Risk*, A. Dorsman, T. Gök, and M.B. Karan, Editors. 2014, Springer-Verlag Berlin Heidelberg: London. p. 9-27.
4. Brock, H., *Competition over Resources: Drivers of Insecurity and the Global South*. 2011, Oxford Research Group.
5. World Economic Forum, *The Future Availability of Natural Resources - A New Paradigm for Global Resource Availability*, in *World Scenario Series*. 2014, World Economic Forum.
6. International Security Advisory Board, *Report on Energy Geopolitics: Challenges and Opportunities*. 2014.
7. European Environment Agency, *Intensified Global Competition for Resources*, in *SOER 2015 - Global Megatrends*. 2015, European Environment Agency.
8. Longo, M., et al., *Analysis of Sustainable and Competitive Energy System*, in *2014 International Conference on Renewable Energy Research and Application*. 2014, Ieee: New York. p. 80-86.
9. Soni, A., C.S. Ouml;zveren, and Ieee, *Renewable energy market potential in UK*. 2007 42nd International Universities Power Engineering Conference, Vols 1-3. 2007, New York: Ieee. 717-720.
10. United Nations, *Paris Agreement*, 2015, United Nations Framework Convention on Climate Change.
11. United Nations, *Paris Agreement - Entry into Force*, 2016, United Nations.
12. UK Department of Energy & Climate Change, *Updated Energy and Emissions Projections*, Department of Energy & Climate Change. 2015, UK Government: UK Government website.
13. International Atomic Energy Agency, *Climate Change and Nuclear Power 2016*. 2016, International Atomic Energy Agency: Vienna, Austria.
14. International Atomic Energy Agency, *Energy, Electricity and Nuclear Power Estimates for the Period up to 2050*. Reference Data Series No. 1. 2016, Austria: International Atomic Energy Energy.

15. Bodansky, D., *Nuclear Energy Principles, Practices and Prospects*. 2nd ed. 2004, New York, United States of America: Springer-Verlag. 693.
16. Bennet, D.J. and J.D. Thompson, *The Elements of Nuclear Power*. 1st ed. 1989: Longman. 320.
17. Lamarsh, J.R. and A.J. Baratta, *Introduction to Nuclear Engineering*. 3rd ed. 2001, New York: Prentice Hall. 783.
18. Marshall, W., *Nuclear Power Technology*. Vol. 2 Fuel Cycle. 1983: Oxford Press.
19. Almenas, K. and R. Lee, *Nuclear Engineering, An Introduction*. 1st ed. 1992: Springer-Verlag Berlin Heidelberg. 566.
20. Garland, W.J. *The Essential CANDU, A Textbook on the CANDU Nuclear Power Plant Technology*. 2014 [cited 2016 05 July]; A web-based textbook on CANDU Nuclear Plant Technology. This source is subject to change at any time.]. Available from: <http://www.nuceng.ca/candu/>.
21. International Atomic Energy Agency, *Nuclear Power Reactors in the World*. Reference Data Series No. 2. 2016, Vienna, Austria: International Atomic Energy Agency. 86.
22. Kim, Y., M. Kim, and W. Kim, *Effect of the Fukushima nuclear disaster on global public acceptance of nuclear energy*. Energy Policy, 2013. **61**: p. 822-828.
23. World Nuclear Association. *World Nuclear Power Reactors & Uranium Requirements*. Information Library - Facts and Figures 2016 1 September 2016 [cited 2016 28 September]; Table of energy generation, operable, under construction, planned and proposed reactors, and uranium requirements by country 2015-16]. Available from: <http://www.world-nuclear.org/information-library/facts-and-figures/world-nuclear-power-reactors-and-uranium-requireme.aspx>.
24. World Nuclear News. *Swiss reject rapid nuclear phase out*. 2016 28 November 2016 [cited 2016 04 December]; Available from: <http://www.world-nuclear-news.org/NP-Swiss-reject-rapid-nuclear-phase-out-2711161.html>.
25. OECD Nuclear Energy Agency and International Atomic Energy Agency, *Uranium 2014: Resources, Production and Demand*. 2014: OECD Nuclear Energy Agency. 422.
26. Parliamentary Office of Science and Technology, *Mixed Oxide Nuclear Fuel (MOX)*, P.O.o.S.a. Technology. 2000, Parliamentary Office of Science and Technology: UK Parliament Website.
27. Gilmour, A. and L. Greenlees. *The 'PLEX-Ready' Power Station: A Sustainable Solution in Sustainable Nuclear Energy Conference*. 2016. Nottingham, UK.
28. World Nuclear Association. *Material Balance in the Nuclear Fuel Cycle*. The Nuclear Fuel Cycle 2016 June 2016 [cited 2016 15 November]; Available from: <http://www.world->

- [nuclear.org/information-library/nuclear-fuel-cycle/introduction/nuclear-fuel-cycle-overview.aspx](http://www.world-nuclear.org/information-library/nuclear-fuel-cycle/introduction/nuclear-fuel-cycle-overview.aspx).
29. World Nuclear Association. *Processing of Used Nuclear Fuel*. The Nuclear Fuel Cycle 2016 June 2016 [cited 2016 15 November]; Available from: <http://www.world-nuclear.org/information-library/nuclear-fuel-cycle/introduction/nuclear-fuel-cycle-overview.aspx>.
 30. Van Den Durpel, L., "Millenium" view on nuclear energy sustainability, in *Talk to students*. 2011, AREVA S.A.: TU Delft, Netherland.
 31. Iwamura, T., et al., *Concept of innovative water reactor for flexible fuel cycle (FLWR)*. Nuclear Engineering and Design, 2006. **236**(14–16): p. 1599-1605.
 32. Yamashita, J.i., T. Mochida, and F. Kawamura, *Next-generation nuclear reactor systems for future energy*. Hitachi Hyoron, 2004. **86**(2): p. 193-196.
 33. Andrews, N., K. Shirvan, and M.S. Kazimi, *Viability of uranium nitride fueled high-conversion PWR*. Progress in Nuclear Energy, 2015. **82**: p. 28-32.
 34. International Atomic Energy Agency, *Thorium fuel cycle — Potential benefits and challenges*. 2005: Vienna.
 35. Mathai, M.V., *Nuclear Power, Economic Development Discourse and the Environment*. Routledge Explorations in Environmental Studies. 2013: Routledge.
 36. Taiwo, T.A., T.K. Kim, and R.A. Wigeland, *Thorium Fuel Cycle Option Screening in the United States*. Nuclear Technology, 2016. **194**(2): p. 127-135.
 37. National Nuclear Laboratory, *The Thorium Fuel Cycle: An independent assessment by the UK National Nuclear Laboratory*. 2010
 38. National Nuclear Laboratory, *Comparison of Thorium and Uranium Fuel Cycles*. 2012 p. 31.
 39. Martin, R. *Uranium Is So Last Century — Enter Thorium, the New Green Nuke*. Wired 2009 21 December [cited 2012 5 Sep]; Available from: http://www.wired.com/magazine/2009/12/ff_new_nukes/.
 40. Martin, R., *Superfuel - Thorium, The Green Energy Source for the Future*. 2012, Palgrave Macmillan: Houndmills, Basingstoke. p. 5226.
 41. Arnold, N., *Comparing recent uranium supply scenarios*, in *IAEA Technical Meeting on the Nuclear Fuel Cycle Information System*. 2014: Vienna, Austria.
 42. Zhu, Z., Y. Pranolo, and C.Y. Cheng, *Separation of uranium and thorium from rare earths for rare earth production – A review*. Minerals Engineering, 2015. **77**: p. 185-196.
 43. OECD Nuclear Energy Agency, *Introduction of Thorium in the Nuclear Fuel Cycle*. 2015: OECD Publishing.
 44. Brown, N.R., et al., *Thorium Fuel Cycles with Externally Driven Systems*. Nuclear Technology, 2016. **194**(2): p. 233-251.

45. Shibata, K., et al., *JENDL-4.0: A New Library for Nuclear Science and Engineering*. Journal of Nuclear Science and Technology, 2011. **48**(1): p. 1-30.
46. Schaffer, M.B., *Abundant thorium as an alternative nuclear fuel: Important waste disposal and weapon proliferation advantages*. Energy Policy, 2013. **60**: p. 4-12.
47. International Atomic Energy Agency. *Power Reactor Information Service, United Kingdom Country Statistics*. 2015-05-28 [cited 2015 29 May]; List of all operational and decommissioned nuclear power reactors in the United Kingdom with basic statistics]. Available from: <http://www.iaea.org/pris/CountryStatistics/CountryDetails.aspx?current=GB>.
48. McKeen, T., *Advanced Gas Cooled Reactors*, in *Nuclear Energy Materials and Reactors*, Y.A. Hassan and R.A. Chaplin, Editors. 2010, Eolss Publishers. p. 364.
49. Nonbøl, E., *Description of the Advanced Gas Cooled Type of Reactor (AGR)*. 1996, Risø National Laboratory, Roskilde, Denmark.
50. Parliamentary Office of Science and Technology, *The Nuclear Energy Option in the UK*, P.O.o.S.a. Technology. 2003, Parliamentary Office of Science and Technology: UK Parliament Website.
51. Hill, C.N., *An Atomic Empire: A Technical History of the Rise and Fall of the British Atomic Energy Programme*. 2013: Imperial College Press. 250.
52. Taylor, S., *The Fall and Rise of Nuclear Power in Britain - a History*. 2016, Cambridge, UK: UIT Cambridge Ltd.
53. UK Department for Energy and Climate Change, *Nuclear Energy Research and Development Roadmap: Future Pathways*. 2013, UK Department for Energy and Climate Change.
54. Reilly, F. *Financing Nuclear New Build in Introduction to Nuclear New Build*. 2016. Rotherham, UK: Nuclear Institute.
55. Department for Business, E.I.S. *Electricity Market Reform: Contracts for Difference*. 2015 8 February 2017 [cited 2017 26 April]; Available from: <https://www.gov.uk/government/collections/electricity-market-reform-contracts-for-difference#the-cfd-contract>.
56. Nuclear Advanced Manufacturing Research Centre. *Developers*. UK New Build Plans 2017 [cited 2017 26 April]; Available from: <http://namrc.co.uk/intelligence/uk-new-build-plans/developers/>.
57. EDF Energy. *Nuclear New Build projects*. 2017 [cited 2017 26 April]; Available from: <https://www.edfenergy.com/energy/nuclear-new-build-projects>.
58. Xing, J., D. Song, and Y. Wu, *HPR1000: Advanced Pressurized Water Reactor with Active and Passive Safety*. Engineering, 2016. **2**(1): p. 79-87.
59. Hitachi-GE Nuclear Energy, l. *ABWR GDA leaflet*. [cited 2017 26 April]; Available from: http://www.hitachi-hgne-uk-abwr.co.uk/downloads/gda_leaflet.pdf.

60. NuGeneration ltd. *Our Plans*. 2017 [cited 2017 26 April]; Available from: http://www.nugeneration.com/our_plan.html.
61. UK Nuclear Decommissioning Authority, *2016 UK Radioactive Waste Inventory: Radioactive Wastes and Materials Not Reported in the 2013 UKRWI, in 2016 UK Radioactive Waste Inventory*. 2017, UK Nuclear Decommissioning Authority: www.nda.gov.uk.
62. Parker, D.R. and R.W. Mills, *FISPIN10 Validation Review*. 2001, British Nuclear Fuels Ltd. : www.oecd-nea.org. p. 115.
63. Simper, A., *Plutonium Management*. 2014, Cambridge Nuclear Energy Centre: www.cnec.group.cam.ac.uk.
64. *Progress on approaches to the management of separated plutonium*. 2014, UK Nuclear Decommissioning Authority: <http://www.nda.gov.uk/publication/progress-on-approaches-to-the-management-of-separated-plutonium-position-paper/>.
65. UK Committee of Public Accounts, *Progress at Sellafield*. 2014, UK Parliament: www.publications.parliament.uk. p. 36.
66. UK House of Commons and M. Wicks, *House of Commons Hansard written answers - Sellafield*, in *House of Commons Hansard written answers*. 2008, UK Parliament: <http://www.publications.parliament.uk/>.
67. McDonald, M.H. and B.P. Bromley, *Checkerboard Heterogeneous Uranium-Thorium Seed-Blanket Cores for Pressure-Tube Heavy Water Reactors*, in *GLOBAL 2015*. 2015, Societe Francaise d'energie nucleaire: Paris, France. p. 675-682.
68. Reid, P.J. *Candu Energy Academic Seminar in Candu Energy Academic Information Series*. 2015. University of Manchester, 18-19 March: unpublished.
69. Kayasth, S.R., H.B. Desai, and M. Sundaresan, *Determination of traces of rare earth elements in high-purity uranium by ion-exchange separation and neutron activation γ -spectrometry*. *Analytica Chimica Acta*, 1989. **219**: p. 313-315.
70. Todd, T., *Spent Nuclear Fuel Reprocessing*, in *Nuclear Regulatory Commission Seminar*. 2008, US Department of Energy: Rockville, Maryland.
71. Horwitz, E.P., et al., *The TRUEX Process - A Process for the Extraction of the Transuranic Elements from Nitric Acid Wastes Utilizing Modified PUREX Solvent*. *Solvent Extraction and Ion Exchange*, 1985. **3**(1-2): p. 75-109.
72. Zhang, Y., et al., *Extraction of Uranium and Thorium from Nitric Acid Solution by TODGA in Ionic Liquids*. *Separation Science and Technology*, 2014. **49**(12): p. 1895-1902.
73. Sharma, J.N., et al., *Separation studies of uranium and thorium using tetra(2-ethylhexyl) diglycolamide (TEHDGA) as an extractant*. *Journal of Radioanalytical and Nuclear Chemistry*, 2008. **278**(1): p. 173-177.
74. Nash, K.L. and G.J. Lumetta, eds. *Advanced Separation Techniques for Nuclear Fuel Reprocessing and Radioactive Waste Treatment*. 1st ed.

- Woodhead Publishing Series in Energy. 2011, Woodhead Publishing Limited: Philadelphia, USA.
75. Choppin, G., et al., *Radiochemistry and Nuclear Chemistry*. 2013: Elsevier Science.
 76. Nash, K.L., et al., *Actinide Separation Science and Technology*, in *The Chemistry of the Actinide and Transactinide Elements*, L.R. Morss, et al., Editors. 2006, Springer: Dordrecht, The Netherlands. p. 2622-2798.
 77. Rydberg, J., et al., eds. *Solvent Extraction Principles and Practice*. 2nd ed. 2004, Marcel Dekker, Inc.: New York, United States of America. 480.
 78. Ritcey, G.M., *Solvent Extraction in Hydrometallurgy: Present and Future*. Tsinghua Science & Technology, 2006. **11**(2): p. 137-152.
 79. Kislik, V.S., *Solvent Extraction - Classical and Novel Approaches*. 2012, Amsterdam: Elsevier.
 80. Rakesh, K.B., A. Suresh, and P.R.V. Rao, *Third Phase Formation in the Extraction of Th(NO₃)(₄) by Tri-*n*-Butyl Phosphate and Tri-*iso*-Amyl Phosphate in *n*-Dodecane and *n*-Tetradecane from Nitric Acid Media*. *Solvent Extraction and Ion Exchange*, 2014. **32**(3): p. 249-266.
 81. Peppard, D.F., et al., *Separation of Scandium from Thorium and Rare Earths Using a Tributyl Phosphate-Hydrochloric Acid System*, in *Summary Report for April, May and June, 1950*, D.W. Osborne, Editor. 1950, Argonne National Laboratory. p. 62-64.
 82. Peppard, D.F., G.W. Mason, and M.V. Gergel, *The Mutual Separation of Thorium, Protactinium, and Uranium by Tributyl Phosphate Extraction from Hydrochloric Acid*. *Journal of Inorganic & Nuclear Chemistry*, 1957. **3**(6): p. 370-378.
 83. Zhang, Y., et al., *Study on thorium recovery from bastnaesite treatment process*. *Journal of Rare Earths*, 2012. **30**(4): p. 374-377.
 84. Wang, Y., et al., *Kinetics of thorium extraction with di-(2-ethylhexyl) 2-ethylhexyl phosphonate from nitric acid medium*. *Hydrometallurgy*, 2013. **140**: p. 66-70.
 85. Sarkar, S.G., S.V. Bandekar, and P.M. Dhadke, *Solvent extraction separation of Th(IV) and U(VI) with PC-88A*. *Journal of Radioanalytical and Nuclear Chemistry*, 2000. **243**(3): p. 803-807.
 86. Borai, E.H., et al., *Subsequent Separation and Selective Extraction of Thorium (IV), Iron (III), Zirconium (IV) and Cerium (III) from Aqueous Sulfate Medium*. *South African Journal of Chemistry-Suid-Afrikaanse Tydskrif Vir Chemie*, 2016. **69**: p. 148-156.
 87. Shabana, R. and H. Ruf, *Extraction and Separation of Uranium, Thorium and Cerium from Different Mixed Media with HDEHP*. *Journal of Radioanalytical Chemistry*, 1977. **36**: p. 389-397.
 88. Sato, T., *Extraction of Thorium from Hydrochloric Acid Solutions by Di-(2-ethylhexyl)-phosphoric acid*. *Zeitschrift für anorganische und allgemeine Chemie*, 1968. **358**(5-6): p. 296-&.

89. Sahu, S.K., et al., *The synergistic extraction of thorium(IV) and uranium(VI) with mixtures of 3-phenyl-4-benzoyl-5-isoxazolone and crown ethers*. *Talanta*, 2000. **51**(3): p. 523-530.
90. Du, H.S., et al., *Separation of thorium from lanthanides by solvent extraction with ionizable crown ethers*. *Talanta*, 1993. **40**(2): p. 173-177.
91. Agrawal, Y.K. and S.B. Vora, *Selective Extraction and Separation of Thorium from Monazite Using N-Phenylbenzo-18-crown-6-hydroxamic Acid*. *Microchimica Acta*, 2003. **142**(4): p. 255-261.
92. Li, Y.L., et al., *Extraction and separation of thorium and rare earths with 5,11,17,23-tetra (diethoxyphosphoryl)-25,26,27,28-tetraacetoxycalix 4 arene*. *Journal of Rare Earths*, 2012. **30**(11): p. 1142-1145.
93. Tran, Q.H., V.T. Le, and V.C. Nguyen, *Solvent Extraction of Thorium Using 5,11,17,23-Tetra (2-ethyl acetoethoxyphenyl)(azo)phenyl calix 4 arene*. *Journal of Chemistry*, 2016: p. 6.
94. Montavon, G., et al., *Solvent Extraction of Uranium(VI) and Thorium(IV) with a Tetra-Carboxylated Calix[4]Arene and Effect of Alkali Ions (Na+, K+)*. *Solvent Extraction and Ion Exchange*, 1997. **15**(2): p. 169-188.
95. ITER Organization. *ITER website*. 2016 [cited 2016 15 November]; Available from: <https://www.iter.org/>.
96. Chadwick, M.B., et al., *ENDF/B-VII.1 Nuclear Data for Science and Technology: Cross Sections, Covariances, Fission Product Yields and Decay Data*. *Nuclear Data Sheets*, 2011. **112**(12): p. 2887-2996.
97. Merriam-Webster Visual Dictionary Online, *Nuclear fission*, nuclear-fission.jpg. 2016, Merriam-Webster: Merriam-Webster Visual Dictionary Online.
98. Nuclear Power for Everybody. *Macroscopic Slowing Down Power - MSDP*. Glossary 2017 [cited 2017 24 April]; Available from: <http://www.nuclear-power.net/glossary/macroscopic-slowng-down-power-msdp/>.
99. World Nuclear Association. *Nuclear Power in Russia*. Country Profiles 2017 [cited 2017 11 August]; Available from: <http://www.world-nuclear.org/information-library/country-profiles/countries-o-s/russia-nuclear-power.aspx>.
100. Cameco Corporation. *Types of Reactors*. Uranium 101 [cited 2016 1 October]; Available from: https://www.cameco.com/uranium_101/electricity-generation/types-of-reactors/.
101. Arafat, Y., et al., *Radiotoxicity Characterization of HLW from Reprocessing of Uranium-Based and Thorium- Based Fuel*, in *WM2011*. 2011: Phoenix, Arizona, USA.
102. Gerasimov, A.S., et al., *Long-Term Behavior of Radiotoxicity and Decay Heat Power of Spent Uranium-Plutonium and Thorium Fuel*, in

- Scientific research on the back-end of the fuel cycle for the 21. century.* 2000: Paris, France.
103. Boczar, P.G., et al. *Achieving Resource Sustainability in China through the Thorium Fuel Cycle in the CANDU Reactor* in *The 18th International Conference on Nuclear Engineering 2010, Vol 6.* 2011. New York: American Society of Mechanical Engineers.
 104. Achuthan, P.V. and A. Ramanujam, *Aqueous Reprocessing by THOREX Process*, in *Thoria-based Nuclear Fuels: Thermophysical and Thermodynamic Properties, Fabrication, Reprocessing, and Waste Management*, D. Das and S.R. Bharadwaj, Editors. 2013, Springer London: London. p. 279-333.
 105. Blanchard, A., et al., *Updated Critical Mass Estimates for Plutonium-238*, in *Sixth International Conference on Nuclear Criticality Safety.* 1999: Versailles, France.
 106. Le Brun, C., et al., *Impact of the MSBR concept technology on long-lived radio-toxicity and proliferation resistance*, in *Technical Meeting on Fissile Material Management Strategies for Sustainable Nuclear Energy.* 2007: Vienna, Austria.
 107. OECD Nuclear Energy Agency, *Perspectives on the Use of Thorium in the Nuclear Fuel Cycle.* 2015, Organisation for Economic Co-operation and Development.
 108. Andrews, N., et al., *Steady State and Accident Transient Analysis Burning Weapons-Grade Plutonium in Thorium and Uranium with Silicon Carbide Cladding.* Nuclear Technology, 2016. **194**(2): p. 204-216.
 109. Worrall, L.G., et al., *Safeguards Considerations for Thorium Fuel Cycles.* Nuclear Technology, 2016. **194**(2): p. 281-293.
 110. Betzler, B.R., J.J. Powers, and A. Worrall, *Molten salt reactor neutronics and fuel cycle modeling and simulation with SCALE.* Annals of Nuclear Energy, 2017. **101**: p. 489-503.
 111. Lindley, B.A. and G.T. Parks, *The performance of closed reactor grade plutonium-thorium fuel cycles in reduced-moderation pressurised water reactors.* Annals of Nuclear Energy, 2012. **47**: p. 192-203.
 112. Demkowicz, P.A., et al., *Aqueous Dissolution of Urania-Thoria Nuclear Fuel.* Nuclear Technology, 2004. **147**(1): p. 157-170.
 113. Hall, V., *A Review of the Benefits and Applications of the Thorium Fuel Cycle*, in *Ralph E. Martin Department of Chemical Engineering.* 2010, University of Arkansas: ScholarWorks@UARK. p. 26.
 114. Alhaj, M.Y., et al., *Towards proliferation-resistant thorium fuels.* Annals of Nuclear Energy, 2017. **101**: p. 586-590.
 115. Vapirev, E.I., et al., *Conversion of high enriched uranium in thorium-232-based oxide fuel for light and heavy water reactors: MOX-T fuel.* Nuclear Engineering and Design, 1996. **167**(2): p. 105-112.
 116. Croff, A.G. and S.L. Krahn, *Comparative Assessment of Thorium Fuel Cycle Radiotoxicity.* Nuclear Technology, 2016. **194**(2): p. 271-280.

117. Shelley, A., et al., *Radiotoxicity hazard of U-free PuO₂+ZrO₂ and PuO₂+ThO₂ spent fuels in LWR*. Progress in Nuclear Energy, 2000. **37**(1-4): p. 377-382.
118. *Operation TEAPOT Technical Summary of Military Effects, Programs 1-9*, Office of the Deputy Chief of Staff for Weapons Effects Tests. 1960: Albuquerque, New Mexico. p. 231.
119. Langford, R.E., *Introduction to Weapons of Mass Destruction: Radiological, Chemical, and Biological*. 2004: John Wiley & Sons.
120. Kang, J. and F.N. von Hippel, *U-232 and the proliferation-resistance of U-233 in spent fuel*. Science & Global Security, 2001. **9**(1): p. 1-32.
121. Ashley, S.F., et al., *Thorium fuel has risks*. Nature, 2012. **492**(7427): p. 31-33.
122. Ashley, S.F., et al., *Open cycle thorium-uranium fuelled nuclear energy systems*. Proceedings of Institution of Civil Engineers: Energy, 2013. **166**(2): p. 74-81.
123. Yemel'Yanov, V.S., A.I. Yevstyukhin, and J.V. Dunworth, *The Metallurgy of Nuclear Fuel: Properties and Principles of the Technology of Uranium, Thorium and Plutonium*. 2013: Elsevier Science.
124. Herring, J.S., et al., *Low cost, proliferation resistant, uranium-thorium dioxide fuels for light water reactors*. Nuclear Engineering and Design, 2001. **203**(1): p. 65-85.
125. Raj, K., C.P. Kaushik, and R.K. Mishra, *Radioactive Waste Management in U/Th Fuel Cycles*, in *Thoria-Based Nuclear Fuels: Thermophysical and Thermodynamic Properties, Fabrication, Reprocessing, and Waste Management*, D. Das and S.R. Bharadwaj, Editors. 2013, Springer: New York. p. 335-405.
126. Colmenares, C.A., *Oxidation mechanisms and catalytic properties of the actinides*. Progress in Solid State Chemistry, 1984 **15**(4): p. 257-364.
127. Srinivas, C., et al., *Studies on Improvements in Thoria Dissolution Process for Reprocessing Application*. BARC (Bhabha Atomic Research Centre) Newsletter, 2012(326).
128. Jorgensen, P.J. and W.G. Schmidt, *Final Stage Sintering of ThO₂*. Journal of the American Ceramic Society, 1970. **53**(1): p. 24-27.
129. Shiratori, T. and K. Fukuda, *Fabrication of very high density fuel pellets of thorium dioxide*. Journal of Nuclear Materials, 1993. **202**(1-2): p. 98-103.
130. Weaver, K.D. and J.S. Herring, *Performance of thorium-based mixed-oxide fuels for the consumption of plutonium in current and advanced reactors*. Nuclear Technology, 2003. **143**(1): p. 22-36.
131. Jess C. Gehin, J.J.P., *Liquid Fuel Molten Salt Reactors for Thorium Utilization*. Nuclear Technology, 2016. **194**(2): p. 152-161.
132. United States Atomic Energy Commission, *An Evaluation of the Molten Salt Breeder Reactor*. 1972, United States Atomic Energy Commission. p. 59.

133. Furukawa, K., et al., *A road map for the realization of global-scale thorium breeding fuel cycle by single molten-fluoride flow*. Energy Conversion and Management, 2008. **49**(7): p. 1832-1848.
134. Generation IV International Forum, *A Technology Roadmap for Generation IV Nuclear Energy Systems*. 2014, OECD Nuclear Energy Agency.
135. Ade, B., et al., *Analysis of Key Safety Metrics of Thorium Utilization in LWRs*. Nuclear Technology, 2016. **194**(2): p. 162-177.
136. Golesorkhi, S. and M. Kaye, *An Investigation of the Feasibility of Net-Breeding Thorium Cycles in Pressure-Tube Heavy Water Reactors*, in *GLOBAL 2015*. 2015, Societe francaise d'energie nucleaire: Paris, France. p. 731-737.
137. US Department of Energy Nuclear Energy Research Advisory Committee, *Molten Salt Reactor*, 900px-Molten_Salt_Reactor.svg. 2002, United States Department of Energy. p. Diagram extracted from Generation IV roadmap published by US Department of Energy and cleaned up to remove excess grouping.
138. U.S. Geological Survey, *Mineral Commodity Summaries 2014*, ed. U.S. Geological Survey. 2014. 196.
139. Jha, M.K., et al., *Review on hydrometallurgical recovery of rare earth metals*. Hydrometallurgy, 2016. **165, Part 1**: p. 2-26.
140. Ault, T., et al., *Natural Thorium Resources and Recovery: Options and Impacts*. Nuclear Technology, 2016. **194**(2): p. 136-151.
141. Katz, J.J., G.T. Seaborg, and L.R. Morss, eds. *The Chemistry of the Actinide Elements*. 2 ed. Vol. 1. 1986, Chapman and Hall Ltd.: New York. 41-101.
142. Cuthbert, F.L., *Thorium Production Technology*. Atoms for Peace, Geneva, 1958, United States of America, ed. United States Atomic Energy Commission. 1958, Reading, Mass.: Addison-Wesley. 303.
143. Gambogi, J., *Thorium*, in *2011 Minerals Yearbook*, U.S. Geological Survey, Editor. 2013. p. 76.1-3.
144. Deer, W.A., R.A. Howie, and J. Zussman, *Rock Forming Minerals, Volume 5 - Non-Silicates*. 1st ed. Rock Forming Minerals. Vol. 5 Non-Silicates. 1962, London: Longman Group Ltd. 371.
145. Clavier, N., R. Podor, and N. Dacheux, *Crystal chemistry of the monazite structure*. Journal of the European Ceramic Society, 2011. **31**(6): p. 941-976.
146. Hudson Institute of Mineralogy. *Monazite*. [cited 2015 03 November]; Available from: <http://www.mindat.org/min-2750.html>.
147. Thompson, W., et al. *Mineralogical Studies in Assisting Beneficiation of Rare Earth Element Minerals from Carbonatite Deposits in 10th International Congress for Applied Mineralogy (ICAM)*. 2011. Trondheim, Norway.
148. Kul, M., Y. Topkaya, and İ. Karakaya, *Rare earth double sulfates from pre-concentrated bastnasite*. Hydrometallurgy, 2008. **93**(3-4): p. 129-135.

149. International Atomic Energy Agency, *Extent of Environmental Contamination by Naturally Occurring Radioactive Material (NORM) and Technological Options for Mitigation*, in *Technical Reports Series*. 2003, International Atomic Energy Agency: Vienna, Austria. p. 198.
150. Acharya, B.C., B.K. Nayak, and S.K. Das, *Mineralogy and Mineral Chemistry of Placer Deposit around Jhatipodar, Odisha*. Journal of the Geological Society of India, 2015. **86**(2): p. 137-147.
151. Holder, R.M., et al., *Monazite trace-element and isotopic signatures of (ultra) high-pressure metamorphism: Examples from the Western Gneiss Region, Norway*. Chemical Geology, 2015. **409**: p. 99-111.
152. Wang, S., et al., *Rare metal elements in surface sediment from five bays on the northeastern coast of the South China Sea*. Environmental Earth Sciences, 2015. **74**(6): p. 4961-4971.
153. Das, S.K., *Characteristics of zircon of Chhatrapur beach placer deposit, Ganjam District, Odisha*. Journal of the Geological Society of India, 2015. **86**(4): p. 383-390.
154. Savel'eva, V.B., E.P. Bazarova, and S.V. Kanakin, *The Mineralogy and Geochemistry of Quartz-Tourmaline Schlieren in the Granites of the Primorsky Complex, Western Baikal Region*. Geology of Ore Deposits, 2014. **56**(8): p. 617-628.
155. Pal-Molnar, E., et al., *Geochemical implications for the magma origin of granitic rocks from the Ditrau Alkaline Massif (Eastern Carpathians, Romania)*. Geologia Croatica, 2015. **68**(1): p. 51-66.
156. Mahar, M.A., T.M.M. Ibrahim, and P.C. Goodell, *Provenance of the heavy mineral-enriched alluvial deposits at the west coast of the Red Sea. Implications for evolution of Arabian-Nubian crust*. Journal of African Earth Sciences, 2014. **100**: p. 510-523.
157. Santana, I.V., F. Wall, and N.F. Botelho, *Occurrence and behavior of monazite-(Ce) and xenotime-(Y) in detrital and saprolitic environments related to the Serra Dourada granite, Goias/Tocantins State, Brazil: Potential for REE deposits*. Journal of Geochemical Exploration, 2015. **155**: p. 1-13.
158. Goswami-Banerjee, S. and M. Robyr, *Pressure and temperature conditions for crystallization of metamorphic allanite and monazite in metapelites: a case study from the Miyar Valley (high Himalayan Crystalline of Zaskar, NW India)*. Journal of Metamorphic Geology, 2015. **33**(5): p. 535-556.
159. Scherrer, N.C., et al., *Monazite analysis; from sample preparation to microprobe age dating and REE quantification*. Schweizerische Mineralogische Und Petrographische Mitteilungen, 2000. **80**(1): p. 93-105.
160. Forbes, C., et al., *Glacial dispersion of hydrothermal monazite in the Prominent Hill deposit: An exploration tool*. Journal of Geochemical Exploration, 2015. **156**: p. 10-33.
161. Frondel, J.W. and M. Fleischer, *Glossary of Uranium- and Thorium-Bearing Minerals*. 1954. p. 42.

162. Deer, W.A., R.A. Howie, and J. Zussman, *An Introduction to the Rock-Forming Minerals*. 1st ed. 1966, London: Longman Group Limited.
163. Maitre, R.W.L., ed. *Igneous Rocks: A Classification and Glossary of Terms*. 2nd ed. 2002, Cambridge University Press: New York. 236.
164. Foster, G.L. and R.R. Parrish, *Metamorphic monazite and the generation of P-T-t paths*, in *Geochronology: Linking the Isotopic Record with Petrology and Textures*, D. Vance, W. Muller, and I.M. Villa, Editors. 2003, Geological Society of London: London, UK. p. 25-47.
165. Ni, Y., J.M. Hughes, and A.N. Mariano, *Crystal chemistry of the monazite and xenotime structures*. *American Mineralogist*, 1995. **80**: p. 21-26.
166. U.S. Geological Survey, *Mineral Commodity Summaries 2016*, ed. U.S. Geological Survey. 2016.
167. Grover, R.B., *Opening up of international civil nuclear cooperation with India and related developments*. *Progress in Nuclear Energy*.
168. da Costa Lauria, D. and E.R.R. Rochedo, *The legacy of monazite processing in Brazil*. *Radiation Protection Dosimetry*, 2005. **114**(4): p. 546-550.
169. Peiris, B.A., *Occurrence of Thorium Bearing Minerals in Sri Lanka, and Progress of Survey of Nuclear Raw Material with Emphasis on Locating Thorium and Uranium Mineralization and Demarcating Radiogenically Hazardous Areas (Project SLR-2009)*, in *UNFC Workshop*. 2013, UNECE: Santiago, Chile.
170. Rupasinghe, M.S., W. Gocht, and C.B. Dissanayake, *The Genesis of Thorium-Rich Monazite Placer Deposits in Sri Lanka* *J. Natn. Sci. Coun. Sri Lanka*, 1983. **11**: p. 99-110.
171. AL-Areqi, W.M., et al., *Thorium: Issues and prospects in Malaysia*. *AIP Conference Proceedings*, 2015. **1659**(1): p. 040005.
172. International Atomic Energy Agency, *Radiation Protection and NORM Residue Management in the Production of Rare Earths from Thorium Containing Minerals*. 2011, Vienna, Austria: IAEA. 259.
173. Hermes, W. and J. Terry. *Removing The Source Term - Thorium Nitrate Disposal at the Nevada Test Site in Proceedings of the Health Physics Society 2007 Midyear Topical Meeting: Decontamination, Decommissioning and Environmental Cleanup*. 2007. Knoxville, Tennessee, USA.
174. Meeley, W.A., M.J. Snyder, and R.B.J. Filbert, *Recovery of Thorium from Brazilian Monazite Sludge by Nitric Acid Digestion*. 1954. p. 28.
175. Taylor, C.W., A.M. Ross, and J.O. Davis, *Solvent Extraction of Thorium from Brazilian Sludges*. 1954. p. 11.
176. Hermes, W.H., et al., *Thorium Nitrate Stockpile - From Here to Eternity*, in *Waste Management Symposium*. 2003: Tucson, AZ, USA.
177. Agence nationale pour la gestion des déchets radioactifs, *Inventaire national des matières et déchets radioactifs - Rapport de Synthèse*. 2015, ANDRA.

178. Ashley, S.F., et al., *Life-cycle impacts from novel thorium-uranium-fuelled nuclear energy systems*. Energy Conversion and Management, 2015. **101**: p. 136-150.
179. Moustafa, M.I. and N.A. Abdelfattah, *Physical and Chemical Beneficiation of the Egyptian Beach Monazite*. Resource Geology, 2010. **60**(3): p. 288-299.
180. Kumari, A., et al., *Process development to recover rare earth metals from monazite mineral: A review*. Minerals Engineering, 2015. **79**: p. 102-115.
181. Nagaiyar Krishnamurthy, C.K.G., *Extractive Metallurgy of Rare Earths*. illustrated ed. 2004: CRC Press. 504.
182. Blickwedel, T.W., *Decomposition of Monazite - Effect of a Number of Variables on the Decomposition of Monazite Sand with Sulfuric Acid*. 1949. p. 28.
183. Shaw, K.G., M. Smutz, and G.L. Bridger, *A Process for Separating Thorium Compounds from Monazite Sands*. 1954. p. 109.
184. Bearse, A.E., et al., *Recovery of Thorium and Uranium from Monazite Sands*. 1954, Battelle Memorial Institute.
185. Calkins, G.D. and E.G. Bohlmann, *Processing of Monazite Sand*, Patent number 390770, United States Patent Office, Editor. 1957, United States Atomic Energy Commission: United States of America. p. 5.
186. Clarke, J.V., *Process for Separating Thorium from other Rare Earths and for the Manufacture of Thorium Nitrate and other Thorium Salts*, Patent number 256096, United States Patent Office, Editor. 1920: United States of America. p. 2.
187. Dietsche, O., *Process of Separating Thorium from the Other Metals of the Rare Earths*, Patent number 21588, United States Patent Office, Editor. 1920, The Chemical Foundation, Inc.: United States of America. p. 2.
188. Willigman, M. and E.E. Slowter, *Literature Survey of Treatments for Monazite Sands*. 1947. p. 41.
189. Mukherjee, T.K., *Processing of Indian Monazite for the recovery of thorium and uranium values*, in *Characterization and Quality Control of Nuclear Fuels (CQCNF-2002)*. 2003, Allied Publishers, New Delhi, India: Hyderabad, India.
190. Zhang, J. and C. Edwards, *Mineral decomposition and leaching processes for treating rare earth ore concentrates*. Canadian Metallurgical Quarterly, 2013. **52**(3): p. 243-248.
191. Jordens, A., Y.P. Cheng, and K.E. Waters, *A review of the beneficiation of rare earth element bearing minerals*. Minerals Engineering, 2013. **41**: p. 97-114.
192. Peelman, S., et al., *Leaching of Rare Earth Elements: Past and Present*, in *ERES2014: 1st European Rare Earth Element Resources Conference*. 2014, EURARE: Milos, Greece. p. 446-456.
193. Huang, X., et al., *Comprehensive recovery of rare earth and thorium from rare earth ore*, Patent number CN1721559-A CN10085230 21

- Jul 2005. 2006, Beijing Gen Res Inst Non Ferrous Metals (Beij-Non-Standard), Grirem Advanced Materials Co L (Gir-Non-Standard), Beijing Non Ferrous Metal Inst (Beij-Non-Standard).
194. Kumari, A., et al., *Thermal treatment for the separation of phosphate and recovery of rare earth metals (REMs) from Korean monazite*. Journal of Industrial and Engineering Chemistry, 2015. **21**: p. 696-703.
 195. Merritt, R.R., *High temperature methods for processing monazite: I. Reaction with calcium chloride and calcium carbonate*. Journal of the Less Common Metals, 1990. **166**(2): p. 197-210.
 196. Borai, E.H., et al., *Modified acidic leaching for selective separation of thorium, phosphate and rare earth concentrates from Egyptian crude monazite*. International Journal of Mineral Processing, 2016. **149**: p. 34-41.
 197. You, W. and S.G. Hong, *A Core Physics Study of Advanced Sodium-Cooled TRU Burners with Thorium- and Uranium-Based Metallic Fuels*. Nuclear Technology, 2016. **194**(2): p. 217-232.
 198. White, G.D., L.A. Bray, and P.E. Hart, *Optimization of thorium oxalate precipitation conditions relative to derived oxide sinterability*. Journal of Nuclear Materials, 1981. **96**(3): p. 305-313.
 199. Beller, D.E., et al., *A closed ThUOX fuel cycle for LWRs with ADTT (ATW) backend for the 21(st) century*. Back-End of the Fuel Cycle in a 1000 GWe Nuclear Scenario. 1999, Paris: Organization Economic Cooperation & Development. 91-104.
 200. Bergelson, B., et al., *Operation of CANDU Power Reactor in Thorium Self-sufficient Fuel Cycle, in 18th International Conference on Structural Mechanics in Reactor Technology*. 2005: Beijing, China. p. 4606-4611.
 201. Blanco, R.E., L.M. Ferris, and D.E. Ferguson, *Aqueous Processing of Thorium Fuels*. 1962.
 202. Blanco, R.E., et al., *Aqueous Processing of Thorium Fuels part 2*. 1962.
 203. Altmaier, M., X. Gaona, and T. Fanghänel, *Recent Advances in Aqueous Actinide Chemistry and Thermodynamics*. Chemical Reviews. Vol. 113. 2013: American Chemical Society. 901-943.
 204. Mailen, J.C., *Interpretation of the Extraction Mechanism of the Purex and Thorex Processes from Kinetics Data*. Separation Science and Technology, 1981. **16**(10): p. 1373-1387.
 205. Ramanujam, A., et al., *Partitioning of actinides from high level waste of PUREX origin using octylphenyl-N,N(prime)-diisobutylcarbamoylmethyl phosphine oxide (CMPO)-based supported liquid membrane*. Separation Science and Technology, 1999: p. 1717-1728.
 206. Van Den Durpel, L., *Discussion on thorium purification methods used by a large chemical company*, R. Peel. 2016.
 207. Parhi, P.K., *Supported Liquid Membrane Principle and Its Practices: A Short Review*. Journal of Chemistry, 2013. **2013**: p. 11.

208. Pitchaiah, K.C., et al., *Influence of Co-Solvent on the Extraction Behaviour of Uranium and Thorium Nitrates with Organophosphorous Compounds*. International Journal of Analytical Mass Spectrometry and Chromatography, 2014. **2**: p. 33-42.
209. Fu, J., et al., *Extraction of Th(IV) from aqueous solution by room-temperature ionic liquids and coupled with supercritical carbon dioxide stripping*. Separation and Purification Technology, 2013. **119**: p. 66-71.
210. Palamalai, A., et al., *Final Purification of U-233 Oxide Product from Reprocessing Treatment of Irradiated Thorium Rods*. Journal of Radioanalytical and Nuclear Chemistry-Articles, 1994. **177**(2): p. 291-298.
211. Suresh, A., et al., *Studies on U-Th Separation using Tri-sec-butyl Phosphate*. Solvent Extraction and Ion Exchange, 1995. **13**(3): p. 415-430.
212. Nasab, M.E., *Solvent extraction separation of uranium(VI) and thorium(IV) with neutral organophosphorus and amine ligands*. Fuel, 2014. **116**: p. 595-600.
213. Croff, A.G., et al., *ORNL Experience and Perspectives Related to Processing of Thorium and U-233 for Nuclear Fuel*. Nuclear Technology, 2016. **194**(2): p. 252-270.
214. Choppin, G.R., *Studies of the Synergistic Effect*. Separation Science and Technology, 1981. **16**(9): p. 1113-1126.
215. Zangen, M., *Some aspects of synergism in solvent extraction—I*. Journal of Inorganic and Nuclear Chemistry, 1963. **25**(5): p. 581-594.
216. Kumar, J.R., et al., *A Brief Review on Solvent Extraction of Uranium from Acidic Solutions*. Separation and Purification Reviews, 2011. **40**(2): p. 77-125.
217. Su, W., J. Chen, and Y. Jing, *Aqueous Partition Mechanism of Organophosphorus Extractants in Rare Earths Extraction*. Industrial & Engineering Chemistry Research, 2016. **55**(30): p. 8424-8431.
218. Kim, J.S., et al., *Studies on selection of solvent extractant system for the separation of trivalent Sm, Gd, Dy and Y from chloride solutions*. International Journal of Mineral Processing, 2012. **112**: p. 37-42.
219. Wang, X., W. Li, and D. Li, *Extraction and stripping of rare earths using mixtures of acidic phosphorus-based reagents*. Journal of Rare Earths, 2011. **29**(5): p. 413-415.
220. Xie, F., et al., *A critical review on solvent extraction of rare earths from aqueous solutions*. Minerals Engineering, 2014. **56**: p. 10-28.
221. Narayanan, N.S., V.R. Nair, and V.D. Narayanan, *Separation of rare earths, thorium and uranium during monazite processing by solvent extraction using 2-ethyl hexyl phosphonic acid mono 2-ethyl hexyl ester*. Rare Earths: Science, Technology & Applications Iii, ed. R.G. Bautista, et al. 1996, Warrendale: Minerals, Metals & Materials Soc. 3-8.

222. Gupta, C.K. and G.T. Krishnamurthy, *Extractive Metallurgy of Rare Earths*. 2005, USA: CRC Press.
223. Whatley, M.E. and G.L. Bridger, *Solvent Extraction of Solutions Containing Rare Earths. Preparation of Thorium Compounds from Monazite by Sulfuric Acid Decomposition and Solvent Extraction*. 1950.
224. Whatley, M.E., M. Smutz, and G.L. Bridger, *Purification of Thorium by Solvent Extraction*, in *Other Information: Decl. Feb. 26, 1957. Orig. Receipt Date: 31-DEC-57*. 1953. p. 92.
225. Sato, T., *Extraction of Uranium(6) and Thorium from Hydrochloric Acid Solutions by Tri-n-butyl Phosphate*. Journal of Applied Chemistry, 1966. **16**(2): p. 53-+.
226. El-Sweify, F.H., A.A. Abdel-Fattah, and S.M. Ali, *Extraction thermodynamics of Th(IV) in various aqueous organic systems*. The Journal of Chemical Thermodynamics, 2008. **40**(5): p. 798-805.
227. Suresh, A., T.G. Srinivasan, and P.R.V. Rao, *Extraction of U(VI), Pu(IV) and Th(IV) by some Trialkyl Phosphates*. Solvent Extraction and Ion Exchange, 1994. **12**(4): p. 727-744.
228. Haggag, A., et al., *Solvent Extraction Studies on Thorium Sulphate and Halides*. Journal of Radioanalytical Chemistry, 1976. **33**: p. 139-152.
229. Saleh, F.A., *Effect of diluents on the extraction of thorium nitrate with tributyl phosphate*. Zeitschrift für anorganische und allgemeine Chemie, 1969. **371**(1-2): p. 106-112.
230. Mandal, K., et al., *Hydrodynamic and mass transfer studies of 125 mm centrifugal extractor with 30% TBP/nitric acid system*. Progress in Nuclear Energy, 2015. **85**: p. 1-10.
231. Wu, S., R. Zhong, and X. Zhong, *Extraction of uranium, thorium, zirconium, titanium, and scandium involves mixing organic phase and material liquid, extracting, stirring, standing, separating water phase from organic phase, and extracting uranium from organic phase*, Patent number CN104263930-A CN10534634 13 Oct 2014. 2014, UNIV NANCHANG HANGKONG (UYNA-Non-standard). p. 5.
232. Ross, W.J. and J.C. White, *The Use of Tri-n-octylphosphine Oxide in the Solvent Extraction of Thorium from Acidic Solutions*. 1958, ; Oak Ridge National Lab., Tenn. p. Medium: ED.
233. Sato, T. and M. Yamatake, *The extraction of thorium (IV) from hydrochloric acid solutions by tri-n-octyl phosphine oxide*. Journal of Inorganic and Nuclear Chemistry, 1969. **31**(11): p. 3633-3642.
234. Sengupta, A., et al., *ICP-AES determination of trace metallic constituents in thorium matrix after preferential extraction of thorium using TBP, TOPO and DHOA: a comparative study*. Journal of Radioanalytical and Nuclear Chemistry, 2016. **310**(1): p. 59-67.
235. Sato, T., *Liquid-liquid extraction of thorium(IV) from hydrochloric acid solutions by dihexyl sulphoxide*. Solvent Extraction Research and Development-Japan, 2008. **15**: p. 61-69.
236. Mishra, S. and V. Chakravorty, *Binary Mixture of PC88a and TOPO as Extractant for Thorium(IV) from Aqueous HNO₃ and H₂SO₄ Media*.

- Journal of Radioanalytical and Nuclear Chemistry, 1996. **207**(1): p. 53-62.
237. Kedari, C.S., S.S. Pandit, and P.M. Gandhi, *Separation by competitive transport of uranium(VI) and thorium(IV) nitrates across supported renewable liquid membrane containing trioctylphosphine oxide as metal carrier*. Journal of Membrane Science, 2013. **430**: p. 188-195.
238. Dinkar, A.K., et al., *Carrier facilitated transport of thorium from HCl medium using Cyanex 923 in n-dodecane containing supported liquid membrane*. Journal of Radioanalytical and Nuclear Chemistry, 2013. **298**(1): p. 707-715.
239. Tong, H., et al., *Synergistic extraction of Ce(IV) and Th(IV) with mixtures of Cyanex 923 and organophosphorus acids in sulfuric acid media*. Separation and Purification Technology, 2013. **118**(0): p. 487-491.
240. Mallick, S., et al., *Third phase formation in the extraction of nitric acid and metal ions by octyl(phenyl)-N,N-diisobutyl carbamoyl methyl phosphine oxide (O Phi CMPO) based solvents*. Desalination and Water Treatment, 2011. **25**(1-3): p. 216-225.
241. Peppard, D.F., G.W. Mason, and S. McCarty, *Extraction of thorium(IV) by di esters of orthophosphoric acid, (GO)2PO(OH)*. Journal of Inorganic and Nuclear Chemistry, 1960. **13**(1): p. 138-150.
242. Baes, C.F., *The extraction of metallic species by dialkylphosphoric acids*. Journal of Inorganic and Nuclear Chemistry, 1962. **24**(6): p. 707-720.
243. Yoshizuka, K., et al., *Solvent extraction and molecular modeling of uranyl and thorium ions with organophosphorus extractants*. Solvent Extraction Research and Development-Japan, 2006. **13**: p. 115-122.
244. Nasab, M.E., A. Sam, and S.A. Milani, *Determination of optimum process conditions for solvent extraction of thorium using Taguchi method*. Journal of Radioanalytical and Nuclear Chemistry, 2011. **287**(1): p. 239-245.
245. Zangen, M., *Some aspects of synergism in solvent extraction—II: Some di-, tri- and tetravalent metal ions*. Journal of Inorganic and Nuclear Chemistry, 1963. **25**(8): p. 1051-1063.
246. Gasser, M.S., E.E. Zaki, and H.F. Aly, *Effect of an electric field on the transport of Th(IV) in the presence of Eu(III) and U(VI) through supported liquid membrane containing di-2-ethylhexylphosphoric acid*. Journal of Chemical Technology and Biotechnology, 2001. **76**(12): p. 1267-1272.
247. Mason, G.W., I. Bilobran, and D.F. Peppard, *Extraction of U(VI), Th(IV), Am(III) and Eu(III) by bis para-octylphenyl phosphoric acid in benzene diluent*. Journal of Inorganic and Nuclear Chemistry, 1978. **40**(10): p. 1807-1810.
248. Vandegrift, G.F. and E.P. Horwitz, *Interfacial activity of liquid-liquid extraction reagents—I*. Journal of Inorganic and Nuclear Chemistry, 1980. **42**(1): p. 119-125.

249. Zhong, X.M. and Y.H. Wu, *Recovery of uranium and thorium from zirconium oxychloride by solvent extraction*. Journal of Radioanalytical and Nuclear Chemistry, 2012. **292**(1): p. 355-360.
250. Peppard, D.F., et al., *Acidic Esters of Orthophosphoric Acid as Selective Extractants for Metallic Cations - Tracer Studies*. Journal of Inorganic & Nuclear Chemistry, 1958. **7**: p. 276-285.
251. Singh, D.K., et al., *Extraction of thorium with 2-ethyl hexyl phosphonic acid mono-2-ethyl hexyl ester (PC-88A)*. Journal of Radioanalytical and Nuclear Chemistry, 2001. **250**(1): p. 123-128.
252. Rout, K.C., et al., *Extraction of Thorium(IV) by CYANEX Reagents, PC-88a and their Mixtures from Aqueous Hydrochloric-acid Media*. Radiochimica Acta, 1993. **62**(4): p. 203-206.
253. Dinkar, A.K., et al., *Studies on the Separation and Recovery of Thorium from Nitric Acid Medium using (2-ethyl hexyl) Phosphonic Acid, Mono (2-ethyl hexyl) Ester (PC88A)/N-Dodecane as Extractant System*. Separation Science and Technology, 2012. **47**(12): p. 1748-1753.
254. Mansingh, P.S., V. Chakravorty, and K.C. Dash, *Solvent extraction of thorium(IV) by Cyanex 272 Cyanex 302 Cyanex 301 PC-88A and their binary mixtures with TBP/DOSO from aq HNO₃ and H₂SO₄ media*. Radiochimica Acta, 1996. **73**(3): p. 139-143.
255. Wang, L., et al., *Thermodynamics and kinetics of thorium extraction from sulfuric acid medium by HEH(EHP)*. Hydrometallurgy, 2014. **150**: p. 167-172.
256. Otu, E.O., *The synergistic extraction of thorium(IV) and uranium(VI) by 2-ethylhexyl phenylphosphonic acid and micelles of dinonyl naphthalene sulphonic acid*. Solvent Extraction and Ion Exchange, 1997. **15**(1): p. 1-13.
257. Otu, E.O., *The effect of temperature on the synergistic extraction of thorium(IV) and uranium(VI) by 2-ethylhexyl phenylphosphonic acid and micelles of dinonyl naphthalene sulphonic acid*. Solvent Extraction and Ion Exchange, 1998. **16**(5): p. 1161-1176.
258. Rao, C., et al., *Studies on extraction of actinides by unsymmetrical diamylbutyl phosphonate*. Radiochimica Acta, 2015. **103**(4): p. 235-243.
259. Tan, M.L., et al., *Highly efficient extraction separation of uranium(VI) and thorium(IV) from nitric acid solution with di(1-methyl-heptyl) methyl phosphonate*. Separation and Purification Technology, 2015. **146**: p. 192-198.
260. Vyas, C.K., et al., *Phosphonates as alternative to tributyl phosphate for the separation of actinides from fission products*. Radiochimica Acta, 2015. **103**(4): p. 277-285.
261. Flett, D.S., *Solvent extraction in hydrometallurgy: the role of organophosphorus extractants*. Journal of Organometallic Chemistry, 2005. **690**(10): p. 2426-2438.

262. Nasab, M.E., S.A. Milani, and A. Sam, *Extractive separation of Th(IV), U(VI), Ti(IV), La(III) and Fe(III) from Zarigan ore*. Journal of Radioanalytical and Nuclear Chemistry, 2011. **288**(3): p. 677-683.
263. Nasab, M.E., A. Sam, and S.A. Milani, *Determination of optimum process conditions for the separation of thorium and rare earth elements by solvent extraction*. Hydrometallurgy, 2011. **106**(3-4): p. 141-147.
264. Nasab, M.E., *Synergistic extraction of uranium(VI) and thorium(IV) with mixtures of Cyanex272 and other organophosphorus ligands*. Journal of Radioanalytical and Nuclear Chemistry, 2013. **298**(3): p. 1739-1747.
265. Shaeri, M., M. Torab-Mostaedi, and A.R. Kelishami, *Solvent extraction of thorium from nitrate medium by TBP, Cyanex272 and their mixture*. Journal of Radioanalytical and Nuclear Chemistry, 2015. **303**(3): p. 2093-2099.
266. Didi, M.A., et al., *Liquid-liquid extraction of thorium(IV) by fatty acids: a comparative study*. Journal of Radioanalytical and Nuclear Chemistry, 2014. **299**(3): p. 1191-1198.
267. Turanov, A.N., et al., *Effect of the structure of phosphorylated carboxylic acids on extraction of uranium and thorium from nitric acid solutions*. Radiochemistry, 2000. **42**(3): p. 251-256.
268. Gaur, P.K. and S.R. Mohanty, *Extraction of Thorium from Hydrochloric Acid Solutions by Dipentyl Sulphoxide*. Naturwissenschaften, 1963. **50**(19): p. 614-&.
269. Mohanty, S.R. and A.S. Reddy, *Solvent-Extraction of Thorium from Hydrochloric-Acid Solutions by Sulfoxides and their Mixtures*. Journal of Inorganic & Nuclear Chemistry, 1975. **37**(9): p. 1977-1982.
270. Yu, S.-N., et al., *The solvent extraction of UO₂²⁺ and Th⁴⁺ with petroleum sulfoxide*. Journal of Radioanalytical and Nuclear Chemistry, 1998. **232**(1): p. 249-251.
271. Chaohong, S., et al., *Extraction of U(VI), Th(IV) and some fission products from nitric acid medium by sulfoxides and effect of γ -irradiation on the extraction*. Journal of Radioanalytical and Nuclear Chemistry, 1994. **178**(1): p. 91-98.
272. Liu, B.-f., L.-b. Liu, and J.-k. Cheng, *Separation of thorium, uranium and rare-earth elements with 2-[(2-arsenophenyl)-azo]-1,8-dihydroxy-7-[(2,4,6-tribromophenyl)azo]-naphthalene-3,6-disulfonic acid by capillary electrophoresis*. Analytica Chimica Acta, 1998. **358**(2): p. 157-162.
273. Deshmukh, B.K. and D. Maheshwari, *Spectrophotometric Determination of Thorium(IV) and Fluoride with 2-carboxy-2'-hydroxy-3',5'-demethylazobenzene-4-sulphonic acid*. Chemia Analityczna, 1981. **26**(2): p. 313-317.
274. Crouse, D.J. and K.B. Brown, *The AMEX Process for Extracting Thorium Ores with Alkyl Amines*. Industrial and Engineering Chemistry, 1959. **51**(12): p. 1461-1464.

275. Higginson, M.A., et al., *Synthesis of functionalised BTPhen derivatives - effects on solubility and americium extraction*. Dalton Transactions, 2015. **44**(37): p. 16547-16552.
276. Shimojo, K., et al., *Highly Efficient Extraction Separation of Lanthanides Using a Diglycolamic Acid Extractant*. Analytical Sciences, 2014. **30**: p. 263-269.
277. Desouky, O.A., et al., *Liquid-liquid extraction of yttrium using primene-JMT from acidic sulfate solutions*. Hydrometallurgy, 2009. **96**(4): p. 313-317.
278. Jain, A., O.V. Singh, and S.N. Tandon, *Separation of Lanthanides and some Associated Elements by Liquid-Liquid-Extraction and Reverse Phase Thin-Layer Chromatography using High-Molecular-Weight Amine-Citrate System*. Indian Journal of Chemistry Section a-Inorganic Bio-Inorganic Physical Theoretical & Analytical Chemistry, 1991. **30**(2): p. 196-197.
279. Huifa, G., S. Jinglan, and M.A. Hughes, *A study of the extraction of ReO₄ with primary amine N1923*. Hydrometallurgy, 1990. **25**(3): p. 293-304.
280. Li, D., Y. Zuo, and S. Meng, *Separation of thorium(IV) and extracting rare earths from sulfuric and phosphoric acid solutions by solvent extraction method*. Journal of Alloys and Compounds, 2004. **374**(1-2): p. 431-433.
281. Liu, J.J., Y.L. Wang, and D.Q. Li, *Extraction kinetics of thorium(IV) with primary amine N1923 in sulfate media using a constant interfacial cell with laminar flow*. Separation Science and Technology, 2008. **43**(2): p. 431-445.
282. Ichikawa, F. and S. Uruno, *Separation of Uranium and Protactinium from Thorium by Amine Extraction*. Bulletin of the Chemical Society of Japan, 1960. **33**(5): p. 569-575.
283. Awwal, M.A. and D.J. Carswell, *Extraction of Thorium by Secondary Amines*. Journal of Inorganic & Nuclear Chemistry, 1968. **30**(4): p. 1057-&.
284. Florence, T.M. and Y.J. Farrar, *Liquid-liquid Extraction of Manganese, Chromium, Thorium by Long-chain Amines from Concentrated Halide Media*. Australian Journal of Chemistry, 1969. **22**(2): p. 473-&.
285. Elyamani, I.S. and E.I. Shabana, *Extraction of Protactinium(V) Chloro Complexes by Tri Capryl Amine and its Separation from Thorium(IV), Uranium(VI) and Rare-earths*. Journal of Radioanalytical and Nuclear Chemistry, 1985. **88**(2): p. 209-216.
286. Burcik, I. and V. Mikulaj, *Separation of Thorium, Uranium and Plutonium by Neutral and Basic Organic Extractants*. Journal of Radioanalytical and Nuclear Chemistry-Articles, 1991. **150**(2): p. 247-253.
287. Moore, F.L., *Liquid-liquid Extraction of Uranium and Plutonium from Hydrochloric Acid Solution with Tri(Iso-octyl) Amine Separation of*

- Uranium and Plutonium from Thorium and Fission Products*. 1957. p. 21.
288. Moore, F.L., *Liquid-liquid Extraction of Uranium and Plutonium from Hydrochloric Acid Solution with Tri(Iso-Octyl)Amine - Separation from Thorium and Fission Products*. Analytical Chemistry, 1958. **30**(5): p. 908-911.
289. Ejaz, M. and D.J. Carswell, *Amine Oxides as Solvents for Uranium, Thorium and some Fission-products*. Journal of Inorganic & Nuclear Chemistry, 1975. **37**(1): p. 233-237.
290. Ishimori, T., K. Kimura, and R. Ono, *Isolation of Uranium-233 from Irradiated Thorium Oxide - An Amine Extraction Procedure*. Journal of Nuclear Science and Technology-Tokyo, 1968. **5**(1): p. 39-&.
291. Abdel-Gawad, A.S., et al., *Amine Extraction of Protactinium(V) and Thorium(IV) from Aqueous Organic Acid Media*. Journal of Inorganic & Nuclear Chemistry, 1970. **32**(6): p. 2079-&.
292. Shivade, M.R. and V.M. Shinde, *Solvent-extraction Studies of Throium(IV) with Aliquat-336 as an Extractant*. Analyst, 1983. **108**(1290): p. 1155-1157.
293. Ali, A.M.I., et al., *Recovery of thorium (IV) from leached monazite solutions using counter-current extraction*. International Journal of Mineral Processing, 2007. **81**(4): p. 217-223.
294. Belova, V.V., et al., *Extraction of rare earth metals, uranium, and thorium from nitrate solutions by binary extractants*. Theoretical Foundations of Chemical Engineering, 2015. **49**(4): p. 545-549.
295. Borai, E.H., et al., *Extraction and Separation of Some Naturally Occurring Radionuclides from Rare Earth Elements by Different Amines*. Arab Journal of Nuclear Science and Applications, 2014. **47**(3): p. 48-60.
296. Patkar, S.N., A.S. Burungale, and R.J. Patil, *Separation and Liquid-Liquid Extraction of Thorium(IV) as Sulphate Complex with Synergistic Mixture of N-N-Octylaniline and Trioctylamine as an Extractant*. Rasayan Journal of Chemistry, 2009. **2**(4): p. 825-832.
297. Siddall III, T.H., *Application of Amides as Extractants*. 1961, ; Du Pont de Nemours (E. I.) ; Co. Savannah River Lab., Aiken, S.C. p. Medium: X; Size: Pages: 14.
298. Wang, Y.-S., et al., *Extraction of uranium(VI) and thorium(IV) ions from nitric acid solutions by N,N,N',N'-tetrabutyladipicamide*. Journal of Radioanalytical and Nuclear Chemistry, 1996. **214**(1): p. 67-76.
299. Shen, C., et al., *The structure effect of N,N,N',N'-alkylamide in the extraction of uranium and thorium*. Journal of Radioanalytical and Nuclear Chemistry, 1996. **212**(3): p. 187-196.
300. Ren, P., et al., *Synthesis and characterization of N,N,N',N'-tetraalkyl-4-oxaheptanediamide as extractant for extraction of uranium(VI) and thorium(IV) ions from nitric acid solution*. Journal of Radioanalytical and Nuclear Chemistry, 2014. **300**(3): p. 1099-1103.

301. Prabhu, D.R., et al., *Role of diluents in the comparative extraction of Th(IV), U(VI) and other relevant metal ions by DHOA and TBP from nitric acid media and simulated wastes: Reprocessing of U-Th based fuel in perspective*. Hydrometallurgy, 2015. **158**: p. 132-138.
302. Qureshi, M.A., et al., *High Molecular-weight Pyridine Amines as Solvents for Uranium(VI) and its Separation from Thorium*. Separation Science and Technology, 1978. **13**(10): p. 843-868.
303. Jankowska, M., J. Mikulski, and E. Ochab, *Extraction Properties of Octaethyltetraamidopyrophosphate (OETAPP). 2. Extraction of Thorium and Hafnium from Hydrochloric- and/or Nitric-acid Media*. Journal of Radioanalytical Chemistry, 1979. **50**(1-2): p. 61-67.
304. Lu, Y.C., et al., *Selective extraction and separation of thorium from rare earths by a phosphorodiamidate extractant*. Hydrometallurgy, 2016. **163**: p. 192-197.
305. Lu, Y.C., et al., *Extraction and separation of thorium and rare earths from nitrate medium with p-phosphorylated calixarene*. Journal of Chemical Technology and Biotechnology, 2013. **88**(10): p. 1836-1840.
306. Singh, S., et al., *Liquid-liquid-extraction of Th-4+ and UO-2(2+) by LIX-26 and its Mixtures*. Journal of Radioanalytical and Nuclear Chemistry-Articles, 1988. **120**(1): p. 65-73.
307. Singh, S., V. Chakravorty, and K.C. Dash, *Liquid-liquid-extraction of Thorium(IV) by LIX-54 and its Mixtures*. Journal of Radioanalytical and Nuclear Chemistry-Letters, 1988. **127**(5): p. 349-356.
308. Mohanty, R.N., et al., *Lix-84 as an Extractant for Thorium(IV), Uranium(VI) and Molybdenum(VI)*. Journal of Radioanalytical and Nuclear Chemistry-Articles, 1989. **132**(2): p. 359-367.
309. Liu, Y.H., J. Chen, and D.Q. Li, *Application and Perspective of Ionic Liquids on Rare Earths Green Separation*. Separation Science and Technology, 2012. **47**(2): p. 223-232.
310. Tian, G.-c., J. Li, and Y.-x. Hua, *Application of ionic liquids in hydrometallurgy of nonferrous metals*. Transactions of Nonferrous Metals Society of China, 2010. **20**(3): p. 513-520.
311. Takao, K., T.J. Bell, and Y. Ikeda, *Actinide Chemistry in Ionic Liquids*. Inorganic Chemistry, 2013. **52**(7): p. 3459-3472.
312. Stojanovic, A., et al., *Quaternary Ammonium and Phosphonium Ionic Liquids in Chemical and Environmental Engineering*. Ionic Liquids: Theory, Properties, New Approaches, 2011: p. 657-680.
313. Baba, Y., et al., *Recent Advances in Extraction and Separation of Rare-Earth Metals Using Ionic Liquids*. Journal of Chemical Engineering of Japan, 2011. **44**(10): p. 679-685.
314. Singh, M., et al., *Comparative study on the radiolytic stability of TBP, DHOA, Cyanex 923 and Cyanex 272 in ionic liquid and molecular diluent for the extraction of thorium*. Journal of Radioanalytical and Nuclear Chemistry, 2016. **309**(2): p. 615-625.

315. Zuo, Y., J. Chen, and D.Q. Li, *Reversed micellar solubilization extraction and separation of thorium(IV) from rare earth(III) by primary amine N1923 in ionic liquid*. Separation and Purification Technology, 2008. **63**(3): p. 684-690.
316. Zuo, Y., et al., *The separation of Cerium(IV) from nitric acid solutions containing Thorium(IV) and Lanthanides(III) using pure C(8)mim PF6 as extracting phase*. Industrial & Engineering Chemistry Research, 2008. **47**(7): p. 2349-2355.
317. Shen, Y.L., et al., *Extraction of Th(IV) from an HNO₃ Solution by Diglycolamide in Ionic Liquids*. Industrial & Engineering Chemistry Research, 2011. **50**(24): p. 13990-13996.
318. Shiri-Yekta, Z., M.R. Yaftian, and A. Nilchi, *Extraction-separation of Eu(III) and Th(IV) ions from nitrate media into a room-temperature ionic liquid*. Journal of the Iranian Chemical Society, 2013. **10**(2): p. 221-227.
319. Turanov, A.N., et al., *Extraction of U(VI), Th(IV), and Lanthanides(III) from Nitric Acid Solutions with CMPO-functionalized Ionic Liquid in Molecular Diluents*. Solvent Extraction and Ion Exchange, 2015. **33**(6): p. 540-553.
320. Karamzadeh, Z., et al., *Extraction-separation of Eu(III)/Th(IV) Ions with a Phosphorylated Ligand in an Ionic Liquid*. Iranian Journal of Chemistry & Chemical Engineering-International English Edition, 2016. **35**(2): p. 89-95.
321. Priya, S., et al., *Piperidinium based ionic liquid in combination with sulphoxides: Highly efficient solvent systems for the extraction of thorium*. Hydrometallurgy, 2016. **164**: p. 111-117.
322. Chen, Q., et al., *Extraction of uranyl ion or thorium ion from water phase involves using trialkyl phosphine oxide, diethylene glycol mono(tetramethylbutyl)phenylether and 1-alkyl-3-methylimidazolium bis(trifluoromethanesulfonyl)imide ionic liquid*, Patent number CN103045869-A CN10581639 27 Dec 2012 CN103045869-B CN10581639 27 Dec 2012. 2012, Univ Peking (Uypk-C).
323. Shen, X., Q. Chen, and J. Fu, *Extraction of thorium ion from aqueous phase thorium comprises taking ionic liquid diluting agent, adding N,N-dimethyl isobutylamine as extracting agent and mixing with solution containing thorium ion*, Patent number CN103045881-A CN10580027 27 Dec 2012 CN103045881-B CN10580027 27 Dec 2012. 2012, Univ Peking (Uypk-C).
324. Wu, W., et al., *Separation of uranium and thorium comprises extracting uranyl nitrate from uranium thorium nitrate solution using 1- or 2-methyl imidazole as extractant dissolved in ionic liquid diluent or n-pentanol*, Patent number CN103451426-A CN10436595 24 Sep 2013 CN103451426-B CN10436595 24 Sep 2013. 2013, Univ Lanzhou (Ulan-C).
325. Sahu, K.K. and R.P. Das, *Mixed solvent systems for the extraction and stripping of iron(III) from concentrated acid chloride solutions*.

- Metallurgical and Materials Transactions B-Process Metallurgy and Materials Processing Science, 2000. **31**(6): p. 1169-1174.
326. Baena, A., et al., *Effect of sintering atmosphere on the hardness of ThO₂*. Journal of Nuclear Materials, 2016. **477**: p. 222-227.
 327. Tel, H., M. Eral, and Y. Altaş, *Investigation of production conditions of ThO₂-UO₃ microspheres via the sol-gel process for pellet type fuels*. Journal of Nuclear Materials, 1998. **256**(1): p. 18-24.
 328. Yang, J.H., et al., *Fabrication and thermal conductivity of (Th,U)O₂ pellets*. Nuclear Technology, 2004. **147**(1): p. 113-119.
 329. Kutty, T.R.G., et al., *Characterization of ThO₂-UO₂ pellets made by co-precipitation process*. Journal of Nuclear Materials, 2009 **389**(3): p. 351-358.
 330. Kutty, T.R.G., et al., *Characterization of (Th,U)O₂ pellets made by advanced CAP process*. Journal of Nuclear Materials, 2009 **384**(3): p. 303-310.
 331. Silva, G.W.C., et al., *Fluoride-Conversion Synthesis of Homogeneous Actinide Oxide Solid Solutions*. Inorganic Chemistry, 2011. **50**(21): p. 11004-11010.
 332. Sokucu, A.S., M. Bedir, and M.T. Aybers, *Study on Preparation and First-Stage Sintering Kinetics of ThO₂-UO₂ Pellets Made by Sol-Gel Microspheres Technique*. Acta Physica Polonica A, 2015. **127**(4): p. 987-991.
 333. Lahoda, E.J., *Costs for manufacturing thorium-uranium dioxide fuels for light water reactors*. Nuclear Technology, 2004. **147**(1): p. 102-112.
 334. Todosow, M., et al., *Use of thorium in light water reactors*. Nuclear Technology, 2005. **151**(2): p. 168-176.
 335. Radkowsky, A. and A. Galperin, *The nonproliferative light water thorium reactor: A new approach to light water reactor core technology*. Nuclear Technology, 1998. **124**(3): p. 215-222.
 336. MacDonald, P.E. and C.B. Lee, *Use of thoria-urania fuels in PWRs: A general review of a NERI project to assess feasible core designs, economics, fabrication methods, in-pile thermal/mechanical behavior, and waste form characteristics*. Nuclear Technology, 2004. **147**(1): p. 1-7.
 337. Rubbia, C., et al., *Conceptual Design of a Fast Neutron Operated High Power Energy Amplifier*, CERN (European Organisation for Nuclear Research), Editor. 1995.
 338. World Nuclear Association. *Accelerator-driven Nuclear Energy*. 2011 [cited 2012 5 Sep]; Available from: <http://www.world-nuclear.org/info/inf35.html>.
 339. Lidsky, L.M., *Fission-Fusion Systems - Hybrid, Symbiotic and Augean*. Nuclear Fusion, 1975 **15**(1): p. 151-173.
 340. Sahin, S., H. Yapici, and N. Sahin, *Neutronic performance of proliferation hardened thorium fusion breeders*. Fusion Engineering and Design, 2001. **54**(1): p. 63-77.

341. Ubeyli, M. and E. Tel, *Effect of different structural materials on neutronic performance of a hybrid reactor*. Journal of Fusion Energy, 2003. **22**(2): p. 173-179.
342. Yapici, H. and M. Bayrak, *Neutronic analysis of denaturing plutonium in a thorium fusion breeder and power flattening*. Energy Conversion and Management, 2005. **46**(7-8): p. 1209-1228.
343. Acir, A. and M. Ubeyli, *Burning of reactor grade plutonium mixed with thorium in a hybrid reactor*. Journal of Fusion Energy, 2007. **26**(3): p. 293-298.
344. Ubeyli, M. and A. Acir, *Incineration of weapon grade plutonium in a (DT) fusion driven hybrid reactor using various coolants*. Kerntechnik, 2007. **72**(1-2): p. 27-32.
345. Zhirkin, A.V., et al., *Neutronics analysis of blankets for a hybrid fusion neutron source*. Nuclear Fusion, 2015. **55**(11): p. 10.
346. Galperin, A., P. Reichert, and A. Radkowsky, *Thorium fuel for light water reactors—reducing proliferation potential of nuclear power fuel cycle*. Science & Global Security, 1997. **6**(3): p. 265-290.
347. Radkowsky, A., *Seed-blanket reactors (a nuclear reactor having a core including a plurality of seed-blanket units)*, Patent number, United States Patent Office, Editor. 1998, Radkowsky Thorium Power Corp.: United States of America. p. 24.
348. Radkowsky, A., *Seed-blanket reactors (a method for operating a nuclear reactor core comprised of at least first and second groups of seed-blanket units)*, Patent number, United states patent Office, Editor. 1999, Radkowsky Thorium Power Corp.: United States of America. p. 24.
349. Radkowsky, A., *Seed-blanket reactors (a nuclear reactor having a core including a plurality of seed-blanket unit)*, Patent number, United States Patent Office, Editor. 1999, Radkowsky Thorium Power Corp.: United States of America. p. 25.
350. Radkowsky, A., *Seed-blanket reactors (a seed-blanket unit fuel assembly for a nuclear reactor)*, Patent number, United States Patent Office, Editor. 2000, Radkowsky Thorium Power Corp.: United States of America. p. 24.
351. Lightbridge. *Thorium-based Seed & Blanket Fuel Assembly*. 2009 [cited 2013 13 May]; Available from: <http://www.ltbridge.com/technologyservices/fueltechnology/thoriumbasedseedandblanketfuel>.
352. Fridman, E. and S. Kliem, *Pu recycling in a full Th-MOX PWR core. Part I: Steady state analysis*. Nuclear Engineering and Design, 2011. **241**(1): p. 193-202.
353. Lau, C.W., et al., *Improvement of LWR thermal margins by introducing thorium*. Progress in Nuclear Energy, 2012. **61**: p. 48-56.
354. Subkhi, M.N., Z. Su'ud, and A. Waris, *Design Study of Long-Life PWR using Thorium Cycle*, in *3rd International Conference on Advances in*

- Nuclear Science and Engineering 2011*, Z. Suud and A. Waris, Editors. 2012, Amer Inst Physics: Melville. p. 101-106.
355. Lombardi, C., et al., *Inert matrix and thoria fuels for plutonium elimination*. *Progress in Nuclear Energy*, 2001. **38**(3-4): p. 395-398.
356. Shelley, A., et al., *Parametric studies on plutonium transmutation using uranium-free fuels in light water reactors*. *Nuclear Technology*, 2000. **131**(2): p. 197-209.
357. Oggianu, S.M., H.C. No, and M.S. Kazimi, *Analysis of burnup and economic potential of alternative fuel materials in thermal reactors*. *Nuclear Technology*, 2003. **143**(3): p. 256-269.
358. Dziadosz, D., et al., *Weapons-grade plutonium-thorium PWR assembly design and core safety analysis*. *Nuclear Technology*, 2004. **147**(1): p. 69-83.
359. Trellue, H.R., C.G. Bathke, and P. Sadasivan, *Neutronics and material attractiveness for PWR thorium systems using monte carlo techniques*. *Progress in Nuclear Energy*, 2011. **53**(6): p. 698-707.
360. Waris, A., et al., *Study on Equilibrium Characteristics of Thorium-Plutonium-Minor Actinides Mixed Oxides Fuel in PWR*, in *2nd International Conference on Advances in Nuclear Science and Engineering - Icanse 2009*, Z. Suud and A. Waris, Editors. 2010, Amer Inst Physics: Melville. p. 85-90.
361. Permana, S., N. Takaki, and H. Sekimoto, *Preliminary study on feasibility of large and small water cooled thorium breeder reactor in equilibrium states*. *Progress in Nuclear Energy*, 2008. **50**(2-6): p. 320-324.
362. Tsigé-Tamirat, H., *Neutronics assessment of the use of thorium fuels in current pressurized water reactors*. *Progress in Nuclear Energy*, 2011. **53**(6): p. 717-721.
363. Takaki, N. and D. Mardiansah, *Core Design and Deployment Strategy of Heavy Water Cooled Sustainable Thorium Reactor*. *Sustainability*, 2012. **4**(8): p. 1933-1945.
364. Bi, G.W., S.Y. Si, and C.Y. Liu, *Core Design, Spent-Fuel Characteristics Assessment, and Fuel Cycle Analysis for Thorium-Uranium Breeding Recycle in Pressurized Water Reactors*. *Nuclear Technology*, 2013. **183**(3): p. 308-320.
365. Marshalkin, V.E. and V.M. Povyshev, *Utilization of Non-Weapons-Grade Plutonium and Highly Enriched Uranium with Breeding of the U-233 Isotope in the VVER Reactors Using Thorium and Heavy Water*. *Physics of Atomic Nuclei*, 2015. **78**(11): p. 1287-1300.
366. Tucker, L.P., A. Alajo, and S. Usman, *Thorium-based mixed oxide fuel in a pressurized water reactor: A beginning of life feasibility analysis with MCNP*. *Annals of Nuclear Energy*, 2015. **76**: p. 323-334.
367. Alhaj, M.Y., et al., *Partial Loading of Thorium-Plutonium Fuel in a Pressurized Water Reactor*. *Nuclear Technology*, 2016. **194**(3): p. 314-323.

368. McDeavitt, S.M., et al., *Zirconium matrix cermet for a mixed uranium-thorium oxide fuel in an SBWR*. Nuclear Technology, 2007. **157**(1): p. 37-52.
369. Bjork, K.I., V. Fhager, and C. Demaziere, *Comparison of thorium-based fuels with different fissile components in existing boiling water reactors*. Progress in Nuclear Energy, 2011. **53**(6): p. 618-625.
370. Galahom, A.A., Bashter, II, and M. Aziz, *Design of an MCNPX model to simulate the performance of BWRs using thorium as fuel and its validation with HELIOS code*. Annals of Nuclear Energy, 2015. **77**: p. 393-401.
371. Venneri, F., et al., *The Analysis of the Thorium-fuelled Modular Helium-cooled reactor*. Proceedings of the 4th International Topical Meeting on High Temperature Reactor Technology, Vol 1. 2009, New York: Amer Soc Mechanical Engineers. 385-390.
372. Sahin, H.M., O. Erol, and A. Acir, *Utilization of thorium in a Gas Turbine - Modular Helium Reactor*. Energy Conversion and Management, 2012. **63**: p. 25-30.
373. Talamo, A., *A novel concept of QUADRISO particles – Part III: Applications to the plutonium–thorium fuel cycle*. Progress in Nuclear Energy, 2009 **51**(2): p. 274-280.
374. Allelein, H.J., et al., *Thorium fuel performance assessment in HTRs*. Nuclear Engineering and Design, 2014. **271**: p. 166-170.
375. Acir, A. and H. Coskun, *Neutronic analysis of the PBMR-400 full core using thorium fuel mixed with plutonium or minor actinides*. Annals of Nuclear Energy, 2012. **48**: p. 45-50.
376. Critoph, E., et al., *Prospects for Self-sufficient Equilibrium Thorium Cycles in CANDU Reactors*, in *ANS 1975 Winter Meeting*. 1976: San Francisco, 16-21 November 1975.
377. Bonin, H.W., *CANDU Pressurized Heavy-water Reactor Thorium-U233 Oxide Fuel Evaluation Based on Optimal Fuel-management*. Nuclear Technology, 1987. **76**(3): p. 390-399.
378. Golesorkhi, S., B.P. Bromley, and M.H. Kaye, *Simulations of a Pressure-Tube Heavy Water Reactor Operating on Near-Breeding Thorium Cycles*. Nuclear Technology, 2016. **194**(2): p. 178-191.
379. Bromley, B.P., *Multiregion Annular Heterogeneous Core Concepts for Plutonium-Thorium Fuels in Pressure-Tube Heavy Water Reactors*. Nuclear Technology, 2016. **194**(2): p. 192-203.
380. Mardiansah, D. and N. Takaki, *Deployment Scenario of Heavy Water Cooled Thorium Breeder Reactor*, in *2nd International Conference on Advances in Nuclear Science and Engineering - Icanse 2009*, Z. Suud and A. Waris, Editors. 2010, Amer Inst Physics: Melville. p. 109-120.
381. Gholamzadeh, Z., et al., *Burn-up calculation of different thorium-based fuel matrixes in a thermal research reactor using MCNPX 2.6 code*. Nukleonika, 2014. **59**(4): p. 129-136.
382. Türkmen, M. and O.H. Zabunoğlu, *Use of Th and U in CANDU-6 and ACR-700 on the once-through cycle: Burnup analyses, natural U*

- requirement/saving and nuclear resource utilization*. Journal of Nuclear Materials, 2012. **429**(1-3): p. 263-269.
383. Saldideh, M., M. Shayesteh, and M. Eshghi, *Neutronic calculations for CANDU thorium systems using Monte Carlo techniques*. Chinese Physics C, 2014. **38**(8): p. 5.
384. Trellue, H.R., et al., *Salt-cooled Modular Innovative Thorium Heavy Water-moderated Reactor System*. Nuclear Technology, 2013. **182**(1): p. 26-38.
385. Sahin, S., M.J. Khan, and R. Ahmed, *CANDU reactors with reactor grade plutonium/thorium carbide fuel*. Kerntechnik, 2011. **76**(4): p. 268-272.
386. Lau, C.W., et al., *Feasibility Study of 1/3 Thorium-Plutonium Mixed Oxide Core*. Science and Technology of Nuclear Installations, 2014: p. 10.
387. Wood-Black, F., *Considerations for Scale-Up – Moving from the Bench to the Pilot Plant to Full Production*, in *Academia and Industrial Pilot Plant Operations and Safety*. 2014, American Chemical Society. p. 37-45.
388. Danesi, P.R., R. Chiarizia, and G. Scibona, *The meaning of slope analysis in solvent extraction chemistry*. Journal of Inorganic and Nuclear Chemistry, 1970. **32**(7): p. 2349-2355.
389. McCabe, W.L. and E.W. Thiele, *Graphical Design of Fractionating Columns*. Industrial and Engineering Chemistry, 1925. **17**(6): p. 605-611.
390. Zhang, Y., et al., *Synergistic extraction of vanadium(IV) in sulfuric acid media using a mixture of D2EHPA and EHEHPA*. Hydrometallurgy, 2016. **166**: p. 87-93.
391. Kolarik, Z., *Review: Dissociation, Self-Association, and Partition of Monoacidic Organophosphorus Extractants*. Solvent Extraction and Ion Exchange, 2010. **28**(6): p. 707-763.
392. Binghua, Y., et al., *Solvent extraction of metal ions and separation of nickel(II) from other metal ions by organophosphorus acids*. Solvent Extraction and Ion Exchange, 1996. **14**(5): p. 849-870.
393. Miralles, N., et al., *On the Interaction of Metal Extractant Reagent .4. The Aggregation of Organophosphorus Acid Compounds in Toluene*. Analytical Sciences, 1992. **8**(6): p. 773-777.
394. Peppard, D.F., M.N. Namboodiri, and G.W. Mason, *Extraction of Th(IV) as a Mixed Complex, Nitrate or Chloride, by 2-ethylhexyl hydrogen 2-ethylhexyl phosphonate*. Journal of Inorganic & Nuclear Chemistry, 1962. **24**(DEC): p. 979-988.
395. National Centre for Biotechnology Information. *CID=8182*. [cited 2016 19th April]; Dodecane physical data]. Available from: <https://pubchem.ncbi.nlm.nih.gov/compound/dodecane>.
396. Luo, J., et al., *Theoretical studies on the AnO_{2n+} (An = U, Np; n = 1, 2) complexes with di-(2-ethylhexyl)phosphoric acid*. Dalton Transactions, 2015. **44**(7): p. 3227-3236.

397. Singh, D.K., H. Singh, and J.N. Mathur, *Synergistic extraction of U(VI) with mixtures of 2-ethyl hexyl phosphonic acid-mono-2-ethyl hexyl ester (PC-88A) and TBP, TOPO or Cyanex 923*. *Radiochimica Acta*, 2001. **89**: p. 573-578.
398. Sujata Mishra, M. and V. Chakravortty, *Extraction of uranium(VI) by the binary mixture of Aliquat 336 and PC88A from aqueous H₃PO₄ medium*. *Hydrometallurgy*, 1997. **44**(3): p. 371-376.
399. Singh, D.K., H. Singh, and J.N. Mathur, *Synergistic extraction of U(VI) with mixtures of 2-ethyl hexyl phosphonic acid-mono-2-ethyl hexyl ester (PC-88A) and TBP, TOPO or Cyanex 923*. *Radiochimica Acta*, 2001. **89**(9): p. 573-578.
400. Biswas, S., et al., *Synergistic extraction of uranium with mixtures of PC88A and neutral oxodors*. *Journal of Radioanalytical and Nuclear Chemistry*, 2010. **284**(1): p. 13-19.
401. Jayachandran, J. and P.M. Dhadke, *Liquid-liquid extraction separation of iron (III) with 2-ethyl hexyl phosphonic acid mono 2-ethyl hexyl ester*. *Talanta*, 1997. **44**(7): p. 1285-1290.
402. Sandhibigraha, A., P. Sarma, and V. Chakravortty, *Solvent extraction of iron(III) from aqueous hydrochloric acid solutions using D2EHPA, PC-88A, cyanex-272 and their mixtures*. *Scandinavian Journal of Metallurgy*, 1996. **25**(3): p. 135-140.
403. Biswas, R.K. and D.A. Begum, *Solvent extraction of Fe³⁺ from chloride solution by D2EHPA in kerosene*. *Hydrometallurgy*, 1998. **50**(2): p. 153-168.
404. Sahu, K.K. and R.P. Das, *Synergistic extraction of iron(III) at higher concentrations in D2EHPA-TBP mixed solvent systems*. *Metallurgical and Materials Transactions B*, 1997. **28**(2): p. 181-189.
405. Sandhibigraha, A., P.V.R.B. Sarma, and V. Chakravortty, *Stripping studies of iron(III) extracted by D2EHPA, PC88A, and CYANEX 272 from chloride solutions using sulphuric and hydrochloric acids*. *Solvent Extraction Research and Development Japan*, 2000. **7**: p. 93-105.
406. Xiao, C., et al., *Solvent Extraction of Molybdenum (VI) from Hydrochloric Acid Leach Solutions Using P507. Part I: Extraction and Mechanism*. *Solvent Extraction and Ion Exchange*, 2017. **35**(2): p. 130-144.
407. Zhang, Y., et al., *Synergistic extraction of rare earths by mixture of HDEHP and HEH/EHP in sulfuric acid medium*. *Journal of Rare Earths*, 2008. **26**(5): p. 688-692.
408. Luo, X., et al., *Synergistic extraction of cerium from sulfuric acid medium using mixture of 2-ethylhexyl phosphonic acid mono 2-ethylhexyl ester and Di-(2-ethyl hexyl) phosphoric acid as extractant*. *Journal of Rare Earths*, 2009. **27**(1): p. 119-122.
409. Job, P., *Formation and Stability of Inorganic Complexes in Solution*. *Annali di Chimica Applicata*, 1928. **9**: p. 113-203.

410. Huang, C.Y., *Determination of binding stoichiometry by the continuous variation method: The job plot*, in *Methods in Enzymology*, L.P. Daniel, Editor. 1982, Academic Press. p. 509-525.
411. Gao, S., et al., *Characterization of reversed micelles formed in solvent extraction of thorium(IV) by bis(2-ethylhexyl) phosphoric acid. Transforming from rodlike to wormlike morphology*. *Radiochimica Acta*, 2016. **104**(7): p. 457-469.
412. Gal, I.J. and R.M. Nikolić, *The method of continuous variations applied to the extraction of metal ions with mixed solvents*. *Journal of Inorganic and Nuclear Chemistry*, 1966. **28**(2): p. 563-569.
413. Nelms, S., ed. *Inductively Coupled Plasma Mass Spectrometry Handbook*. 1 ed. 2005, Blackwell Publishing. 504.
414. Taylor, H.E., *Inductively Coupled Plasma-Mass Spectrometry: Practices and Techniques*. 1st ed. 2000, Boulder, Colorado: Academic Press. 308.
415. Profrock, D. and A. Prange, *Inductively Coupled Plasma-Mass Spectrometry (ICP-MS) for Quantitative Analysis in Environmental and Life Sciences: A Review of Challenges, Solutions, and Trends*. *Applied Spectroscopy*, 2012. **66**(8): p. 843-868.
416. May, T.W. and R.H. Weidmeyer, *A Table of Polyatomic Interferences in ICP-MS*. *Atomic Spectroscopy*, 1998. **19**(5): p. 150-155.
417. PerkinElmer Life and Analytical Sciences, *Elan DRC II Mass Spectrometer Brochure*. 2004, PerkinElmer Life and Analytical Sciences: Shelton, Connecticut, USA.
418. Boss, C.B. and K.J. Fredeen, *Concepts, Instrumentation and Techniques in Inductively Coupled Plasma Optical Emission Spectrometry*. 3rd ed. 2004, United States of America: The Perkin-Elmer Corporation.
419. Nolte, J., *ICP Emission Spectrometry: A Practical Guide*. 1st ed. 2003: Wiley-VCH. 290.
420. Evans, E.H., et al., *Atomic spectrometry update: review of advances in atomic spectrometry and related techniques*. *Journal of Analytical Atomic Spectrometry*, 2016. **31**(5): p. 1057-1077.
421. Quinn, J.E., et al., *Solvent extraction of rare earth elements using phosphonic/phosphinic acid mixtures*. *Hydrometallurgy*, 2015. **157**: p. 298-305.
422. Kao, H.-C., P.-S. Yen, and R.-S. Juang, *Solvent extraction of La(III) and Nd(III) from nitrate solutions with 2-ethylhexylphosphonic acid mono-2-ethylhexyl ester*. *Chemical Engineering Journal*, 2006. **119**(2-3): p. 167-174.
423. Castro, P. and M.E. Huber, *Marine Biology*. 4th ed. 2003: McGraw-Hill. 461.
424. Wilson, R.E., et al., *Structures of Dimeric Hydrolysis Products of Thorium*. *Inorganic Chemistry*, 2007. **46**(7): p. 2368-2372.
425. Acharya, S., S. Mishra, and P.K. Misra, *Studies on extraction and separation of La(III) with DEHPA and PC88A in petrofin*. *Hydrometallurgy*, 2015. **156**: p. 12-16.

426. Reddy, B.R. and P.V.R. Bhaskara Sarma, *Extraction of iron(III) at macro-level concentrations using TBP, MIBK and their mixtures*. Hydrometallurgy, 1996. **43**(1-3): p. 299-306.
427. Wang, Y., et al., *Preparation of high-purity thorium by solvent extraction with di-(2-ethylhexyl) 2-ethylhexyl phosphonate*. Journal of Radioanalytical and Nuclear Chemistry, 2013. **298**(3): p. 1651-1657.
428. Singh, S.K., S.C. Tripathi, and D.K. Singh, *Studies on the Separation and Recovery of Uranium from Phosphoric Acid Medium Using a Synergistic Mixture of (2-Ethylhexyl)phosphonic Acid Mono 2-Ethyl Hexyl Ester (PC-88A) and Tri-n-octylphosphine Oxide (TOPO)*. Separation Science and Technology, 2010. **45**(6): p. 824-831.
429. Singh, S.K., et al., *Studies on the recovery of uranium from phosphoric acid medium using synergistic mixture of (2-Ethyl hexyl) Phosphonic acid, mono (2-ethyl hexyl) ester (PC88A) and Tri-n-butyl phosphate (TBP)*. Hydrometallurgy, 2009. **95**(1-2): p. 170-174.
430. Gray, M., P. Zalupski, and M. Nilsson, *Activity Coefficients of di-(2-ethylhexyl) Phosphoric Acid in Select Diluents*. Procedia Chemistry, 2012. **7**: p. 209-214.
431. Quinn, J.E., D. Wilkins, and K.H. Soldenhoff, *Solvent extraction of uranium from saline leach liquors using DEHPA/Alamine 336 mixed reagent*. Hydrometallurgy, 2013. **134**: p. 74-79.
432. Sato, T., *The extraction of uranium (VI) from sulphuric acid solutions by di-(2-ethylhexyl)-phosphoric acid*. Journal of Inorganic and Nuclear Chemistry, 1962. **24**(6): p. 699-706.
433. Tyrpekl, V., et al., *Alterations of thorium oxalate morphology by changing elementary precipitation conditions*. Journal of Nuclear Materials, 2017. **493**: p. 255-263.
434. Aspen Technology Inc., *Aspen Plus*. 2012: Burlington, Massachusetts, USA.
435. Peel, R., et al., *Three-component U-Pu-Th fuel for plutonium irradiation in heavy water reactors*. EPJ Nuclear Sci. Technol., 2016. **2**: p. 29.
436. Hertzler, T.J., D.D. Nishimoto, and M.D. Otis, *Depleted Uranium Disposal Options Evaluation*. 1994.
437. Ovanes, M., et al. *Enhanced CANDU 6 : Reactor Core Design & Fuel Cycle Flexibility in SIEN (International Symposium on Nuclear Energy)*. 2011. Bucharest, Romania: CANDU Energy.
438. Candu Energy Inc., *Enhanced CANDU 6 Technical Summary*. 2012, Candu Energy Inc.: www.candu.com.
439. Meneley, D.A. and Y.Q. Ruan, *CANDU6 Calandria*, 19980102_002.jpg. 1998, Atomic Energy of Canada Ltd.: CANTEACH website. p. Photograph of CANDU6 calandria, with two workers.
440. Meneley, D.A. and Y.Q. Ruan, *CANDU6 Reactor Assembly*, 19980101_012.jpg. 1998, Atomic Energy of Canada Ltd.: CANTEACH website. p. Diagram of selected components of CANDU 6 reactor, focussing on fuel channels.

441. Su, J.J., *Thermalhydraulic Evaluations for a CANFLEX Bundle with Natural or Recycled Uranium Fuel in the Uncrept and Crept Channels of a CANDU-6 Reactor* Nuclear Engineering and Technology, 2005. **37**(5): p. 479-490.
442. Inch, W.W.R., et al. *Increasing CANDU Operating Margins with CANFLEX Fuel in COG/IAEA 6th Technical Committee Meeting on the Exchange of Operational Safety Experience of Pressurised Heavy Water Reactors*. 2000. Trois Rivieres, Quebec.
443. Colton, A., et al., *Code-to-code comparisons of lattice physics calculations for thorium-augmented and thorium-based fuels in pressure tube heavy water reactors*. Annals of Nuclear Energy, 2017. **103**: p. 194-203.
444. Blair, D.P., *UK EPR Pre-Construction Safety Report, Sub-chapter 4.3 - Nuclear Design*, in *UK EPR Pre-Construction Safety Report*. 2012, EDF: UK EPR Generic Design Assessment website. p. 71.
445. *Geological Disposal – Assessment of the implications for the products of reprocessing compared to direct disposal of the spent fuel*. 2012, UK Nuclear Decommissioning Authority: www.nda.gov.uk. p. 31.
446. Azeez, S. and J. Hopwood. *The Enhanced CANDU 6™ Reactor - Generation III CANDU Medium Size Global Reactor in the International conference on opportunities and challenges for water cooled reactors in the 21st century*. 2009. Vienna, Austria: <http://www-pub.iaea.org/>.
447. Aleyaseen, V., C.M. Cottrell, and S. Kuran, *Demonstration of a New Recycled Fuel for CANDU*, in *Nuclear Engineering International*. 2014: www.neimagazine.com.
448. Hopwood, J., et al., *Enhanced CANDU 6: An Upgraded Reactor Product with Optimal Fuel Cycle Capability*. Proceedings of the 18th International Conference on Nuclear Engineering 2010, Vol 6. 2011, New York: Amer Soc Mechanical Engineers. 369-373.
449. Nuclear-21.net, *UK NPP-Park Projection*. 2016, Nuclear-21.net: Unpublished data.
450. Zheng, S., J. Lonchamp, and B. Winterholer, *Etudes de combustibles au Thorium dans les réacteurs PHWR (Modélisation au niveau "grappe du combustible")*. 2012, AREVA NP: Unpublished internal data.
451. Carlier, B., et al., *Caractéristiques techniques des coeurs des réacteurs nucléaires*. 2009, CEA Direction d'Energie Nucléaire: Centre de Cadarache.
452. Lonchamp, J., *Evaluation des performances du CANDU 100% MOX*. 2013, AREVA NP: AREVA internal report. p. 12.
453. Popov, S.G., et al., *Thermophysical Properties of MOX and UO₂ Fuels Including the Effects of Irradiation*. 2000, Oak Ridge National Laboratory: <http://web.ornl.gov/>. p. 9-13.
454. Santamarina, A., et al., *The JEFF-3.1.1 Nuclear Data Library*, in *JEFF Report Series*, A. Santamarina, D. Bernard, and Y. Rugama, Editors. 2009, OECD Nuclear Energy Agency.

455. Obložinský, P., et al., *Evaluated Nuclear Data File ENDF/B-VII.0* ENDF/B-VII.0: Next Generation Evaluated Nuclear Data Library for Nuclear Science and Technology. Nuclear Data Sheets, 2006. **107**(12): p. 2931-3060.
456. Kim, Y., D. Hartanto, and W. Kim, *A Lattice-Based Monte Carlo Evaluation of Canada Deuterium Uranium-6 Safety Parameters*. Nuclear Engineering and Technology, 2016. **48**(3): p. 642-649.
457. Bennet, D.J. and J.R. Thompson, *The Fast Fission Factor*, in *The Elements of Nuclear Power*, J.R. Thompson, Editor. 1989, Longman. p. 79.
458. Crist, J.E., et al. *Neutron Multiplication Factor and Reactivity*. Nuclear Theory, Course 227, Nuclear Training Centre 20053700 1979 [cited 2016 05 July]; Introductory reactor physics covering the basic phenomena without extensive use of equations.]. Available from: <https://canteach.candu.org/Content%20Library/20053706.pdf>.
459. *Module 14 - Annulus Gas System*. Course 233 - Reactor & Auxiliaries [cited 2016 05 July]; 3rd:[Teaching materials on the subject of the CANDU annulus gas system]. Available from: <https://canteach.candu.org/Content%20Library/20053816.pdf>.
460. Yee, F., et al. *AFCR and EC6: The Two Sister Products* in *ICONE21 - 21st International Conference on Nuclear Energy*. 2013. Chengdu, China: The American Society of Mechanical Engineers.
461. *Reactor Physics Constants*, in *Other Information: Orig. Receipt Date: 31-DEC-63*. 1963. p. Medium: ED; Size: Pages: 876.
462. Palleck, S.J., R. Sejnoha, and B.J. Wong, *Bundle Uranium Content and Performance of CANDU Fuel*, in *5th International CNS CANDU Fuel Conference*. 1997, Canadian Nuclear Society: Toronto, Canada. p. 243-255.
463. Ioffe, B.L. and L.B. Okun, *Fuel burn-up in nuclear reactors*. The Soviet Journal of Atomic Energy, 1956. **1**(4): p. 529-544.
464. Pusa, M., *Numerical Methods for Nuclear Fuel Burnup Calculations*, in *Department of Mathematics and Systems Analysis*. 2013, Aalto University, Finland. p. 174.
465. Chyba, C.F. and C.R. Milne, *Simple calculation of the critical mass for highly enriched uranium and plutonium-239*. American Journal of Physics, 2014. **82**(10): p. 977-979.
466. Clercq, G.D. and B. Mallet. *EDF says Hinkley Point cost could rise 3 billion pounds, timing slips*. [Press article] 2016 12 May [cited 2016 10 August]; Available from: <http://uk.reuters.com/article/uk-edf-nuclear-britain-idUKKCN0Y30Q6>.
467. Ko, W.I. and F. Gao, *Economic Analysis of Different Nuclear Fuel Cycle Options*. Science and Technology of Nuclear Installations, 2012. **2012**: p. 10.
468. Yang, M.S., et al., *The Status and Prospect of DUPIC Fuel Technology*. 38, 2006. **4**.

469. Greenwood, S., et al., *Solid Radioactive Waste Strategy Report*, in *UK EPR Generic Design Assessment Supporting Documents*. 2008, AREVA NP: www.epr-reactor.co.uk. p. 257.
470. Muzumdar, A. and D. Meneley, *Large LOCA Margins & Void Reactivity In CANDU Reactors*. 2007, CANDU Owner's Group Inc.
471. Goorley, T., et al., *Initial MCNP6 Release Overview*. Nuclear Technology, 2012. **180**(3): p. 298-315.
472. Griffiths, J., *WIMS-AECL Users Manual*. 1994, Atomic Energy of Canada Ltd.
473. Rouben, B., *Overview of Current RFSP-Code Capabilities for CANDU Core Analysis*. 1996, Atomic Energy of Canada Ltd. p. 74.
474. Marleau, G., R. Roy, and A. Hebert, *DRAGON - A Collision Probability Transport Code for Cell and Supercell Calculations*. 1993, Ecole Polytechnique de Montreal: Montreal, Canada.
475. Hebert, A., D. Sekki, and R. Chambron, *A User Guide for DONJON Version 4*. 2016, Ecole Polytechnique de Montreal: Montreal, Canada.
476. Van Den Durpel, L., et al., *DANESS v4. 0: An Integrated Nuclear Energy System Assessment Code*, in *PHYSOR*. 2008: Interlaken, Switzerland.
477. Leppänen, J., *Serpent – a Continuous-energy Monte Carlo Reactor Physics Burnup Calculation Code*. 2013, VTT Technical Research Centre of Finland: VTT Technical Research Centre of Finland.
478. Leppänen, J., et al., *The Serpent Monte Carlo code: Status, development and applications in 2013*. *Annals of Nuclear Energy*, 2015. **82**: p. 142-150.
479. Leppanen, J., *Serpent User's Manual*. 2015: Available from: http://montecarlo.vtt.fi/download/Serpent_manual.pdf.
480. Curtis, C.E. and J.R. Johnson, *Properties of Thorium Oxide Ceramics*. *Journal of the American Ceramic Society*, 1957. **40**(2): p. 63-68.
481. Novog, D.R., A.C. Morreale, and J. Luxat, *The potential production of molybdenum 99 in CANDU reactors*, in *Canadian Nuclear Society Annual Conference*. 2011, Canadian Nuclear Society: Niagara Falls, Canada.
482. Bae, J.H. and J.Y. Jeong, *Thermal-hydraulic Characteristics for CANFLEX Fuel Channel Using Burnable Poison in CANDU Reactor*. *Nuclear Engineering and Technology*, 2015. **47**: p. 559-566.
483. Rouben, B. and W. Garland, *Supercell*, Chapter21-image010.jpg. 2016, UNENE: CANTEACH website. p. Figure 3 Supercell for Calculation of Device Incremental Cross Sections.
484. Zainuddin, N.Z., G.T. Parks, and E. Shwageraus, *The factors affecting MTC of thorium-plutonium-fuelled PWRs*. *Annals of Nuclear Energy*, 2016. **98**: p. 132-143.
485. Phillips, J.F. and H.D. Huber, *Process for the Dissolution of Aluminum-clad Thoria Fuel Elements*. 1968, ; Battelle-Northwest, Richland, Wash. Pacific Northwest Lab. p. Medium: ED; Size: Pages: 36.

486. Knope, K.E. and L. Soderholm, *Solution and Solid-State Structural Chemistry of Actinide Hydrates and Their Hydrolysis and Condensation Products*. Chemical Reviews, 2012. **113**(2): p. 944-994.
487. Neck, V., et al., *Solubility of crystalline thorium dioxide*. Radiochimica Acta, 2003. **91**(5): p. 253-262.
488. Johnson, G.L. and L.M. Toth, *Plutonium(IV) and Thorium(IV) Hydrous Polymer Chemistry*. 1978, Oak Ridge National Laboratory. p. 19.
489. John, K.S., et al., *Solvent extraction of tetravalent titanium from acidic chloride solutions by 2-ethylhexyl phosphonic acid mono-2-ethylhexyl ester*. Hydrometallurgy, 1999. **53**(3): p. 245-253.
490. Wang, L., H. Lee, and M. Lee, *Solvent Extraction Separation of Zr and Hf from Nitric Acid Solutions by PC 88A and Its Mixture with Other Extractants*. Metals and Materials International, 2015. **21**(1): p. 166-172.
491. Banda, R. and M.S. Lee, *Solvent Extraction for the Separation of Zr and Hf from Aqueous Solutions*. Separation and Purification Reviews, 2015. **44**(3): p. 199-215.
492. Fiorina, C., et al., *Comparative analysis of thorium and uranium fuel for transuranic recycle in a sodium cooled Fast Reactor*. Annals of Nuclear Energy, 2013. **62**: p. 26-39.
493. Montgomery, M.H., et al., *The Role of Thorium Fuel in the Future of the LWR Fuel Cycle*. 2010.
494. International Atomic Energy Agency, *Role of Thorium to Supplement Fuel Cycles of Future Nuclear Energy Systems*, in *Nuclear Energy*. 2012: Vienna. p. 171.
495. Reimer, L., *Scanning Electron Microscopy - Physics of Image Formation and Microanalysis*. Springer Series in Optical Sciences. 1998: Springer Berlin Heidelberg.
496. Goldstein, J., et al., *Scanning Electron Microscopy and X-ray Microanalysis*. 3rd ed. 2003: Springer US.
497. Australian Microscopy & Microanalysis Research Facility. *Principles of SEM Operation*. MyScope training 2013 [cited 2015 08 September]; Available from: <http://www.ammrf.org.au/myscope/sem/practice/principles/>.
498. Pyle, J.M., et al., *Monazite-Xenotime-Garnet Equilibrium in Metapelites and a New Monazite-Garnet Thermometer*. Journal of Petrology, 2001. **42**(11): p. 2083-2107.
499. *Discussion forum for Serpent users*. [cited 2016 01 December]; Available from: <http://ttuki.vtt.fi/serpent/>.
500. *Serpent Wiki*. [cited 2016 01 December]; Available from: http://serpent.vtt.fi/mediawiki/index.php/Main_Page.

APPENDIX A. MONAZITE SAMPLE ELECTRON MICROSCOPY STUDIES

A.1 ANALYSIS OF SOME MONAZITE SAMPLES

Several monazite samples were loaned for study by the Manchester Museum. These samples were studied using Scanning Electron Microscopy (SEM) and Energy Dispersive X-ray Spectroscopy (EDS).

A.1.1 SCANNING ELECTRON MICROSCOPY

SEM is a common technique in materials analysis, used to produce high quality images of small scale objects and features. The technique is analogous to standard light microscopy, with the key difference that electrons are used for imaging, rather than photons of visible light, allowing much smaller features to be resolved. An electron source produces electrons which are directed and focussed by electromagnets onto the surface of the sample of interest, producing a variety of detectable emissions which may be analysed to gain information about the sample.

Secondary electrons produce images in which contrast indicates sample morphology, while backscattered electrons produce images in which contrast shows average atomic mass. EDS is used to perform semi-quantitative chemical analyses with spatial resolution over the sample. This technique was used to estimate the elemental composition of different phases in the monazite samples, and thus make inferences about the fractions of individual minerals in each sample.

Detailed information on SEM and EDS is available in a variety of sources [495, 496].

A.1.2 SAMPLE PREPARATION AND ANALYTICAL PROCEDURE

For bulk minerals, samples were cut using a Buehler Isomet low-speed saw and cold mounted in Buehler EpoxiCure resin. The sample was then polished on a Buehler Metaserv polishing wheel using 0.25 μm diamond suspension. Acheson Silver DAG 1415 conductive paint was applied over the sides and base of the resin, and the polished face was sputter-coated with carbon using an Edwards Speedivac carbon coating unit. Sand samples could not be successfully mounted in resin, as polishing caused the sand grains to be pulled out of the resin surface. Instead sand grains were pressed onto an adhesive carbon pad on an aluminium sample holder disc, and this was then sputter-coated with carbon.

Analysis was performed using a JEOL JSM-6400 scanning electron microscope with beam accelerating voltage set to 20 keV, as required for EDS analysis when using this instrument. The EDS system used was an Oxford INCA X-sight.

A.1.3 RESULTS AND DISCUSSION

A.1.3.1 BULK MONAZITE SAMPLE

Figure A.1 shows secondary and backscatter electron images of a Norwegian bulk monazite sample. A number of components of different average atomic mass were observed in the backscatter image, and EDS spectra were gathered for each phase, according to the marked positions in Figure A.1.

The EDS spectra for each investigated position in the image are presented through Figure A.2 to Figure A.6.

THE PREPARATION AND APPLICATION OF THORIUM-BASED NUCLEAR FUELS

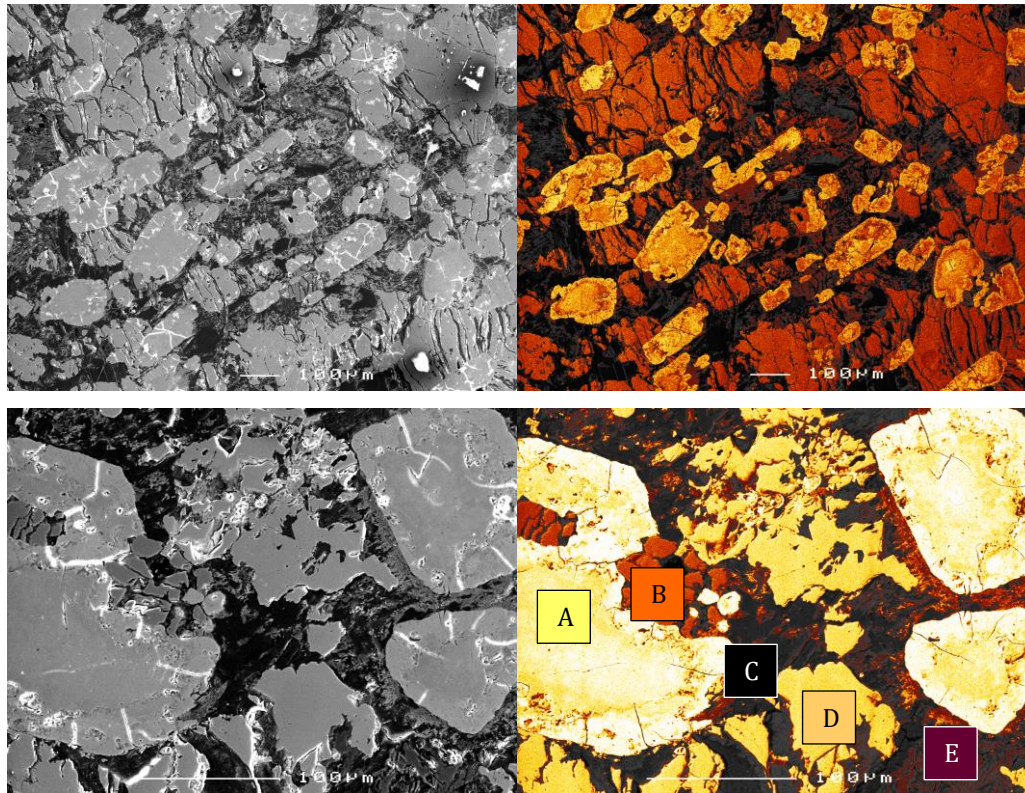


FIGURE A.1 – SECONDARY ELECTRON (LEFT) AND BACKSCATTER ELECTRON (RIGHT) IMAGES OF NORWEGIAN BULK MONAZITE, TAKEN AT 90X MAGNIFICATION (TOP) AND 350X MAGNIFICATION (BOTTOM).

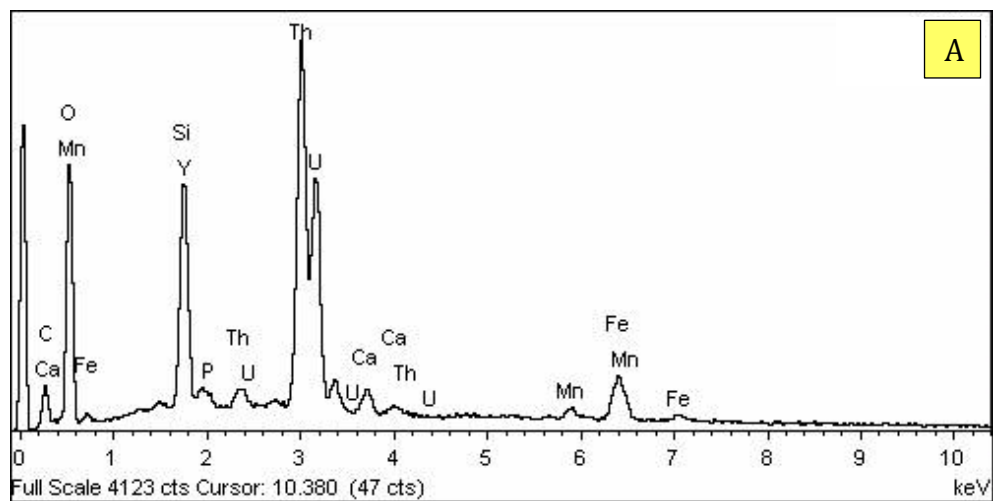


FIGURE A.2 – EDS SPECTRUM FOR POSITION A IN BULK MONAZITE SAMPLE. PHASE SUGGESTED TO BE THORITE, HUTTONITE, OR URANOTHORITE (Th,U)SiO₄.

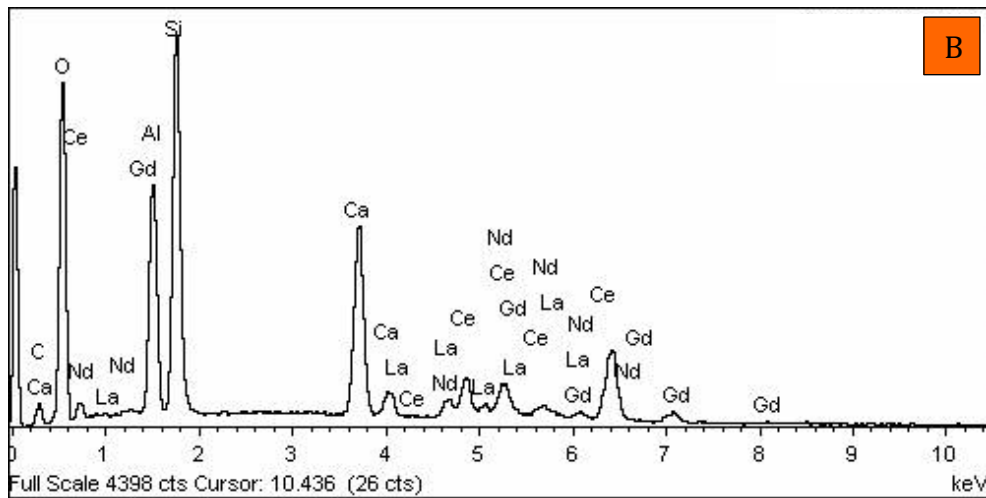


FIGURE A.3 – EDS SPECTRUM FOR POSITION B IN BULK MONAZITE SAMPLE. PHASE SUGGESTED TO BE ALLANITE $(\text{Ce,Ca,Y,La})_2(\text{Al,Fe}^{3+})_3(\text{SiO}_4)_3(\text{OH})$, OR SIMILAR.

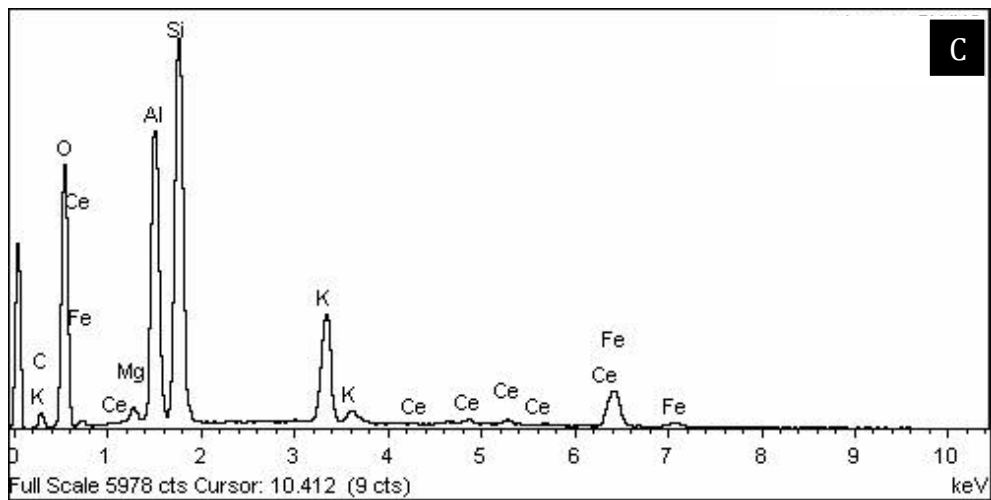


FIGURE A.4 – EDS SPECTRUM FOR POSITION C IN BULK MONAZITE SAMPLE. PHASE SUGGESTED TO BE MICROCLINE OR OTHER POTASSIUM FELDSPAR KAIS_3O_8 .

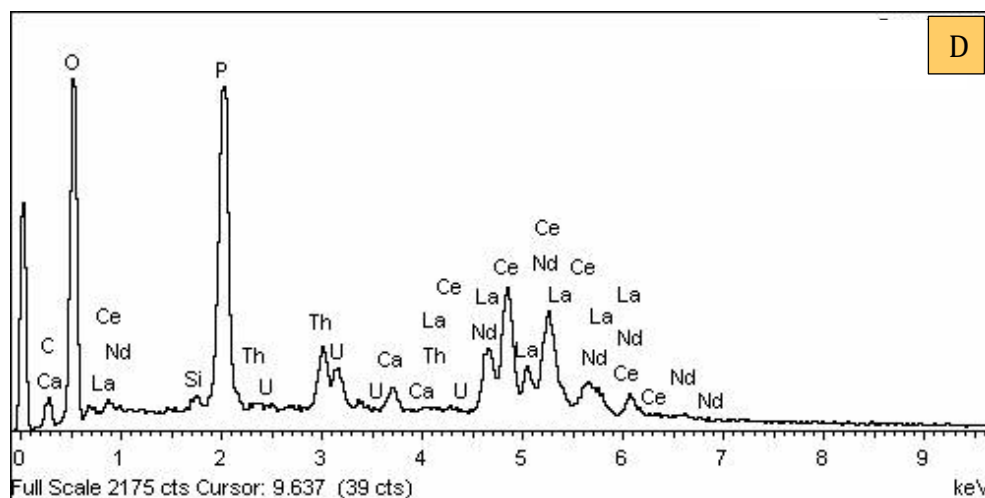


FIGURE A.5 – EDS SPECTRUM FOR POSITION D IN BULK MONAZITE SAMPLE. PHASE SUGGESTED TO BE MONAZITE (Ce,La,Ca,Th)PO₄.

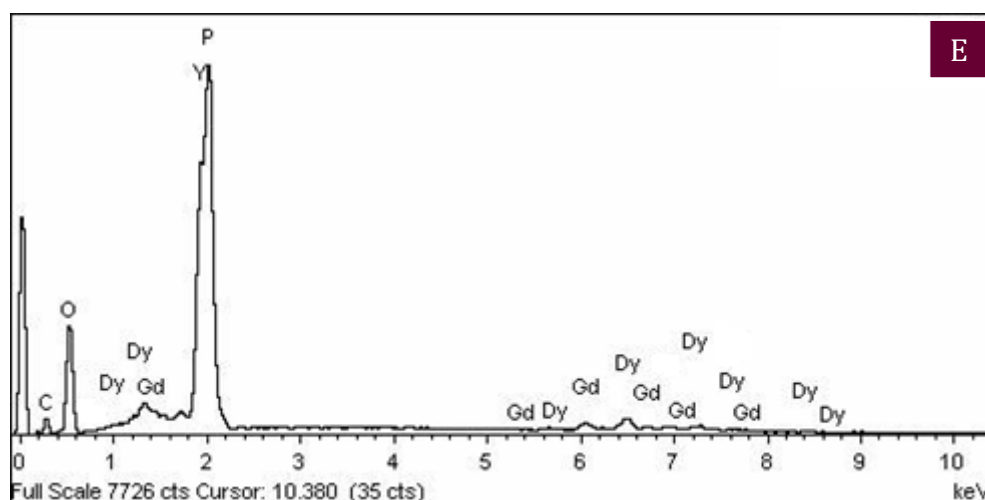


FIGURE A.6 – EDS SPECTRUM FOR POSITION E IN BULK MONAZITE SAMPLE. PHASE SUGGESTED TO BE XENOTIME YPO₄.

The EDS results for position A were indicative of huttonite or uranothorite. Position B was indicative of a calcium/rare earth, aluminium silicate mineral, such as allanite (Ca,Ce,La,Y)₂(Al,Fe)₃(SiO₄)₃(OH). Allanite can include uranium and thorium and is found in similar geological deposits to monazite [158, 162]. Position C was indicative of a potassium feldspar mineral such as microcline KAlSi₃O₈, which is another common accompanying mineral to monazite [162, 163]. Position D was the monazite

phase, including rare earths, phosphorous and small amounts of U and Th. Finally position E exhibits a large yttrium peak with phosphorous, suggesting xenotime YPO_4 [157].

A.1.3.2 MONAZITE SAND SAMPLE

A Brazilian monazite sand was also studied, and secondary and backscatter electron images are presented in Figure A.7. There are horizontal bands of contrast changes in these images. These are artefacts of the analysis due to sample charging, and do not represent real features of the samples being analysed [497].

Three principal phases were identified, marked as A-C in Figure A.7. The spectra for these positions are presented through Figure A.8 to Figure A.10.

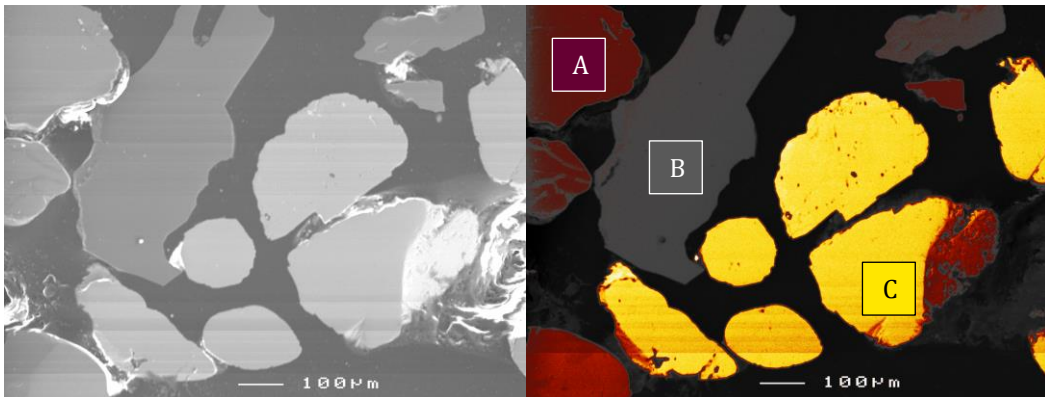


FIGURE A.7 – SECONDARY ELECTRON IMAGE OF BRAZILIAN MONAZITE SAND SAMPLE, TAKEN AT 100X MAGNIFICATION.

THE PREPARATION AND APPLICATION OF THORIUM-BASED NUCLEAR FUELS

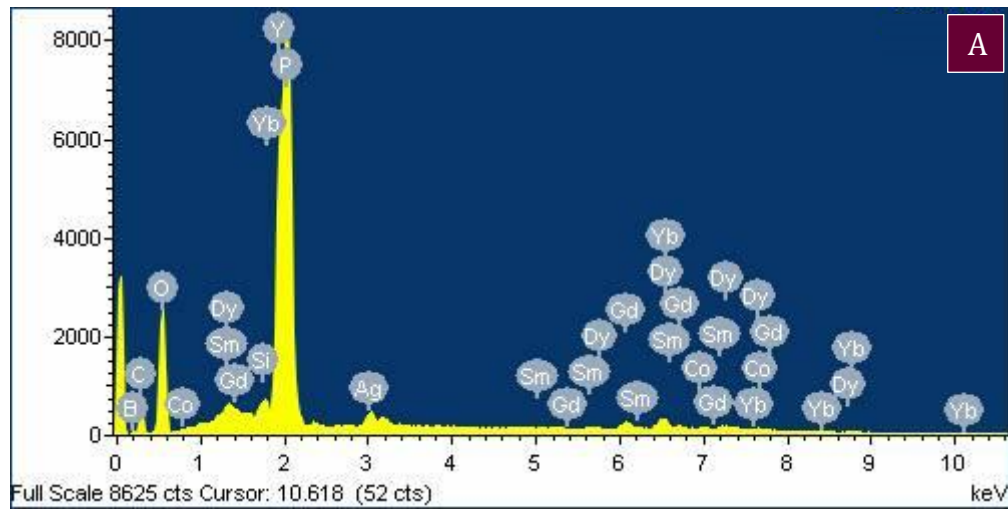


FIGURE A.8 – EDS SPECTRUM FOR POSITION A IN MONAZITE SAND SAMPLE . PHASE SUGGESTED TO BE XENOTIME YPO_4 .

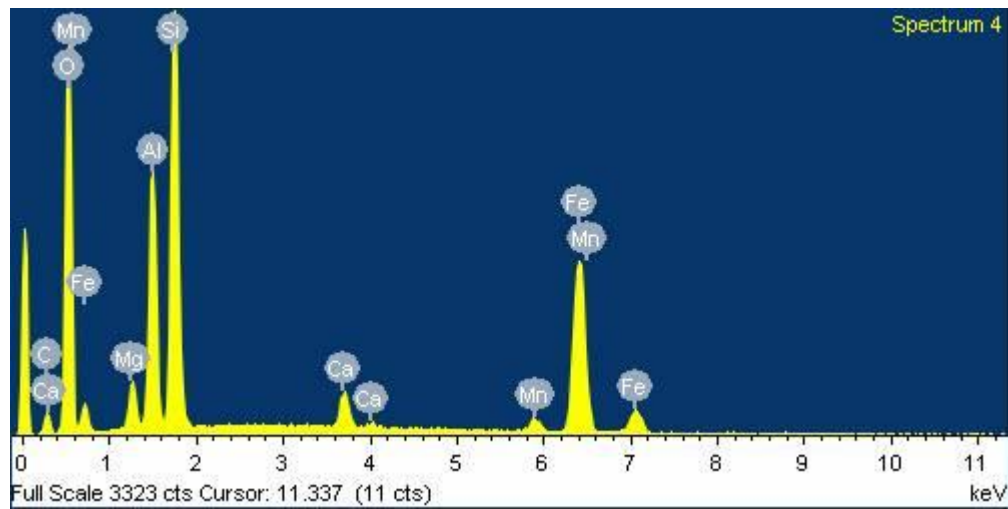


FIGURE A.9 – EDS SPECTRUM FOR POSITION A IN MONAZITE SAND SAMPLE. PHASE SUGGESTED TO BE THORITE, HUTTONITE, OR URANOTHORITE $(Th,U)SiO_4$.

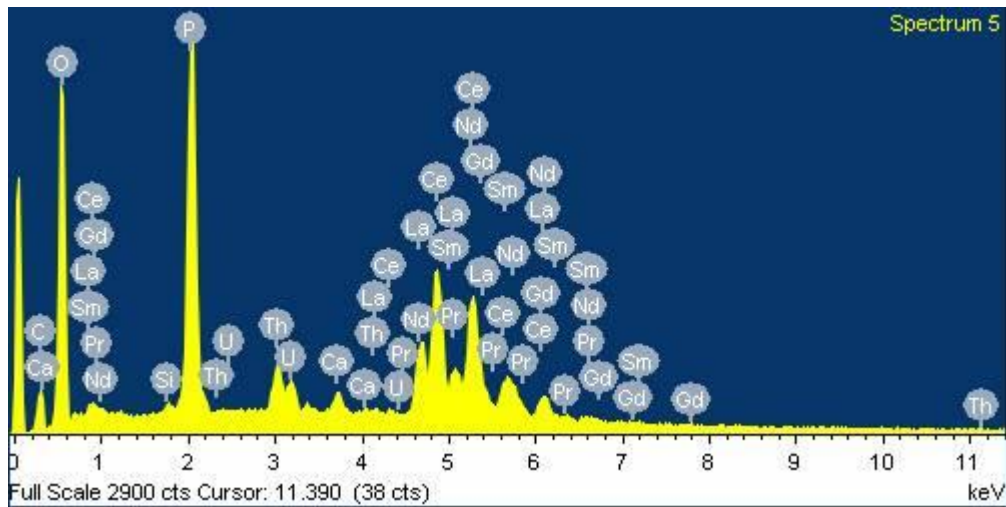


FIGURE A.10 – EDS SPECTRUM FOR POSITION A IN MONAZITE SAND SAMPLE. PHASE SUGGESTED TO BE MONAZITE (Ce,La,Ca,Th)PO₄.

Position A was found to be xenotime. The spectrum at position B contained a number of elements associated with garnet group minerals, which are formed in metamorphic rocks and can accompany monazite [150, 498]. Position C is the monazite phase.

The analysed monazite samples were found to contain a number of other minerals. The additional minerals identified are all known to accompany monazites. Xenotime was present in both samples. The bulk sample contained components of common pegmatite deposits, while the sand sample contained garnet group minerals which are commonly found in metamorphic deposits where monazite may occur. However, for the sand sample the presence of other minerals not normally associated with thorium could be expected, given that the sand was produced by weathering and concentration of heavy minerals across a potentially large geographical region.

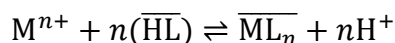
APPENDIX B. MATHEMATICAL DERIVATIONS OF SOLVENT EXTRACTION EQUATIONS

B.1 EQUILIBRIUM EXTRACTION CONSTANTS FOR CATION EXCHANGE LIQUID-LIQUID DISTRIBUTION

In this sub-section, starting from the simplest reaction for cation exchange, the reaction for extraction with two dimeric extractants by a combination of cation exchange and neutral adduct formation is described. Associated equilibrium extraction coefficients are derived throughout.

B.1.1 BASIC CATION EXCHANGE REACTION AND EQUILIBRIUM EXTRACTION CONSTANT FOR AN ACIDIC EXTRACTANT

The simplest solvent extraction reaction, liquid cation exchange, has the general biphasic exchange reaction for metals of charge n [250]

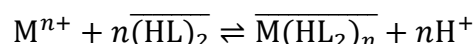


The equilibrium extraction constant of the reaction is

$$K_{ex} = \frac{[\overline{ML}_n][H^+]^n}{[M^{n+}][\overline{HL}]^n} \quad (B.1)$$

B.1.2 CATION EXCHANGE REACTION AND EQUILIBRIUM EXTRACTION CONSTANT FOR A DIMERIC ACIDIC EXTRACTANT

Some extractants form dimers $(HL)_2$. These usually exchange for a single proton, binding as (HL_2) . For extractants which form dimers such as HDEHP and HEHEHP (PC-88a), the reaction is simply modified to [247]



This has the equilibrium extraction constant

$$K_{ex} = \frac{[\overline{M(HL_2)_n}][H^+]^n}{[M^{n+}][\overline{(HL)_2}]^n} \quad (B.2)$$

We can use the definition of the distribution ratio D_M to simplify this equation, where

$$D_M = \frac{[\overline{M(HL_2)_n}]}{[M^{n+}]} \quad (B.3)$$

This gives

$$K_{ex} = D_M \frac{[H^+]^n}{[\overline{(HL)_2}]^n} \quad (B.4)$$

B.1.3 MIXED CATION EXCHANGE AND SOLVATION WITH ONE DIMERIC EXTRACTANT

In addition to those binding through cation exchange, more ligands may bind to the metal through adduct formation, in which case the interfacial exchange reaction becomes

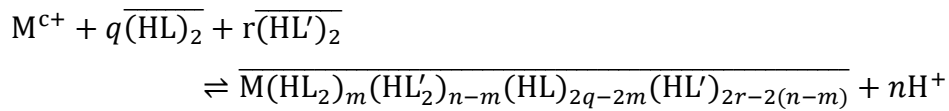


This gives the extraction constant

$$K_{ex} = \frac{[\overline{M(HL_2)_n(HL)_{2q-2n}}][H^+]^n}{[M^{n+}][\overline{(HL)_2}]^q} = D_M \frac{[H^+]^n}{[\overline{(HL)_2}]^q} \quad (B.5)$$

B.1.4 MIXED CATION EXCHANGE AND ADDUCT FORMATION WITH TWO EXTRACTANTS

When considering synergic extraction systems using multiple cation exchange extractants, and including the possibility of neutral adduct formation with the extractant, the general reaction is given by



Where M^{c+} is a metal cation in the aqueous phase, of charge c ,
 $\overline{(\text{HL})}_2$ is an acidic extractant dimer in the organic phase, whose ligand is denoted L,
 $\overline{(\text{HL}')}_2$ is an acidic extractant dimer in the organic phase, whose ligand is denoted L', and
 q, r, m and n are constants specific to the reaction.

The associated reaction equilibrium constant is given by

$$K_{ex} = \frac{[\overline{M(\text{HL}_2)_m(\text{HL}'_2)_{n-m}(\text{HL})_{2q-2m}(\text{HL}')_{2r-2(n-m)}}][\text{H}^+]^n}{[M^{c+}][\overline{(\text{HL})}_2]^q[\overline{(\text{HL}')}_2]^r} \quad (\text{B.6})$$

Using the definition of distribution ratio D_M as

$$D_M = \frac{[\overline{M(\text{HL}_2)_m(\text{HL}'_2)_{n-m}(\text{HL})_{2q-2m}(\text{HL}')_{2r-2(n-m)}}]}{[M^{c+}]} \quad (\text{B.7})$$

This allows the general reaction to be simplified as

$$K_{ex} = D_{Th} \frac{[\text{H}^+]^n}{[\overline{(\text{HL})}_2]^q[\overline{(\text{HL}')}_2]^r} \quad (\text{B.8})$$

B.1.5 SLOPE ANALYSIS TO FIND PARAMETERS N , Q AND R

Taking the logarithm of Equation (B.8) gives

$$\begin{aligned} \log D_M - n \cdot \text{pH} \\ = q \log[\overline{(\text{HL})}_2] + r \log[\overline{(\text{HL}')}_2] + \log K_{ex} \end{aligned} \quad (\text{B.9})$$

n , q and r may be determined experimentally by slope analysis using Equation (B.9).

The determination of n may be made from the variable pH experiment. If the organic phase is fixed then $q \log[(\text{HL})_2]$ and $r \log[(\text{HL}')_2]$ are constants, as long as there is a large excess of extractant to minimise the changes in effective concentration of free extractant in the organic phase. The equation above then simplifies to

$$\log D_M = n \cdot \text{pH} + C \quad (\text{B.10})$$

Where C is a constant. Plotting $\log D_M$ against pH should give a straight line of slope n , which will represent the number of hydrated protons released per thorium complex produced.

q and r may be determined by a similar method, from the variable [PC-88a] and [HDEHP] experiments, where q and r represent the number of PC-88a and HDEHP ligands in each thorium complex. The pH should be held constant and the concentration of one extractant varied while the other is held constant. Similar mathematical treatment yields

$$\log D_M = q \log[(\text{HL})_2] + C \quad (\text{B.11})$$

$$\log D_M = r \log[(\text{HL}')_2] + C \quad (\text{B.12})$$

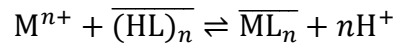
Plotting $\log D_M$ against $\log[(\text{HL})_2]$ or $\log[(\text{HL}')_2]$ should give a straight line of slope n or q respectively.

The substitution of these values into Equation (B.8) will give the equilibrium extraction constant for the interfacial extraction reaction.

B.2 MCCABE-THIELE EXTRACTION ISOTHERM

B.1.6 CATION EXCHANGE WITH A SINGLE EXTRACTANT

The McCabe-Thiele isotherm is derived for a cation exchange reaction as follows.



This gives the extraction coefficient

$$k_{ex} = \frac{[\overline{ML}_n][H^+]}{[M^{n+}][\overline{(HL)}_n]}$$

Some conventions are defined:

$$y = [\overline{ML}_n] \quad (B.13)$$

$$x = [M^{n+}] \quad (B.14)$$

$$k_{ex} = \frac{y}{x} \frac{[H^+]}{[\overline{(HL)}_n]} \quad (B.15)$$

There is also a need to define the total extractant concentration, which is denoted S , being the sum of the free extractant and the complexed ligand.

$$S = y + [\overline{(HL)}_n] \quad (B.16)$$

$$[\overline{(HL)}_n] = S - y \quad (B.17)$$

By substituting this back into the equation for the extraction constant

$$K_{ex} = \frac{y [H^+]^n}{x (S - y)} \quad (B.18)$$

$$K_{ex} x = \frac{y [H^+]^n}{S - y} \quad (B.19)$$

$$y [H^+]^n = K_{ex} x S - K_{ex} x y \quad (B.20)$$

$$y ([H^+]^n + K_{ex} x) = K_{ex} x S \quad (B.21)$$

$$y = \frac{K_{ex}xS}{[H^+]^n + K_{ex}x} \quad (\text{B.22})$$

$$y = \frac{K_{ex}xS/[H^+]^n}{1 + K_{ex}x/[H^+]^n} \quad (\text{B.23})$$

The modified extraction coefficient K'_{ex}

$$K'_{ex} = \frac{K_{ex}}{[H^+]^n} \quad (\text{B.24})$$

Recalling that

$$D_M = \frac{[\overline{ML}_n]}{[M^{n+}]} = \frac{y}{x} \quad (\text{B.25})$$

Substituting Equations (B.24) and (B.25) into Equation (B.23) gives

$$D_M = \frac{SK'_{ex}}{1 + xK'_{ex}} \quad (\text{B.26})$$

$$D_M(1 + xK'_{ex}) = SK'_{ex} \quad (\text{B.27})$$

$$D_M + D_MxK'_{ex} = SK'_{ex} \quad (\text{B.28})$$

$$D_M = SK'_{ex} - D_MxK'_{ex} \quad (\text{B.29})$$

$$D_M = K'_{ex}(S - xD_M) \quad (\text{B.30})$$

$$K'_{ex} = \frac{D_M}{S - xD_M} \quad (\text{B.31})$$

Thus, the extraction coefficient is a function of the metal distribution and the extractant concentration.

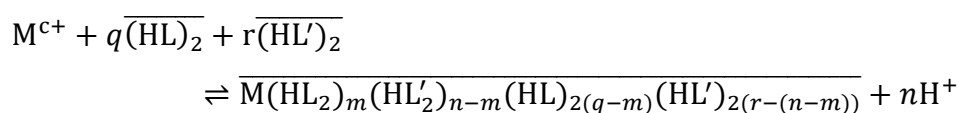
Equation (B.31) may be reduced using Equation (B.25) in order to give a function of y in terms of x

$$y = \frac{K'_{ex}xS}{1 + K'_{ex}x} \quad (\text{B.32})$$

This equation may be used to predict a McCabe-Thiele extraction isotherm for solvent extraction systems, based on the extraction constant K_{ex} and the total amount of extractant in the system S .

B.1.7 MIXED SOLVATION AND CATION EXCHANGE BY MULTIPLE EXTRACTANTS

Considering now the reaction for extraction by two extractants with a mixed solvation and cation exchange mechanism, taken from Section 3.2.6



With the extraction constant defined as

$$K_{ex} = \frac{[\overline{M(HL_2)_m(HL'_2)_{n-m}(HL)_{2(q-m)}(HL')_{2(r-(n-m))}}][H^+]^n}{[M^{c+}][\overline{(HL)}_2]^q[\overline{(HL')}_2]^r} \quad (B.33)$$

We redefine x as

$$x = [M^{c+}] \quad (B.34)$$

And y as

$$y = [\overline{M(HL_2)_m(HL'_2)_{n-m}(HL)_{2(q-m)}(HL')_{2(r-(n-m))}}] \quad (B.35)$$

The modified extraction constant is retained as

$$K'_{ex} = \frac{K_{ex}}{[H^+]^n} \quad (B.36)$$

The use of Equations (B.34) and (B.35) allows Equation (B.33) to be reduced to

$$K_{ex} = \frac{y}{x} \frac{[H^+]^n}{[\overline{(HL)}_2]^q[\overline{(HL')}_2]^r} \quad (B.37)$$

In order to determine the free quantity of each extractant in the system at equilibrium, required in the denominator of Equation (B.37), we can define

two parameters α and β which represent the total concentration of the extractant dimers L_2 and L'_2 respectively. Each total concentration is given by the sum of the free extraction and the complexed ligand.

$$\alpha = [(\text{HL})_2] + y \frac{2m + 2(q - m)}{2} \quad (\text{B.38})$$

$$\beta = [(\text{HL}')_2] + y \frac{2(n - m) + 2(r - (n - m))}{2} \quad (\text{B.39})$$

Simplifying the numerators of the fractions in Equations (B.38) and (B.39) and rearranging gives

$$[(\text{HL})_2] = \alpha - qy \quad (\text{B.40})$$

$$[(\text{HL}')_2] = \beta - ry \quad (\text{B.41})$$

These can be substituted into Equation (B.37) to give

$$K_{ex} = \frac{y}{x} \frac{[\text{H}^+]^n}{(\alpha - qy)^q (\beta - ry)^r} \quad (\text{B.42})$$

Equation (B.36) may then be used to give

$$K'_{ex} = \frac{y}{x} \frac{1}{(\alpha - qy)^q (\beta - ry)^r} \quad (\text{B.43})$$

Finally, this may be rearranged to give x as a function of y , as shown

$$x = \frac{y}{K'_{ex} (\alpha - qy)^q (\beta - ry)^r} \quad (\text{B.44})$$

By inserting values of y , the corresponding values of x may be determined, allowing the prediction of an isotherm. It can be seen that this equation allows the calculation of an isotherm directly, based on knowledge of the total amount of each extractant, the extraction constant, the acidity of the system and the values of q and r determined from slope analysis.

APPENDIX C. SERPENT INPUT FILE FOR 3% PLUTONIUM IN FUEL CONCEPT 19

C.1 SERPENT CODE INTERPRETATION

The input code in Serpent is organised into “cards” and “set” options. Cards are used to define major aspects of the simulation, such as material compositions, geometry, fuel pin lattice layouts, and burnup histories. The keyword “set” is used to enable/disable options, make minor changes and define aspects of the simulation that do not require a full card. The % symbol is used to mark a comment line, with anything on the same line and following the % symbol being ignored by Serpent.

The user manual and supporting documentation for Serpent is not complete. However the reader will be able to find information on using Serpent in the version 1 manual [479], the users discussion forums [499] and the users wiki page, which is intended to act as the user’s manual for Serpent version 2 [500].

The file below includes a burnup history to 30 MWd/tHM, and produces a materials composition restart file, as would be required to perform voiding calculations.

C.2 INPUT FILE TEXT

```

% --- START -----
% --- Enhanced CANDU 6 with 43-element bundle, Fuel Concept 19 (InvPu and TPU
MOX) ---
% --- 3% average plutonium in MOX
% --- Includes burnup history to 400 MWd/kg

set title "C19, 3%Pu, burnup towards 30 GWd/t"
set seed 1234567890          % Fix random seed value to allow replication

% --- Define fuel elements:

pin 1          % Centre element, large diameter
ThO2 0.6290
sheath 0.6750
cool

pin 2          % Inner 7 elements, large diameter
ThO2 0.6290
sheath 0.6750
cool

pin 3          % Intermediate 14 elements, small diameter
RichMOX 0.5325
sheath 0.5750
cool

pin 4          % Outer 21 elements, small diameter
LeanMOX 0.5325
sheath 0.5750
cool

% ===== GEOMETRY DEFINITIONS =====

% --- Define pin lattice in bundle (type = 4 (rings), 4 rings, 3rd ring rotated
to 12.857 deg.):

lat 10 4 0.0 0.0 4          % Lattice, universe 10, type 4, centrally
    positioned, 4 rings
  1 0.0000 0.000 1          % Centre pin
  7 1.7340 0.000 2 2 2 2 2 2 % Inner ring, 7 pins
 14 3.0750 12.857 3 3 3 3 3 3 3 3 3 3 3 3 3 3 % Intermediate ring, 14 pins
 21 4.3840 0.000 4 4 4 4 4 4 4 4 4 4 4 4 4 4 4 4 4 4 4 4 % Outer ring, 21
    pins

% --- Define surfaces (core lattice pitch = 28.6 cm):

surf 1 cyl 0.0 0.0 5.16890 % Pressure tube inner wall
surf 2 cyl 0.0 0.0 5.60320 % Pressure tube outer wall
surf 3 cyl 0.0 0.0 6.44780 % Calandria tube inner wall
surf 4 cyl 0.0 0.0 6.58750 % Calandria tube outer wall
surf 5 sqc 0.0 0.0 14.30000 % Domain extent boundary halfway between bundles

% --- Cell definitions:

cell 1 0 fill 10 -1        % Pin lattice inside pressure tube
cell 2 0 prstube 1 -2      % Pressure tube
cell 3 0 anulgas 2 -3      % Inter-tube gas annulus
cell 4 0 caltube 3 -4      % Calandria tube
cell 5 0 calan 4 -5        % Moderator in calandria
cell 6 0 outside 5        % Domain extent boundary

% ===== MATERIAL DEFINITIONS =====

% --- Define ThO2 as blanket:

```

THE PREPARATION AND APPLICATION OF THORIUM-BASED NUCLEAR FUELS

```

mat ThO2      -10.42  rgb 153 76 0   burn 1  % 95 percent of interpolated
densities
90232.09c    1.0000  % Thorium-232 atom fraction in fuel
8016.09c     2       % Oxygen-16 atom fraction in fuel

% --- Define intermediate ring as rich mox:

mat RichMOX   -10.44  rgb 153 51 255 burn 1  % 95 percent of interpolated
densities
94238.09c    0.0001  % Plutonium-238 atom fraction in fuel
94239.09c    0.0307  % Plutonium-239 atom fraction in fuel
94240.09c    0.0101  % Plutonium-240 atom fraction in fuel
94241.09c    0.0007  % Plutonium-241 atom fraction in fuel
94242.09c    0.0005  % Plutonium-242 atom fraction in fuel
95241.09c    0.0006  % Americium-241 atom fraction in fuel
92234.09c    0.0002  % Uranium-234 atom fraction in fuel
92235.09c    0.0086  % Uranium-235 atom fraction in fuel
92236.09c    0.0024  % Uranium-236 atom fraction in fuel
92238.09c    0.9463  % Uranium-238 atom fraction in fuel
8016.09c     1.999998085 % Oxygen-16 atom fraction in fuel

% --- Define outer ring as lean mox:

mat LeanMOX   -10.43  rgb 255 255 0   burn 1  % 95 percent of interpolated
densities
94238.09c    0.0000  % Plutonium-238 atom fraction in fuel
94239.09c    0.0154  % Plutonium-239 atom fraction in fuel
94240.09c    0.0050  % Plutonium-240 atom fraction in fuel
94241.09c    0.0003  % Plutonium-241 atom fraction in fuel
94242.09c    0.0002  % Plutonium-242 atom fraction in fuel
95241.09c    0.0003  % Americium-241 atom fraction in fuel
92234.09c    0.0002  % Uranium-234 atom fraction in fuel
92235.09c    0.0087  % Uranium-235 atom fraction in fuel
92236.09c    0.0024  % Uranium-236 atom fraction in fuel
92238.09c    0.9673  % Uranium-238 atom fraction in fuel
8016.09c     1.999998043 % Oxygen-16 atom fraction in fuel

% --- Define sheath as zircaloy-4 (mass densities):

mat sheath    -7.48      rgb 255 0 0   % Sheath (cladding) density 7.48 g/cm3
50000.06c    -1.45000E+0   % Natural tin mass fraction in sheath
26000.06c    -1.50000E-1   % Natural iron mass fraction in sheath
28000.06c    -7.00000E-3   % Natural nickel mass fraction in sheath
24000.06c    -1.00000E-1   % Natural chromium mass fraction in sheath
40000.06c    -9.82930E+1   % Natural zirconium mass fraction in sheath

% --- Define pressure tube as Zr-2.5%Nb:

mat prstube   -6.57      rgb 192 192 192 % Pressure tube density 6.57 g/cm3
40000.06c    -9.75000E+1   % Natural zirconium mass fraction in pressure tube
41093.06c    -2.25000E+0   % Natural niobium mass fraction in pressure tube

% --- Define annulus as carbon dioxide

mat anulgas   -0.001253 rgb 229 204 255 % CO2 density at 1 bar, 150oC = 1.253
kg/m3
6000.06c     1.00000E+0   % 1 carbon atom in CO2
8016.06c     2.00000E+0   % 2 oxygen atoms in CO2

% --- Define calandria tube as zircaloy-2:

mat caltube   -6.44      rgb 96 96 96   % Calandria tube density 6.44 g/cm3
50000.06c    -1.45000E+0   % Natural tin mass fraction in sheath
26000.06c    -1.35000E-1   % Natural iron mass fraction in sheath
28000.06c    -5.50000E-2   % Natural nickel mass fraction in sheath
24000.06c    -1.00000E-1   % Natural chromium mass fraction in sheath
40000.06c    -9.82600E+1   % Natural zirconium mass fraction in sheath

% --- Define coolant water with reference to thermal scattering data libraries:

mat cool      -0.8121200  moder lwtr 1001 moder hwtr 1002  rgb 0 255 255
8016.06c     -7.99449E-1   % Oxygen-16 mass fraction in coolant

```

APPENDIX C SERPENT INPUT FILE FOR 3% PLUTONIUM IN FUEL CONCEPT 19

```

1002.06c -1.99768E-1 % Deuterium mass fraction in coolant
1001.06c -7.83774E-4 % Protium mass fraction in coolant

% --- Define moderator water with reference to thermal scattering data libraries:

mat calan -1.082885 moder lwtr 1001 moder hwtr 1002 rgb 0 0 255
8016.06c -7.98895E-1 % Oxygen-16 mass fraction in coolant
1002.06c -2.01016E-1 % Deuterium mass fraction in coolant
1001.06c -8.96000E-5 % Protium mass fraction in coolant

% ===== LIBRARY DEFINITIONS =====

% --- Thermal scattering data for light and heavy water:

therm lwtr lwj3.11t
therm hwtr hwj3.11t

% --- Cross section data library file path

set acelib "/opt/gridware/apps/intel-12.0/serpent/2.1.28-
fix/xsdata/jeff311/sss_jeff311u.xsdata"

% --- Set outer boundary condition to periodic (type = 3)

set bc 3

% --- Neutron population and criticality cycles:

set pop 5000 2500 20 % 5000 neutrons, 2500 active cycles, 20 inactive cycles

% === Burnup calculation definition =====

% --- Decay and fission yield data library file paths

set declib "/opt/gridware/apps/intel-12.0/serpent/2.1.28-
fix/xsdata/jeff311/sss_jeff311.dec"
set nfylib "/opt/gridware/apps/intel-12.0/serpent/2.1.28-
fix/xsdata/jeff311/sss_jeff311.nfy"

% --- Write binary restart file

set rfw 1 RF-BUto30MWd % Writes binary restart file with name "RF-BUto30MWd"

% --- Irradiation cycle history definition

set powdens 0.025809 % calculated as 2084 MWt over core HM mass with 3% Pu in
MOX

dep butot % Burnup steps at which to calculate, cumulative, MWd/kgHM
0.1
0.5
1
2
3
4
6
8
10
12.5
15
20
25
30

% --- ENDS -----

```

APPENDIX D. SCREENING STUDY

DISTRIBUTION RATIO RESULTS

TABLES

TABLE D.1 – DISTRIBUTION CONSTANTS FOR THORIUM EXTRACTION FROM ACID MEDIA BY PC-88A AND POTENTIAL SYNERGISTS.

D_{Th}	0.5 M HCl	3.0 M HCl	0.5 M HNO ₃	3.0 M HNO ₃	0.5 M H ₂ SO ₄	3.0 M H ₂ SO ₄
PC-88a alone	1535	2.399	6902	6902	0.5383	0.00001
TBP	905.7	2.056	6902	6902	0.03936	0.03155
TOPO	123.6	9.333	6902	6902	0.00001	0.05559
HDEHP	3846	68.23	6902	6902	41.11	0.00001
MOA	2009	2.449	6902	6902	0.5035	0.00193
TOA	94.62	0.6730	6902	6902	0.00001	0.00001
<i>Tert</i> -OA	966.1	2.270	6902	6902	0.6152	0.00001
Aliquat-336	590.2	0.4966	6902	6902	0.00001	0.00001
Cyphos 101	153.1	0.9462	6902	6902	1.072	0.00001
BMIM Cl ⁻	935.4	2.208	6902	6902	0.6592	0.00001

APPENDIX D SCREENING STUDY DISTRIBUTION COEFFICIENT RESULTS TABLES

TABLE D.2 – DISTRIBUTION CONSTANTS FOR URANIUM EXTRACTION FROM ACID MEDIA BY PC-88A AND POTENTIAL SYNERGISTS.

<i>D_U</i>	0.5 M HCl	3.0 M HCl	0.5 M HNO₃	3.0 M HNO₃	0.5 M H₂SO₄	3.0 M H₂SO₄
PC-88a alone	164.1	3.034	134.6	25.586	22.39	0.4775
TBP	202.3	3.428	50.12	115.1	25.18	0.8414
TOPO	2716	616.6	173.8	1227	204.6	8375
HDEHP	818.5	16.07	153.5	83.946	121.9	4.375
MOA	203.2	3.258	159.2	28.708	22.80	0.5984
TOA	272.9	96.61	487.5	92.683	143.2	0.7551
<i>Tert</i> -OA	182.8	3.304	381.9	26.915	23.66	0.4634
Aliquat-336	166.3	35.32	299.2	65.766	21.28	0.2911
Cyphos 101	238.8	437.5	459.2	83.176	57.41	1.021
BMIM Cl ⁻	160.0	3.090	136.8	24.210	22.08	0.5768

TABLE D.3 – DISTRIBUTION CONSTANTS FOR IRON EXTRACTION FROM ACID MEDIA BY PC-88A AND POTENTIAL SYNERGISTS.

<i>D_{Fe}</i>	0.5 M HCl	3.0 M HCl	0.5 M HNO₃	3.0 M HNO₃	0.5 M H₂SO₄	3.0 M H₂SO₄
PC-88a alone	4.227	0.1355	1.581	0.8551	0.1343	0.0190
TBP	2.099	0.03155	0.4477	0.5200	0.1125	0.00001
TOPO	3.184	57.02	0.3289	0.5521	0.2104	0.00001
HDEHP	22.80	0.2239	6.026	3.443	2.188	0.2333
MOA	5.188	0.1079	0.1901	0.5754	0.3069	0.00001
TOA	4.446	207.0	0.4169	0.4898	0.2818	0.00001
<i>Tert</i> -OA	2.754	0.1262	0.8356	0.8433	0.3784	0.00001
Aliquat-336	6.223	98.401	0.2506	0.4898	0.6839	0.00001
Cyphos 101	4.753	233.9	0.3334	0.5058	1.567	0.0538
BMIM Cl ⁻	3.622	0.06982	2.070	0.6761	0.4426	0.00001

THE PREPARATION AND APPLICATION OF THORIUM-BASED NUCLEAR FUELS

TABLE D.4 – DISTRIBUTION CONSTANTS FOR ZIRCONIUM EXTRACTION FROM ACID MEDIA BY PC-88A AND POTENTIAL SYNERGISTS.

<i>D_{Zr}</i>	0.5 M HCl	3.0 M HCl	0.5 M HNO₃	3.0 M HNO₃	0.5 M H₂SO₄	3.0 M H₂SO₄
PC-88a alone	5012	411.1	5012	5012	345.9	62.37
TBP	5012	400.9	5012	5012	285.1	9.638
TOPO	5012	1837	5012	5012	122.7	22.28
HDEHP	5012	5012	5012	5012	553.4	90.57
MOA	5012	5012	5012	5012	567.5	276.7
TOA	5012	227.5	5012	5012	650.1	28.84
<i>Tert</i> -OA	5012	5012	5012	5012	799.8	98.86
Aliquat-336	5012	343.6	5012	5012	914.1	37.24
Cyphos 101	5012	1387	5012	5012	5012	31.33
BMIM Cl ⁻	5012	5012	5012	5012	1950	94.84